ELECTRICAL PERFORMANCE OF ESTER LIQUIDS UNDER IMPULSE VOLTAGE FOR APPLICATION IN POWER TRANSFORMERS

A thesis submitted to The University of Manchester for the degree of PhD
in the Faculty of Engineering and Physical Sciences

2011

QIANG LIU

School of Electrical and Electronic Engineering

CONTENTS

Word count: 47 607

LIST OF FIGURES

LIST OF TABLES

ABSTRACT

Ester liquids including both natural ester and synthetic ester are being considered as potential alternatives to mineral oil, due to their better environmental performance and for some liquids their higher fire point. Although these liquids have been widely used in distribution and traction transformers, it is still a significant step to adopt ester liquids in high-voltage power transformers because the high cost and severe consequence of a factory test failure and the high level of safety and reliability required in service for these units, tend to lead to a cautious approach to any step change in technology. Lightning impulse strength as basic insulation level is of importance for insulation design of power transformers and lightning impulse test is commonly required in the factory routine tests for high-voltage power transformers, so this thesis is aimed to investigate the electrical performances including pre-breakdown and breakdown of natural ester and synthetic ester under impulse voltage.

Two types of field geometry were considered in the study, one is sphere-sphere configuration which represents the quasi-uniform fields inside a transformer and another is strongly non-uniform point-plane configuration which represents the situation of a defect or a source of discharge. In quasi-uniform field study, standard breakdown tests were carried out under negative lightning and switching impulse voltages. Influence of various testing methods on the measured lightning breakdown voltage was studied and the 1% lightning withstand voltage was obtained based on Weibull distribution fitting on the cumulative probability plot built up using the approximately 1000 impulse shots. As for strongly non-uniform field study, streamer propagation and breakdown event in ester liquids either with or without pressboard interface were investigated at various gap distances under both positive and negative lightning impulse voltages. A relationship between the results under lightning impulse and previously published results under step voltage was built up to predict the lightning breakdown voltage of ester liquids at very large gaps.

The results indicated that impulse strengths of ester liquids for both breakdown and withstand in a quasi-uniform field, are comparable to those of mineral oil. In a strongly non-uniform field, streamers in ester liquids propagate faster and further, than in mineral oil at the same voltage level. Thus breakdown voltages of ester liquids are generally lower than those of mineral oil, which could be as low as 40% at a large gap distance of approximately 1000 mm. Introduction of parallel pressboard interface has no influence on the streamer propagation and thus does not weaken the breakdown voltage, but it tends to reduce the acceleration voltage particularly for mineral oil under positive polarity.

Last but not least, a unique phenomenon of secondary reverse streamer (SRS) was observed in ester liquids, which occurs subsequently and well after the extinction of the primary streamer (PS) propagation within a single shot of impulse voltage and has the reverse polarity to the PS. The formation mechanism of SRS is explained mainly due to the reverse electric field induced by the residual space charges left by the PS.

DECLARATION

I declare that no portion of the work referred to in the thesis has been submitted in support of an application for another degree or qualification of this or any other university or other institute of learning.

COPYRIGHT STATEMENT

ACKNOWLEDGEMENT

When I finished the last word of the technical part of this thesis, the moment was exciting. I suddenly realized that I had grown up a lot for both scientific knowledge and life experience during the PhD study. I would like to express my sincere gratitude to my supervisor Professor Zhongdong Wang, since any tiny step of my improvements in the last three years was tied closely with her great effort and kind encouragement. I thank her for her supervision, guidance and support to my PhD research, and her trust in my ability, when necessary, to 'play' in the research activities.

I would also like to thank all the sponsoring companies, who provided the PhD research studentship and gave the continuous support to the project at the University of Manchester. In particular, they are Alan Darwin, Fabrice Perrot and Christophe Perrier of ALSTOM Grid, Mark Lashbrook and Russell Martin of M&I Materials, Paul Jarman and Gordon Wilson of National Grid, Dave Walker of Scottish Power, Sue Northcote, John Noakhes and the team of TJH2b Analytical Services, Paul Dyer of UK Power Networks, Tony Byrne and Darren Jones of Electricity North West. Their technical comments and kind patience guaranteed the success of the project and are greatly appreciated here.

Great thanks are also given to Dr. Keith Cornick, Prof. Ian Cotton, Dr. Olivier Lesaint and Dr. Lars Lundgaard for some inspirational advices during the talks with them. I would also like to thank CIGRE WG D1.31 for offering me an opportunity to learn, EPSRC Instrument Pool for loans of High-speed camera and Mr Frank Hogan for teaching me the operation of a 2 MV impulse generator.

To all my colleagues in the transformer research group and others in the corridor of Ferranti building and the School of Electrical and Electronic Engineering, I appreciate for your company and thank you for offering me an enjoyable working environment. Special thanks to Miss Xiao Yi and Mr Xin Wang who worked together with me in the same project of alternative oils.

Last but not least, I wish to give my heartful thanks to my family, to my parents for their continuous backup and understanding, to my wife Mrs Linqing Zhang for her selfless support and love.

CHAPTER 1. INTRODUCTION

1.1 Background

A reliable supply of power in the form of electricity to industrial, commercial and domestic consumers ensures today's economies and standard of living of the industrialised world. The efficient transmission of bulk electrical power from where it is generated to where it is consumed relies significantly on the ability to reduce transmission losses by reducing the transmitted current [1]. The invention of power transformer towards the end of the nineteenth century made possible the development of modern high-voltage power transmission system [2]. Nowadays a typical national electricity transmission and distribution network would be connected by a few hundred transmission and a few thousand distribution transformers. The majority of power transformers so far are still oil filled type, which, to be simplified, is a laminated iron core with paper insulated copper conductors, contained in an oil filled steel tank [1].

The oil used in power transformers has several main functions as it acts as electrical insulation, cooling medium and information carrier. Besides those main functions there are several secondary properties being expected from transformer oil, e.g. compatibility with cellulose solid insulation, fire safety consideration and environmental requirements etc. Up to now, the dominant oil insulation for power transformers remains as mineral oil since it has been widely and successfully used in practice for over a century.

Ester liquids including both natural ester and synthetic ester are being considered as potential alternatives to mineral oil, due to their better environmental performance and for some liquids their higher fire point. Although these liquids have been widely used in distribution and traction transformers, it is still a significant step to adopt ester liquids in high-voltage power transformers because the high cost and severe consequence of a factory test failure and the high level of safety and reliability required in service for these units, tend to lead to a cautious approach to any step change in technology. To mitigate these risks and open up the possibility of gaining the benefit from these materials, an extensive effort has been made by many researchers [3-7] to gain as much

understanding of the material characteristics as possible, including dielectric, thermal and chemical properties, material compatibility and ageing performance relative to the conventional mineral oil.

Results from laboratory experiments have revealed both pros and cons of ester liquids for application in power transformers. In terms of positive aspects, besides the good biodegradability and high fire point, ester liquids could retard cellulose paper's ageing rate due to their large absorption of water from paper, which slows down the hydrolysis process of cellulose paper [8, 9]. In addition, AC breakdown strength of ester liquids was found to be comparable to that of mineral oils [4, 5, 10, 11]. In terms of negative aspects, higher viscosity of ester liquids could cause higher top oil rise and higher hot-spot temperature even ester liquids have higher specific heat and thermal conductivity, compared with mineral oils [12]. Some papers also reported that ester liquids have inferior performance under impulse voltage [13, 14].

With the progressing research activities in laboratory, manufacturers are making every endeavour to launch field trials of ester liquids filled power transformers. Indeed, a few successful application cases can be traced up to 238 kV for synthetic ester [15] and 230 kV (242 kV, if considering shunt reactor) for natural ester [16]. Transformers with higher voltage rating e.g. 400 kV are under development in factory with consideration of possible design changes.

Facing towards the application in high-voltage large power transformers, electrical performance of ester liquids under impulse voltage becomes more important than ever for the insulation design. Transformer in service shall be exposed to voltages in excess of the normal operating voltage, such as transient overvoltages due to lightning strokes to earth near overhead lines connected to the transformer, represented by standard lightning impulse 1.2/50 μs or when equipment is connected to or disconnected from the power system, represented by standard switching impulse 250/2500 μs. It is acknowledged that those impulse strokes external to the transformer are one of the main modes to cause in-service failures. To verify the reliability of large power transformers under impulse voltage, both lightning and switching impulse tests are usually required for transformers with voltage rating higher than 170 kV [17]. Furthermore, lightning impulse strength as basic insulation level (BIL) is commonly used as the criterion of

insulation design for large power transformers. Therefore the increasing interests on use of ester liquids in large power transformers press for the comprehensive investigations on electrical performance of these liquids under impulse voltage.

In contrast to AC breakdown strength, which indicates the liquid condition, e.g. contaminations of moisture or particles, impulse breakdown strength, particularly under lightning impulse, is normally regarded to be predominated by the intrinsic properties of liquids. The possible reason is that some of the mechanisms known to influence AC breakdown e.g. particle migration become less important in the case under impulse voltage since those activities require a considerable period of time while the duration of the impulse is relatively too short to allow these to operate [18]. However particle contamination might have some effects on the impulse performance of a liquid, depending on the contamination level. For low and normal contamination levels [19], an increase of particle number does not reduce the liquid's lightning breakdown voltage [20]; for marginal and high contamination levels [19], an increase of particle number does reduce the liquid's lightning breakdown strength [21, 22]. In addition, an AC pre-stress of about 3.5 kV/mm could reduce the 63% switching impulse breakdown voltage by 20% for the liquid with high contamination level [23].

Nevertheless, it is generally acknowledged that breakdown voltage of mineral oils under negative lightning impulse in a divergent field decreases with the increase of their aromatic content (especially poly-aromatic content). In other words, liquids with different chemical compositions are likely to perform differently under impulse voltage, so application of ester liquids (with composition quite different from mineral oil) in power transformers calls for detailed investigations under impulse voltage.

1.2 Research Objectives

The aim of this PhD thesis is to evaluate the electrical performance of ester liquids under impulse voltage for the application in power transformers. Two types of ester liquid including a synthetic ester and a natural ester will be studied. Tests will also be conducted on a mineral oil as the benchmark. Both breakdown strength and pre-breakdown phenomenon of ester liquids under impulse voltage will be investigated

at various testing conditions e.g. field geometry, voltage polarity and gap distance. Overall the following topics will be covered in this thesis:

(i) Breakdown strength of ester liquids in a quasi-uniform field

The main electric fields distributed inside a transformer e.g. between turn to turn and disk to disk, are quasi-uniform fields, so the first attempt is to know the impulse breakdown strength of ester liquids in such a quasi-uniform field. Both lightning and switching impulse voltages and various testing methods are considered in the study.

(ii) Streamer characteristic and breakdown strength of ester liquids in a non-uniform field

A point-plane electrode configuration, which aids the initiation of a streamer, is usually used in non-uniform field study. Although this strongly non-uniform field is avoided to the upmost in the transformer design and manufacture, there is always the possibility for the existence of manufacturing defects e.g. protrusion on the copper conductor, and contaminations resulting from long term in-service degradation e.g. particle and moisture in the oil, all of which could cause local electric field enhancement (non-uniform field) and thus might initiate a discharge. In addition, impulse tests in a strongly non-uniform field are able to show the difference among liquids if there is. Therefore, it is of importance to understand the behaviour of ester liquids under impulse voltage in a strongly non-uniform field in terms of pre-breakdown phenomenon i.e. streamer characteristic and breakdown strength.

(iii) Streamer characteristic and breakdown strength on ester/pressboard interface in a non-uniform field

As pressboards are generally used in transformers as barriers between windings or winding and earth to enhance the dielectric strength of oil gaps, it is necessary to investigate the streamer and breakdown performances of ester liquids by taking into account the presence of pressboard. When a streamer or discharge propagates along the pressboard surface, it could be driven by the tangential electric field on the surface or self built-up divergent electric field. This type of discharge is also called ‘creepage discharge’, which is attributed to one of the failure modes for large power transformers.

(iv) <u>Phenomenon of secondary reverse streamer in ester liquids in a non-uniform field</u>

Secondary reverse streamer is a newly observed phenomenon in this thesis, depicting a streamer in liquids which has the reverse polarity to the primary streamer and subsequently occurs well after the extinction of the primary streamer propagation within a single shot of impulse voltage. This phenomenon is speculated as being caused by the space charge induced reverse electric field. In addition it exists in ester liquids but is difficult to be observed in mineral oil.

1.3 Major Contributions

The major contributions of this thesis are given as follows:

(i) 1% withstand voltage and 50% breakdown voltage of ester liquids in a quasi-uniform sphere-sphere field are determined, of which both are comparable to those of mineral oil.

(ii) Streamer characteristics of ester liquids in a non-uniform point-plane field are recorded. At the same voltage level, streamers in ester liquids generally propagate faster, further, and with more branches for those negative ones, than in mineral oil.

(iii) A relationship between the breakdown results under lightning impulse and the previously published results under step voltage is built up. Based on the relationship, the lightning breakdown voltages of ester liquids in a non-uniform field at very large gaps are predicted, which could be as low as 40% of that of mineral oil at a gap distance of approximately 1000 mm.

(iv) Introduction of pressboard surface in the parallel direction to the point-plane gap does not influence the streamer propagation and 50% breakdown voltage, but it tends to reduce the acceleration voltage, particularly for mineral oil under positive polarity.

(v) Secondary reverse streamer (SRS), as a newly observed phenomenon in liquids, is introduced. It occurs well after the extinction of the primary streamer (PS) and has the reverse polarity to the PS, which might be due to the reverse electric field induced by the residual space charges left by the PS.

1.4 Outline of Thesis

The following is a summary of the chapters presented in this thesis:

Chapter 1 Introduction

This chapter introduces the background and motivation of the PhD study and also gives an overview of the thesis.

Chapter 2 Literature Review

This chapter provides a brief introduction of pre-breakdown and breakdown phenomena in liquids under impulse voltage and summarizes the most recent research findings on ester liquids, as well as compared with mineral oil.

Chapter 3 Experimental Description

This chapter first introduces the liquids under test and the preparation procedures for liquid and solid samples. Then detailed descriptions of test setups, together with verification tests, are provided for quasi-uniform field and non-uniform field tests respectively.

Chapter 4 Breakdown Strength of Ester Liquids in Quasi-uniform Field

This chapter reports the lightning and switching impulse breakdown strengths of ester liquids in a quasi-uniform field under negative polarity. Various testing methods including rising-voltage method, up-and-down method and multiple-level method are investigated for determining the lightning breakdown voltage. Based on the large amount of data, lightning withstand voltages of ester liquids are deduced and also compared with other data in the literatures.

Chapter 5 Streamer and Breakdown of Ester Liquids in Non-uniform Field

This chapter describes the characteristics of streamer and breakdown of ester liquids in a strongly non-uniform point-plane field under the standard lightning impulse voltage. Streamer length, velocity, shape and mode are analyzed under both positive and negative polarities. A relationship between the results under lightning impulse and

previously published results under step voltage is built up and empirical formulas are obtained to predict the lightning breakdown voltage of ester liquids at very large gaps.

Chapter 6 Influence of Pressboard on Streamer and Breakdown of Ester Liquids in Non-uniform Field

This chapter investigates the influence of pressboard (in parallel direction to the electric field) on the streamer and breakdown of ester liquids in a strongly non-uniform point-plane field under the standard lightning impulse voltage. Current and light signals together with streamer images are used to characterize the streamer propagation on liquid/solid interface. In addition, breakdown voltage and acceleration voltage of ester liquids with and without the presence of pressboard interface are compared at various gap distances.

Chapter 7 Secondary Reverse Streamer of Ester Liquids in Non-uniform Field

This chapter depicts a secondary reserve streamer (SRS) in ester liquids which occurs subsequently and well after the extinction of the primary streamer (PS) propagation within a single shot of impulse voltage and has the reverse polarity to the PS. Characteristics of SRS including stopping length, average velocity and time of occurrence are obtained at various gap distances from 25 mm to 100 mm. In addition, the formation mechanisms of SRS under both positive and negative impulse voltages are discussed and verification tests under tail-chopped impulse voltages are provided.

Chapter 8 Conclusions and Future Work

This chapter summaries the main conclusions of this thesis and provides the suggestions for future work which is required to further understand the behaviour of ester or general liquids under impulse voltage.

CHAPTER 2. LITERATURE REVIEW

2.1 Introduction

Insulating liquids have been widely used in high-voltage power equipment, e.g. transformers and cables for many decades. Breakdown strength is one of the essential properties of insulating liquids. To understand the breakdown mechanism in liquids, pre-breakdown phenomenon has been intensively studied. The discharge event leading to a failure in liquids is generally called streamer, of which the characteristics including length, velocity, shape, current and light signals were thoroughly investigated in a strongly non-uniform field under impulse voltage in the past decades [24-32]. It was found that those streamer characteristics are influenced by various testing conditions e.g. voltage polarity [33, 34], gap distance [35, 36], electrode geometry [37, 38] and hydrostatic pressure [39-41]. In addition, molecular structure of liquids and some additives have a great influence on the streamer propagation [42-44]. A number of review papers [24, 30, 45, 46] and books [47, 48] have summarized the streamer phenomena in liquids, however a universally agreed conclusion has not yet been achieved.

With the fast progress of electrical and optical technologies, the facilities used in the pre-breakdown and breakdown study of liquids have been well developed. Point-plane electrode configuration with impulse voltage and fast photographing setup have remained the most widely used techniques [49]. Voltage, current, charge and light signals are generally monitored during the streamer initiation and propagation. In addition, emission spectrometry [50] and chromatographic technique [51] have been used to understand the nature of a streamer. For the mechanism study, tests were usually carried out in a pure hydrocarbon liquid, e.g. n-hexane or benzene. For the engineering practise, tests were normally done in a commercial insulating liquid, e.g. transformer mineral oil.

This chapter first introduces the fundamental concepts of pre-breakdown and breakdown phenomena in liquids and then summarizes the most recent research findings on ester liquids under impulse voltage.

2.2 Pre-breakdown and Breakdown Phenomena in Liquids

2.2.1 General Breakdown Phenomenon in Liquids

A breakdown event in liquids generally involves two processes including initiation and propagation of a streamer. If the streamer stops before reaching the opposite electrode, the phenomenon might be called partial discharge. Breakdown mechanism is closely related to the electric field in the electrode geometry. Field enhancement factor (inhomogeneity factor or non-uniform field factor) f is commonly used to describe the degree of non-uniformity of a field configuration [52, 53],

$$f = \frac{E_{\max}}{E_{average}} \tag{2-1}$$

where E_{max} stands for the maximum field in the configuration which can be calculated by using empirical formulas or computational simulation;

$E_{average}$ stands for the average field in the configuration i.e. applied voltage divided by the gap distance.

The higher the field enhancement factor, the higher degree of non-uniformity a field configuration has. As for uniform fields with small enhancement factor e.g. at a short plane-plane gap, the breakdown is dominated by streamer initiation; and for non-uniform fields with large enhancement factor e.g. at a long point-plane gap, the breakdown is dominated by streamer propagation.

The underlying mechanism of breakdown in liquids remains still unclear, there are in fact numerous speculations existing. Experimental results vary largely upon the test setups and conditions, so they have normally to be interpreted by either one or some of the speculations. Broadly speaking, it is difficult to produce a unified theory which is able to explain all or at least the majority of experimental results. Overall there have been two main streams of theory competing with each other: (1) the electronic ionization model; (2) the so called gaseous ‘bubble theory’. [24, 40, 46]

Early studies of electrical breakdown in gases showed that breakdown is due to the electron avalanches caused by the continuous collision ionization. Similar concepts with some modifications were introduced to explain the breakdown phenomenon in liquids i.e. the electronic ionization model [47]. Influence of electron scavenger and low ionization potential additives on the streamer propagation supports that an electronic process is present. For example Devins proposed a two-step model for negative streamers: electrons injecting into the liquid are first trapped to form a concentration of negative ions; the ionic space charges build up an electric field till reaching a critical value at which the ionization occurs in the liquid. This process repeats itself as electrons are readily supplied by the trailing plasma channel [42].

In the gaseous bubble theory, a streamer initiates from local micro bubbles which could be either the natural existence due to the impurity of the liquid or formed by the vaporization of liquid due to the charge injection induced heating process [24]. The nature of streamer channels is believed as gaseous phase which is confirmed by the optical observation and the chromatographic analysis. The phase transition from liquid to gas, however, can be induced by very high local fields at the channel's extremity (some MV/cm), which is able to induce an intense and localised energy dissipation via charge injection and or multiplication. Due to the charge injection at the filament tip, a fast intense and localized injection of thermal energy occurs. This brings the liquid into supercritical state and a shockwave is radiated. Also a vapour phase instantaneously develops, and afterwards expands while its pressure and temperature decrease. Thus the filament tip acts as a moving point source of heat of about 10 W in power, and the streamer channel is formed by the expanding vapour track left behind [35]. This theory is supported by a large number of pressure effect experiments, in which both initiation and propagation are influenced by the applied hydrostatic pressure [28, 39-41].

With more and more experience accumulated, one tends to accept a harmonious voice that both gaseous and electronic processes are responsible for the breakdown in liquids and the dispute seems changing to which is dominant at the different stages of a streamer. In addition, most of the discussions on breakdown mechanism focus on the relatively slow streamers (1^{st} and 2^{nd} modes) at below breakdown voltage rather than the fast events (3^{rd} and 4^{th} modes) at overstressed voltages, so there is little knowledge about the nature of fast events. Instead of discussing the detailed mechanism, the

following contents will mainly review the macro characteristics of streamers in liquids from an engineering point of view.

2.2.2 Streamer Initiation in Liquids

2.2.2.1 Influence of tip radius

No matter what kind of mechanism is involved, local electric field is of importance for the initiation of a streamer. In a non-uniform point-plane field, the maximum electric field mainly depends on the tip radius rather than the gap distance. Figure 2-1 shows the inception voltages of positive and negative streamers in a mineral oil using various tip radii [37]. Tests with tip radii from 1 μm to 200 μm were carried out at the gap distance of 6 mm under rectangular high-voltage pulses with rise time of ~20 ns while tests with rod radii from 0.5 mm to 20 mm were conducted at the gap distances of 20 mm and 50 mm under 0.4/1400 μs step impulse voltage.

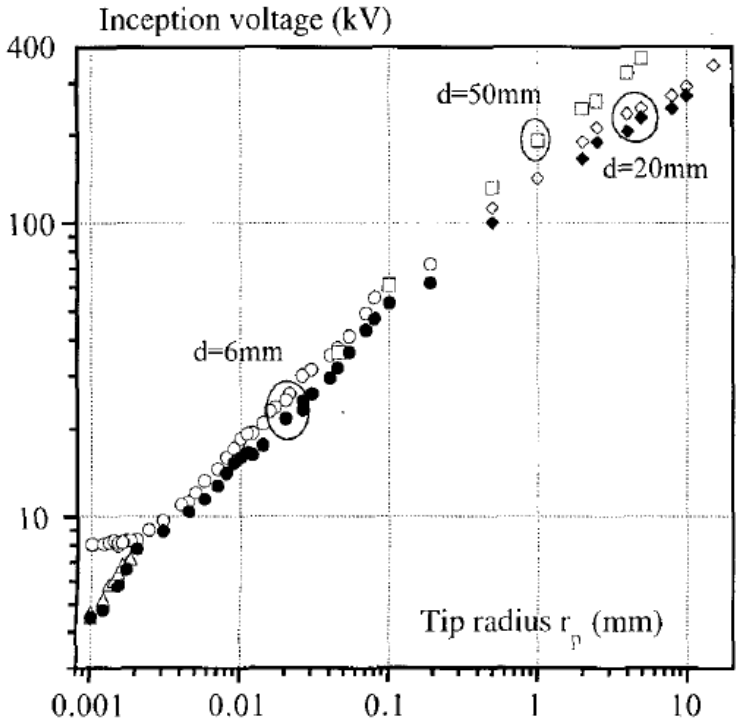

Figure 2-1 Inception voltage of positive streamers (open symbols) and negative streamers (solid symbols) versus tip radius in mineral oil; d=6 mm for tip radii from 1 μm to 200 μm, d=20 mm and 50 mm for rod radii from 0.5 mm to 20 mm [37].

It was observed that inception voltages of both positive and negative streamers increase with the tip radius. It was also noted that there are a few μs time delay for the streamer initiation at large tip radii e.g. 0.5 mm and 2.5 mm [37]. Slight polarity effect exists i.e. inception voltage of negative streamer is slightly lower than that of positive streamer.

The theory of space charge induced field distortion used in the gas discharge might be borrowed for liquids to explain the observed polarity effect. For positive polarity, after ionization occurs in the near tip region, electrons move quickly into the positive point electrode while positive ions move slowly towards the negative plane electrode. Therefore, positive space charges accumulated ahead of the positive tip weaken the near tip field and thus suppress an effective streamer initiation. For negative polarity, after ionization occurs in the near tip region, the positive ions move back slowly towards the negative point electrode while electrons dissipate away quickly into the liquids probably forming negative ions. Therefore, positive space charges accumulated ahead of the negative tip enhance the near tip field and further decrease the inception voltage.

With the increase of tip radius being reflected by effective electrode area, the inception voltage is increasing, but the inception field, calculated based on the inception voltage and electrode geometry, actually is reducing as shown in Figure 2-2 under positive polarity [37]. This probably can be explained by the area effect that large surface area of electrode increases the probability of defects on the electrode and in the locally stressed liquids. It was noted that the decreasing trend of electric field with electrode area fits well with the breakdown tests at large area uniform electrode configuration.

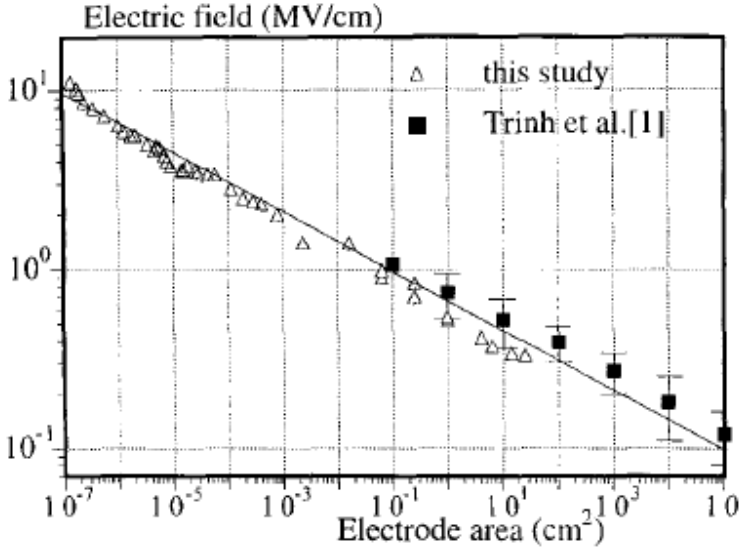

Figure 2-2 Inception field of positive streamers versus electrode area in mineral oil; solid symbols stand for breakdown tests at large area uniform electrode configuration [37].

2.2.2.2 Influence of field geometry

Semi-uniform field was used in the initiation study trying to bridge the knowledge gap between uniform plane-plane field and non-uniform point-plane field. Inception

voltages of positive and negative streamers in a semi-uniform field were studied in a mineral oil, as shown in Figure 2-3 [54]. The semi-uniform field was achieved by placing an adjustable point tip at the centre of one of the two plane electrodes (diameter of 45 mm) through a 0.2 mm diameter hole. The point tip was a tungsten wire with diameter of 100 μm. Tests were carried out under rectangular high-voltage pulses with rise time of ~20 ns.

As similar to the point-plane gaps, only slow streamer (1st mode) was observed under negative polarity and both filamentary (2nd mode) and slow (1st mode) streamers were observed under positive polarity [54]. It was found that streamer inception voltages under semi-uniform field are higher than that at normal point-plane gaps, due to the electrostatic influence of the plane electrode behind the triggering tip. When the point length increases, the inception voltages of both negative and positive streamers decrease rapidly. Overall if the point tip increases to a critical long length, the results resemble those at the point-plane gaps, if the point tip decreases to an extremely short length, the results represent those at the plane-plane gaps.

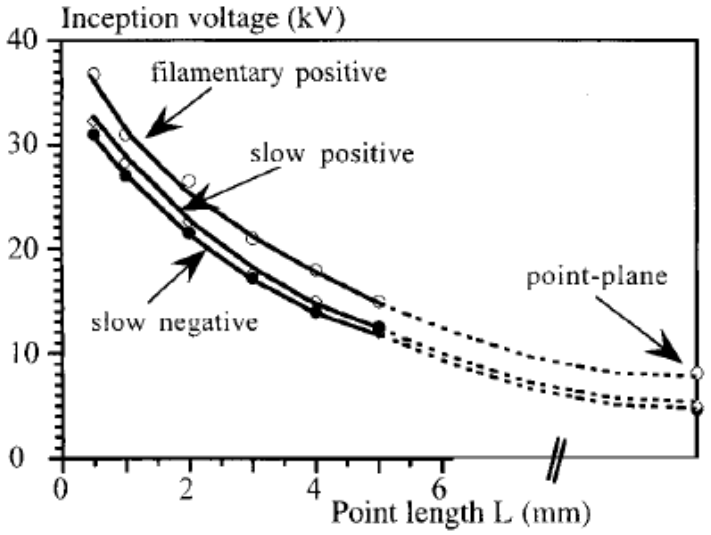

Figure 2-3 Streamer inception voltage of mineral oil in semi-uniform field; tip radius 1 μm, d=6 mm [54].

The above mentioned results were extrapolated to extremely small point length to simulate the electrode surface protrusion or defect using a charge simulation method (CSM) [54]. The mean inception field E_0 was obtained using the applied voltage divided by the gap distance. As shown in Figure 2-4, mean inception field reduces with the increase of point length and the decrease of tip radius [54]. It should be stressed that

mean inception field could drop to below 10 kV/mm when either long (1 mm length, 20 μm radius) or thin (0.3 mm length, 1 μm radius) metallic protrusion exists on the electrode surface.

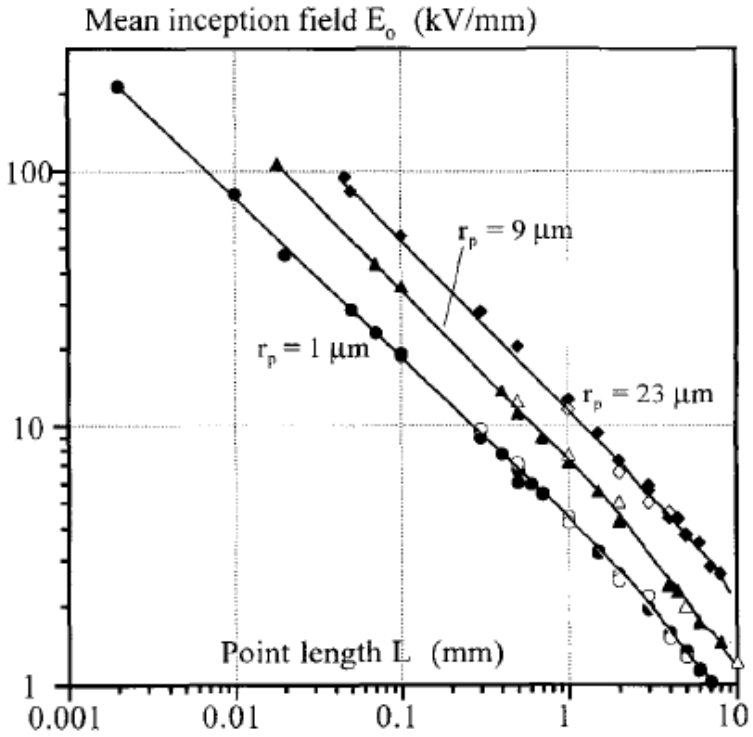

Figure 2-4 Mean inception field of streamer in mineral oil in semi-uniform field; open symbols represent experimental results and solid symbols represent calculation results [54].

2.2.3 Streamer Propagation in Liquids

2.2.3.1 Basic characteristic

When a streamer propagates in a liquid, several methods including measuring current, light signals and photography images are commonly used to describe its characteristic. Figure 2-5 shows an example of typical recordings for a positive streamer in mineral oil at the gap distance of 200 mm under 0.4/1400 μs step impulse voltage [35, 55]. Streak image (Figure 2-5 A) records the time-resolved trace of light emission during the streamer propagation. Besides streak image, other photography techniques like shadowgraph and integral light image (also called still image) are used to capture the streamer shape feature [55]. Corresponding to the photography image, a trace of transient current and light signals are usually observed (Figure 2-5 B). The intensity and occurrence time of current pulses normally correlate to those of light signals [35, 55].

The shape of current signal varies significantly with the testing conditions e.g. voltage polarity and voltage level [27, 33, 35, 36, 42, 45, 56]. However in most of the cases, a train of discrete pulses can be observed either with or without a continuous DC component. It was summarized in [45] that for small gaps (roughly smaller than 50 mm), a continuous component usually exists for positive streamers; for large gaps (roughly larger than 50 mm), both positive and negative streamer currents tend to consist of irregularly spaced discrete pulses and a notable continuous component might be only observed when fast event occurs at high-voltage levels under both polarities [29, 35].

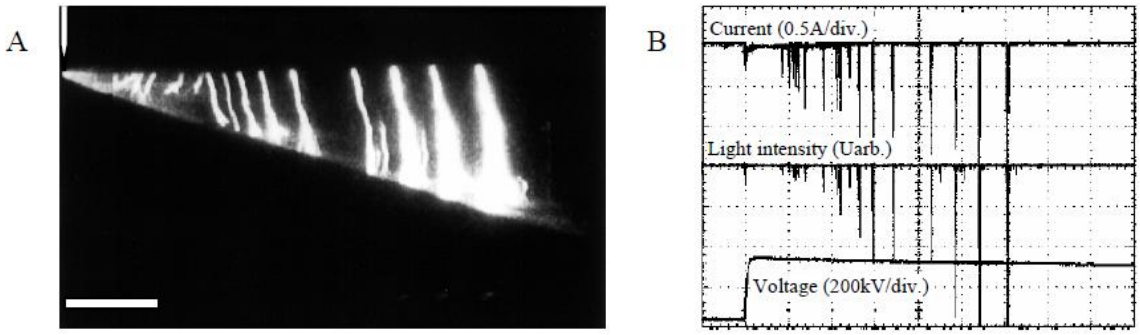

Figure 2-5 Typical recordings of a streamer propagation in mineral oil under positive polarity; A streak image, B current, light and voltage recordings; tip radius 100 μm, d=200 mm, V=256 kV [55].

Below breakdown voltage, the streamer would normally stop after propagating for a certain distance. Accordingly the propagating length, i.e. the straight-line distance from the farthest tip point of a streamer to the point electrode, can be measured from the streamer images. The final length is usually called stopping length, which is one of the most useful parameters to characterize a streamer.

Figure 2-6 shows a comparison of stopping lengths between positive and negative streamers in a mineral oil at a 100 mm point-plane gap under 0.4/1400 μs step impulse voltage [33]. It was found that the stopping length of a streamer increases on average with the applied voltage till reaching the breakdown voltage V_b. There was an obvious polarity effect that negative streamer is much shorter than positive streamer at the same voltage. The theory of space charge induced field distortion is used again to explain the polarity effect. For positive polarity, after ionization occurs in the near tip region, electrons move quickly into the positive point electrode while positive ions move slowly towards the negative plane electrode. Therefore, the concentration of positive charges, like an extension of the positive tip, enhances the boundary field at the head of charge cloud. The enhanced field further facilitates the streamer propagation and then decreases the positive breakdown voltage. For negative polarity, after ionization occurs

in the near tip region, the positive ions move back slowly towards the negative point electrode while electrons dissipate away quickly into the surrounding liquid probably forming negative ions. Therefore the diluted negative space charges, like a shielding of the negative tip, weaken the boundary field, which slows down the streamer propagation and then increases the negative breakdown voltage.

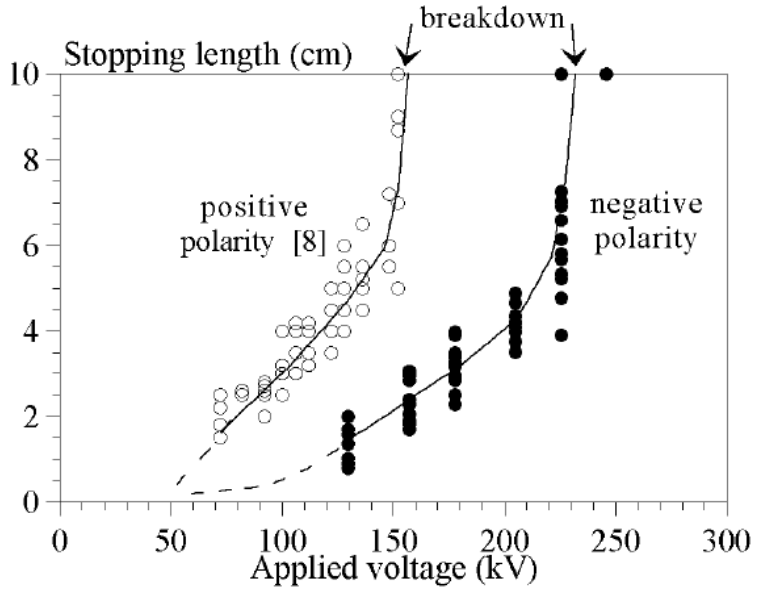

Figure 2-6 Streamer stopping length versus applied voltage in mineral oil under both polarities; tip radius 100 μm, d=100 mm [33].

By knowing the stopping length and propagating time (generally obtained from the current and light signals), average velocity of streamer propagation can be deduced, which is another important parameter to describe a streamer. Unless stated otherwise, the streamer velocity in this thesis means the average velocity of a streamer.

Figure 2-7 shows a comparison of average velocities between positive and negative streamers in a mineral oil at the same 100 mm point-plane gap under 0.4/1400 μs step impulse voltage [33]. It was found that streamer velocity increases slightly at a large range of applied voltages, till reaching a voltage level, above which streamer velocity increases dramatically. This transition voltage is named acceleration voltage V_a, which indicates the ability of a liquid to withstand fast streamer (fast event). Similar to the stopping length, polarity effect exists that positive streamer is faster than negative streamer at the same voltage. The typical velocities responsible for point-plane breakdown in a mineral oil are 2 km/s under positive polarity and 1 km/s under negative polarity.

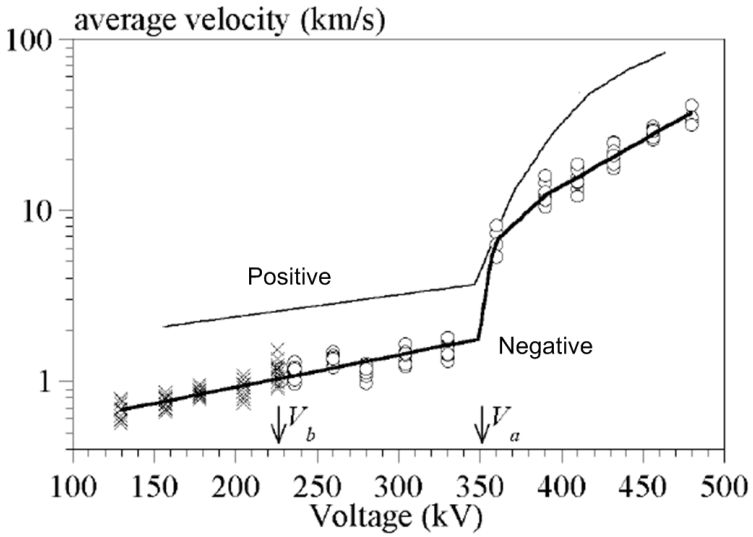

Figure 2-7 Streamer average velocity versus applied voltage in mineral oil under both polarities; tip radius 100 μm, d=100 mm [33].

2.2.3.2 Propagation mode

Characteristics of streamer propagation have been comprehensively investigated for many decades, during which many adjectives were used to describe streamer mode, such as "fast" and "slow", "primary" and "secondary", "subsonic" and "supersonic". The meaning of those terms varies according to the authors which might lead to a confusing situation for comparison among literatures. A velocity-based classification, proposed by Hebner [57] and then developed by Lesaint [35], is a much clearer description and becomes popularly used, in which the streamer propagations are separated into 1st, 2nd, 3rd and 4th modes as given in Table 2-1. This classification is mainly based on the experience of positive streamers.

Table 2-1 Typical velocity of various streamer modes in mineral oil [55].

Streamer mode	1st mode	2nd mode	3rd mode	4th mode
Propagation velocity (km/s)	0.1	1-2	10	100

Figure 2-8 and Figure 2-9 show the evolution of streamer mode associated with the applied voltage in a mineral oil under positive 0.4/1400 μs step impulse voltage [35, 55]. The 1st mode streamer concerns slow streamers propagating at velocity of ~0.1 km/s. In mineral oil this mode is only observed at low voltages in short gaps with very thin tips (about a few μm) [58]. The 2nd mode streamer with the typical velocity of 1-2 km/s is recorded for a sufficiently wide range of applied voltage from well below V_b to about V_a. Its velocity is quasi-constant during the whole propagating process. When the voltage is increased, the propagation becomes to consist of two distinct phases. The fast phase with velocity of 10-50 km/s that lasts for a few μs and the slow phase analogous to the

2nd mode with velocity of 1-2 km/s are clearly seen in the streak photographs, the schematic transition process is shown in Figure 2-9 [35]. The fast phase is called the 3rd mode streamer. As the voltage is further increased above acceleration voltage V_a, streak images show that the streamer starts as a 3rd mode streamer and then switches to a much faster and very different phase that quickly bridges the remaining gap. This very fast phase is classified as the 4th mode usually with velocity higher than 100 km/s [29, 35].

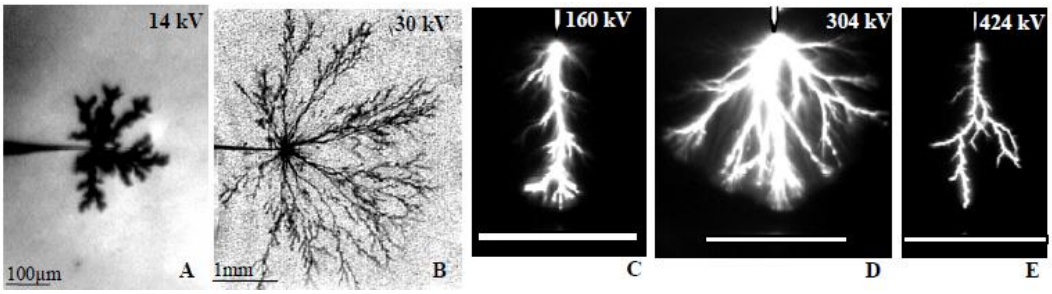

Figure 2-8 Typical images of positive streamer at various modes in mineral oil; A, B for 1st mode, C for 2nd mode, D for 3rd mode and E for 4th mode [55].

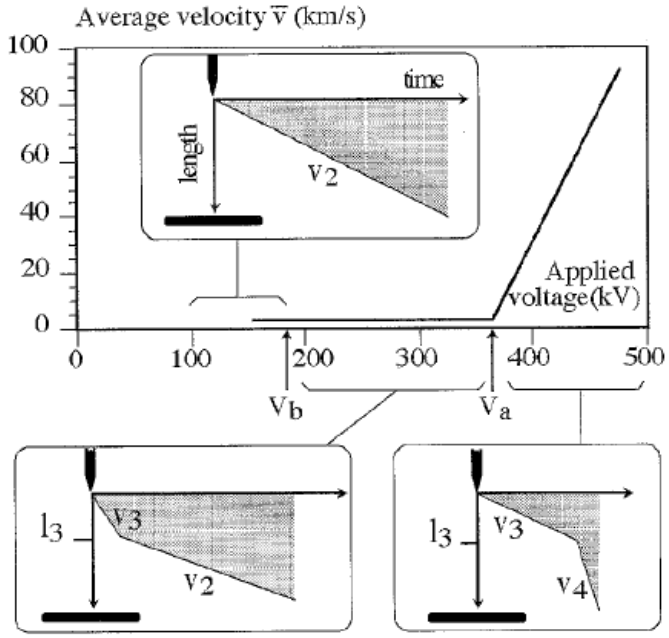

Figure 2-9 Schematic diagram of streak photographs showing streamer mode transition; V2, V3 and V4 stand for 2nd, 3rd and 4th modes respectively [35].

2.2.3.3 Breakdown voltage and acceleration voltage

Figure 2-10 shows the 50% breakdown voltage V_b and acceleration voltage V_a of a mineral oil in a non-uniform point-plane field at various gap distances under 0.4/1400 μs step impulse voltage [33]. Generally breakdown voltage and acceleration voltage increase with the gap distance under both positive and negative polarities. V_a could be as high as double of V_b in most of the cases.

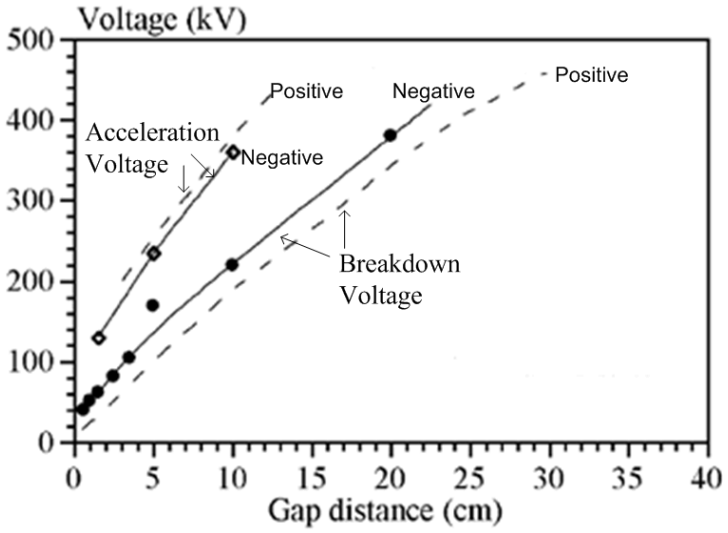

Figure 2-10 Breakdown voltage and acceleration voltage of mineral oil at various gap distances under both polarities; tip radius 100 μm [33].

It was also predicted in [35] that fast streamers (3rd and 4th modes) are likely responsible for lightning breakdown at large gaps, since measured acceleration voltages at small gaps under step impulse (0.4/1400 μs) match well the breakdown voltages at large gaps under lightning impulse (1/40 μs) as shown in Figure 2-11. Similarly, slow streamers (2nd mode) tend to account for the breakdown at large gaps under switching impulse (600/3600 μs). To sum up, the acceleration voltage, which shows the ability to withstand fast streamers, could be an important parameter as supplement of the traditional 50% breakdown voltage to indicate electrical strength of a liquid.

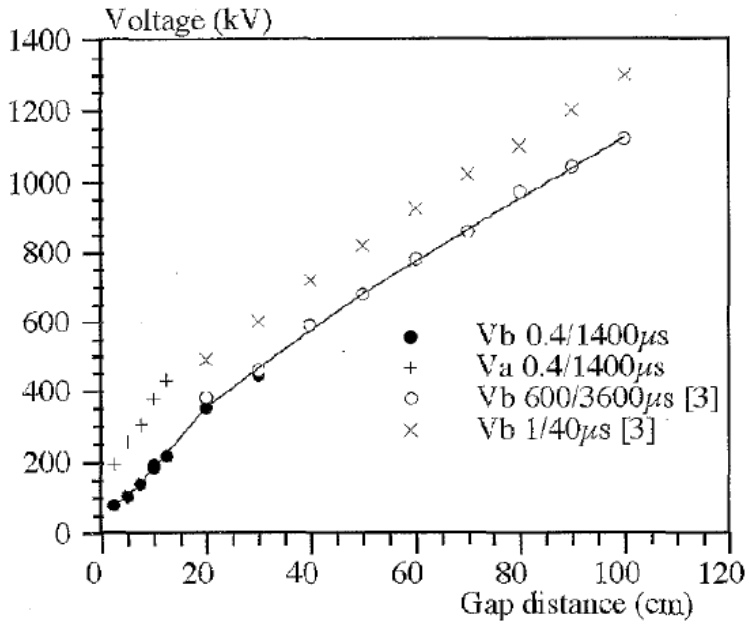

Figure 2-11 Comparison of breakdown voltage and acceleration voltage with 'lightning' (1/40 μs) and 'switching' (600/3600 μs) breakdown voltages at large gaps [35].

2.2.4 Influence of Liquid Composition

It has been acknowledged that liquid composition has a great influence on the liquid's pre-breakdown and breakdown performances under impulse voltage. Initially, aromatic content especially polyaromatic content was proved to be related to the lightning impulse breakdown voltage of mineral oil. As the aromatic content in particular the presence of polyaromatic molecules increases, the negative lightning impulse breakdown voltage in a divergent field decreases. In addition, it was found that aromatic content is related to the gassing tendency. Overall the lower the aromatic content, the higher positive gassing tendency and higher negative impulse strength a mineral oil will possess, as shown in Table 2-2 [59]. The polyaromatic content seems to affect the impulse breakdown voltage more than aromatic content. This phenomenon was observed in various types of mineral oil [60].

Table 2-2 Influence of aromatic content on gassing tendency and negative lightning impulse breakdown voltage of mineral oil [59].

Polyaromatic content BS 2000-346 (%W)	Aromatic content IEC 60590 (%)	Negative impulse breakdown voltage ASTM D 3300 (kV)	Gassing tendency (μL/minute)
0.02	5	>300	+33
0.03	7	282	+26
0.11	10	220	+16
0.48	10	196	+11
1.20	10	148	+4

Influence of aromatic additives on the streamer growth was examined in [42], of which the results indicated that the decrease of impulse strength is indeed due to the increase of streamer velocity. Adding 2-methyl naphthalene, a typical diaromatic constituent of transformer oil, could notably accelerate both the positive and negative streamers, even at very low concentrations. Therefore it was considered that the aromatic compounds (or polyaromatic) could have two electronic properties: low ionization potentials (electron-releasing) and large electron-trapping cross sections (electron-attaching). By adding different additives with only one of the above properties, it was clarified that electron-attaching function influences negative streamer as confirmed in [27, 42] and electron-releasing function works for positive streamer as confirmed in [42, 61].

A detailed study on the additive effect was reported in a series of publications [43, 44, 62], in which 15 additives were examined to see the influence on streamer initiation and propagation. Tests were carried out in a 10 mm point-plane gap under high-voltage

rectangular pulses with rise time of 15-20 ns. The tip radius of point electrode was in the range of 1.3-1.5 μm. Streamer charge was measured using a sensitive differential technique and a sudden increase of the recorded charge was used to indicate the initiation of a streamer. The probability for streamer initiation versus voltage was based on 60 to 100 tests at each voltage level around onset. However it was stated that it is difficult to assess additive effect on the initiation voltage by comparing inception voltage from one experiment to another since the initiation probabilities vary with time and the streamer initiations are not independent of each other with the delay interval of three minutes between two consecutive shots.

Under positive polarity, conclusive influence of additive concentrations on initiation voltage was only observed for tetramethyl-p-phenylenediamine (TMPD) and tetrakis-dimethylamino-ethylene (TDAE) solutions [62]. Generally additives that are ionized more easily than the base liquid could accelerate positive streamer propagation. As shown in Figure 2-12, both streamer length and average streamer velocity increase with the concentration of additive N.N-dimethylaniline (DMA) [44]. It was also found that the transition voltage from the slow (1^{st}) to the faster (2^{nd}) mode of propagation decreases by increasing concentrations and decreasing ionization potentials of the electron-releasing additives. Overall for positive streamer, the results supported that impact ionization takes place in the liquid phase outside the gaseous phase of streamer channel [62].

Under negative polarity, effects of additives on streamer initiation were not observed [43], but those electro-attaching additives could facilitate the negative streamer propagation. As shown in Figure 2-13, both streamer length and average streamer velocity increase with the concentration of additive perfluoro-n-hexane [44]. For negative streamers, it was proposed that injection of thermal electrons from a gaseous phase is dominant for the streamer mechanism [44].

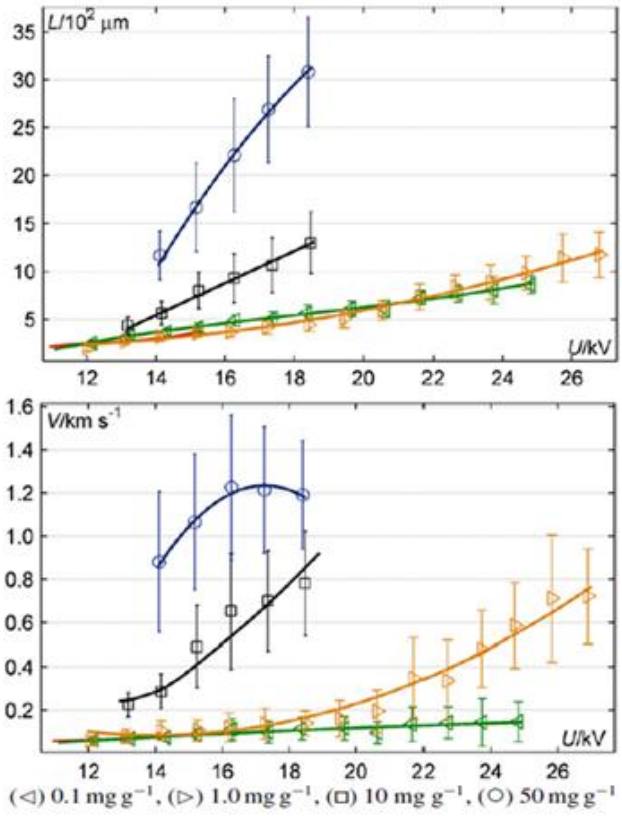

Figure 2-12 Stopping length and average velocity of positive streamers in cyclohexane with additive N.N-dimethylaniline (DMA); tip radius 1.3-1.5 µm [44].

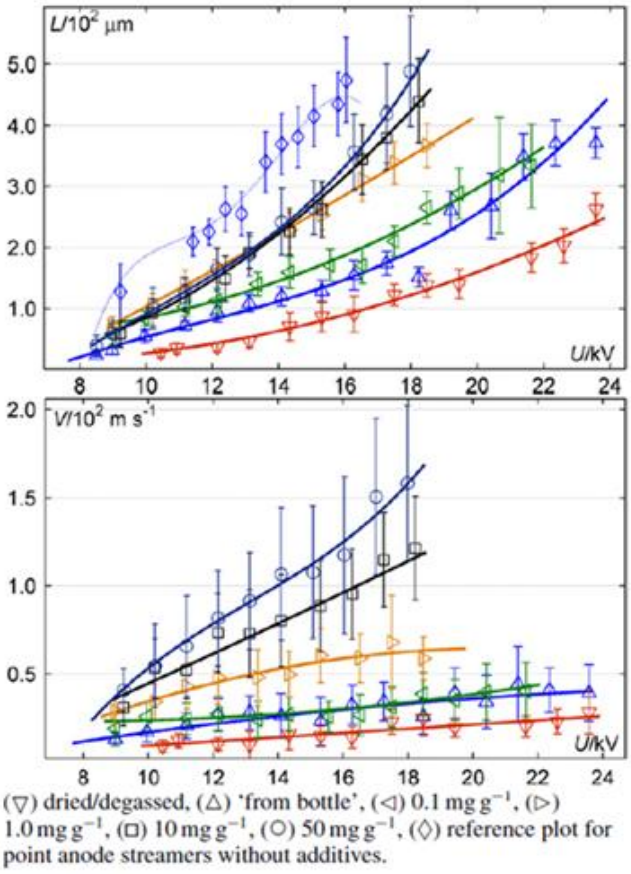

Figure 2-13 Stopping length and average velocity of negative streamers in cyclohexane with additive perfluoro-n-hexane; tip radius 1.3-1.5 µm [44].

Influences of additive pyrene (with low ionization potential) on the streamer propagation and breakdown in cyclohexane were studied at a gap distance of 50 mm under positive 0.4/1400 μs step impulse voltage [63]. Same as the previous description, the positive streamer propagation was promoted by adding electron-releasing additive and thus breakdown voltage V_b was reduced accordingly, as shown in Figure 2-14. However it was surprising that acceleration voltage V_a was inversely increased by adding the pyrene additive. It was observed that with pyrene additive, propagation of streamer becomes easier and more branches are formed; however when the density of branches increases at overstressed voltage, the branches tend to shield each other and this process produces a self-regulation of the tip field and velocity, and thus leads to the increase of acceleration voltage [63].

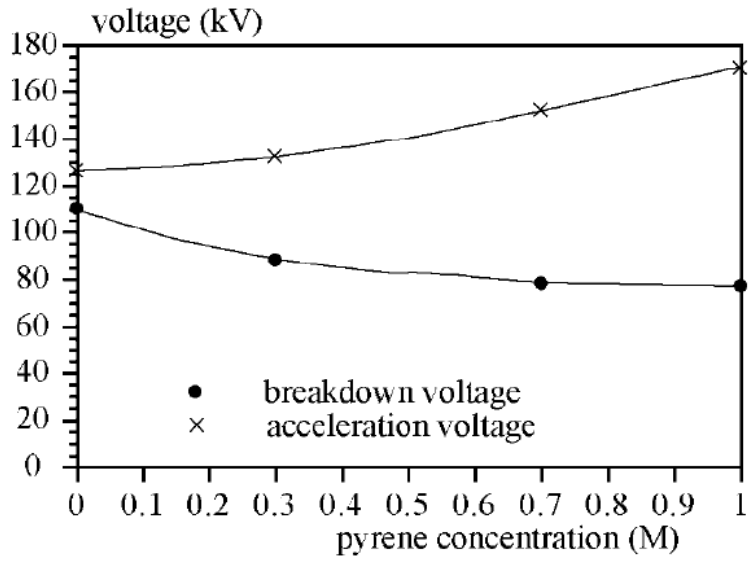

Figure 2-14 Breakdown voltage and acceleration voltage of cyclohexane with additive pyrene; tip radius 40 μm, d=50 mm [63].

2.2.5 Influence of Solid Interface

As liquid/solid composite insulation is widely used in power transformers as well as in other power equipment, it is of importance to know the integral electrical performance of liquid/solid insulation. When a streamer propagates along an oil/pressboard interface, it is also called 'creepage discharge', and creepage discharge is attributed to one of the failure modes for large power transformers [64]. In the field of creepage discharge study, two types of arrangement were usually used: solid interface in parallel direction to the electric field [65-67] and solid interface in perpendicular direction to the electric field [65, 68-74], as shown in Figure 2-15 [65].

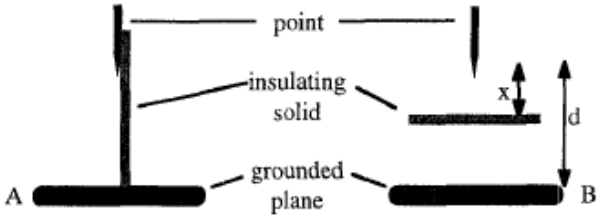

Figure 2-15 Arrangement of solid interface in a non-uniform field; A in parallel direction to the electric field, B in perpendicular direction to the electric field [65].

2.2.5.1 In parallel direction to the electric field

Influence of pressboard on the breakdown voltage and streamer velocity in mineral oil was investigated under positive 0.4/1400 μs step impulse voltage [65]. The tip radius of the point electrode was 100 μm and the diameter of the plane electrode was 200 mm. Pressboard with 2 mm thickness was placed in parallel to the point-plane axis. The results indicated that introducing the pressboard surface does not influence the breakdown voltage as shown in Figure 2-16 [65]. It was also observed that streamers are always propagating along the liquid/solid interface. At overstressed voltages, it was found that presence of pressboard obviously promotes the streamer velocity and thus leads to a large reduction of acceleration voltage, as shown in Figure 2-17 [65].

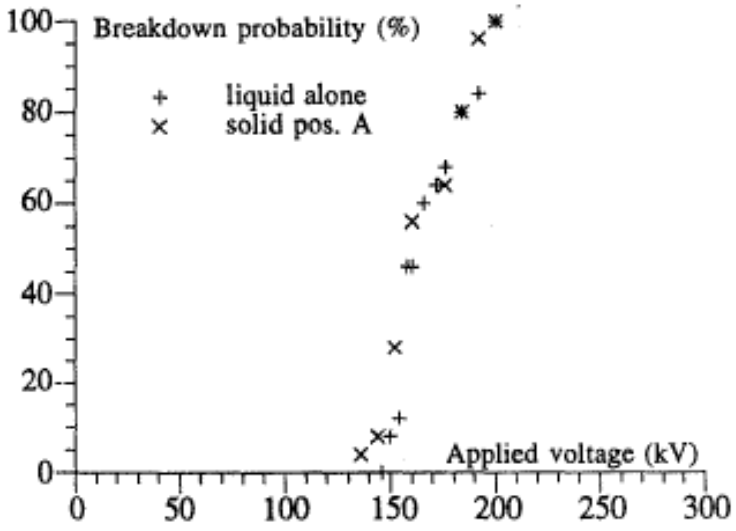

Figure 2-16 Influence of pressboard (parallel) on breakdown voltage under positive polarity; tip radius 100 μm, d=100 mm [65].

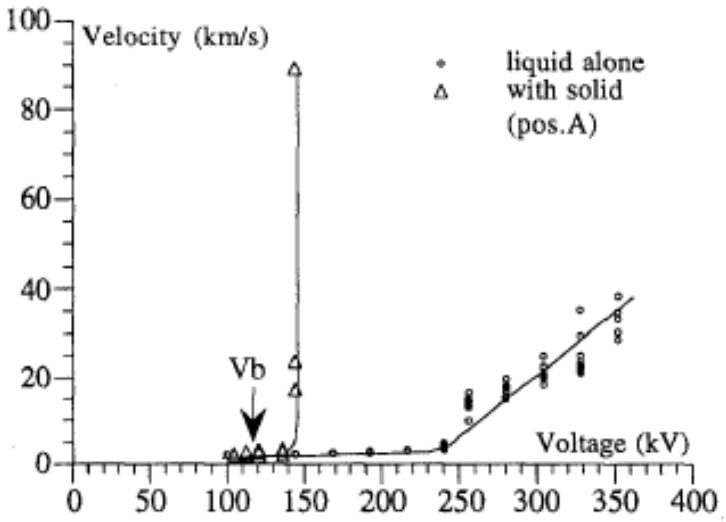

Figure 2-17 Influence of pressboard (parallel) on streamer velocity under positive polarity; tip radius 100 μm, d=50 mm [65].

Another study [66] carried out in a mineral oil at a 150 mm gap using 190 μm tips under positive 1/190 μs impulse, depicted similar results that pressboard does not change the breakdown voltage but reduces the acceleration voltage. In addition, it was observed that slow streamer (<4 km/s) tends to leave a weak darkening on the pressboard surface while fast streamer (fast event) tends to leave a burnt track with branches on the pressboard surface, as shown in Figure 2-18. The easier formation of fast events with a pressboard surface in parallel might be due to the removal of half of the spherical streamer geometry which results in a more inhomogeneous field close to the pressboard surface [65, 66].

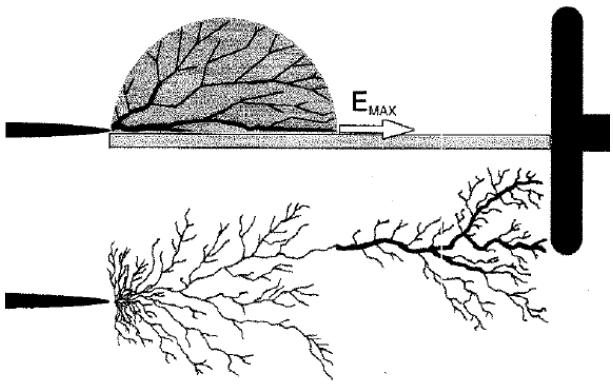

Figure 2-18 Illustration of streamer propagation on pressboard interface under positive polarity [66].

2.2.5.2 In perpendicular direction to the electric field

When the pressboard is placed in the perpendicular direction to the electric field, the phenomenon is also called barrier effect. Paper [65] investigated the barrier effect at the

gap distance of 100 mm under positive 0.4/1400 μs step impulse voltage. The diameter of pressboard barrier was 150 mm. It was found that presence of pressboard barrier significantly increases the breakdown voltage, especially when the barrier is close to the tip electrode as shown in Figure 2-19.

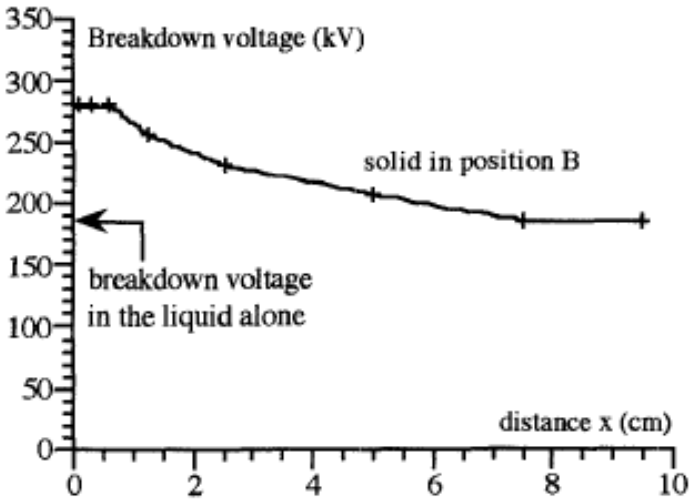

Figure 2-19 Influence of pressboard disk (perpendicular) on breakdown voltage under positive polarity; d=100 mm; x stands for the distance between the point electrode and the pressboard barrier [65].

Research on barrier effect in a mineral oil under both positive and negative lightning impulse voltages (1.2/50 μs) was reported in [68]. Similar conclusion was made that introduction of pressboard barrier obviously increases the breakdown voltage under both polarities. Moreover the dimension of barriers was considered, of which the results showed that barrier with larger radius leads to higher breakdown voltage, as shown in Figure 2-20 [68].

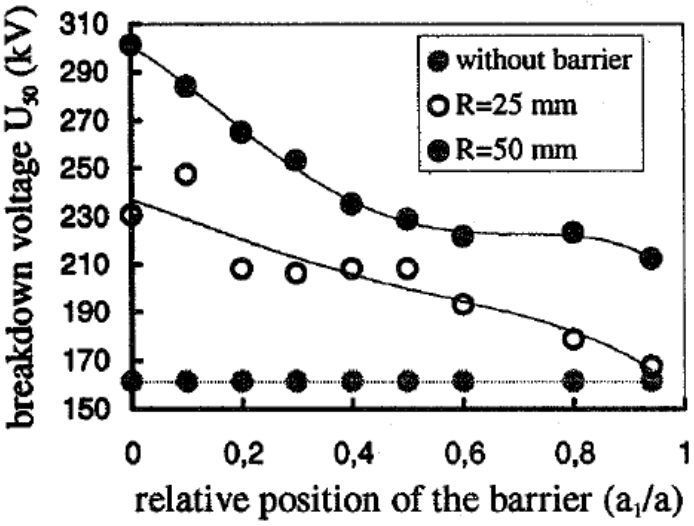

Figure 2-20 Influence of pressboard disk with different radii (perpendicular) on breakdown voltage under negative polarity; a=50 mm, which stands for the gap distance and a_1 stands for the distance between the point electrode and the pressboard barrier [68].

Effect of pressboard barrier to increase the breakdown strength is simply explained as due to the increase of equivalent discharge path between the high-voltage point electrode and the ground plane electrode. As shown in Figure 2-21, with the presence of pressboard barrier, the discharge path roughly equals to the sum of distance from the point electrode to the edge of the barrier and distance from the edge of the barrier to the plane electrode.

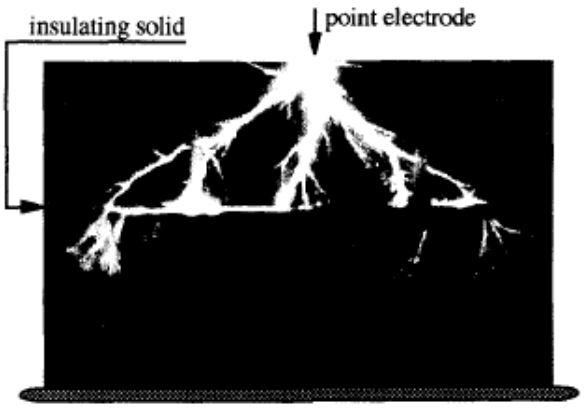

Figure 2-21 Streamer propagation getting around a pressboard barrier [65].

2.3 Research Findings Relevant to Ester Liquids

With growing interests in ester liquids as alternatives to mineral oil used in power transformers, an extensive work has been done by worldwide researchers to compare all the aspects of properties between mineral oils and ester liquids. This section only summarizes the research findings on ester liquids' performances under impulse voltage. Both natural ester and synthetic ester were considered in the literature search, however much more results were found on natural esters rather than on synthetic esters.

A transformer is usually composed of three-phase high-voltage windings, low voltage windings and probably tertiary windings. These windings can be made in the structures of disk or layer, of which each consists of many paper wrapped turn conductors.

The turn to turn insulation is made by multiple layer oil impregnated papers with a thickness of ~1-2 mm. Washers are used to separate the disk conductors and thus oil ducts are formed between the disks with a thickness of ~3-10 mm. The distance between windings is relatively large, which could be tens of mm. However to increase the insulation strength, the oil gap between the windings are usually divided into smaller

ducts by thick pressboard barriers. These insulations between turns, disks and windings are in a quasi-uniform electric field, which is experienced by the majority of insulation materials inside a transformer.

Some other special locations of a transformer may be more challenging for insulation design. At the corner part of end winding insulation, although with the contoured angle rings, there are still tangential electric fields existing on the pressboard surface, which could facilitate the creepage discharge when it happens and creepage discharge is one of the failure reasons for large power transformers. In addition, the bushing lead to grounded tank could form a long distance non-uniform field. Last but not least, manufacturing defects e.g. protrusion on the copper conductor and contaminations resulting from long term in-service degradation e.g. particle and moisture in the oil, could cause local electric field enhancement (non-uniform field) and thus might initiate a discharge. Insulations stressed in all these non-uniform fields are the weak link of a transformer, which requires careful attentions in the processes of design and manufacture.

To sum up, the insulation system of a transformer is stressed in the majority of quasi-uniform fields and somewhat exceptional non-uniform fields. Therefore the following reviews will be classified into two categories to show the impulse performances of ester liquids, i.e. in quasi-uniform fields and in non-uniform fields.

2.3.1 In Quasi-uniform Fields

As quasi-uniform fields resemble the most of the electric fields inside a transformer, impulse breakdown strength of ester liquids in those fields has been thoroughly investigated and compared with that of mineral oil [6, 52, 75-79]. Most of the tests used the standard lightning impulse 1.2/50 μs with either positive or negative polarity. The electrode configuration was usually designed to represent the practical applications in a transformer. The volume of tank used in the tests varied from a few hundred litres to over ten thousand litres, so such a test in quasi-uniform fields, especially for large gaps, was truly costly and time consuming. The following contents are organized in the way of with and without solid interface, and from small to large gap distances.

2.3.1.1 Tests in liquid gaps without solid interface

Positive lightning (1.2/50 μs) breakdown voltages of natural ester (rape-seed oil) at gap distances from 5 mm to 15 mm in a plane-plane field geometry were reported, as shown in Figure 2-22 [78]. The diameter of the plane electrode with Rogowski-profile was 100 mm. The volume of the test vessel was 150 litres. The breakdown voltage was taken as the average of 100 tests at each gap distance. The results indicated that natural ester has similar breakdown voltage to mineral oil.

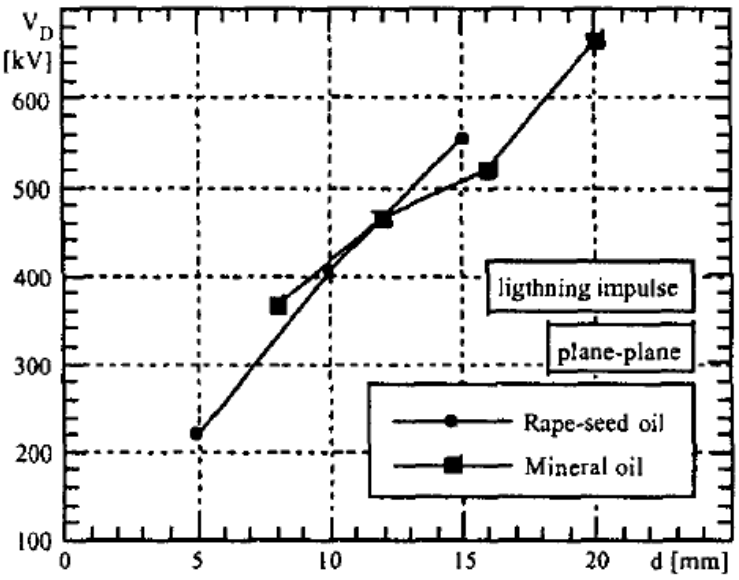

Figure 2-22 Positive lightning breakdown voltage of natural ester (rape-seed oil) and mineral oil in plane-plane geometry at various gap distances from 5 mm to15 mm [78].

Moving to larger gap distances, tests in quasi-uniform field become more difficult, since larger volume of sample and longer time for sample preparation are required. Fortunately an impressive work has been done in [75] which reported the lightning (1.2/50 μs) breakdown strength of natural ester (Envirotemp® FR3) in a quasi-uniform field at gap distances from 12 mm to 50 mm. The quasi-uniform field was achieved by using the symmetric pairs of electrodes, as shown in Figure 2-23. The electrode of both type 1 and type 2 was rectangular aluminium bar (3.05 mm×7.85 mm) covered by three layers of paper. The turn to turn paper thickness in total was 0.56 mm between the electrodes. The electrode dimensions were 381 mm long with 279 mm effective length of parallel facing electrode surface. Type 1 electrode configuration was used for 25 mm and 50 mm gap distance tests in a 2400 litres tank, while type 2 electrode configuration was mounted on a 3.2 mm thick pressboard and used for 12 mm gap distance test in a

210 litres tank. Breakdown tests were conducted by using rising-voltage method with three shots per step.

(a) Type 1 electrodes for 25 mm and 50 mm gaps (b) Type 2 electrodes for 12 mm gap

Figure 2-23 Electrode configurations for lightning impulse tests in quasi-uniform fields at gap distances from 12 mm to 50 mm [75].

The results obtained under negative lightning impulse are shown in Figure 2-24 [75]. As expected, the breakdown strength of liquids generally decreases with the increase of gap distance and volume of the liquid under stress. Importantly, the breakdown strength of natural ester is similar to that of mineral oil, both of which are higher than the Weidmann oil design line [18, 75, 80].

Sample handling procedure (e.g. whether the sample is exposed to the air environment and if yes whether the vacuum is required afterwards) during the processing and testing was emphasized by the authors as an important factor which might influence the test results.

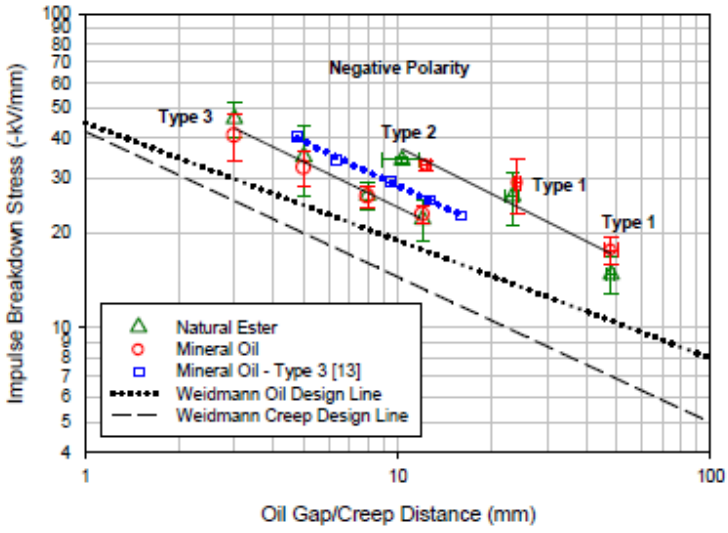

Figure 2-24 Negative lightning breakdown strength of natural ester and mineral oil in quasi-uniform field at various gap distances from 12 mm to 50 mm [75].

Tests under positive polarity showed the similar results to negative polarity, and both of which are summarized in Table 2-3. Overall the authors [75] concluded that the lightning breakdown strength of natural ester in a quasi-uniform field at gap distances from 12 mm to 50 mm is comparable to that of mineral oil. However it should be mentioned that 'comparable' here in fact indicates the lightning breakdown strength of natural ester is generally approximately 10% to 15% lower than that of mineral oil.

Table 2-3 Lightning breakdown strength of natural ester and mineral oil under both negative and positive polarities using type 1 and type 2 electrodes at various gap distances from 12 mm to 50 mm [75].

	Electrode	Type 2		Type 1		Type 1	
	Gap distance	12 mm		25 mm		50 mm	
	Liquid	Natural Ester	Mineral Oil	Natural Ester	Mineral Oil	Natural Ester	Mineral Oil
Positive	Average gap(mm)	11.3	12.0	24.5	24.0	50.4	48.7
	$U_{50\%}$ (kV)	388	387	630	690	722	856
	Std dev. (kV)	20.7	16.5	74.1	103	131	102
	Variance %	5.3	4.3	12	15	18	12
Negative	Average gap(mm)	10.3	12.3	23.3	24.1	48.1	48
	$U_{50\%}$ (kV)	352	404	611	695	712	846
	Std dev. (kV)	8.3	13.9	116	139	97.8	79.4
	Variance %	2.4	3.4	19	20	14	9.4

The most recent tests revealed the lightning (1.2/50 μs) impulse breakdown strength of natural ester (Envirotemp® FR3) at even larger gap distances from 50 mm to 150 mm using a specially designed bushing shield to plate electrode configuration as shown in Figure 2-25 [76]. The bushing shield electrode was machined from a stainless steel disc with final dimensions of 216 mm diameter × 38 mm thick and with edge radius of 4.3 mm. The diameter of steel plate electrode was 463 mm. Tests were carried out by using up-and-down method with applied impulses from 25 to 42 shots in an amazingly big tank with the volume of 12 500 litres.

(a) Top bushing shield disk electrode (b) bottom plate electrode

Figure 2-25 Electrode configuration for lightning impulse tests in slightly non-uniform field at gap distances from 50 mm to 150 mm [76].

The results of negative lightning tests including both 50% breakdown and 1% withstand voltages are given in Figure 2-26 and Table 2-4 [76]. It is surprising that the 50% breakdown strength of natural ester is almost the same as or even higher than that of mineral oil at those large gap distances from 50 mm to 150 mm. It is worth noting that the decreasing trend of 1% withstand strength with gap distance is in parallel to that of 50% breakdown strength.

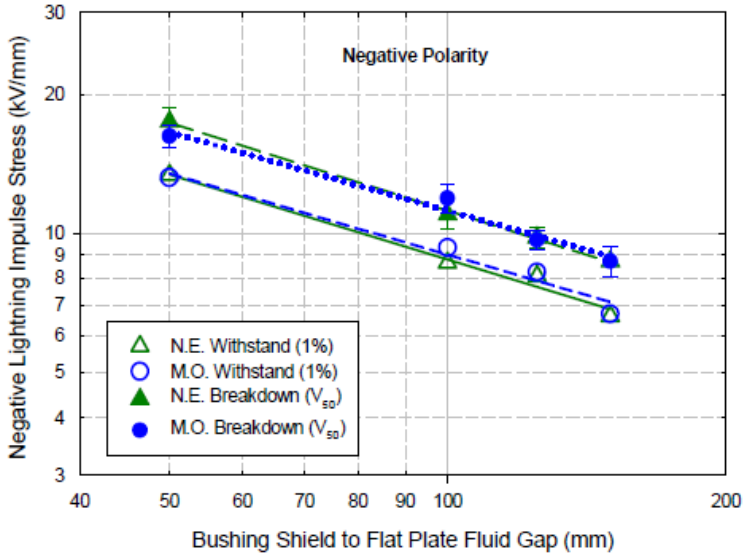

Figure 2-26 Negative lightning impulse breakdown strength of natural ester and mineral oil at various gap distances from 50 mm to 150 mm; N.E. stands for natural ester, M.O. stands for mineral oil [76].

Table 2-4 Lightning breakdown strength of natural ester and mineral oil under negative polarity using bushing shield-plate electrodes at various gap distances from 50 mm to 150 mm [76].

Gap distance	50 mm		100 mm		125 mm		150 mm	
Liquid	Natural Ester	Mineral Oil	Natural Ester	Mineral Oil	Natural Ester	Mineral Oil	Natural Ester	Mineral Oil
U_{avg} (kV)	873	812	1099	1191	1225	1211	1305	1306
Std dev. (kV)	65	48	76	85	64	61	100	97
Variance %	7.5	5.9	6.9	7.1	5.3	4.8	7.6	7.4
$U_{1\%W}$ (kV)	669	661	864	932	1012	1031	995	1005
Scale	901.9	833.4	1133	1229	1256	1240	1350	1349
Shape	15.37	19.90	16.94	16.69	21.27	24.84	15.04	15.63
R^2_W	0.921	0.946	0.898	0.938	0.931	0.964	0.914	0.971

The results of positive lightning tests including both 50% breakdown and 1% washstand voltages are given in Figure 2-27 and Table 2-5 [76]. Similarly, the 50% breakdown strengths of natural ester and mineral oil are very close to each other at various gap distances from 50 mm to 150 mm. However for 1% withstand strength, mineral oil lies lower than the natural ester; this might be caused by the high standard deviation of mineral oil's breakdown strength at the 50 mm gap distance as shown in Table 2-5 and the consequent low withstand strength at the 50 mm gap distance.

Although the bushing shield to plate electrode configuration resembles more likely a slightly non-uniform field rather than a quasi-uniform field, comparing the results under negative and positive polarities, there is no polarity effect observed, so results using this field configuration are classified into the quasi-uniform category.

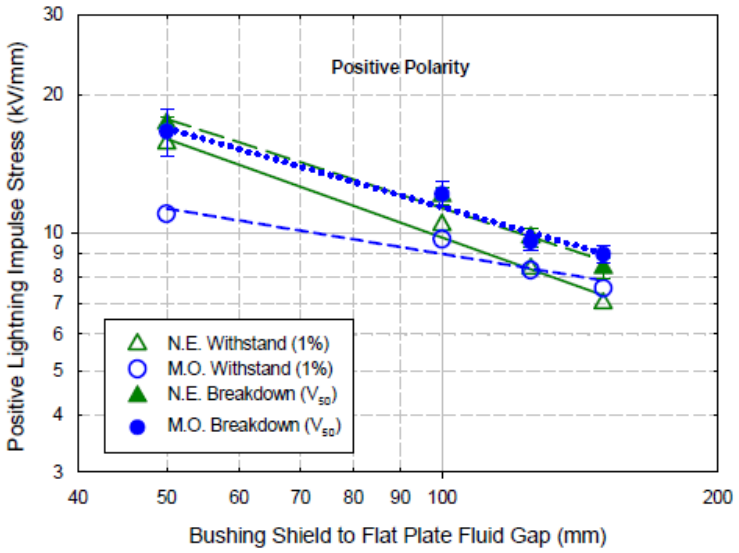

Figure 2-27 Positive lightning impulse breakdown strength of natural ester and mineral oil at various gap distances from 50 mm to 150 mm; N.E. stands for natural ester, M.O. stands for mineral oil [76].

Table 2-5 Lightning breakdown strength of natural ester and mineral oil under positive polarity using bushing shield-plate electrodes at various gap distances from 50 mm to 150 mm [76].

Gap distance	50 mm		100 mm		125 mm		150 mm	
Liquid	Natural Ester	Mineral Oil	Natural Ester	Mineral Oil	Natural Ester	Mineral Oil	Natural Ester	Mineral Oil
U_{avg} (kV)	867	831	1203	1215	1221	1193	1256	1346
Std dev. (kV)	25	98	50	77	56	49	64	62
Variance %	2.9	12	4.1	6.4	4.6	4.1	5.1	4.6
$U_{1\%W}$ (kV)	783	551	1040	967	1042	1035	1051	1134
Scale	878.9	873.2	1226	1250	1246	1216	1286	1377
Shape	39.97	9.984	27.94	17.90	25.70	28.55	22.89	23.74
R^2_W	0.973	0.952	0.924	0.904	0.955	0.952	0.983	0.801

2.3.1.2 Tests in liquid gaps with solid interface

Coil-to-coil electrodes made from opposing lengths of rectangular aluminium secondary winding conductor (the same size as the type 1 and type 2 electrodes in Figure 2-23) represent a common insulation system between the disc coils of a transformer. As shown in Figure 2-28 [75], pressboard spacers (2 or 3 mm thick × 12.7 mm wide × 38.1 mm long) were used to set gaps from 3 mm to 12 mm excluding the turn insulation on the electrodes. The spacers were placed in three locations between the electrodes and secured with nylon wire ties. The parallel length of electrode was about 305 mm. Tests

were carried out under 1.2/50 μs lightning impulse by using rising-voltage method with three shots per step in a 210 litres steel tank.

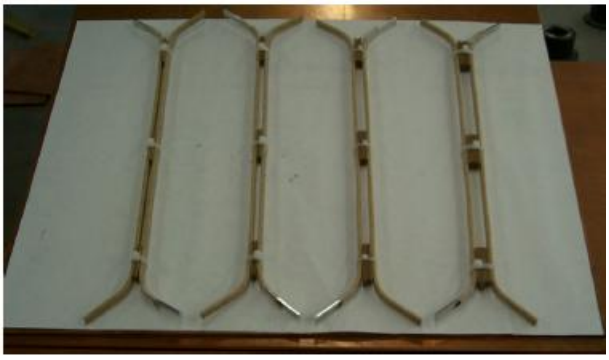

Figure 2-28 Coil-to-coil electrodes used for lightning impulse tests with solid interface at gap distances from 3 mm to 12 mm [75].

The results obtained under both negative and positive lightning impulse voltages using coil-to-coil electrodes are given in Table 2-6 [75]. Creep breakdown at the end spacers in either liquid accounted for 50% to 60% of the failures, 35% to 45% at the middle spacers and the rest 5% in the oil gaps. As oil wedge might exist between the solid spacer and coil electrode, most of the breakdowns were observed at the location of spacers. It indicates that solid interface is indeed the weak link in liquid/solid composite insulation. The breakdown strength of natural ester at gap distances from 3 mm to 12 mm is generally higher than that of mineral oil. This is likely due to the better balanced dielectric constant ratio between ester liquids and pressboard, as in this case, the maximum local stress of the oil wedge for ester liquids is lower than for mineral oil [6].

Table 2-6 Lightning breakdown strength of natural ester and mineral oil using coil-to-coil electrodes at various gap distances from 3 mm to 12 mm [75].

Gap distance	3 mm		5 mm		8 mm		12 mm	
Liquid	Natural Ester	Mineral Oil	Natural Ester	Mineral Oil	Natural Ester	Mineral Oil	Natural Ester	Mineral Oil
Positive Polarity								
$U_{50\%}$ (kV)	132	129	160	140	210	199	274	265
Std dev. (kV)	12.7	14.0	13.3	23.8	14.4	24.7	37.9	17.2
Variance %	10	11	8.3	17	6.9	12	14	6.5
Negative Polarity								
$U_{50\%}$ (kV)	139	122	175	156	211	209	266	275
Std dev. (kV)	18.5	20.3	44.5	21.0	21.0	16.9	38.8	17.3
Variance %	13	17	25	13	10	8.1	15	6.3

U-shape electrode configuration was specially designed for creepage breakdown tests on liquid/solid interface as show in Figure 2-29 [77]. It is important to avoid the

presence of any oil wedge and ensure the breakdown is related to the interfacial stress. The high-voltage electrode consisted of a copper or brass tube shaped into a 'U' form. For each test a Kraft crepe insulation tube was placed over the electrode. The ground electrode was a metallic disc with round radius edge. The exact dimension of the electrode configuration and the breakdown testing method were not mentioned in the paper [77].

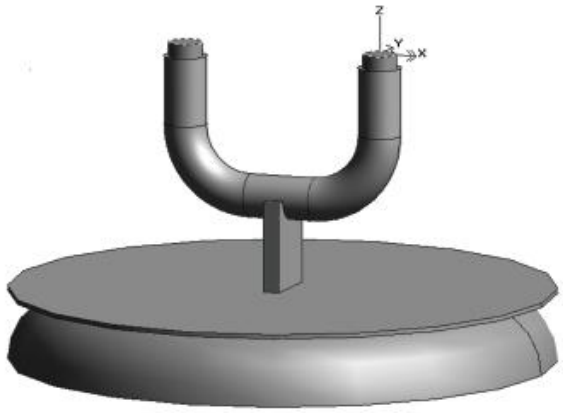

Figure 2-29 U-shape electrode configuration for lightning impulse tests with solid interface at gap distances from 10 mm to 35 mm [77].

The results of creepage breakdown tests in natural ester and mineral oil under both negative and positive 1.2/50 μs lightning impulse voltages are given in Table 2-7 [77]. It was found that lightning creepage breakdown strength of natural ester is close to that of mineral oil at various gap distances from 10 mm to 35 mm.

Table 2-7 Lightning breakdown strength of natural ester and mineral oil using U-shape electrodes at various gap distances from 10 mm to 35 mm [77].

			Natural Ester		Mineral Oil	
	Gap distance	Sample No.	Ave. (kV)	1% W. (kV)	Ave. (kV)	1% W. (kV)
Positive	10 mm	23	358	230	400	256
	20 mm	23	504	379	528	342
	35 mm	23	622	450	644	484
Negative	10 mm	24	386	243	396	259
	20 mm	24	549	425	576	399
	35 mm	24	638	455	674	453

Tap selector electrode configuration, as shown in Figure 2-30 [76], was used to study the creepage failure in an on-load tap changer. Six contacts were equally spaced on a phenolic insulator rod (55 mm wide × 20 mm thick × 850 mm long). The aluminium metal contacts were 65 mm in diameter and the central bolts were 22 mm in diameter. The contact to contact oil gap was 55 mm and the central bolt to central bolt distance was 98 mm. Tests were carried out in a 2400 litres tank. The 1.2/50 μs lightning

impulse voltage was increased step by step under alternatively reverse polarities. Test always started at positive polarity and on average four consecutive steps were conducted before changing the polarity [75].

The results of lightning breakdown voltage and calculated withstand voltage showed that natural ester is comparable with mineral oil as given in Table 2-8 [75]. In this test configuration, breakdown could occur in oil gap or creep on solid surface. For natural ester, 64% of failures broke down in oil gaps while for mineral oil it was 50%. The majority of breakdowns in either liquid, about 75%, occurred under positive polarity.

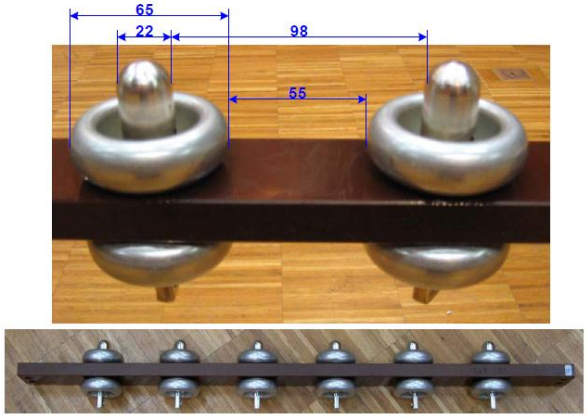

Figure 2-30 Tap selector electrode configuration for lightning impulse tests with solid interface at the gap distance of 55 mm [76].

Table 2-8 Lightning breakdown strength of natural ester and mineral oil using tap selector electrodes at the gap distance of 55 mm [75].

	Natural Ester	Mineral Oil
$U_{50\%N}$ (kV)	682	699
Std dev. (kV)	120	126
Variance (%)	17.6	18.0
R^2_N	0.978	0.973
$U_{1\%W}$ (kV)	358	359
$U_{2.5\%W}$ (kV)	413	417
Scale parameter	732	751
Shape parameter	6.43	6.24
R^2_W	0.930	0.979

2.3.2 In Non-uniform Fields

Point-plane electrode configuration was usually used to create a strongly non-uniform field, which represents the situation when a discharge is initiated locally by some defects in a transformer. Up to now there have been some published results on ester liquids in strongly non-uniform fields [13], which are summarized as follows from inception stage, propagation stage to breakdown stage.

2.3.2.1 Streamer initiation

Streamer inception voltage of natural ester (rape-seed oil) in a non-uniform point-plane field was studied under both positive and negative 1.2/50 μs lightning impulses [81, 82]. The tip radius of point electrode was 50 μm and the diameter of plane electrode was 36 mm. Tests were carried out at gap distances of 8 mm and 20 mm. Results of streamer inception voltage V_{si}, streamer inception field E_{si} and propagation speed v_{ps} under positive and negative polarities are given in Table 2-9 [81].

Inception voltage and field of natural ester are only approximately 50% of those of mineral oil at both gap distances. Streamer propagation velocity of natural ester is similar to that of mineral oil at the inception stage. Streamer inception voltages under negative polarity are lower than those under positive polarity at the gap distance of 20 mm. However it is interesting to see the inception voltages of negative streamers are higher than those of positive streamers at the gap distance of 8 mm, which is converse to the customary experience. In addition, the absolute values of inception voltage obtained in this study seem unreasonably high, which might have exceeded the breakdown voltages reported by others at the similar condition [14].

Table 2-9 Streamer inception voltage, field and speed of natural ester under positive and negative polarities [81].

		Rape-seed Oil		Mineral Oil	
Gap Distance (mm)		8	20	8	20
Positive	V_{si} (kV)	50	120	87	288
	E_{si} (MV/cm)	3.1	6.5	5.4	15.6
	V_{ps} (km/s)	1.0-3.3	1.4-3.7	2.0-3.0	2.0-3.0
Negative	V_{si} (kV)	54	112	103	208
	E_{si} (MV/cm)	3.3	6.1	6.0	11.3
	V_{ps} (km/s)	0.5-2.0	0.5-3.5	1.0-2.0	1.0-3.0

Streamer inception voltage of synthetic ester (Midel 7131) in a non-uniform point-plane field was investigated under both positive and negative impulse voltages [83, 84]. Very sharp point electrode with tip radius of approximately 2.0 μm and plane electrode with diameter of 90 mm were used. Tests were carried out under non-standard impulse waveform of 40 ns/740 μs. Gap distances for Midel 7131 and Nytro 10X (mineral oil) were slightly different, 19.5 mm and 17.0 mm respectively. It should be emphasized that the inception voltage in this study was associated with inception probability, which was determined by counting the number of injected streamers during 30 pulses at a fixed voltage.

The results indicated that inception voltage U_i (corresponding to 50% probability) of synthetic ester Midel 7131 is approximately 60% higher than that of mineral oil Nytro 10X under both positive and negative polarities, as shown in Table 2-10 [83]. As expected, inception voltage under negative polarity is generally slightly lower than that under positive polarity. Even the inception voltage of synthetic ester Midel 7131 is higher than that of mineral oil Nytro 10X, once incepted, the streamer length versus impulse voltage in Midel 7131 follows the streamer lengths measured in Nytro 10X closely under both polarities [84]. It has to be mentioned that results in this study focus on the inception stage, at which the measured streamer lengths are lower than 1.5 mm.

Table 2-10 Streamer inception voltage and field of synthetic ester (Midel 7131) under positive and negative polarities [83].

	Cyclohexane	Midel 7131	Nytro 10 X
Tip radius, r_p (μm)	2.0	2.0	2.3
Gap distance, d (mm)	19.5	19.5	17.0
Inception voltage, U_i positive (kV)	10.5	16.0	9.7
Inception voltage, U_i negative (kV)	9.9	14.7	8.5-9.0

It is worth introducing two other studies on synthetic ester, even the results were not compared with mineral oil. Paper [85] investigated the effect of DC pre-stress on streamer inception voltage in synthetic ester Midel 7131 under step impulse voltage (100 ns rise time), which demonstrated the presence of space charges in the vicinity of electrodes. Paper [86] studied the influence of hydrostatic pressure on the streamer inception voltage in synthetic ester under DC voltage. The results indicated that inception voltage increases with the increase of hydrostatic pressure under both polarities, which supports the gaseous nature of streamers in synthetic ester.

2.3.2.2 Streamer propagation and breakdown

Streamer propagation and breakdown in natural ester (rape-seed oil) were studied at large gap distances under both positive and negative step impulse voltages [13, 87, 88]. The diameter of plane electrode was 200 mm. Point electrodes with various tip radii from 1 μm to 100 μm were used. Gap distances varied from 20 mm to 200 mm. The waveform consisted of a fast rise time and a long tail (0.5/1400 μs), resembling a step voltage. This type of waveform makes the interpretation of results easier. With the lightning impulse (1.2/50 μs), the rapid decay of voltage would have an extra influence on the propagation, and with the switching impulse (250/2500 μs), the long rise time would induce a large jitter on streamer initiation [13].

Figure 2-31 summarises the streamer characteristics of natural ester including stopping length, average velocity and streamer charge at the gap distance of 100 mm under positive polarity [13]. Compared with mineral oil, the increasing trend of stopping length of natural ester with applied voltage follows closely to that of mineral oil. After breakdown, the streamer velocity of natural ester increases quickly with the applied voltage, which appears at much lower voltage levels than for mineral oil. It is noted that breakdown voltage and acceleration voltage of natural ester are identical at the large gap distance of ~100 mm. Breakdown voltage and acceleration voltage of natural ester at various gap distances under positive polarity are shown in Figure 2-32, both of which are lower than those of mineral oil [13].

Similar results of natural ester at the gap distance of 100 mm under negative polarity are summarized in Figure 2-33 and Figure 2-34 [13]. Under negative polarity, there is a big difference of stopping lengths between natural ester and mineral oil that streamer in natural ester propagates further than in mineral oil at the same voltage level. Both breakdown voltage and acceleration voltage of natural ester under negative polarity are lower than those of mineral oil as well. Natural ester's acceleration voltage becomes same as its breakdown voltage at the gap distance of 200 mm.

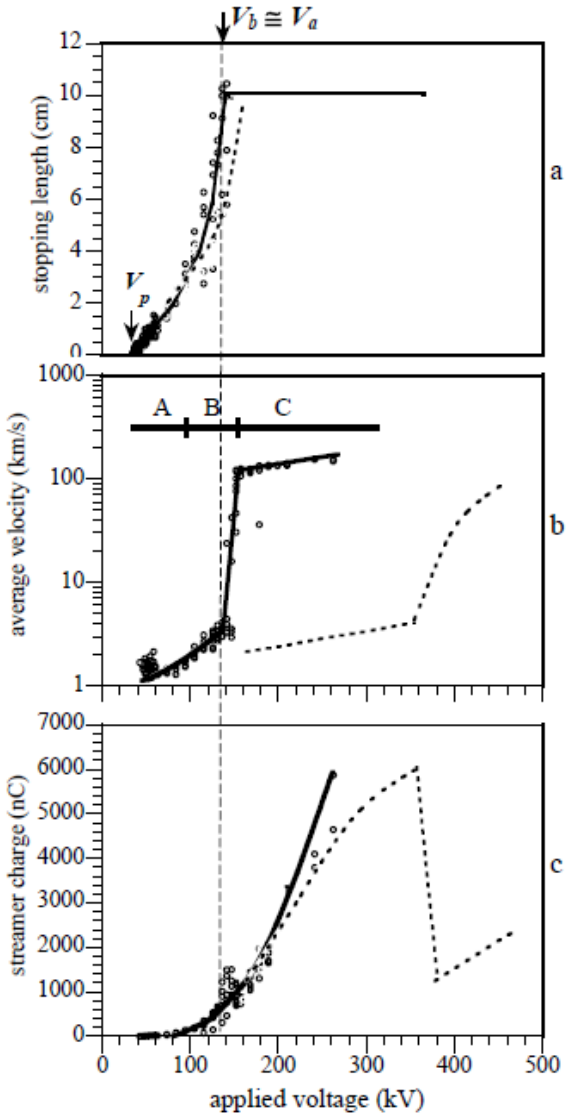

Figure 2-31 Characteristics of positive streamer in natural ester at gap distance of 100 mm; a streamer stopping length, b streamer average velocity, c streamer charge; dash line represents mineral oil [13].

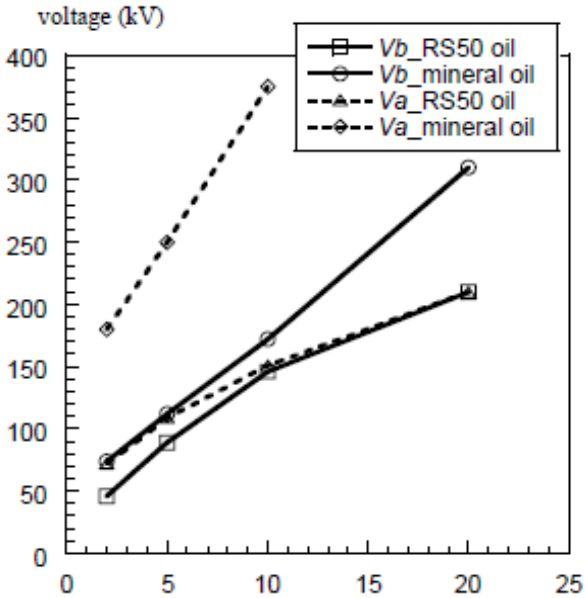

Figure 2-32 Breakdown voltage V_b and acceleration voltage V_a of natural ester at various gap distances under positive step impulse voltage; RS50 stands for natural ester [13].

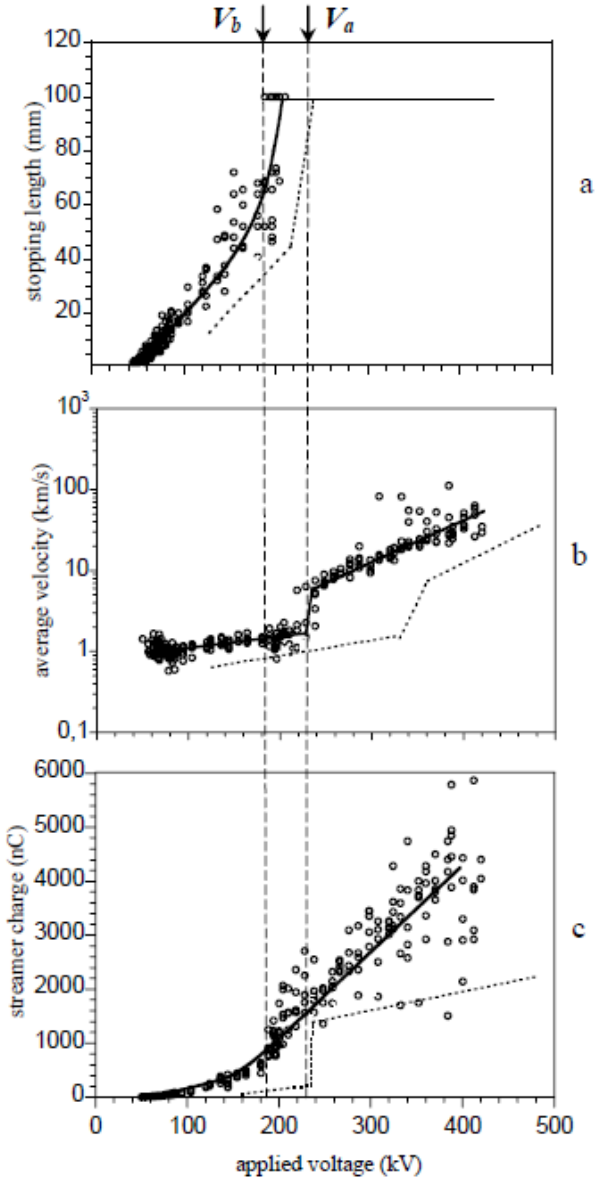

Figure 2-33 Characteristics of negative streamer in natural ester at gap distance of 100 mm; a streamer stopping length, b streamer average velocity, c streamer charge; dash line represents mineral oil [13]

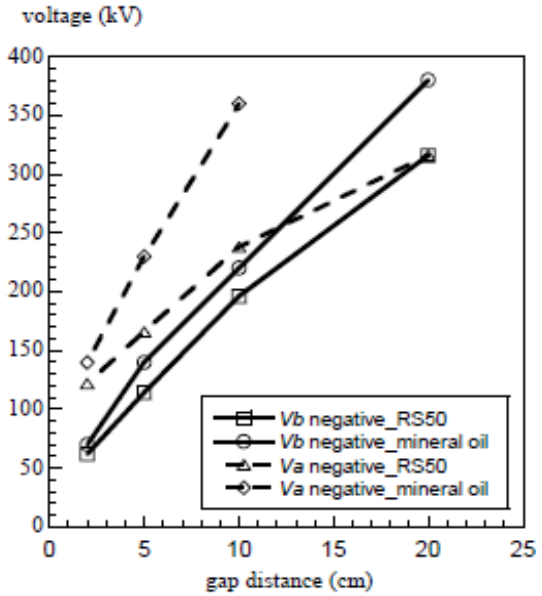

Figure 2-34 Breakdown voltage V_b and acceleration voltage V_a of natural ester at various gap distances under negative step impulse voltage; RS50 stands for natural ester [13].

The most recent study of streamer phenomenon in ester liquids was carried out under 1.2/50 μs lightning impulse, in which a few mineral oils, a few natural esters (vegetable oils) and a synthetic ester were compared [89]. The plane electrode was a brass disc of 40 mm diameter, and the tip radius of point electrode was ~10 μm. The results of stopping length (final length) versus applied voltage at the gap distance of 20 mm under positive and negative polarities are shown in Figure 2-35 and Figure 2-36 respectively [89]. Under positive polarity, relatively small difference exists between ester liquids and mineral oil; under negative polarity, increase of stopping length with voltage is much quicker in ester liquids than in mineral oil; both of which confirm the findings under step impulse voltage.

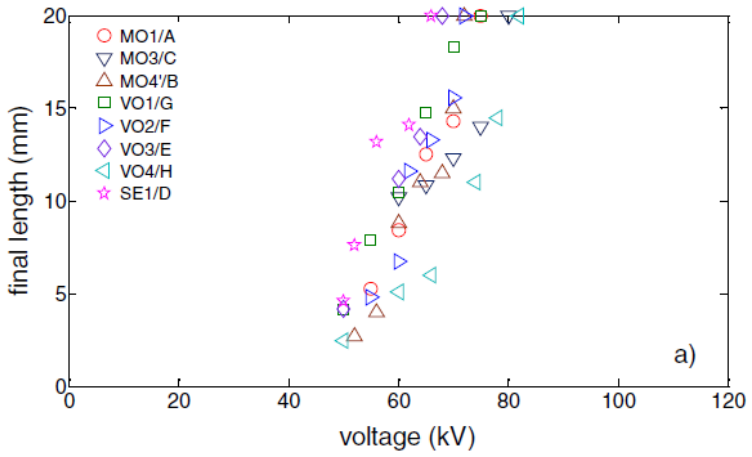

Figure 2-35 Streamer length versus applied voltage of ester liquids and mineral oil under positive lightning impulse voltage; d=20 mm; MO stands for mineral oil, VO stands for natural ester, SE stands for synthetic ester [89].

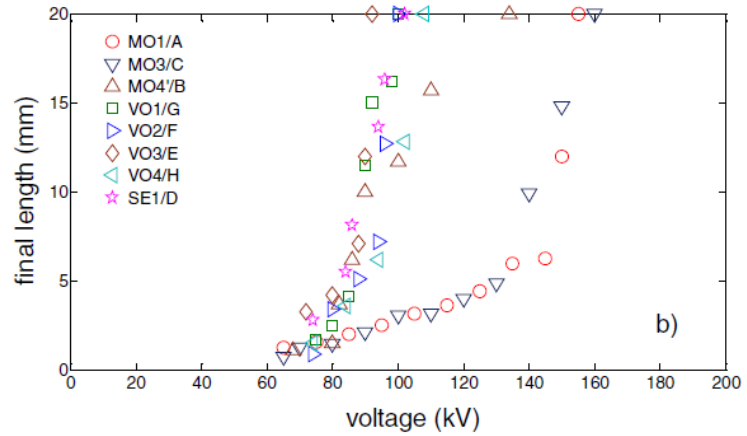

Figure 2-36 Streamer length versus applied voltage of ester liquids and mineral oil under negative lightning impulse voltage; d=20 mm; MO stands for mineral oil, VO stands for natural ester, SE stands for synthetic ester [89].

Streamer velocity and breakdown voltage of ester liquids and mineral oil under 1.2/50 μs lightning impulse voltage were studied in [14]. The tip radius of the point

electrode was 40 μm and the diameter of the plane electrode was 355 mm. Gap distance varied from 25 mm to 200 mm. In addition, influence of pressboard on breakdown voltage and streamer velocity was considered as well.

Results of streamer velocity versus applied voltage under positive and negative polarities are shown in Figure 2-37 and Figure 2-38 respectively [14]. Generally fast streamers appear at lower voltage in ester liquids than in mineral oil especially under positive polarity. Introduction of pressboard accelerates the streamer velocity in mineral oil but not in ester liquids under positive polarity. Under negative polarity, the presence of pressboard promotes the streamer velocity for both ester liquids and mineral oil at the very high-voltage levels.

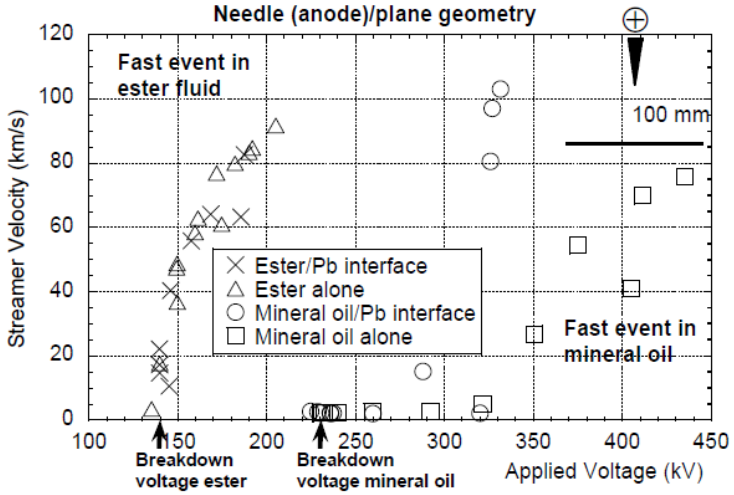

Figure 2-37 Streamer velocity versus applied voltage of ester liquids and mineral oil under positive lightning impulse voltage; d=100 mm; Pb stands for pressboard [14].

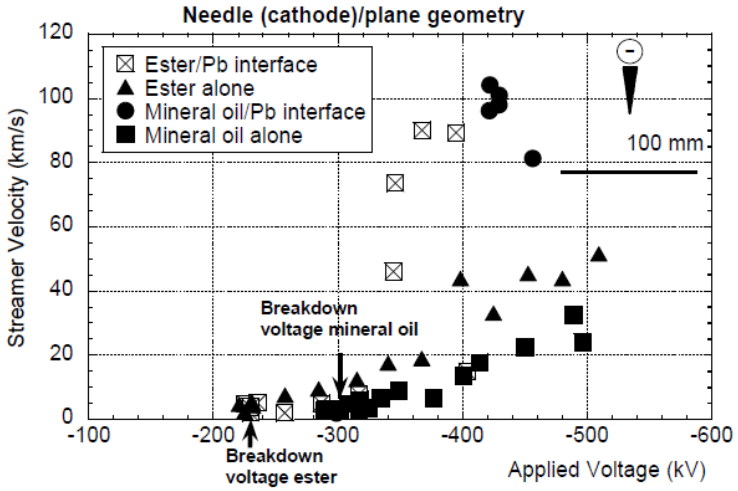

Figure 2-38 Streamer velocity versus applied voltage of ester liquids and mineral oil under negative lightning impulse voltage; d=100 mm; Pb stands for pressboard [14].

Lightning breakdown voltages of ester liquids and mineral oil with and without pressboard under positive polarity are shown in Figure 2-39 [14]. It can be seen that introduction of pressboard at the gap distance of 100 mm does not reduce the lightning breakdown voltage. Overall, lightning breakdown voltages of ester liquids are lower than those of mineral oil, between which the difference is enlarged at larger gap distances.

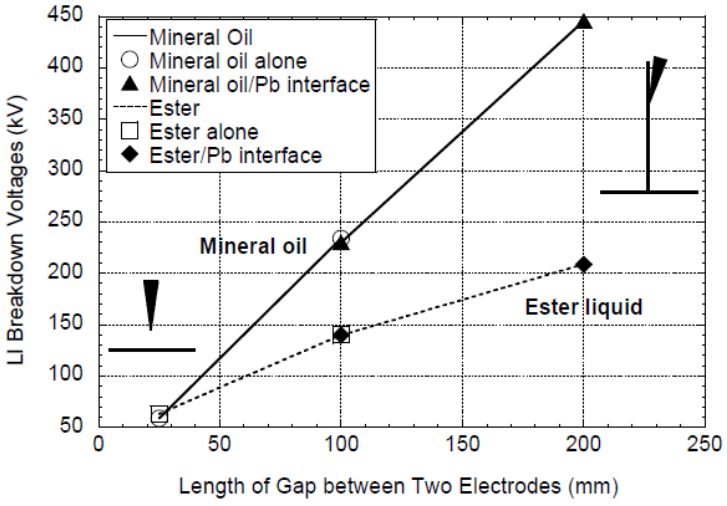

Figure 2-39 Breakdown voltage versus gap distance of ester liquids and mineral oil under positive lightning impulse voltage; Pb stands for pressboard [14].

2.4 Summary

A brief description of pre-breakdown and breakdown phenomena in liquids is given in this chapter mainly based on the mineral oil's experience including the polarity effect, scale effect, additive influence and pressboard influence. The basic knowledge introduced here is going to be used in the descriptions and discussions of the following chapters.

Literature review of ester liquids' performances under impulse voltage are organised in two categories following quasi-uniform field and non-uniform field respectively. As for quasi-uniform field, lightning impulse tests indicated that ester liquids have comparable breakdown strength with mineral oil at gap distances up to 150 mm. It was noted that most of the tests were conducted under lightning impulse voltage by using various testing methods e.g. rising-voltage method, up-and-down method and multiple-level method. In addition, due to the limitation of sample size, 50% breakdown voltage rather

than withstand voltage was usually given. Therefore many issues like influence of the impulse waveform, testing method and withstand voltage deduction need to be studied.

In non-uniform field study, point-plane electrode configuration was commonly used. The results revealed the differences between ester liquids and mineral oil mainly using the step impulse voltage while some others using lightning impulse voltage. What is the impact of waveform? Is there a relationship between the results under different waveforms? In addition, more tests focused on natural ester, and even fewer studies considered the influence of pressboard surface, so cross comparison of streamer and breakdown among natural ester, synthetic ester and mineral oil with and without pressboard surface is worthy of detailed investigation.

CHAPTER 3. EXPERIMENTAL DESCRIPTION

3.1 Liquids under Test

3.1.1 Basic Introduction

Two ester liquids and a mineral oil as benchmark were investigated in this thesis: synthetic ester Midel 7131, natural ester FR3 and mineral oil Gemini X.

Midel 7131 conforms to IEC 61099: 1992 "Specifications for Unused Synthetic Organic Esters for Electrical Purposes". It is classified as type T1, a halogen-free pentaerythritol ester, whose molecular structure is shown in Figure 3-1 (a) [90]. There are four ester groups indicated by '–COOR' at the end of the cross structure, where the 'R' stands for multiple organic groups, and the four organic groups could be either the same or different. The high electronegative performance of oxygen atom in '–COOR' group makes synthetic ester Midel 7131 more polar than the traditional mineral oil with hydrocarbon molecular structure. For Midel 7131, the relative permittivity is therefore higher and the volume resistivity is lower than that of mineral oil.

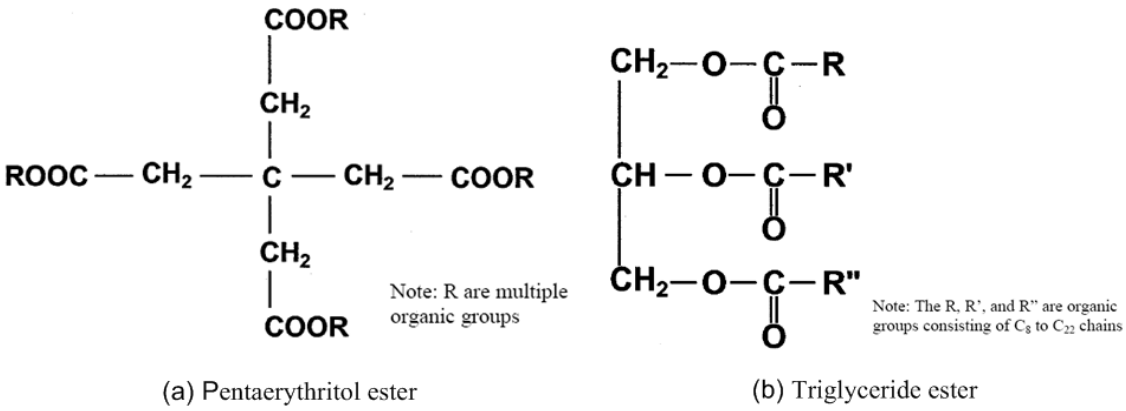

Figure 3-1 Chemical structure of pentaerythritol ester (synthetic ester) and triglyceride ester (natural ester) [90].

Natural ester is refined from vegetable oils which could be soya, sunflower, rapeseed (canola), cottonseed, olive, safflower, jojoba, lesquerella and verona. FR3 is refined from soya bean and its main molecular component is triglyceride fatty acid ester, which contains a mixture of saturated and unsaturated fatty acids with up to 22 carbon length chains containing 1 to 3 double bonds, as shown in Figure 3-1 (b) [90]. The number of double

bonds, 1 to 3, is an optimum choice under careful consideration by the manufacturer, because a high degree of bond saturation will increase the viscosity of the liquid which reduces the cooling function of liquid while low degree of bond saturation will reduce anti-oxidation ability. In addition, anti-oxidation additives and pour point suppressants are added in FR3 to improve the liquid performance. FR3 is also more polar than mineral oil, and has higher relative permittivity and lower volume resistivity than mineral oil.

Mineral oil mainly consists of carbon and hydrogen in molecules with different structures, as shown in Figure 3-2 [91]. Paraffinic, naphthenic and aromatic are the three basic structures, and their percentages are normally specified for a mineral oil. Aromatic components (especially polyaromatic compound) influence the positive and negative streamer characteristics due to their low ionization potential and large electrons-trapping section respectively [42]. A highly refined mineral oil Nytro Gemini X, which contains 10% aromatic content, was tested during all the experiments as the benchmark for cross comparison between ester liquids and mineral oil.

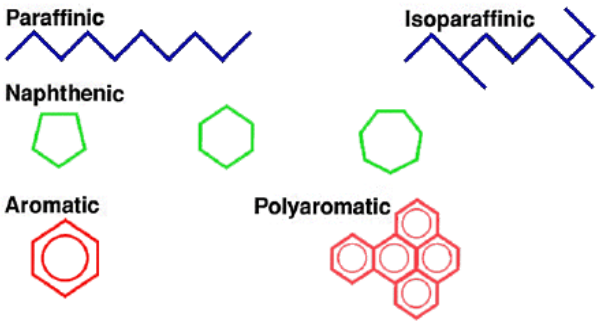

Figure 3-2 Chemical structure of components in mineral oil [91].

3.1.2 Cross Comparison between Ester Liquids and Mineral oil

The basic properties of the investigated liquids including physical, chemical and electrical parameters, based mainly on the Product Data Sheets, are given in Table 3-1. The colour appearance of the liquid samples is shown in Figure 3-3. Natural ester FR3 shows light green colour, synthetic ester Midel 7131 light orange and mineral oil Gemini X light yellow. In addition, all the liquids are transparent.

Table 3-1 Basic property of liquids: Midel 7131, FR3 and Gemini X.

Property	**Unit**	**Midel 7131**	**FR3**	**Gemini X**
Density@20℃	kg/dm^3	0.97	0.92 (25 ℃)	0.882
Viscosity@40℃	mm^2/s	28	34	8.7
Viscosity@-30℃	mm^2/s	1400 (-20 ℃)		1080
Specific heat@20℃	J/kg K	1880	1883	1860
Thermal conductivity@20℃	W/mK	0.144	0.167	0.126
Pour point	℃	-60	-21	-60
Flash point	℃	275	316	144
Acidity	mg KOH/g	<0.03	0.04	<0.01
Aromatic content	%			10
Water content	mg/kg	50	30	<20
Furfural content	mg/kg			<0.1
Antioxidant, phenols	Wt%			0.38
Breakdown voltage (AC)				
- before treatment	kV			40-60 (d=2.5 mm)
- after treatment		>75 (d=2.5 mm)	56 (d=2 mm)	>70 (d=2.5 mm)
Dielectric dispassion factor@90℃		<0.03	0.03 (100℃)	<0.001
Volume resisitivity@25℃	Ωcm	>5×10^{12}	20×10^{12}	
Interfacial tension	mN/m		24	50

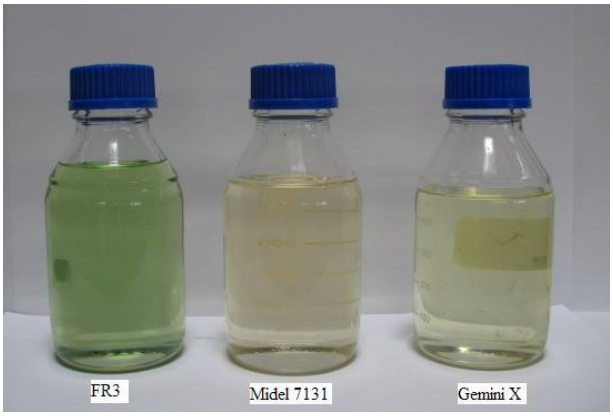

Figure 3-3 Colour appearance of liquid samples.

Comparing ester liquids with mineral oil, there are some major features for ester liquids including pros and cons:

- Ester liquids are more biodegradable than mineral oil which favours the environmental request of modern society.
- Ester liquids have much higher flash point and fire point than mineral oil which means high resistance to ignition, and therefore reduces the risk of fire hazard in electrical power apparatus.
- Ester liquids are non-toxic which meets the safety and health consideration.
- Moisture is an important factor to accelerate cellulose ageing in transformers. Ester liquids are more hygroscopic than mineral oils, thus they can absorb more water from cellulose insulation and thereby slow down the hydrolysis ageing process of cellulose material.

- Compared to mineral oil, permittivity of ester liquids is closer to that of solid insulation which leads to an evener stress distribution between solid and liquid materials where thicknesses of liquid gap and solid insulation are comparable. This will also reduce the local stress in oil wedges which typically sets off a discharge.
- Ester liquids have higher viscosity than mineral oil, and it may reduce the oil flow, further influence (or worsen) the cooling effect of a transformer under ON (Oil Natural) mode. On the other hand, thermal conductivity of ester liquids is higher than that of mineral oils, and this could offer some compensation for heat dissipation.
- Ester liquids are more polar than mineral oils which may aggravate the oil flowing electrification and bring space charge issues. Moreover lower volume resistivity of ester liquids reduces their insulation resistance.
- Due to the divergence of original materials (vegetable or agriculture plant), the uniformity of natural esters' performance is suspected. The oxidation/gelling performance of natural ester under storage, transportation and in service should also be carefully considered. In addition, natural ester has relatively high pour point which may influence its application at very cold environment.

3.2 Sample Preparation

3.2.1 Pre-processing of Liquid Sample

For quasi-uniform field tests, the liquid samples were pre-processed through filtering, degassing and dehydrating to minimize the influence of impurity on the test results. The "as-received" liquid was filtered by Nalgene® MF 75 nylon membrane filter, of which the pore size is 0.2 μm. A HIAC/ROYCO 8000A 8-channel particle counter with a HIAC/ROYCO ABS2 automatic bottle sampler was used to measure the particle number of liquid sample. Particle numbers of unfiltered and filtered liquid samples are shown in Figure 3-4. The cumulative particle number larger than 5 μm of filtered liquid samples could reduce to approximately 500 per 100 mL liquid, which is close to the criterion of clean oil '200 per 100 mL liquid' defined in CIGRE brochure 157 [19].

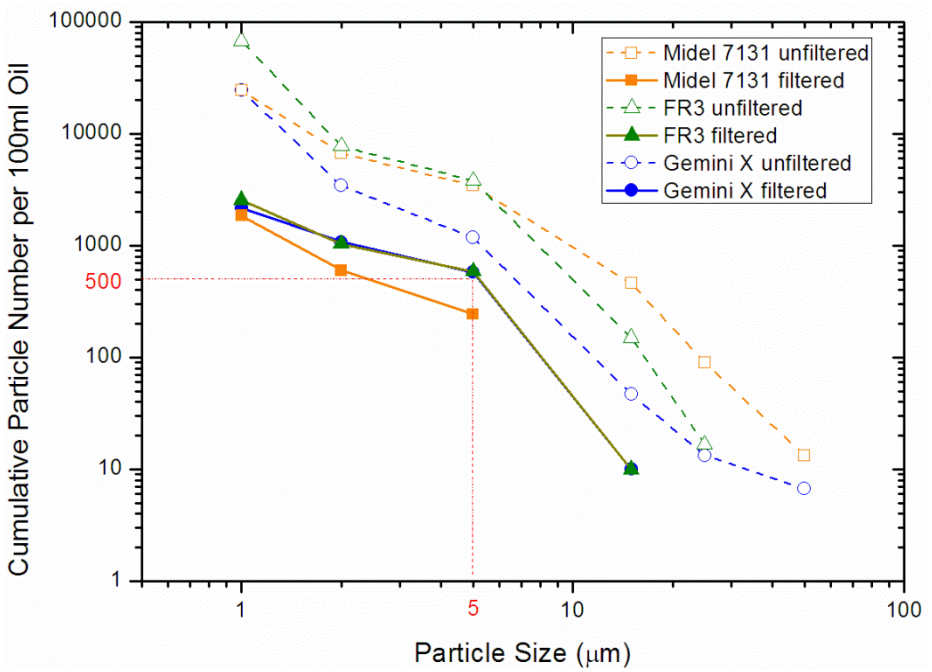

Figure 3-4 Particle numbers of unfiltered and filtered liquid samples.

The filtered liquid samples were then degassed and dehydrated in the vacuum oven under 500 Pa (5 mbar) at 85 ^{o}C for 48 hours, then a further 24 hours was given for the liquids to cool down to ambient temperature under vacuum. Water content was measured according to Karl Fisher titration analysis, using Metrohm 684 coulometer and 832 Termoprep ovens. The results of water content measurements of the processed samples are shown in Table 3-2. Generally the relatively humidity of processed samples is lower than approximately 5%.

Table 3-2 Water content and relative humidity of processed liquid samples at room temperature.

Liquid	Water content (ppm)	Saturation level (ppm)	Relative humidity (%)
Midel 7131	73	2700	2.7
FR3	25	1100	2.3
Gemini X	3	55	5.5

For the strongly non-uniform field tests, liquid samples were taken directly from sealed new oil barrels delivered from the oil manufacturers; once delivered, they were stored in a cool, dry, isolated and well ventilated storage area. The relative humidity of testing liquids was regularly checked during the whole period of experiments, which ranged approximately from 5% to 20% for all the liquids under test. Since streamer propagation is relatively insensitive to the normal contamination level of water and particle in a strongly non-uniform field under lightning impulse [13, 20], no further filtering nor dehydrating process was applied to the liquid samples.

3.2.2 Impregnation of Pressboard Sample

High density pressboards of 1.2 g/cm^3 were cut into the following dimensions for tests at various gap distances: 100 mm long × 40 mm high for 25 mm, 145 mm long × 65 mm high for 50 mm and 210 mm long × 90 mm high for 75 mm gap distances. The thickness of pressboard is 3 mm. The pressboards were firstly dried in an air circulating oven at 105 ^{o}C for 48 hours, and then in vacuum condition below 500 Pa (5 mbar) at 85 ^{o}C for 24 hours. The pressboards were then immersed into the insulating liquids and kept under vacuum below 500 Pa (5 mbar) at 85 ^{o}C for further 48 hours to achieve fully-impregnated conditions. After this procedure, the moisture content of fully impregnated pressboard samples was below 0.5% by weight.

3.3 Test Setup

3.3.1 Quasi-uniform Field Tests

The test setup for quasi-uniform field study is shown in Figure 3-5. A cylindrical test cell with liquid volume of 250 mL, was manufactured according to IEC 60897 "Methods for the Determination of the Lightning Impulse Breakdown Voltage of Insulating Liquids" [92]. The side wall of the test cell was made of transparent Perspex, which was then mounted on a nylon base. Brass sphere-sphere electrodes with diameter of 12.7 mm were used to provide the quasi-uniform field at a gap distance of 3.8 mm.

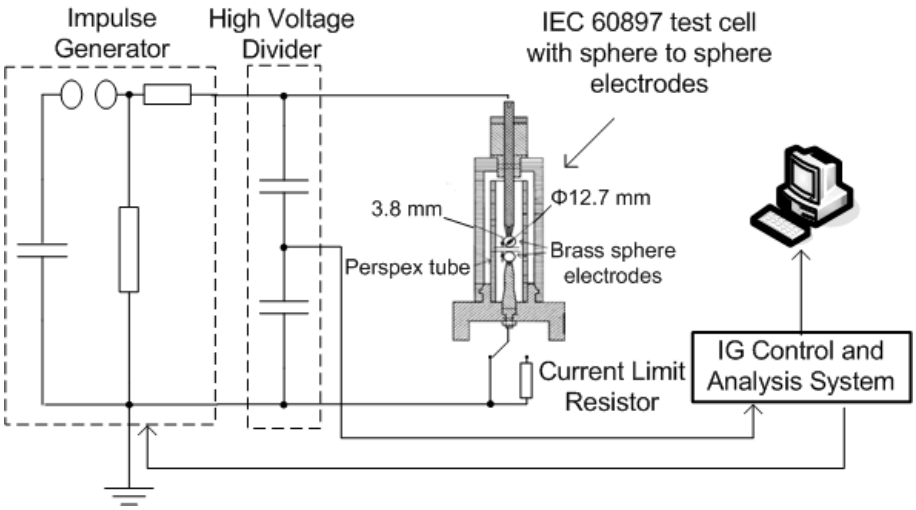

Figure 3-5 Sketch of test setup used in quasi-uniform field tests.

A 10-stage Haefely impulse generator with a maximum voltage 2000 kV and energy 150 kJ was used to deliver the standard lightning impulse 1.2(±30%)/50(±20%) μs and switching impulse 250(±20%)/2500(±60%), as shown in Figure 3-6 (right). Voltage waveform was measured by a high-voltage capacitive divider, as shown in Figure 3-6 (left) and recorded by the DIAS 733 impulse analysis system. In the quasi-uniform field tests, only negative impulse was used since transformers were normally tested under negative polarity.

Figure 3-6 Haefely impulse generator (right) with high-voltage divider (left).

According to standards [92, 93], liquid sample was required to be changed after each breakdown, and it was followed in the present tests. In addition, it was found that an obvious damage spot was left on the surface of sphere electrodes after each breakdown, so the sphere electrodes were changed as well in the present tests. However in the comparison study of testing methods in this thesis, hundreds of breakdowns were needed, and thus it was impractical to change the liquid sample and electrodes after

every breakdown. Therefore a current-limit resistor R_L (40 kΩ) was added in the circuit to limit the current of breakdown arc, further to protect the liquid sample and electrodes.

Both ATP simulation and experimental measurement indicated that the actual voltage waveform applied on the test cell in the test circuit with R_L was slightly distorted i.e. the front time was slowed down to approximately 2 μs without change of tail time and the peak voltage reduction was less than 5%. Further verification tests with and without the current-limit resistor were carried out in the three types of liquid under lightning impulse voltage. Five breakdowns were done at each case. The results confirmed that the current-limit resistor has negligible influence on the measured average breakdown voltage, as shown in Figure 3-7. To sum up, for the quasi-uniform field tests in chapter 4, current-limit resistor of 40 kΩ was used in the tests of method comparison but not in the standard lightning and switching impulse tests.

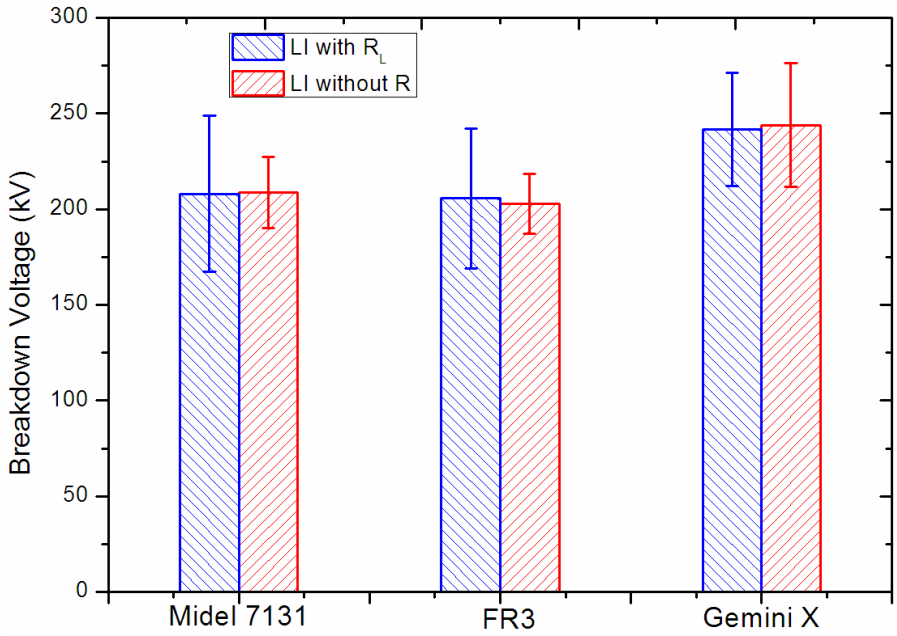

Figure 3-7 Influence of current-limit resistor R_L (40 kΩ) on lightning breakdown voltage; error bars stand for one standard deviation.

3.3.2 Non-uniform Field Tests

The test setup for strongly non-uniform field study is shown in Figure 3-8. The same impulse generator was used to deliver the standard lightning impulse. For tail-chopped impulse tests, a three-stage adjustable chopping gap was connected to the impulse generator.

A cubic-like test cell with volume of 12.5 L was used to hold the liquid sample and point-plane electrodes. Side walls and top lid of the test cell were made of transparent Perspex, which facilitated the streamer observation. Tungsten needle was used as the point electrode, whose tip radius of curvature was guaranteed to be 50±5 μm after selection using a microscope. The needle was regularly changed after each set of tests i.e. per liquid type per gap distance. Plane electrode was made of brass, having a diameter of 200 mm and edge radius of 3 mm. The gap distance between point-plane electrodes can be adjusted by a set of thickness gauges with step of 5 mm. In the tests with solid interface, a pressboard was placed in parallel to the point-plane electrode axis and in the upmost tight contact with the point electrode.

Voltage waveform was measured by the same high-voltage capacitive divider used in quasi-uniform field tests. In addition current was recorded by a 1 Ω non-inductive current shunt. A Hamamatsu made photomultiplier tube (PMT) H5783P with spectral response from 300 nm to 650 nm was used to monitor the light signal of a streamer. Voltage, current and light recordings were synchronized with the camera imaging operation.

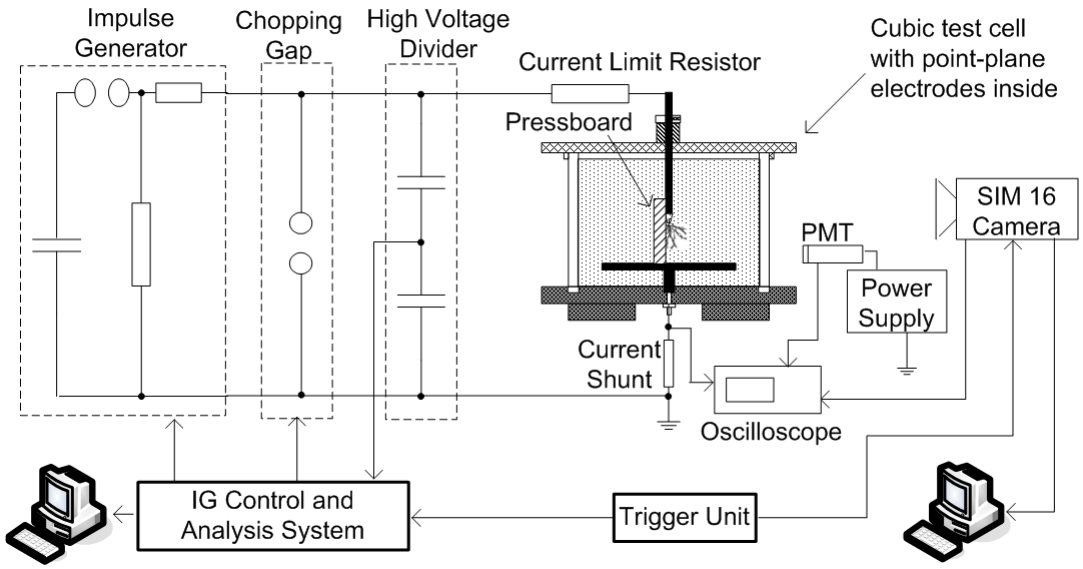

Figure 3-8 Sketch of test setup used in non-uniform field tests.

A high-speed camera Specialized Imaging SIM16, which consisted of 16 high resolution intensified CCD sensors interfaced with a beam splitter, was used to study the streamer characteristics. Each CCD sensor has a resolution of 1360 × 1024 pixels, which allows us to analyze the streamer shape based on the high quality streamer images. Each image can be individually set to a different exposure time from 5 ns to

10 ms in steps of 5 ns. The interframe time between images can also be independently set from 0 ns to 20 ms in steps of 5 ns.

Below breakdown voltage, the streamer could initiate and propagate, but finally stop at a certain distance less than the gap distance. Figure 3-9 shows a typical propagating process of such a stopped streamer. With the help of multi-frame high speed camera, the whole process of streamer propagation was recorded frame by frame with 2 μs interval time. Here, propagation length means the straight-line distance from the farthest tip point of a streamer to the point electrode, which is measured by using self-contained software of the camera. It can be seen from Figure 3-9 that streamer propagates and then stops at 28 μs with a length of 22.75 mm. This final length is named as stopping length of the streamer l_s. Accordingly the average propagation velocity of the streamer can be deduced by using the stopping length l_s divided by the propagating time t_p. Stopping length and average propagation velocity are two commonly used parameters to characterize a streamer.

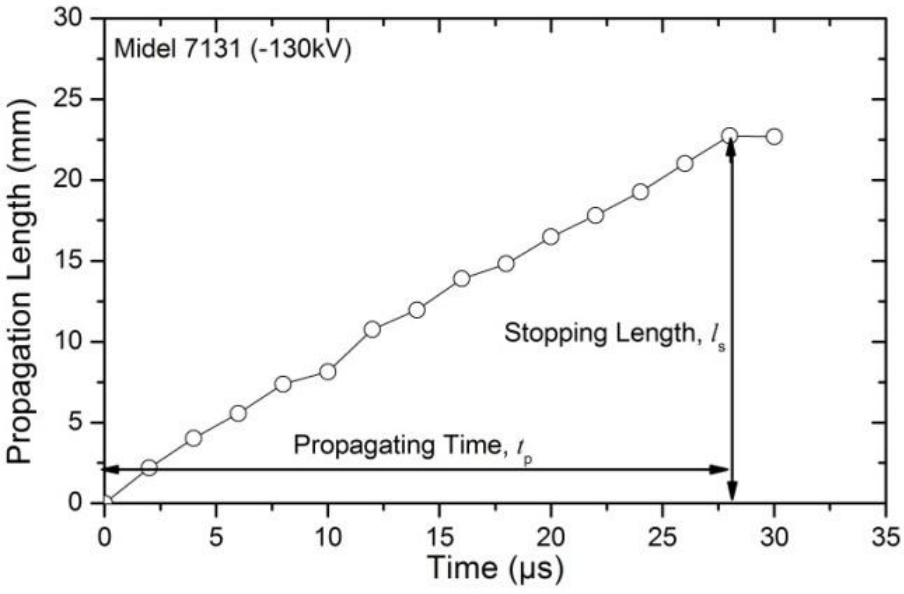

(a) Propagation length versus propagation time

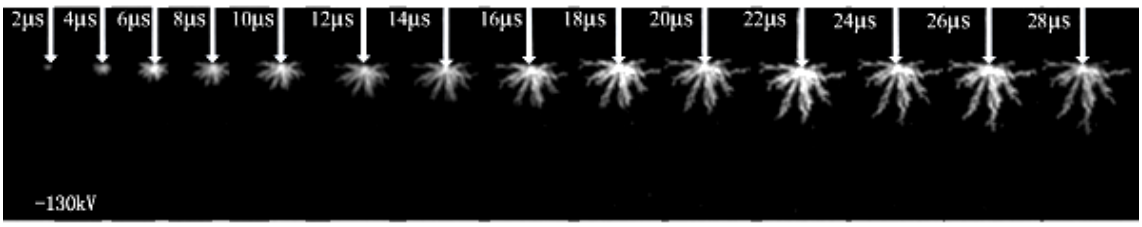

(b) Images of streamer propagation

Figure 3-9 Demonstration of a streamer propagation recorded by multi-frame high speed camera; Midel 7131, negative polarity, V=-130 kV, d=50 mm.

A small current-limit resistor R_L (3.5 kΩ) was added into the circuit to protect point electrode and oil samples especially when a breakdown occurred. Verification tests with and without the current-limit resistor indicated that such a small current-limit resistor does not influence the streamer propagation, as demonstrated by the streamer stopping length of FR3 under both positive and negative polarities shown in Figure 3-10 and Figure 3-11 respectively.

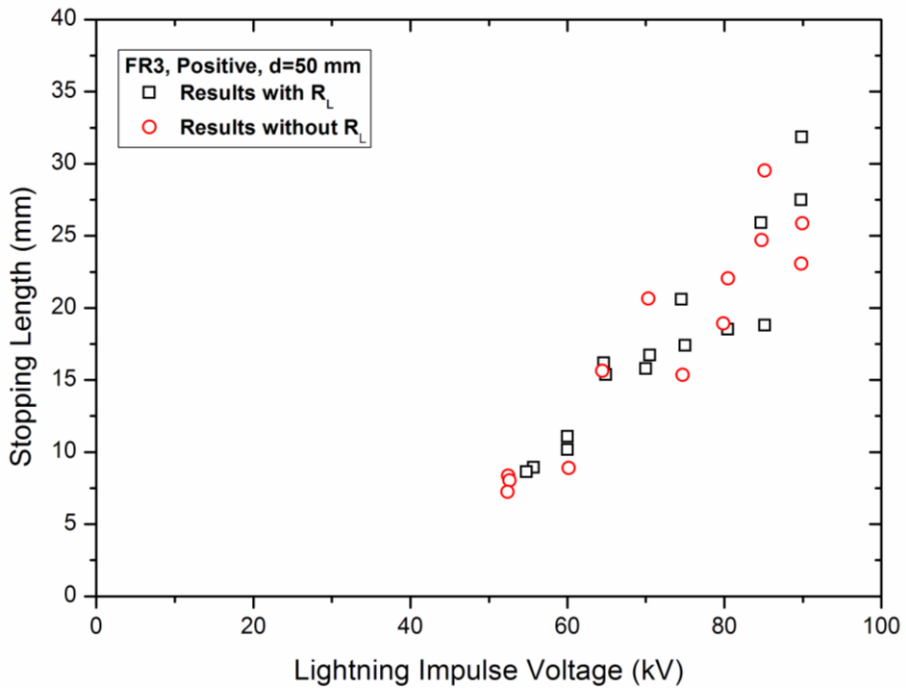

Figure 3-10 Influence of current-limit resistor R_L (3.5 kΩ) on positive streamer length; FR3, d=50 mm.

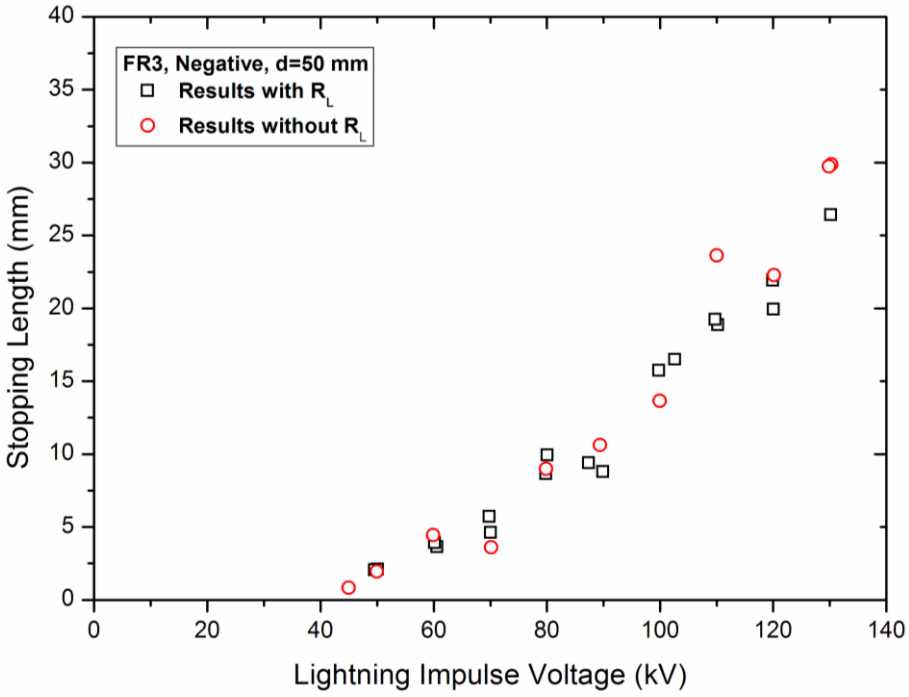

Figure 3-11 Influence of current-limit resistor R_L (3.5 kΩ) on negative streamer length; FR3, d=50 mm.

For tests in open liquid gaps, three photographing setups including shadowgraph, reflective image and integral light image were used, as shown in Figure 3-12. As it is named, shadowgraph shows the shadow projection of a streamer under the illumination of a back light source. This technique has been widely used in streamer study which provides the shape characteristic of the streamer channels, as shown in Figure 3-12 (a) and Figure 3-13 (a). Reflective image, which is rarely used in the literatures, indicates the streamer shape by reflecting the strong side flash light, as shown in Figure 3-12 (b) and Figure 3-13 (b). Compared with shadowgraph, the contrast between streamer and background of reflective image is much better, which is useful for the further image analysis e.g. fractal index calculation. Integral light image collects the self-irradiated light information during the streamer propagation, as shown in Figure 3-12 (c) and Figure 3-13 (c). Tests using the latter two setups reflective image and integral light image were carried out in a dark room.

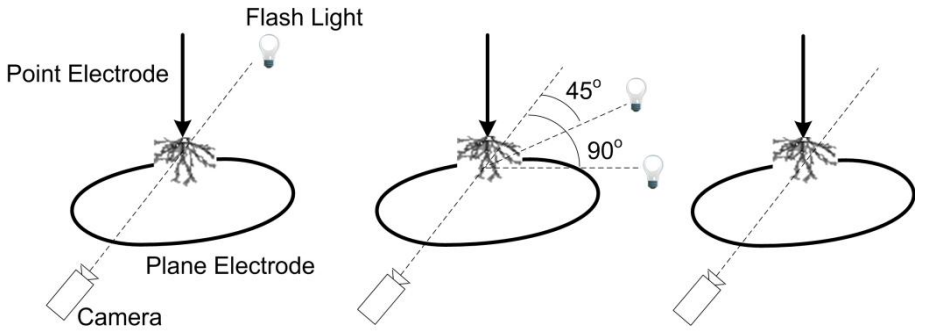

(a) Shadowgraph (b) Reflective image (c) Integral light image

Figure 3-12 Illustration of streamer photographing setups in tests without pressboard interface.

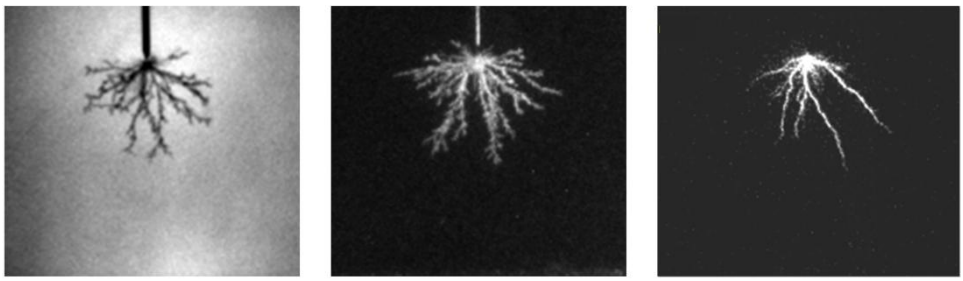

(a) Shadowgraph (b) Reflective image (c) Integral light image

Figure 3-13 Typical images in liquids using various photographing setups; Midel 7131, negative polarity.

Stopping length measured from the streamer image is one of the most useful parameters to show the characteristic of a streamer. It should be emphasized that stopping lengths of streamer scatter in a certain range even at the same voltage level, so multiple tests are usually conducted to produce an average value and its standard deviation.

Figure 3-14 and Figure 3-15 depict the results of stopping length versus applied voltage using the three photographing setups under positive and negative lightning impulses respectively. It can be seen that different techniques provide similar results in terms of stopping length which together are in a reasonable scattering range, so in the open liquid gap study, stopping length will be given as the average of all the measured data using the three photographing setups.

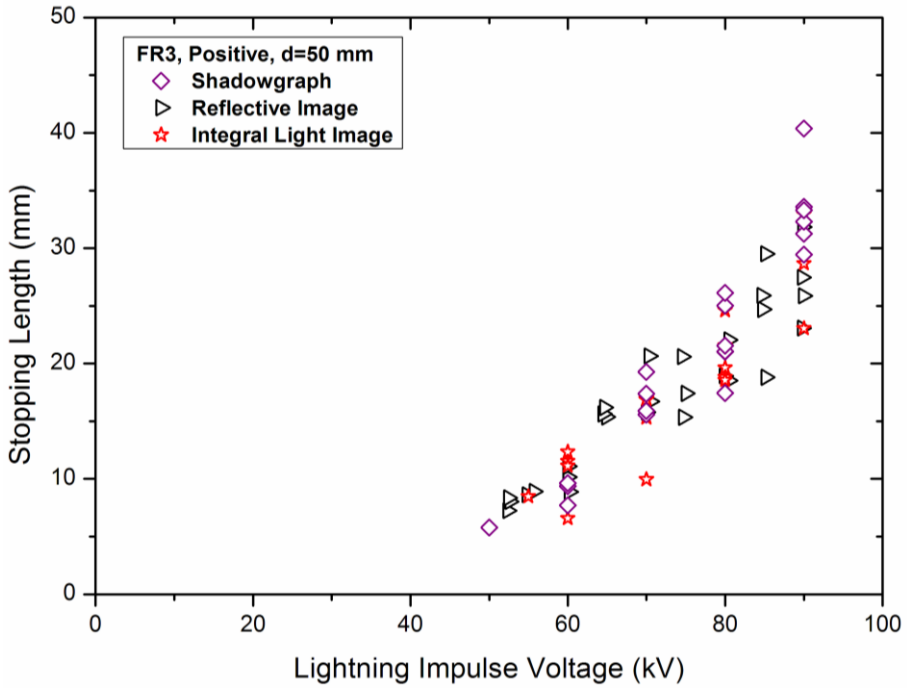

Figure 3-14 Stopping length of positive streamers obtained using various photographing setups; FR3, d=50 mm.

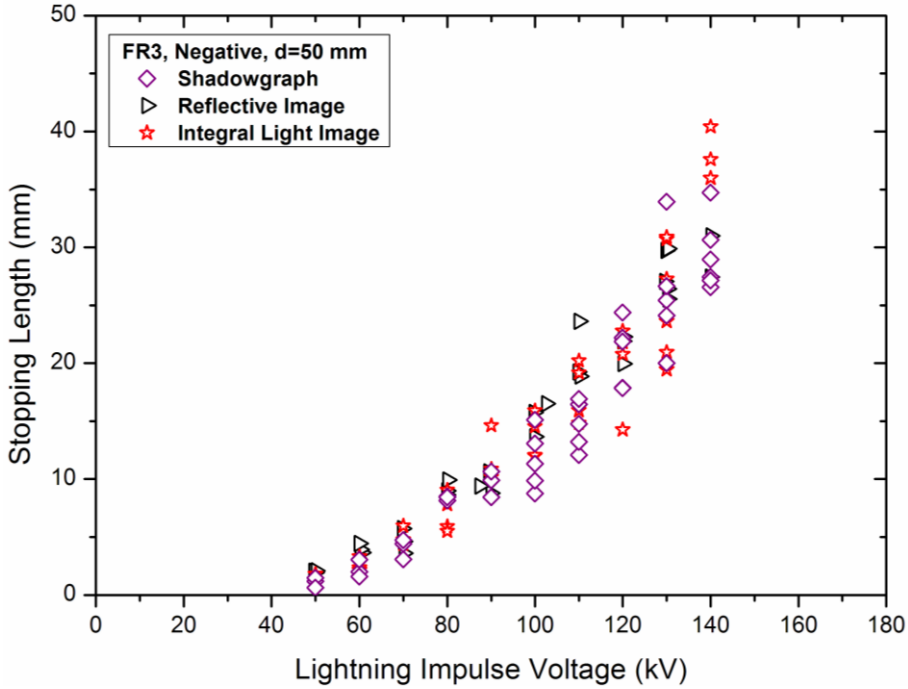

Figure 3-15 Stopping length of negative streamers obtained using various photographing setups; FR3, d=50 mm.

For tests on liquid/pressboard interface, three photographing setups including shadowgraph, integral light images in parallel and perpendicular directions to pressboard were used as well, as shown in Figure 3-16. Shadowgraph setup has the merit to capture the streamer channel shape with the help of back flash light. Since pressboard is not transparent, the camera can only be put in parallel direction to the pressboard surface, as shown in Figure 3-16 (a) and Figure 3-17 (a). Integral light image collects the streamer self-irradiated light information, and camera can be set in both parallel and perpendicular directions to the pressboard surface as shown in Figure 3-16 (b) and (c) respectively. Tests using integral light image must be taken in a dark room and the typical images are shown in Figure 3-17 (b) and (c) for parallel and perpendicular directions respectively. The setups in Figure 3-16 (a) and (b), have the advantage to see whether or not the streamer propagates along the surface, and both require careful manipulations to make sure the camera is properly set in the parallel direction to the pressboard surface.

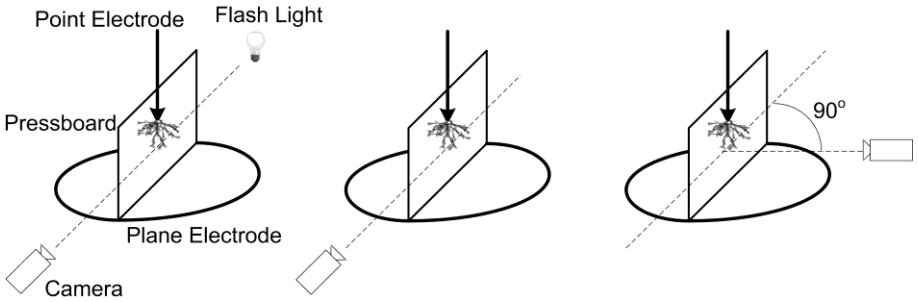

(a) Shadowgraph (b) Integral light image, parallel (c) Integral light image, perpendicular

Figure 3-16 Illustration of streamer photographing setups in tests with pressboard interface.

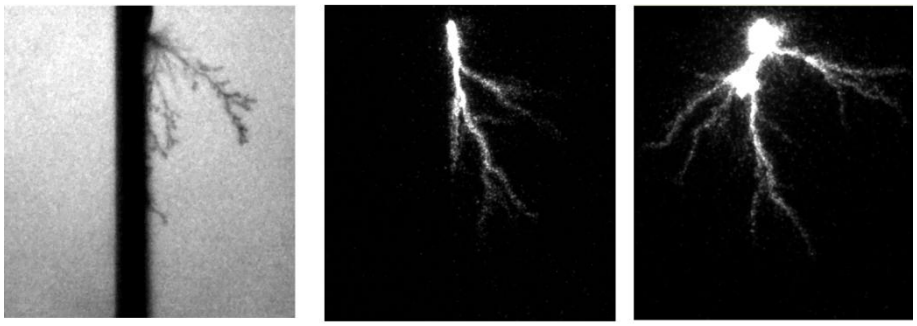

(a) Shadowgraph (b) Integral light image, parallel (c) Integral light image, perpendicular

Figure 3-17 Typical images in liquids with pressboard interface using various photographing setups; Midel 7131, negative polarity.

Verification tests as for stopping length measurements using the three photographing setups under positive and negative lightning impulses are shown in Figure 3-18 and Figure 3-19 respectively. The results indicate that stopping length obtained from different methods are overlapping with one and another in a reasonable scattering range,

so in the liquid/solid interface study, stopping length will be given as the average of all the measured data using the three photographing setups.

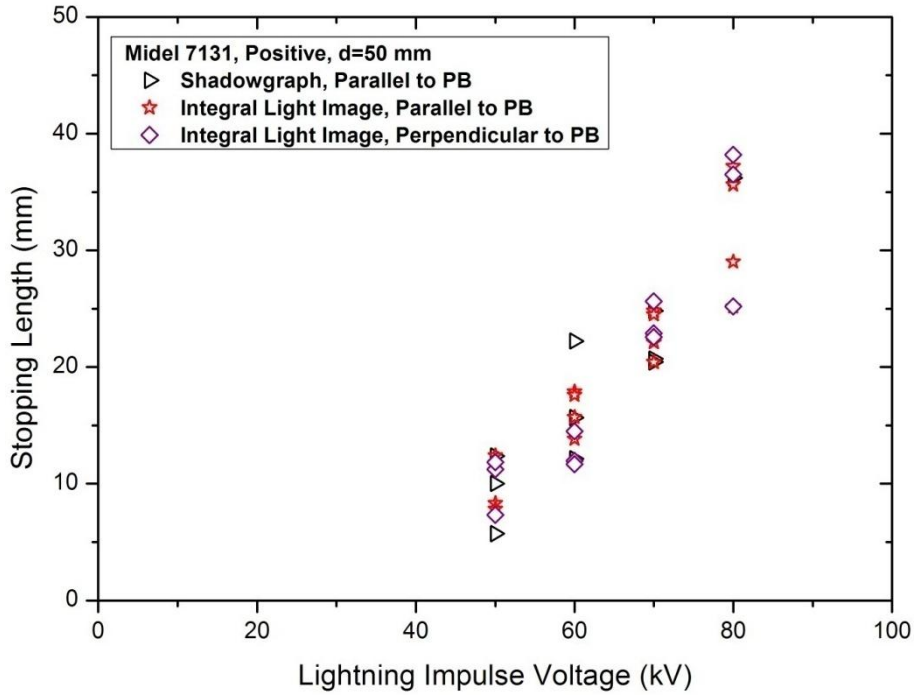

Figure 3-18 Stopping length of positive streamers on liquid/pressboard interface using various photographing setups; Midel 7131, d=50 mm.

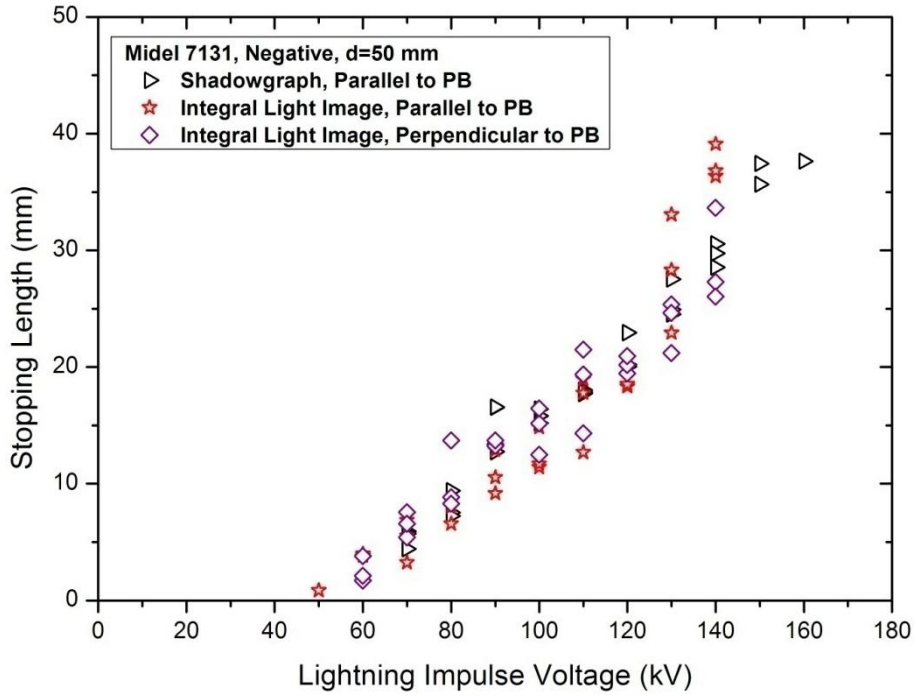

Figure 3-19 Stopping length of negative streamers on liquid/pressboard interface using various photographing setups; Midel 7131, d=50 mm.

3.4 Summary

Three types of liquid including a synthetic ester Midel 7131, a natural ester FR3 and a mineral oil Gemini X, are used in this study.

For the quasi-uniform field tests, the liquid samples are pre-processed through filtering, dehydrating and degassing. Sphere-sphere electrodes with the 3.8 mm gap distance are contained in a cylindrical test cell. A 40 kΩ current-limit resistor is used in the method comparison tests, and it has been proved that this resistor has a negligible influence on the measured breakdown voltages.

For the non-uniform field tests, the liquid samples are directly taken from the sealed new oil barrels. Pressboard is pre-processed in an air circulating oven and a vacuum oven to achieve the dry and fully-impregnated conditions. Point-plane electrodes with variable gap distances are contained in a cubic-like test cell. A high-speed camera, a photomultiplier tube and a current shunt are used to observe the streamer characteristics. Various photographing techniques including shadowgraph, reflective image and integral light image are considered in the study, and all of those techniques can provide the similar information in terms of streamer stopping length.

CHAPTER 4. BREAKDOWN STRENGTH OF ESTER LIQUIDS IN QUASI-UNIFORM FIELD

4.1 Introduction

The inner insulation structure of a power transformer is complex, as there are a large number of components with different potentials existing inside a transformer, and oil/solid composite insulation is generally used to withstand these stresses. Nevertheless the majority of electric fields in a transformer e.g. between turn to turn and disk to disk, are quasi-uniform fields.

A significant amount of experience on impulse breakdown tests has been accomplished in mineral oil. Breakdown and withstand strengths of mineral oil at various gap distances in quasi-uniform fields have been experimentally determined, in order to consider ester liquids as the alternatives for mineral oil, the first attempt of tests in this thesis is to identify the impulse breakdown strength of ester liquids in a quasi-uniform field.

Adopting one of the recommendations in ASTM D 3300 'Dielectric Breakdown Voltage of Insulating Oils of Petroleum Origin under Impulse Conditions' [93], sphere-sphere electrode configuration with a gap distance of 3.8 mm is used to provide the quasi-uniform field. Negative lightning and switching impulse tests are considered since they are normally required as routine tests for power transformers with voltage rating higher than 170 kV [17].

Various testing methods including rising-voltage method [92, 93], up-and-down method [70, 94] and multiple-level method [95] have been used for impulse breakdown tests over the past decades. Each method has its own pros and cons, and also the validity range. When comparing the impulse breakdown strength of various liquids, results based on different methods might be different and lead to a confusing situation. Therefore testing method influence on the breakdown strength of ester liquids and mineral oil is examined under lightning impulse voltage.

Besides 50% breakdown voltage, withstand voltage at low breakdown probabilities e.g. 1% is even more important for the insulation design of power transformers. Using Weibull distribution analysis, lightning withstand voltages of ester liquids are deduced and compared with those of mineral oil.

4.2 Standard Impulse Breakdown Tests

4.2.1 Lightning Impulse Breakdown Voltage

According to standard ASTM D 3300 [93], lightning impulse (LI) breakdown voltages of ester liquids and mineral oil were measured. After filling the liquid sample, the test cell was degassed under vacuum for 20 minutes. Negative impulse voltage with waveform of 1.2/50 μs was applied on a 3.8 mm sphere-sphere gap. The voltage was increased step by step with step increment of 10 kV. At each voltage level, three shots were applied and the time interval between two consecutive shots was fixed at 60 seconds. Current-limit resistor was not used in the tests, so once a breakdown occurred, both the liquid sample and the pair of sphere electrodes were changed. In total, five breakdowns were made for each type of liquid.

Results of the LI breakdown voltages for ester liquids and mineral oil are given in Table 4-1. Mean LI breakdown voltage of Gemini X is the highest, 243.9 kV, followed by Midel 7131, 208.8 kV, and then FR3, 202.8 kV. The lowest measured breakdown voltage for Gemini X is 209.0 kV, followed by 190.0 kV for FR3, and then 180.0 kV for Midel 7131. In the present tests, the standard deviation of breakdown voltages and the coefficient of variance for Gemini X are larger than those for ester liquids Midel 7131 and FR3.

Table 4-1 Lightning impulse breakdown voltages of ester liquids and mineral oil, d=3.8 mm.

Test sequence	Midel 7131	FR3	Gemini X
1	222.6	198.0	219.9
2	180.0	195.5	209.0
3	220.1	200.2	290.0
4	221.5	230.1	260.2
5	200.0	190.0	240.6
Mean LI breakdown voltage (kV)	208.8	202.8	243.9
Standard deviation (kV)	18.6	15.7	32.4
Coefficient of variance	0.09	0.08	0.13

A cross comparison of the LI breakdown voltages between ester liquids and mineral oil is plotted in Figure 4-1. Using mineral oil Gemini X as the baseline, it is found that LI breakdown voltage of synthetic ester Midel 7131 is 14% lower and 17% for natural ester FR3. In addition, time to breakdown was also recorded for each breakdown event. On average, breakdown takes approximately 3.8 μs in both ester liquids, which is slightly shorter than that 5.7 μs in mineral oil. Using the gap distance divided by the time to breakdown, the average streamer velocity is 1 km/s for ester liquids and 0.67 km/s for mineral oil. However there would be an initiation part in the parameter time to breakdown of streamers in a quasi-uniform field, so the actual propagation velocity leading to breakdown should be higher than those calculated based on the time to breakdown.

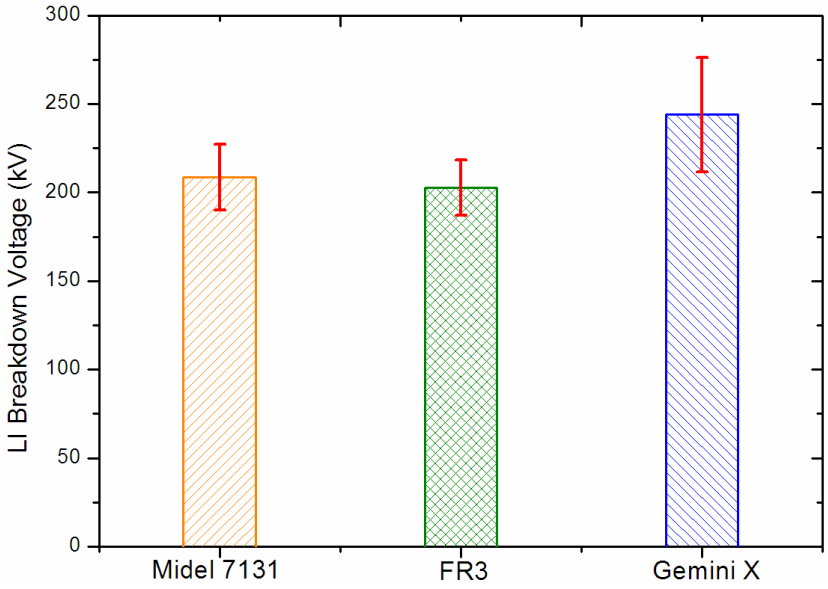

Figure 4-1 Comparison of lightning breakdown voltages between ester liquids and mineral oil; d=3.8 mm; error bars indicate one standard deviation, the same in the following figures.

4.2.2 Switching Impulse Breakdown Voltage

Similarly switching impulse (SI) breakdown voltages of ester liquids and mineral oil were measured according to standard ASTM D 3300 [93]. After filling the liquid sample, the test cell was degassed under vacuum for 20 minutes. Negative impulse voltage with waveform of 215/2500 μs was applied on a 3.8 mm sphere-sphere gap. The voltage was increased step by step with step increment of 10 kV. At each voltage level, three shots were applied and the time interval between two consecutive shots was fixed at 60 seconds. Current-limit resistor was not used in the tests, so once a breakdown

occurred, both the liquid sample and the pair of sphere electrodes were changed. In total, five breakdowns were made for each type of liquid.

Results of the SI breakdown voltages for ester liquids and mineral oil are given in Table 4-2. Mean SI breakdown voltage of Gemini X is still the highest, 184.3 kV, followed by FR3, 169.7 kV and Midel 7131, 169.2 kV. The lowest measured breakdown voltage for Gemini X is 175.0 kV, followed by 160.0 kV for FR3, and 159.8 kV for Midel 7131. The scattering ranges of breakdown voltages for all the liquids are small, as indicated by the coefficients of variance which are generally lower than 0.1.

A cross comparison of the SI breakdown voltages between ester liquids and mineral oil is plotted in Figure 4-2. Using mineral oil Gemini X as the baseline, it is found that SI breakdown voltages of ester liquids Midel 7131 and FR3 are approximately 8% lower.

Table 4-2 Switching impulse breakdown voltages of ester liquids and mineral oil, d=3.8 mm.

Test sequence	Midel 7131	FR3	Gemini X
1	176.3	166.2	189.0
2	160.0	160.0	181.0
3	159.8	162.9	182.0
4	180.0	190.3	194.9
5	170.0	169.0	175.0
Mean SI breakdown voltage (kV)	169.2	169.7	184.3
Standard deviation (kV)	9.2	12.0	7.7
Coefficient of variance	0.05	0.07	0.04

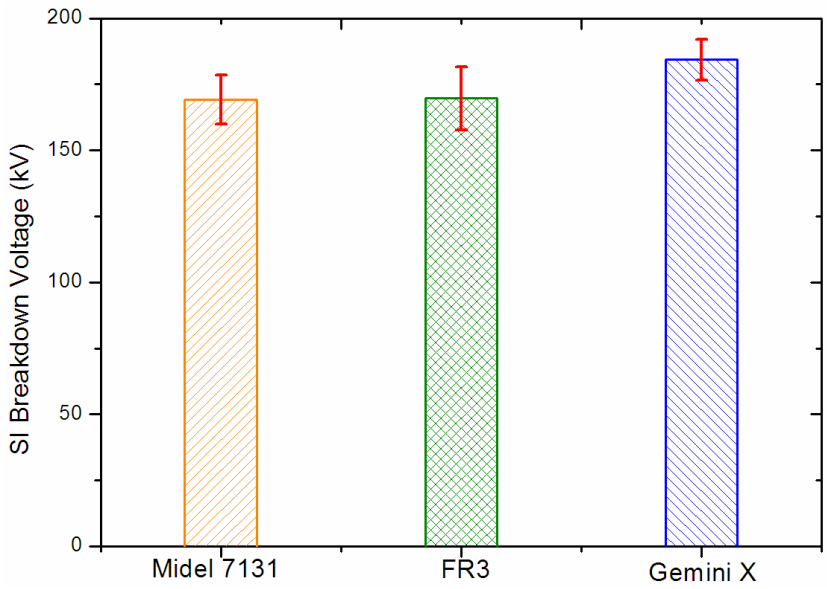

Figure 4-2 Comparison of switching breakdown voltages between ester liquids and mineral oil; d=3.8 mm.

The parameter time to breakdown was recorded as well during the tests. It should be noted that the front time of switching impulse in the present tests is about 215 μs. Most of the breakdowns occurred around the peak of switching impulse. The average time to breakdown for mineral oil Gemini X is 175.6 μs and 4 out of 5 breakdowns occurred slightly before the peak of the applied impulse. However, for synthetic ester Midel 7131, 4 out of 5 breakdowns occurred slightly after the peak of the applied impulse, which results in an average time to breakdown of 247.6 μs. As for natural ester FR3, the average time to breakdown is 232.1 μs, and 3 out 5 breakdowns occurred before the peak of applied impulse while the others after. As there is a large component of initiation time in the parameter time to breakdown under switching impulse, the streamer velocity cannot be deduced without further measurement of pre-breakdown process using current, light signals or fast imaging pictures.

4.2.3 Influence of Waveform on Breakdown Voltage

Besides LI and SI electrical strengths, it is also essential to know AC electrical strength of insulation materials. Generally transformer insulation needs to meet the impulse requirements defined by the basic insulation level (BIL), instead of using lightning strength as the design criterion, another commonly used design method is to use AC criterion with a conversion factor to account for the impulse conditions. This factor is also known as design insulation level (DIL) factor [18].

AC breakdown tests of ester liquids and mineral oil were previously conducted and published in [10], the results were reproduced in Table 4-3. The liquids were pre-processed using the same procedure described in chapter 3 and VDE electrodes with 1 mm gap were used according to ASTM D 1816 [96].

Table 4-3 AC breakdown strength obtained at 1 mm gap VDE electrodes [10].

Liquid	Midel 7131	FR3	Gemini X
E_1 (kV/mm)	45.1	44.5	47.7

To compare with LI and SI breakdown voltages, AC breakdown voltages of ester liquids and mineral oil at the gap distance of 3.8 mm are needed. However we cannot simply transfer the breakdown voltages by multiplying the gap distance ratio, since there is a scale (volume) effect which needs to be taken into account. Therefore a power

law relationship, which represents the scale effect [18, 80], is used to calculate the breakdown strength E_d at the gap distance d, given as follows:

$$E_d = E_1 \times d^{-0.38} \tag{4-1}$$

where E_1 means the electrical strength at 1 unit distance (mm), as given in Table 4-3. The power constant of -0.38 is obtained based on Weidmann AC_{rms} design curve for bulk mineral oil insulation [18, 80]. As ester liquids behaved similarly to mineral oil in quasi-uniform fields, the same constant was used for the calculation of ester liquids' breakdown voltage.

Based on equation (4-1) and Table 4-3, estimated AC breakdown voltages of ester liquids and mineral oil at the gap distance of 3.8 mm were obtained. The results together with LI and SI breakdown voltages are given in Table 4-4. Accordingly the conversion factors from AC_{rms} to LI and SI are calculated and also compared with the reference values of mineral oil [18], as given in Table 4-5.

Table 4-4 LI, SI and AC breakdown voltages of ester liquids and mineral oil, d=3.8 mm.

Liquids	Midel 7131	FR3	Gemini X
LI (kV)	208.8	202.8	243.9
SI (kV)	169.2	169.7	184.3
AC_{rms} (kV)	103.2	101.8	109.1

Table 4-5 Conversion factors (DIL) from AC_{rms} to LI and SI based on breakdown voltage.

Liquids	Midel 7131	FR3	Gemini X	Mineral oil [18]
LI	2.0	2.0	2.2	2.5
SI	1.6	1.7	1.7	1.7
AC_{rms}	1	1	1	1

As expected, the waveform of applied voltage has significant influence on the measured breakdown voltage. The generic trend is that the shorter duration the applied voltage waveform, the higher breakdown voltage it can be measured.

As shown in Figure 4-3, LI breakdown voltages are the highest, followed by SI breakdown voltages and then AC breakdown voltages for all the liquids. Taking the mineral oil as the baseline, the percentage reductions of breakdown voltage for ester liquids are approximately 15% under lightning impulse, 8% under switching impulse

and 6% under AC voltage. It is clear that lightning impulse tests show the relatively large difference between ester liquids and mineral oil.

In terms of DIL, conversion factors from AC_{rms} to SI of both ester liquids and mineral oil are almost identical to the reference value of 1.7 based on mineral oil's experience [18]. However the conversion factors from AC_{rms} to LI obtained in the present tests are generally lower than the reference value of 2.5. Especially when comparing ester liquids and mineral oil, the conversion factor from AC_{rms} to LI for ester liquids 2.0, is further lower than that of Gemini X 2.2. This difference needs to be carefully considered in the insulation design of ester filled transformers for the manufacturers who are using AC design criterion. Bearing in mind, the reference values of conversion factors [18] are mainly based on withstand voltage rather than breakdown voltage.

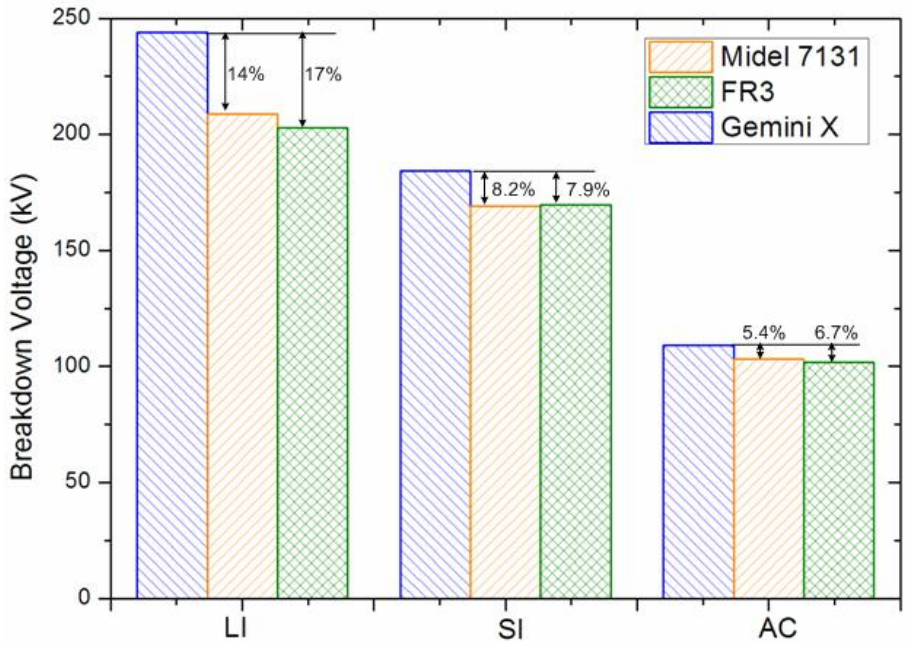

Figure 4-3 Comparison of LI, SI and AC breakdown voltages between ester liquids and mineral oil; d=3.8 mm.

Overall the lightning impulse tests tend to reveal the difference between ester liquids and mineral oil, so the following investigations e.g. comparison of testing methods, will only focus on lightning impulse voltage. In addition, lightning withstand voltage of ester liquids in the quasi-uniform field is going to be studied.

4.3 Comparison of Testing Methods

4.3.1 Rising-voltage Method

Rising-voltage method can be performed under both impulse and AC conditions [97]. For a single test, the applied voltage should be increased from an initial voltage level at a constant rate till the breakdown occurs. Repeat the single test procedure after a resting interval, until a significant number of breakdown voltages are obtained. It is widely and successfully used in AC breakdown tests due to the easy control of voltage increasing process. However for impulse tests, the voltage can only be increased shot by shot or step by step.

Both IEC 60897 and ASTM D 3300 [92, 93], standards for lightning breakdown tests of insulating liquid, adopt the rising-voltage method. The main difference between them is 1 shot per step for IEC standard while 3 shots per step for ASTM standard, as shown in Figure 4-4 (a) and (b) respectively. ΔT_1 is the time interval between two consecutive shots; ΔT_2 is the time interval between two consecutive tests and ΔU is voltage of step increment.

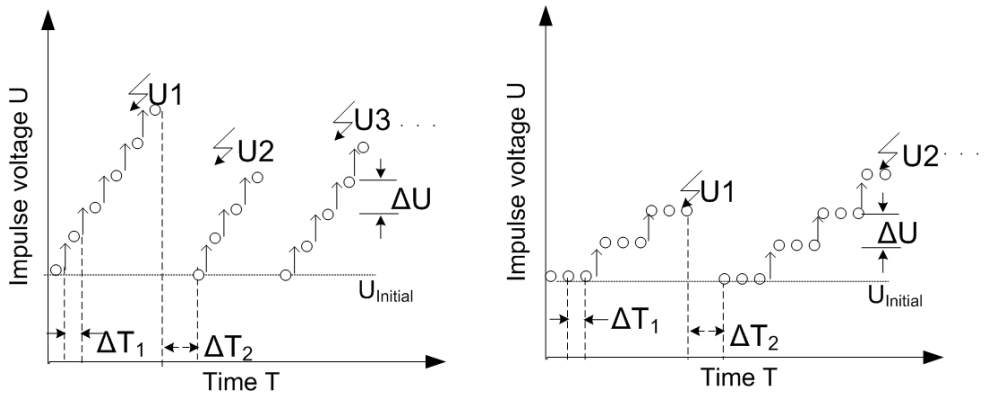

(a) 1shot/step, IEC 60897 (b) 3 shots/step, ASTM D 3300

Figure 4-4 Sketch of rising-voltage method.

Standard 1.2/50 μs lightning impulse voltage was used in the present investigation. The detailed test procedure is given as follows: after filling the liquid sample, test cell together with the liquid sample was degassed under vacuum for 20 minutes. Then a resting time of 5 minutes was given before starting the test. The initial voltage level was 140 kV; the voltage was increased step by step with step increment ΔU of 10 kV and

the time interval ΔT_1 of 60 seconds till a breakdown occurred. The 40 kΩ current-limit resistor was used in the rising-voltage tests.

For rising-voltage method, different increasing rates, 1 shot per step and 3 shots per step referring to IEC 60897 and ASTM D 3300 respectively, were investigated to see the influence on the test results if there is any. Thanks to the energy control of current-limit resistor, 15 breakdowns for each type of liquid at 1 shot per step increasing rate were obtained without changing the electrodes and liquid samples. Weibull distribution was used to fit the test results. Its cumulative distribution function is given as follows:

$$F_{Weibull}(x) = 1 - e^{-(\frac{x}{\beta})^{\alpha}} \tag{4-2}$$

where, α is shape parameter,

β is scale parameter.

The breakdown voltages and the Weibull fitting results are shown in Figure 4-5. Mineral oil Gemini X shows the highest 50% breakdown voltage of 276.4 kV, followed by Midel 7131 of 258.0 kV and then FR3 of 239.3 kV.

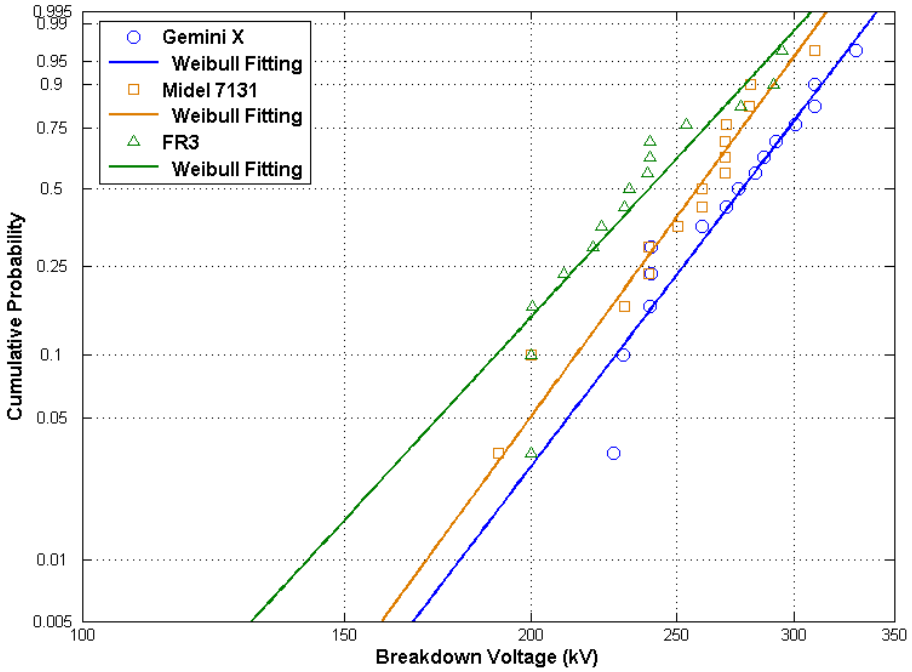

Figure 4-5 Results of lightning breakdown voltage using rising-voltage method; 1 shot/step, d=3.8 mm.

In addition, 14 breakdowns for each type of liquid at 3 shots per step increasing rate were carried out. The results with Weibull fitting are shown in Figure 4-6. Similar to the results using 1 shot per step increasing rate, mineral oil has a higher 50% breakdown voltage than ester liquids. They are 251.9 kV for Gemini X, 205.0 kV for Midel 7131 and 200.4 kV for FR3.

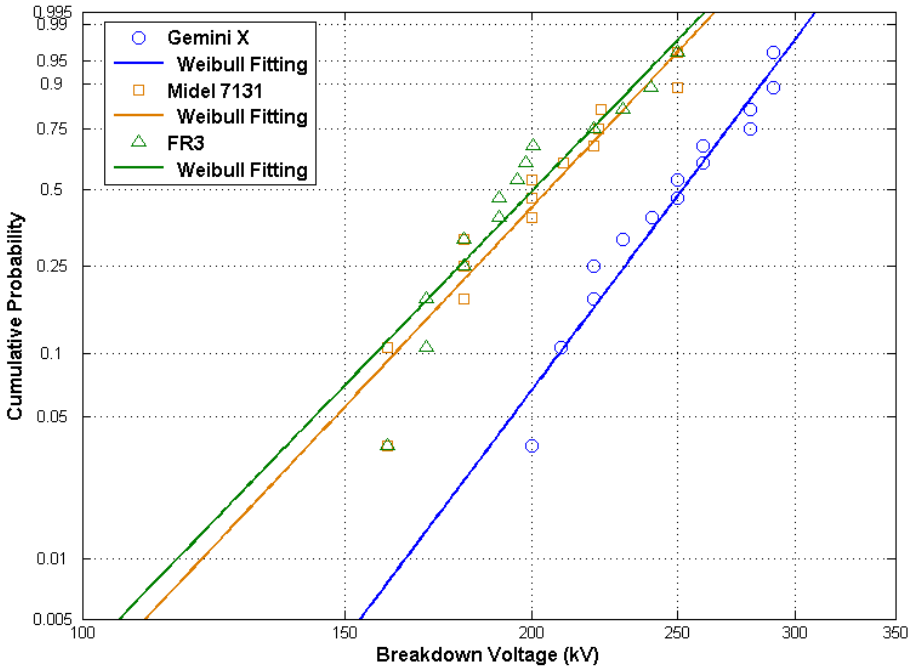

Figure 4-6 Results of lightning breakdown voltage using rising-voltage method; 3 shots/step, d=3.8 mm.

To sum up, the parameters of Weibull fitting and the 50% breakdown voltages are listed in Table 4-6. Comparing the results, it can be found that tests using 3 shots per step procedure result in lower breakdown voltages than those using 1 shot per step procedure. Since more shots at a voltage level (e.g. 3 shots per step) offer more chances for a breakdown to occur at that voltage level, it is reasonable to see 50% breakdown voltage obtained using 3 shots per step procedure is lower than that using 1 shot per step procedure.

Table 4-6 Lightning impulse breakdown voltages using rising-voltage methods (kV).

Liquid		Midel 7131	FR3	Gemini X
1 shot/step	Scale	267.5	250.4	287.0
	Shape	10.1	8.0	9.7
	$U_{50\%}$	258.0	239.3	276.4
3 shots/step	Scale	214.7	210.1	261.4
	Shape	7.9	7.7	9.9
	$U_{50\%}$	205.0	200.4	251.9

4.3.2 Up-and-down Method

Up-and-down method, proposed by Dixon and Mood, permits an estimation of 50% breakdown voltage, when the breakdown voltage is normally distributed [97]. It is widely used in impulse breakdown tests to save the testing time. Procedure of up-and-down method is illustrated in Figure 4-7: (i) The voltage is raised from an initial value, at which with certainty no breakdown would occur, in steps of a fixed amplitude ΔU, and till the first breakdown occurs; (ii) The voltage is reduced by the same step ΔU until breakdown does not occur; (iii) The voltage is raised again till another breakdown occurs, and so on so forth. The average value of the applied voltages of which the lowest voltage level taken into account should have at least two shots, is regarded as the 50% breakdown voltage [97].

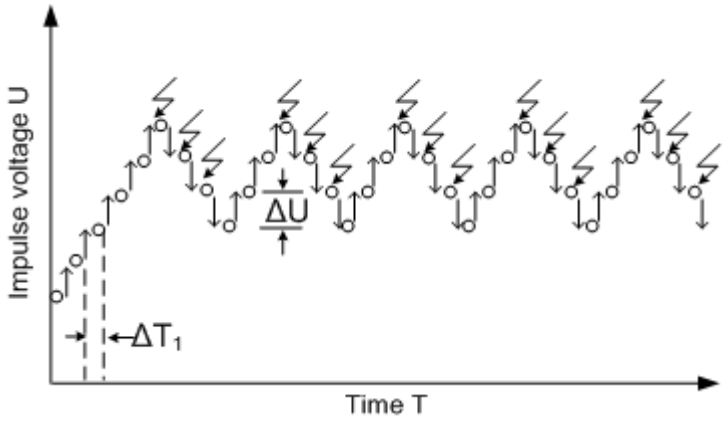

Figure 4-7 Sketch of up-and-down method.

Standard 1.2/50 μs lightning impulse voltage was used in the present tests. The initial voltage level was 150 kV, the step voltage ΔU was 10 kV and the time interval ΔT_1 was 60 seconds. 30 shots were applied for each set of tests. The 40 kΩ current-limit resistor was also used in the up-and-down tests.

Results of the lightning breakdown tests for ester liquids and mineral oil using up-and-down method are shown in Figure 4-8. Since up-and-down method was a continuous procedure, we did not change the liquid sample and electrodes after breakdowns during the one set of tests for a liquid. The applied voltages generally keep stable in a reasonably up-and-down scatting range for all the liquids. There is a small difference observed between ester liquids and mineral oil in terms of lightning

breakdown voltage: 232.8 kV for Gemini X, 223.2 kV for Midel 7131 and 212.9 kV for FR3.

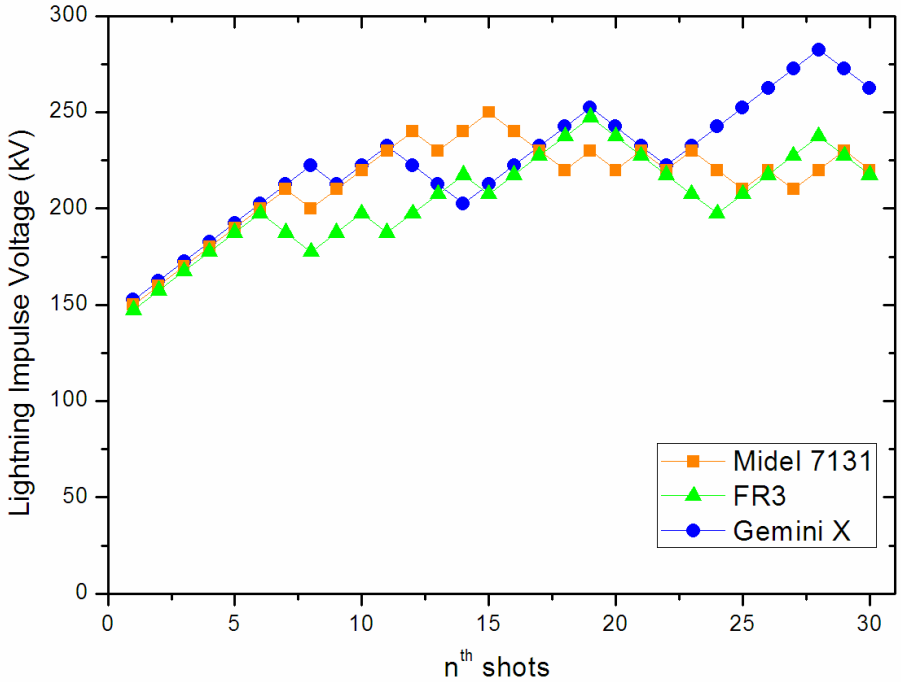

Figure 4-8 Results of lightning breakdown voltage using up-and-down method; d=3.8 mm.

4.3.3 Multiple-level Method

Multiple-level method, also named as constant-voltage method, represents the 'classic' method for determining breakdown probability [97], as shown in Figure 4-9. The procedure is applying a fixed number of shots at various voltage levels and recording the corresponding number of breakdowns at each voltage level. Based on the results, the cumulative frequency plot can be obtained.

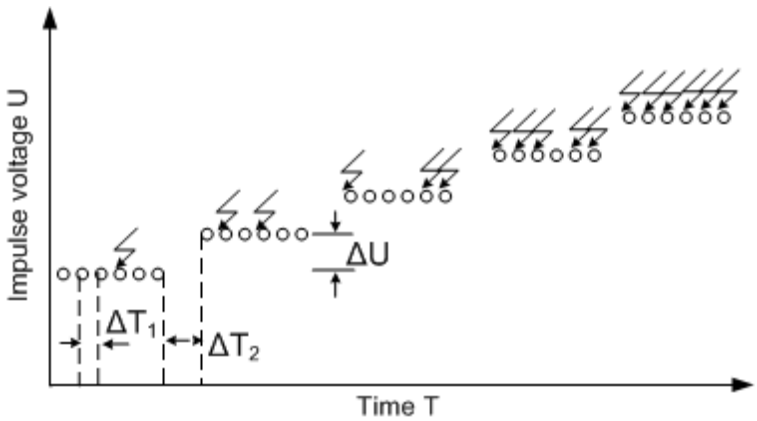

Figure 4-9 Sketch of multiple-level method.

Standard 1.2/50 μs lightning impulse voltage was used in the present tests. 20 shots with time interval ΔT_1 of 60 seconds were applied for each voltage level. Step voltage ΔU between two consecutive voltage levels was 20 kV. According to the experience of the previous tests, the initial level for Gemini X was set at 240 kV and 200 kV for both Midel 7131 and FR3. The 40 kΩ current-limit resistor was used in the multiple-level tests as well.

As for multiple-level method if applying a small number of shots per voltage level, the scatter of cumulative frequency would be large; however if applying a large number of shots per voltage level, the change of oil condition (discharge by-products, space charge accumulation) should be carefully considered and also the time consuming issue pops up. Consequently in the present study, only a small scale of tentative tests were done by using multiple-level method, as shown in Figure 4-10. Accordingly the 50% breakdown voltages are obtained as follows: 270.0 kV for Gemini X, 248.9 kV for Midel 7131 and 230.8 kV for FR3.

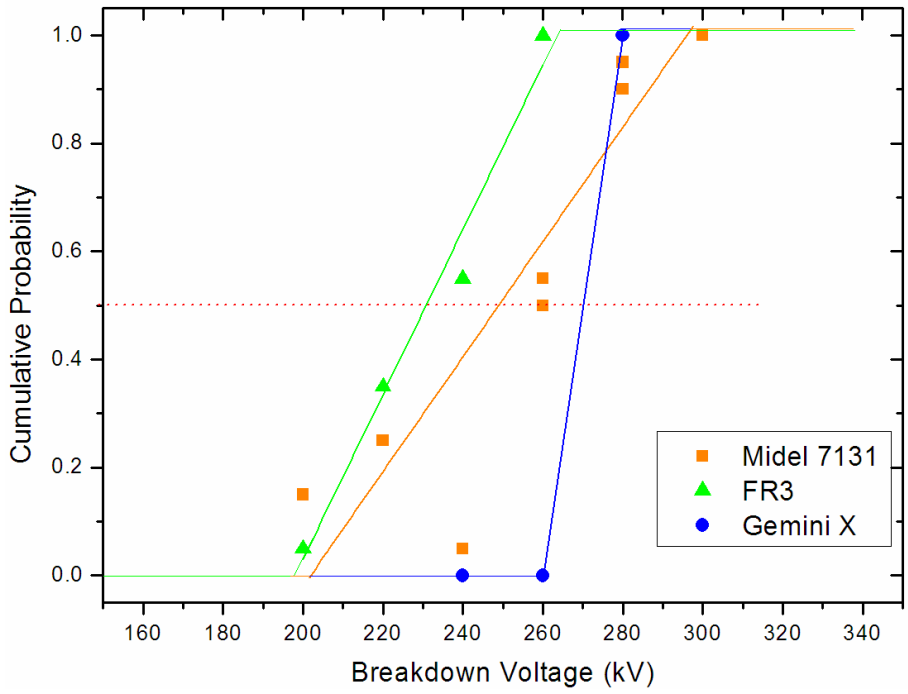

Figure 4-10 Results of lightning breakdown voltage using multiple-level method; d=3.8 mm.

4.3.4 Influence of Method on Measured Breakdown Voltage

50% lightning impulse breakdown voltages of ester liquids and mineral oil using various testing methods are summarized in Table 4-7. It is found that testing methods

have notable influence on the measured breakdown voltage. As for rising-voltage method, results using 3 shots per step procedure are lower than those using 1 shot per step procedure. Multiple-level method and rising-voltage method with 1 shot per step increasing rate provide the closest results, which are generally higher than those obtained using the other two methods.

However the testing methods which influence the absolute breakdown voltages, do not affect the ranking of liquids for the aim of comparison. As indicated in Figure 4-11, ester liquids always show lower lightning breakdown voltage than mineral oil no matter which kind of method is used. Considering mineral oil Gemini X as the baseline, the percentage reductions of breakdown voltage for ester liquids are less than 20%.

Table 4-7 Lightning impulse breakdown voltages of ester liquids and mineral oil using various testing methods, d=3.8 mm (kV).

Liquid	Midel 7131	FR3	Gemini X
Rising-voltage (1 shot/step)	258.0	239.3	276.4
Rising-voltage (3 shots/step)	205.0	200.4	251.9
Up-and-down	223.2	212.9	232.8
Multiple-level	248.9	230.8	270.0

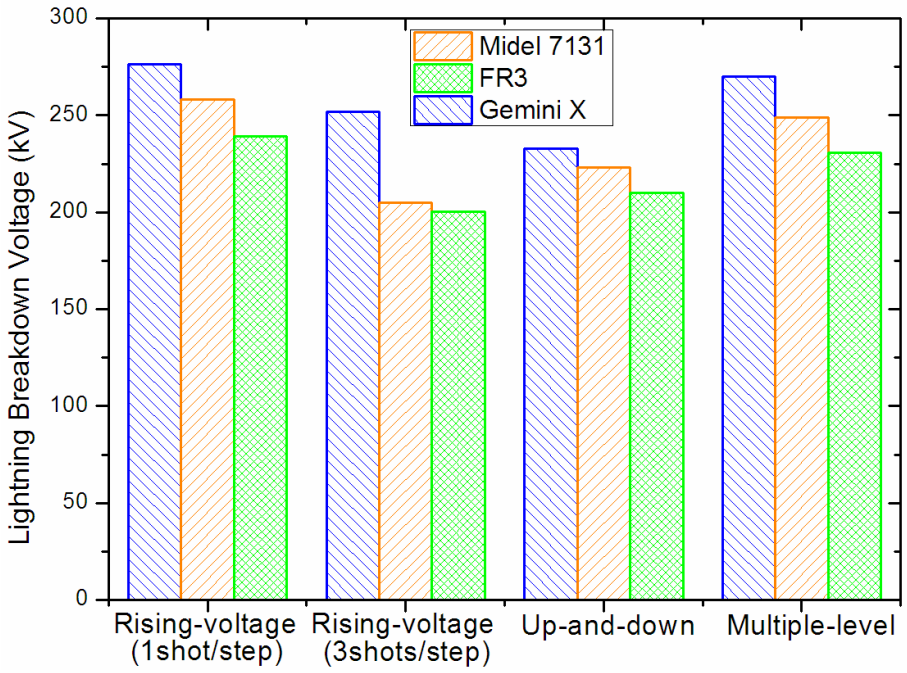

Figure 4-11 Comparison of lightning breakdown voltages between ester liquids and mineral oil using various testing methods; d=3.8 mm.

4.4 Lightning Withstand Voltage

4.4.1 Determination of Withstand Voltage

Withstand voltage is critically important for the insulation design of power transformers. Weibull distribution is usually used to fit the breakdown data, and then withstand voltage can be calculated based on the fitted curve with specific shape and scale parameters. The limitation of this method is the small sample size of the breakdown tests which could result in a large uncertainty of the predicted withstand voltage.

In the methodology studies including rising-voltage method, up-and-down method and multiple-level method, in total a large number of tests have been done for each type of liquid i.e. 1255 shots at various voltage levels for Gemini X, 912 shots for Midel 7131 and 639 shots for FR3. Ideally each single test should be an independent event and the obtained results should be independent of the test procedure. In practice, it is difficult to reach such an ideal condition. However, some tactics can be used to minimize the influence of test procedure and maximally ensure the independence of each single test. In the present methodology studies, the following actions were taken: (i) the liquid sample was filtered, dehydrated and degassed before the tests; (ii) a 60 seconds time interval, according to IEC and ASTM standards [92, 93], was used between two consecutive shots; (ii) a current-limit resistor was used to protect the electrodes and liquid sample when breakdown occurred; (iv) after breakdown occurred, there was at least 5 minutes time interval till next shot and the liquid sample was regularly changed after about 10 breakdowns on average.

To maximally utilize the data obtained by using different procedures, all of those data are combined together as one set of data and sorted according to the applied voltage level. By counting the breakdown events, withstand and breakdown probabilities at each voltage level can be calculated, as given in Table 4-8 to Table 4-10. As it is suggested that at least 10 shots should be applied at each voltage level to calculate the breakdown probability [98], all the data are further processed using the same criterion that data with applied shot $N \leq 10$ are filtered out, as shown in Figure 4-12 to Figure 4-14.

Table 4-8 Lightning breakdown probability at various voltage levels for Midel 7131.

Voltage Level (kV)	Applied Shots N	Withstand Probability	Breakdown Probability
125	36	1.000	0.000
130	30	1.000	0.000
140	63	1.000	0.000
150	62	1.000	0.000
160	60	0.967	0.033
170	53	0.981	0.019
180	50	0.940	0.060
190	46	0.978	0.022
200	73	0.877	0.123
210	46	0.935	0.065
220	89	0.831	0.169
230	42	0.810	0.190
240	56	0.857	0.143
245	10	0.600	0.400
250	29	0.483	0.517
255	10	0.800	0.200
260	57	0.509	0.491
270	11	0.364	0.636
280	65	0.077	0.923
290	2	0.500	0.500
300	21	0.048	0.952
310	1	0.000	1.000

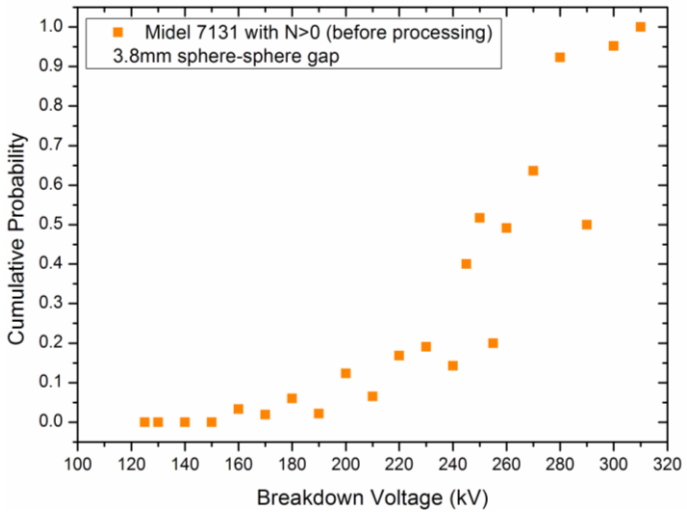

(a) Data before processing

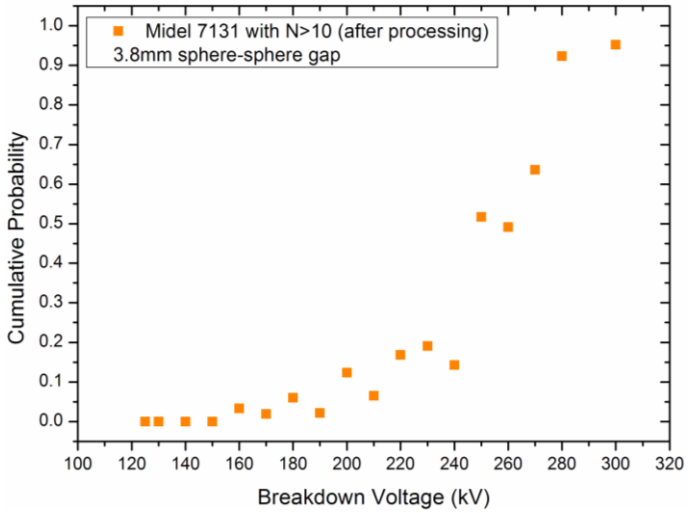

(b) Data after processing, filtered using criterion of N>10

Figure 4-12 Cumulative probability plot for withstand voltage calculation of Midel 7131.

Table 4-9 Lightning breakdown probability at various voltage levels for FR3.

Voltage Level (kV)	Applied Shots N	Withstand Probability	Breakdown Probability
125	33	1.000	0.000
130	30	1.000	0.000
140	58	1.000	0.000
150	58	1.000	0.000
160	56	0.982	0.018
170	52	0.962	0.038
180	50	0.960	0.040
190	43	0.907	0.093
200	57	0.860	0.140
210	28	0.929	0.071
220	47	0.723	0.277
230	21	0.762	0.238
240	66	0.470	0.530
250	8	0.625	0.375
260	23	0.130	0.870
270	3	1.000	0.000
280	3	0.667	0.333
290	2	0.500	0.500
300	1	0.000	1.000

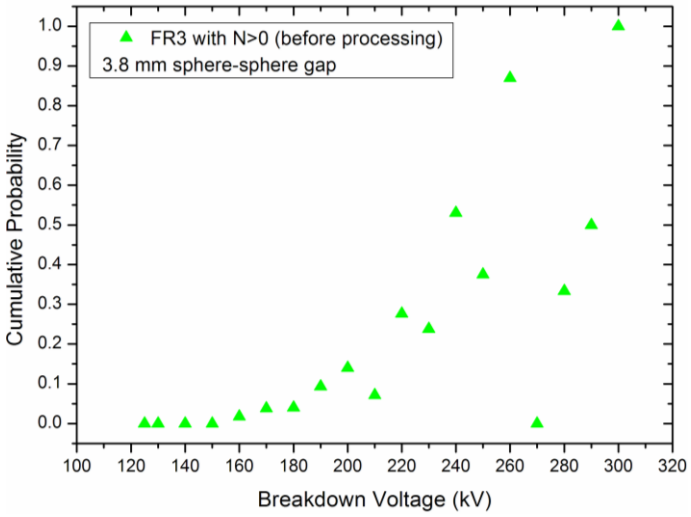

(a) Data before processing

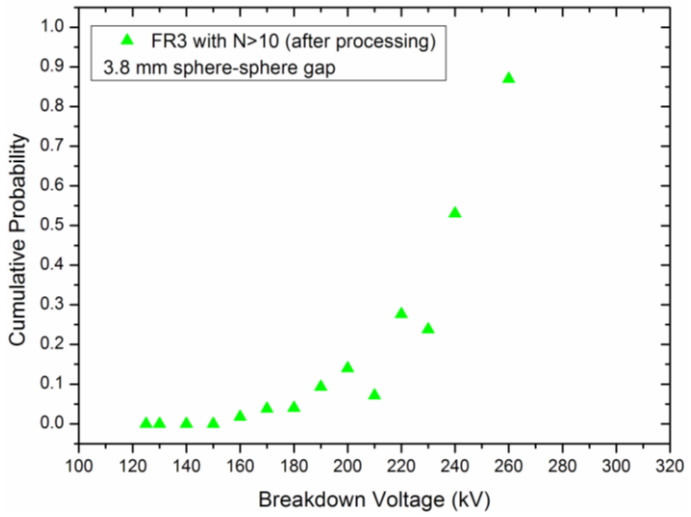

(b) Data after processing, filtered using criterion of N>10

Figure 4-13 Cumulative probability plot for withstand voltage calculation of FR3.

Table 4-10 Lightning breakdown probability at various voltage levels for Gemini X.

Voltage Level (kV)	Applied Shot N	Withstand Probability	Breakdown Probability
125	9	1.000	0.000
130	45	1.000	0.000
140	83	1.000	0.000
150	82	1.000	0.000
160	78	0.974	0.026
170	96	0.979	0.021
180	95	0.979	0.021
190	93	0.978	0.022
200	96	0.927	0.073
210	85	0.965	0.035
220	85	0.906	0.094
230	73	0.918	0.082
240	94	0.904	0.096
250	60	0.733	0.267
260	80	0.600	0.400
270	41	0.634	0.366
280	42	0.381	0.619
290	9	0.667	0.333
300	4	0.750	0.250
310	3	0.333	0.667
320	1	1.000	0.000
330	1	0.000	1.000

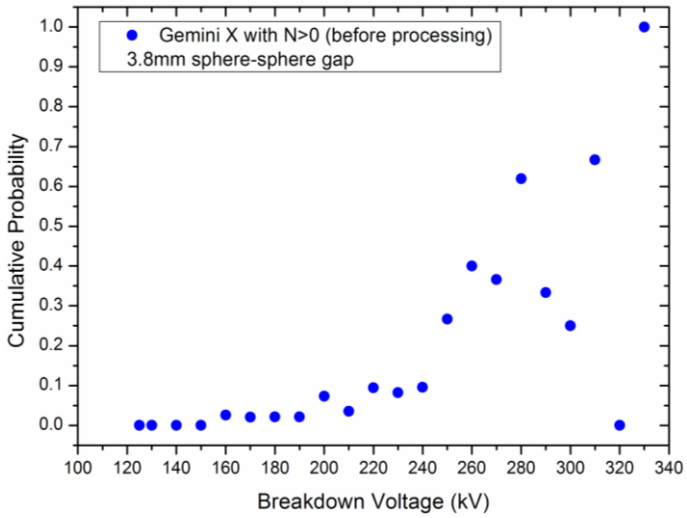

(a) Data before processing

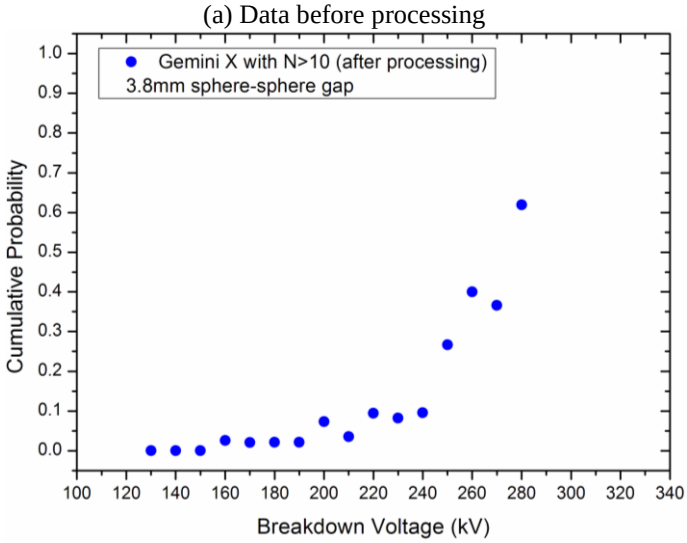

(b) Data after processing, filtered using criterion of N>10

Figure 4-14 Cumulative probability plot for withstand voltage calculation of Gemini X.

The processed data for each type of liquid are plotted together in Figure 4-15. Weibull distribution is used to fit the breakdown probability data and its scale and shape parameters are given in Table 4-11. Knowing the specific shape and scale parameters of Weibull function, the withstand voltage at low breakdown probabilities e.g. 1% can be easily deduced. As indicated in Table 4-11, the 50% breakdown voltages of ester liquids are lower than that of mineral oil which is consistent with previously drawn conclusions using various testing methods. Moving down to the low breakdown probability, the difference between ester liquids and mineral oil becomes smaller. As for withstand voltages at 1% breakdown probability, they are 153.1 kV and 151.0 kV for Midel 7131 and FR3 respectively, which are slightly lower than that of mineral oil 156.7 kV.

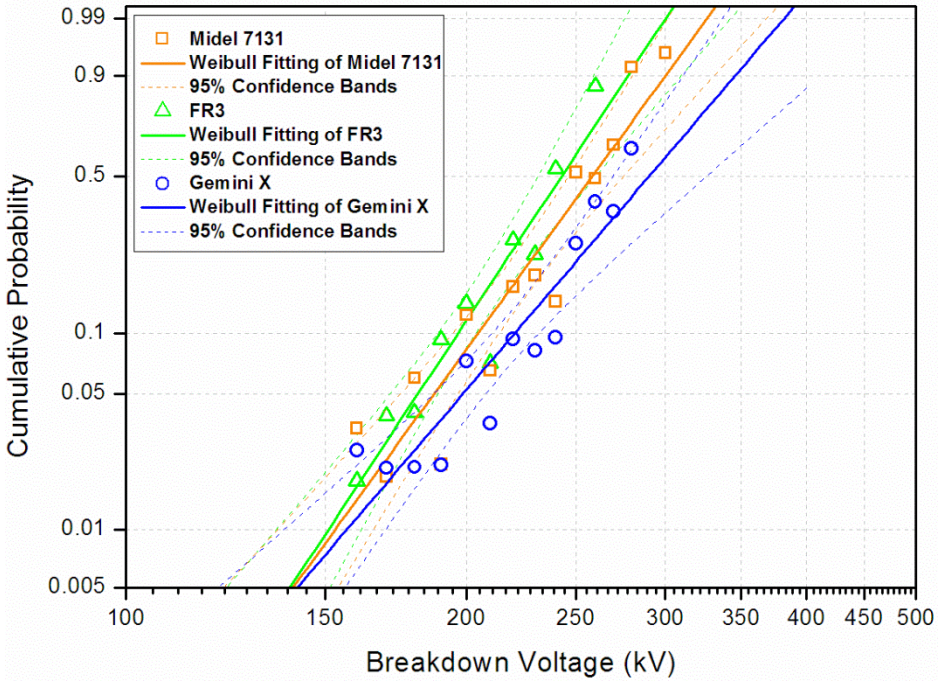

Figure 4-15 Cumulative probability versus breakdown voltage for withstand voltage calculation using Weibull fitting; d=3.8 mm.

Table 4-11 Lightning withstand voltages of ester liquids and mineral oil, d=3.8 mm.

Liquids		Midel 7131	FR3	Gemini X
Weibull fitting parameters	Scale	270.47	252.95	306.04
	Shape	8.08	8.91	6.87
	R^2	0.878	0.906	0.852
Withstand voltage (kV)	50%	258.5	242.8	290.1
	1.0%	153.1	151.0	156.7

4.4.2 Comparison with Tests at Large Gap Distances

The results in the present tests at a 3.8 mm sphere-sphere gap are compared with those results at large gap distances up to 150 mm in the literatures [75, 76, 78], as shown in Figure 4-16, all of these results were conducted under negative 1.2/50 μs lightning impulse voltage.

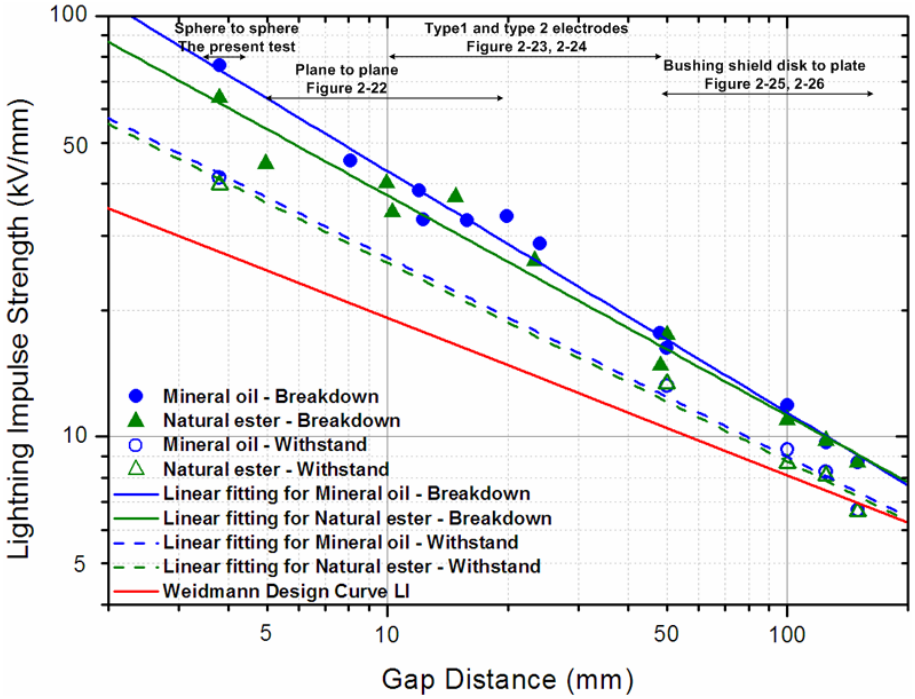

Figure 4-16 Negative lightning impulse strengths of ester liquids and mineral oil versus gap distances in quasi-uniform fields, the data at gaps from 5 mm to 150 mm are obtained from the literatures [75, 76, 78].

50% breakdown strength (50% breakdown voltage divided by the gap distance) 63.9 kV/mm and 76.3 kV/mm for natural ester and mineral oil respectively and 1% withstand strength (1% withstand voltage divided by the gap distance) 39.7 kV/mm and 41.2 kV/mm for natural ester and mineral oil respectively are plotted in Figure 4-16 to represent the results of the present tests.

Tests at gap distances from 5 mm to 20 mm were carried out using plane to plane electrodes, as shown in Figure 2-22 [78]; Tests at gap distance of approximately 10-12 mm were carried out using type 2 electrodes, as shown in Figure 2-23 (b) and Figure 2-24 [75]; tests at gap distances from 25 mm to 50 mm were done using type 1 electrodes, as shown in Figure 2-23 (a) and Figure 2-24 [75]; tests at gap distances from 50 mm to 150 mm were carried out using bushing shield disk to plate electrodes, as shown in Figure 2-25 and Figure 2-26 [76]. The Weidmann design curve for lightning

impulse stress is obtained using the AC discharge inception design curve [80] multiplied by the design insulation level factor of 2.5 [75].

As shown in Figure 4-16, the present results at the small gap distance of 3.8 mm match well those results at large gaps. It is noted that lightning impulse strengths for both breakdown and withstand decrease with the increase of gap distance in a linear relationship under logarithm scale. Therefore the power law function can be used to fit the data, and the deduced empirical formulas for lightning impulse strength *E* at the gap distance *d* are given as follows:

$$E_{\mathrm{MineralOil-breakdown}} = 160.15 \times d^{-0.57} \tag{4-3}$$

$$E_{\mathrm{NaturalEster-breakdown}} = 124.86 \times d^{-0.52} \tag{4-4}$$

$$E_{\mathrm{MineralOil-1\%\,withstand}} = 79.48 \times d^{-0.47} \tag{4-5}$$

$$E_{\mathrm{NaturalEster-1\%\,withstand}} = 76.84 \times d^{-0.47} \tag{4-6}$$

Generally the 1% withstand strengths are lower than 50% breakdown strengths and the decreasing trends with gap distance for both of them are almost in parallel. Comparing natural ester and mineral oil, it is remarkable that the negative lightning impulse strengths of natural ester stay close to those of mineral oil at the gap distances up to 150 mm. Importantly, the withstand strengths of both natural ester and mineral oil are higher than the Weidmann design curve, except for a little overlapping at the gap distance of 150 mm.

4.5 Summary

Electrical strengths of ester liquids in a quasi-uniform field under negative impulse voltage were examined in this chapter. Sphere-sphere electrodes with a gap distance of 3.8 mm were used throughout the investigation.

It was found that breakdown voltages of ester liquids are lower than those of mineral oil under both standard lightning impulse (1.2/50 μs) and switching impulse (215/2500 μs).

In addition lightning impulse breakdown voltages showed relatively larger differences between ester liquids and mineral oil than those of switching impulse.

Therefore the detailed tests and analyses only focused on lightning impulse voltage. Various testing methods including rising-voltage method (1 shot/step and 3 shots/step), up-and-down method and multiple-level method were comparatively studied to determine the lightning breakdown voltage. The results indicated that the testing methods have notable influences on the absolute breakdown voltages, but do not affect the ranking of liquids for the purpose of comparison. No matter which method was used, ester liquids showed lower breakdown voltages than mineral oil. Using mineral oil as the baseline, the percentage reductions of breakdown voltage for ester liquids are generally less than 20%.

By combining the test data obtained in method comparison study and using Weibull distribution fitting, 1% withstand voltages of ester liquids were deduced, which were found to be close to those of mineral oil.

At last both breakdown and withstand voltages of natural ester and mineral oil were compared with those published in the literatures at large gap distances up to 150 mm. It was found that both breakdown and withstand voltages of ester liquids stay close to those of mineral oil and all of them lie above the Weidmann design curve for lightning impulse stress.

In general it is concluded that lightning impulse strengths of ester liquids are comparable to those of mineral oil at various gap distances in a quasi-uniform field. As there is no polarity effect expected in such a quasi-uniform field, the conclusion based on negative polarity tests should be valid for positive polarity as well.

In quasi-uniform fields, breakdown event is mainly controlled by the streamer initiation, of which the results indicate the similarities between ester liquids and mineral oil. As streamer propagation dominates the process leading to a breakdown in a strongly non-uniform field, the following three chapters will focus on the streamer propagation and breakdown performances of ester liquids in a strongly non-uniform field under lightning impulse voltage.

CHAPTER 5. STREAMER AND BREAKDOWN OF ESTER LIQUIDS IN NON-UNIFORM FIELD

5.1 Introduction

A number of studies on traditional mineral oil were published [29, 32, 33, 35, 53, 99], describing the streamer initiation and propagation. It is acknowledged that impulse pre-breakdown and breakdown characteristics are related to chemical composition of the liquid, so application of ester liquids (with composition different to mineral oil) calls for detailed investigation under impulse voltage.

There are rarely comparative studies on streamer and breakdown phenomena across natural ester, synthetic ester and mineral oil. Furthermore, most of the recent studies have been using step impulse voltage (fast front <0.5 μs and long tail >1000 μs), which aimed to distinguish streamer modes and facilitate data interpretation from academic point of view. However, to provide guidance for industry practice there is still a strong need to study the pre-breakdown and breakdown properties of ester liquids under standard lightning impulse voltage.

This chapter focuses on streamer propagation and breakdown event of both natural ester and synthetic ester liquids under the standard lightning impulse voltage. Streamer shape, mode, length and velocity are analyzed under both positive and negative polarities. 50% breakdown voltages at various gap distances are compared between ester liquids and mineral oil. A relationship between the results under lightning impulse and previously published results under step voltage is built up and empirical formulas are obtained to predict the lightning breakdown voltages of ester liquids at very large gaps.

5.2 Basic Characteristics of Streamer

5.2.1 Shape Feature

Shape features, e.g. configuration, branch number and diameter, directly offer the visual information to distinguish the various modes of streamers and can be used to compare the different liquids. Figure 5-1 and Figure 5-2 show the typical shadowgraph images of

both positive and negative streamers in Midel 7131, FR3 and Gemini X. Under positive polarity as shown in Figure 5-1, streamers in the three liquids are with stopping length of ~29.5 mm and the similar tree-like structures. The branch of the positive streamer is so thin that the observation is made difficult. As for negative streamers in the three liquids with the similar stopping length of ~25.0 mm, the shape characteristics are clearly different as shown in Figure 5-2. Streamer in Gemini X normally has one or two main branches with many small offshoots. However streamers in ester liquids have more branches than in mineral oil, especially for Midel 7131, the branches even tend to propagate in lateral directions. In addition, the channel of negative streamer is much thicker than that of positive streamer.

Figure 5-1 Shadowgraph images of positive streamers in ester liquids and mineral oil; d=50 mm, (a) Midel 7131, V=80 kV, length 31.9 mm, exposure time 2 μs, (b) FR3, V=90 kV, length 28.68 mm, exposure time 2 μs, (c) Gemini X, V=90 kV, length 27.64 mm, exposure time 2 μs; plane electrode is adjusted as the bottom line of the image, the same as following figures.

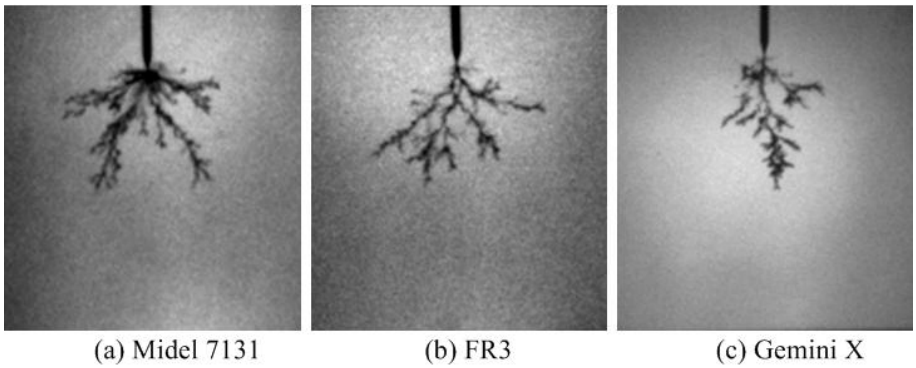

Figure 5-2 Shadowgraph images of negative streamers in ester liquids and mineral oil; d=50 mm, (a) Midel 7131, V=-140 kV, length 26.98 mm, exposure time 2 μs, (b) FR3, V=-130 kV, length 23.62 mm, exposure time 2 μs, (c) Gemini X, V=-220 kV, length 24.58 mm, exposure time 3 μs.

5.2.2 Current and Light Signals

Time-resolved recordings of current and light signals are useful for describing the streamer propagation and understanding the underlying mechanism of a streamer. Based on the previous experience of mineral oil, a train of discrete pulses either with or

without a continuous DC component are generally observed for current and light signals [30, 45]. Those signals of both positive and negative streamers in ester liquids, at from low to breakdown voltage level, are shown in Figure 5-3 to Figure 5-5. Charging process at the wavefront of impulse voltage induces some noises in both current and light signals, and these noises are consequently ignored in the following analysis.

At low voltage level just above inception as shown in Figure 5-3, a short train of discrete pulses with increasing amplitude are commonly observed for both positive and negative streamers. Current and light signals usually correlate with each other in time occurrence. The current and light signals of positive streamers have higher repetition rate but lower amplitude than those of negative streamers. The highly intense signals of positive streamers tend to show a weak continuous DC component, as shown in Figure 5-3 (a).

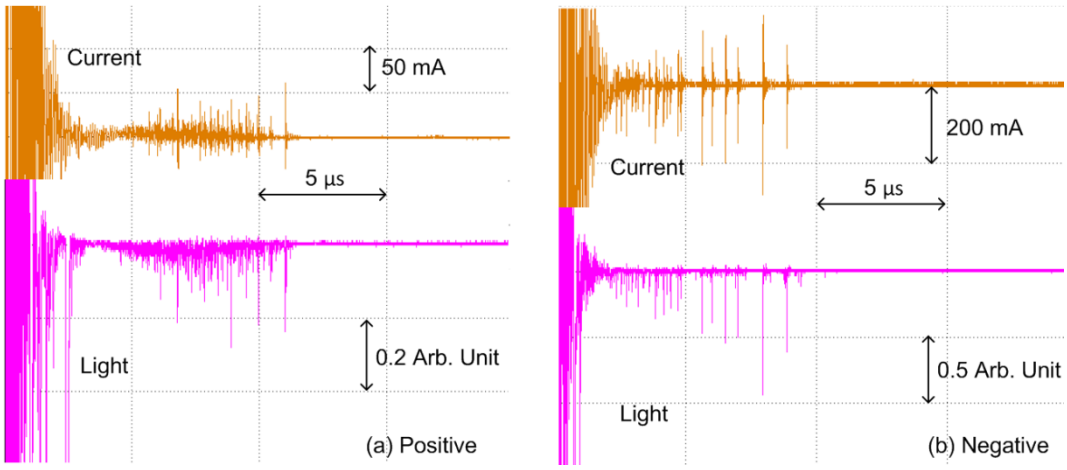

Figure 5-3 Recordings of current and light signals of positive and negative streamers at low voltage level above inception; d=50 mm, (a) positive streamer, V=60 kV, FR3, (b) negative streamer, V=-70 kV, Midel 7131.

With the increase of applied voltage, current and light signals become gradually stronger with larger amplitude. For positive streamers, a continuous DC component imposed by the discrete pulses is usually observed, as shown in Figure 5-4 (a). The continuous component seems to be stronger at the early half duration of the streamer propagation. At high-voltage level close to breakdown, current and light signals clearly show the two-phase propagation of negative streamers: the initial phase of large pulses with similar amplitude and the latter normal phase of a train of discrete pulses with increasing amplitude, as shown in Figure 5-4 (b). The initial phase represents the fast 3rd mode propagation while the latter phase stands for the slow 2nd mode propagation. This

phenomenon exists in both positive and negative streamers, and its existence can also be observed by the fast imaging of streamer propagation as given in the next section.

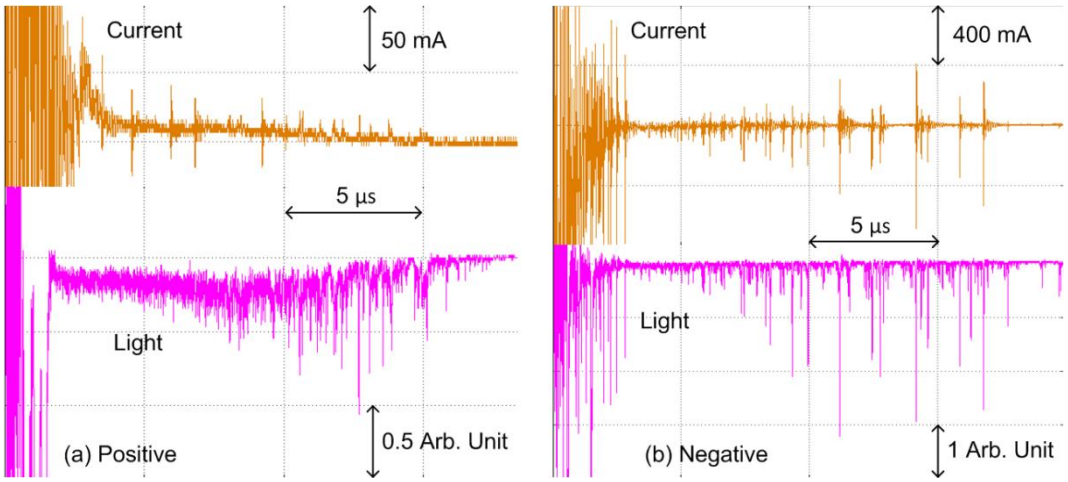

Figure 5-4 Recordings of current and light signals of positive and negative streamers at high-voltage level below breakdown; d=50 mm, (a) positive streamer, V=80 kV, Midel 7131, (b) negative streamer, V=-130 kV, FR3.

Figure 5-5 shows the typical recordings of current and light signals of both positive and negative streamers when a breakdown occurs. The current and light signals of positive streamers before breakdown are still very low compared with those of negative streamers. Large current pulses with amplitude of approximate a few amperes are observed for negative streamers before the breakdown takes place, as shown in Figure 5-5 (b).

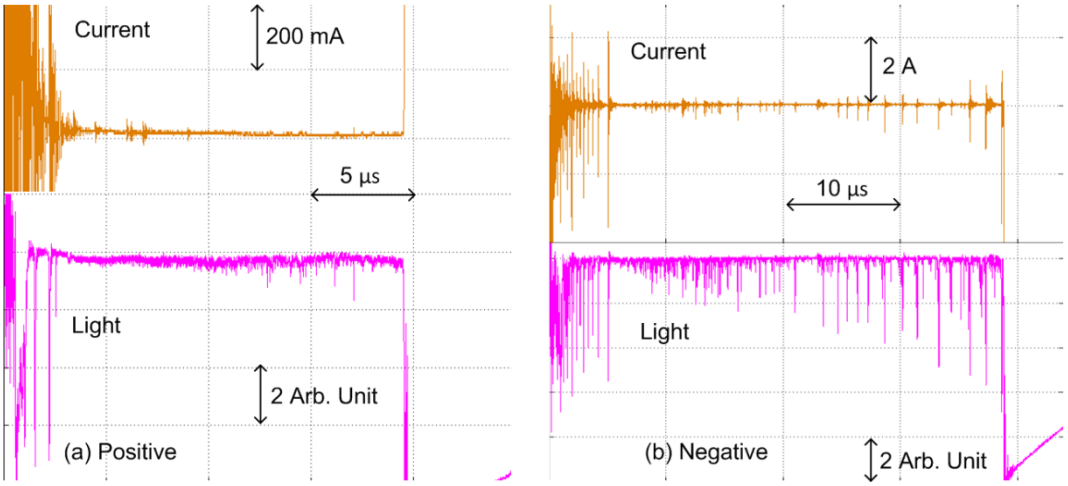

Figure 5-5 Recordings of current and light signals of positive and negative streamers leading to breakdown; d=50 mm, (a) positive streamer, V=90 kV, Midel 7131, (b) negative streamer, V=-150 kV, FR3.

5.2.3 Propagation Mode

Generally two groups of streamers, slow and fast ones were observed in this study. As the detailed propagating process of a streamer is concerned, three modes, however, can be clearly divided, slow mode, fast mode and combination of fast and slow modes, similar to the classification of 2^{nd}, 3^{rd} and 3^{rd}+2^{nd} modes in [35]. An example of the three modes is demonstrated by Midel 7131 under positive polarity in Figure 5-6.

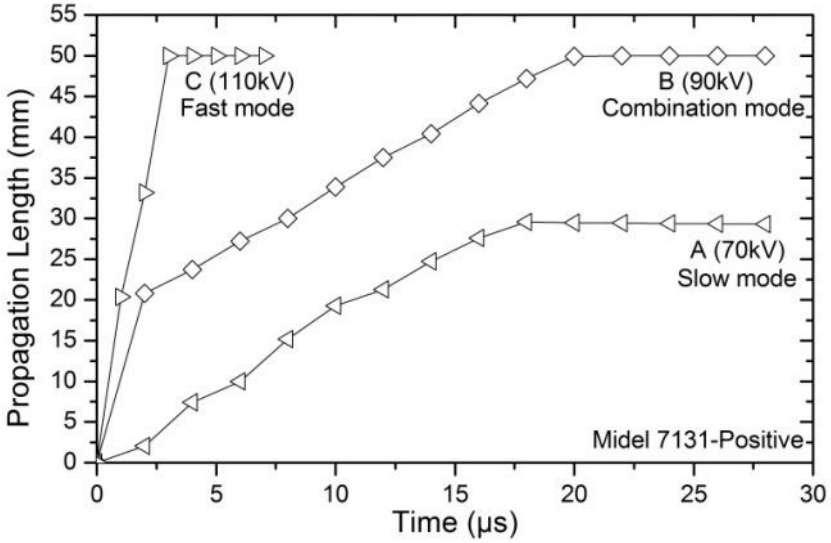

(a) Propagation length versus time

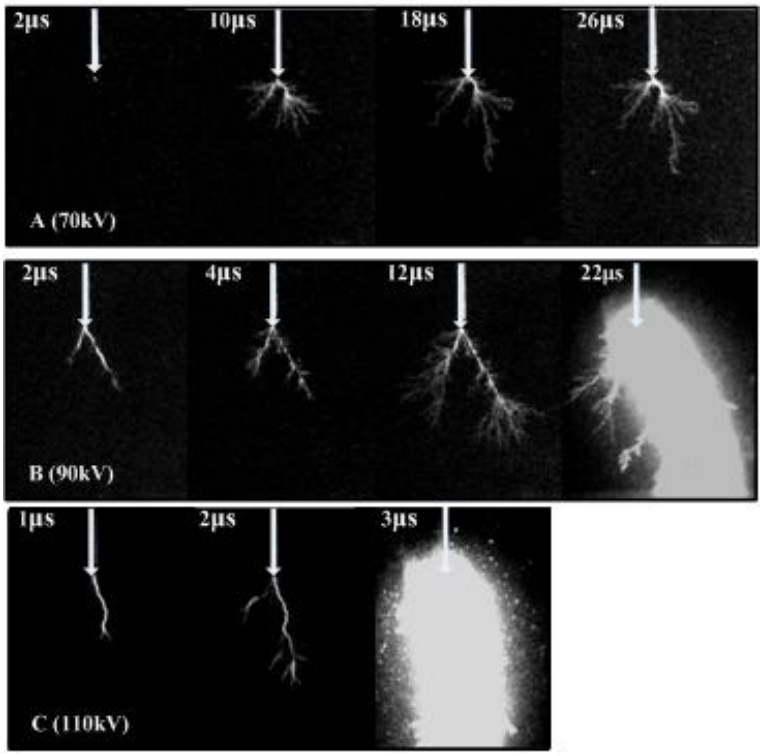

(b) Reflective images of streamer propagation

Figure 5-6 Typical propagation modes in ester liquids using reflective image; Midel 7131, positive polarity, d=50 mm, (a) V=70 kV, exposure time 2 μs, (b) V=90 kV, exposure time 2 μs, (c) V=110 kV, exposure time 1 μs; point electrode is marked by white arrow, the same as following figures.

For slow mode/2nd mode (A), the streamer propagates at a constant speed of less than 3 km/s during the whole propagation process. Streamer in this mode has relatively more branches and small offshoots. For fast mode/3rd mode (C), streamer propagates much faster at the speed from 5 km/s to 50 km/s for the 50 mm gap in the present study. Streamer at this stage is very different from at slow mode, normally has bright filamentary branches and almost no small offshoots. For combination mode/3rd+2nd mode (B), streamer initiates with fast mode/3rd mode and then quickly changes into slow mode/2nd mode. At the beginning of this mode, only the filamentary branch with few offshoots propagates at a high speed, following the fast mode characteristic. Then many small offshoots start to grow around the main branch, and the propagation speed falls into the slow mode range. If average velocity is used as the criterion, this combination mode still belongs to the category of slow mode.

Figure 5-7 shows an example of 3rd+2nd combination mode in Midel 7131 under positive polarity below breakdown voltage, where the 3rd mode and 2nd mode are successfully separated using multi-frame integral light imaging technique. The propagation of 3rd mode streamer with length of 11.19 mm is captured in the beginning 2 μs. Its instant velocity at the duration from 1 μs to 2 μs is 6.84 km/s. Afterwards it changes into the 2nd mode propagation with an average velocity of 1.40 km/s, and finally reaching 37.06 mm long at the time of 20 μs. Although the 3rd mode streamer is obtained with 1 μs short exposure time, it is still much brighter than that of 2nd mode streamer obtained with 17 μs long exposure time.

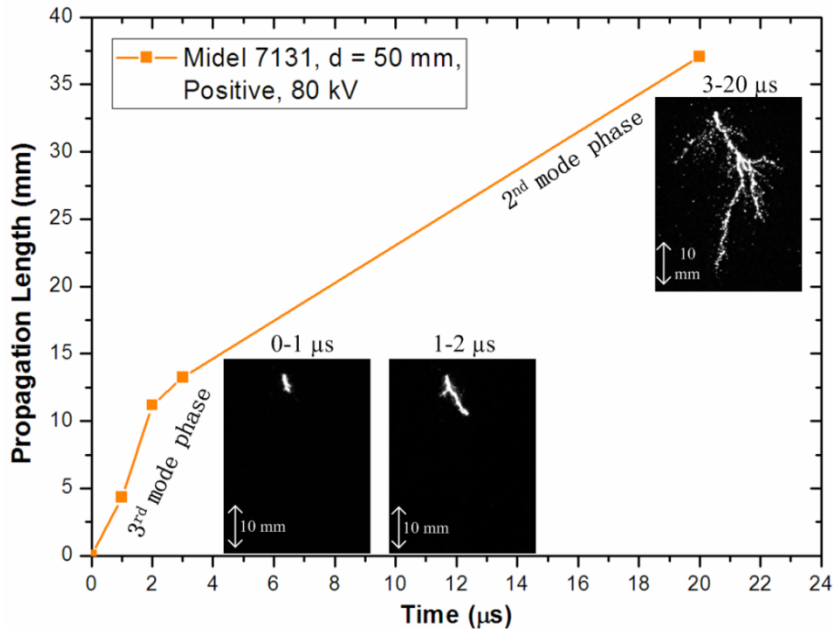

Figure 5-7 Separation of 3rd+2nd combination mode using multi-frame integral light images; Midel 7131, positive polarity, V=80 kV, d=50 mm.

Figure 5-8 shows an unusual case that streamer has touched to the plane electrode but without inducing a breakdown event. A bright zone was usually observed when the streamer head touched to the plane electrode. This phenomenon could be occasionally observed in the three liquids at the voltage level close to 50% breakdown voltage under both positive and negative polarities and at various gap distances. Similar observations were reported in other studies [13, 29, 100].

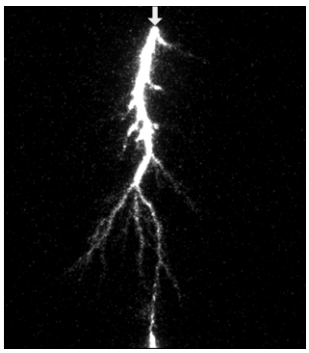

Figure 5-8 Streamer touching the plane electrode without inducing breakdown; Midel 7131, d=100 mm, positive polarity, V=140 kV, exposure time 50 μs.

Figure 5-9 shows an even more rare observation that an upstream 'return streamer' (image exposed from 50 μs to 80 μs) was observed after the downstream propagation of main streamer (image exposed from 0 μs to 50 μs). The root of return streamer consists of a very bright zone. Comparing the shape geometry of main streamer shown in Figure 5-9 (a) and return streamer shown in Figure 5-9 (b), the channel should be somehow connected, but without inducing a breakdown event. In addition, a re-illumination (image exposed from 80 μs to 110 μs) was observed just after the return streamer and following one of its main branches.

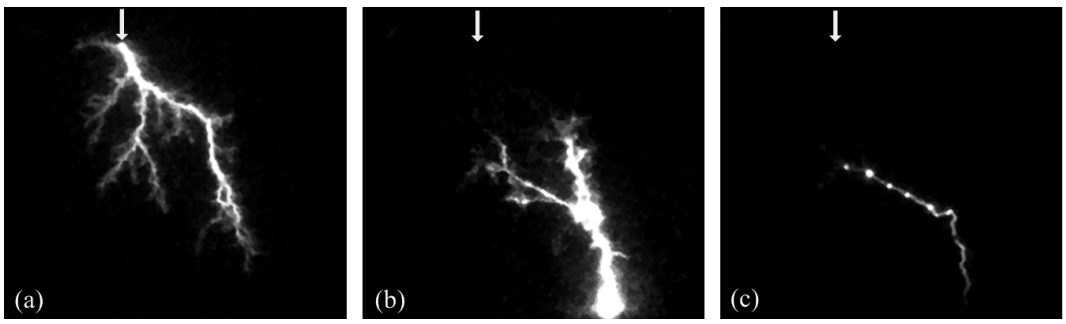

Figure 5-9 'Return streamer' without inducing breakdown; Gemini X, d= 50 mm, negative polarity, V=-30 kV, (a) main streamer, exposure time 50 μs, (b) return streamer, exposure time 30 μs, (c) re-illumination, exposure time 30 μs.

It is commonly difficult to describe the streamer shape in liquid quantitatively due to first the complexity of the phenomena and then the quality of the captured images.

Thanks to the high resolution images obtained by the present experimental setup and the open-source software ImageJ, streamer area information was calculated based on the intensity of the pixels, which means all the areas occupied by the bright channels observed in a streamer image. It has to be emphasized that a streamer is propagating in the 3-dimensional space. However the images obtained only reflect a 2-dimensional projection. Figure 5-10 shows the shape evolution of slow streamer and fast streamer.

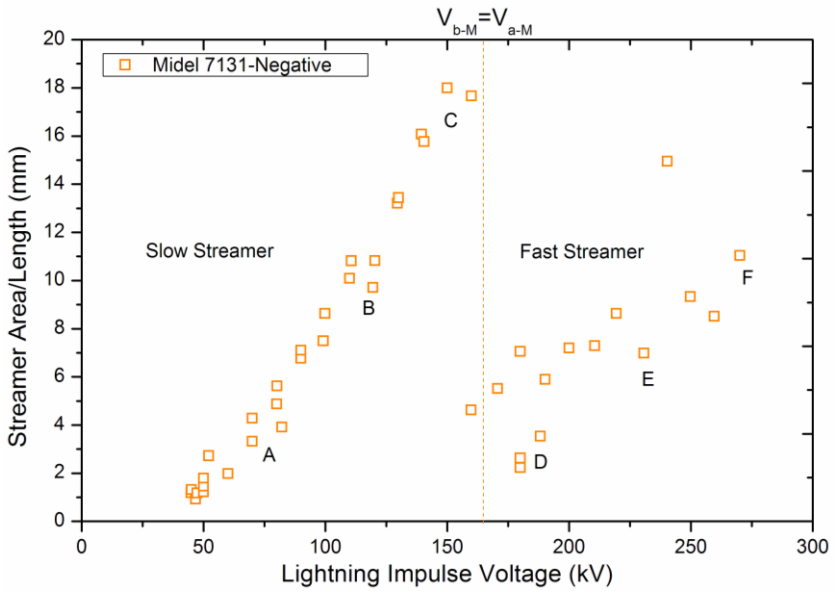

(a) Ratio of streamer area to length versus applied impulse voltage

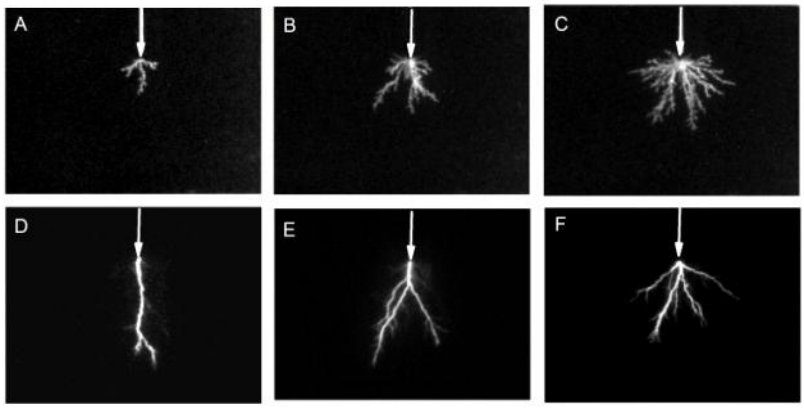

(b) Correlated streamer shape at different stages in (a)

Figure 5-10 Evolution of streamer shape with applied voltage; Midel 7131, negative polarity, d=50 mm.

Once breakdown occurs, the last image obtained about 1 μs before breakdown is used to represent the streamer shape. In this case, the length of captured streamer is scattering due to the increasing velocity of fast streamers. Therefore unified streamer area, ratio of area to length (width) is deduced to compare the slow streamer and fast streamer with fairness. This pseudo width can indicate the branching or expanding of the streamer shape. It is found that the pseudo width of fast streamer and slow streamer follows the same relationship with applied voltage: the higher voltage, the more branches.

A similar relationship between the streamer area and the applied voltage is confirmed for both positive and negative streamers in a paraffinic oil at a 80 mm point-plane gap under step voltage [21].

5.3 Statistical Analysis of Streamer Length and Velocity

Statistical analysis of streamer length and velocity were carried out at a 50 mm gap, after breakdown voltages of liquids at the 50 mm gap were measured first as the reference.

Breakdown voltage was measured by using rising-voltage method. The initial voltage level was set at about 70% to 80% of the expected breakdown voltage. Voltage level was increased step by step (one shot per step) with increment of 5 kV or 10 kV depending on the gap distance or expected breakdown voltage. 15 breakdowns per sample were obtained before changing both the electrode and liquid sample. At least 5 minutes break was given between breakdowns to let the discharge by-products and gas bubbles diffuse. Results of ester liquids and mineral oil under both positive and negative polarities are shown in Figure 5-11.

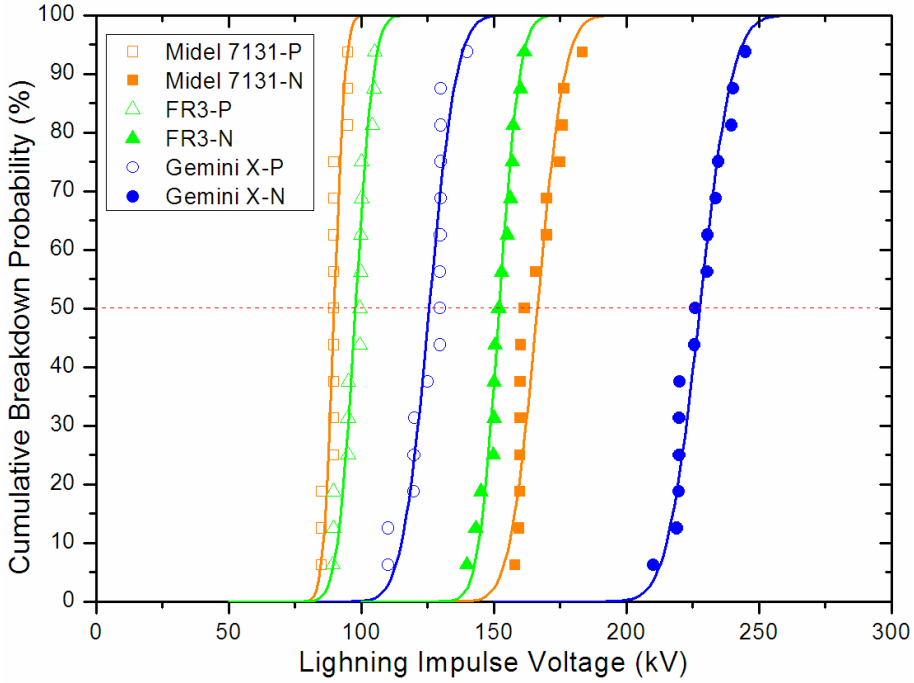

Figure 5-11 Distribution of breakdown voltages at the 50 mm gap distance; open symbols represent positive breakdown, solid symbols represent negative breakdown and lines are normal distribution fitting of results.

According to the distribution of cumulative breakdown probability, 50% breakdown voltage, V_b, can be calculated as given in Table 5-1. For both positive and negative polarities, V_b of Midel 7131 and FR3 are close to each other and lower than that of Gemini X. Moreover similar polarity effect as in mineral oil exists in ester liquids. Breakdown voltages of Midel 7131 and Gemini X under positive polarity are about 55% of those under negative polarity. For FR3, this ratio is slightly higher, about 64%.

Table 5-1 Summary of inception, breakdown and acceleration voltages (kV).

Polarity	Positive (+)			Negative (-)		
Voltage	V_i	V_b	V_a	V_i	V_b	V_a
Midel7131	50.0	89.8	100.0	47.5	166.4	166.4
FR3	52.5	97.8	97.8	45.0	152.0	152.0
Gemini X	55.0	125.6	260.0	50.0	227.6	250.0

5.3.1 Stopping Length

Results on streamer stopping length of ester liquids and mineral oil at a 50 mm gap under both positive and negative polarities are shown in Figure 5-12 and Figure 5-13, where 50% breakdown voltages are also stated as reference ($V_{b\text{-}M}$, $V_{b\text{-}F}$ and $V_{b\text{-}G}$ stand for breakdown voltage of Midel 7131, FR3 and Gemini X respectively). At each voltage level, the average value and standard deviation are given based on about 10 measurements.

Inception voltages of streamer were determined at first. It should be noted that inception voltage is statistically distributed and determination of inception voltage is sensitive to the testing condition (like minimal detectable level of camera setup, light and current measurement, or tip radius of point electrode). Here appearance of streamer is determined by the capture of camera, where the smallest detectable streamer is about 0.5 mm long. Applied voltage is increased step by step (3 shots per step) and the inception voltage is defined as the voltage at which 3 consecutive streamers appear. Results are given in Table 5-1. Inception voltages of negative and positive streamers are very close, negative streamer appears at slightly lower voltage compared to positive streamer. However positive streamer, once captured, already reaches in the range from 5 mm to 10 mm long whereas negative streamer can only reach 1 mm long. It is observed here that inception voltages of ester liquids, about 50 kV, are comparable to that of mineral oil at the present testing condition.

Under positive polarity, ester liquids behave similar to mineral oil, the stopping length increases with applied voltage, in a seemingly linear relationship well before breakdown. Midel 7131 has a higher increasing rate of 0.75 mm/kV thus leads to lower breakdown voltage. It is, however, surprising that FR3 has a similar increasing rate of about 0.50 mm/kV to Gemini X but still has a much lower breakdown voltage.

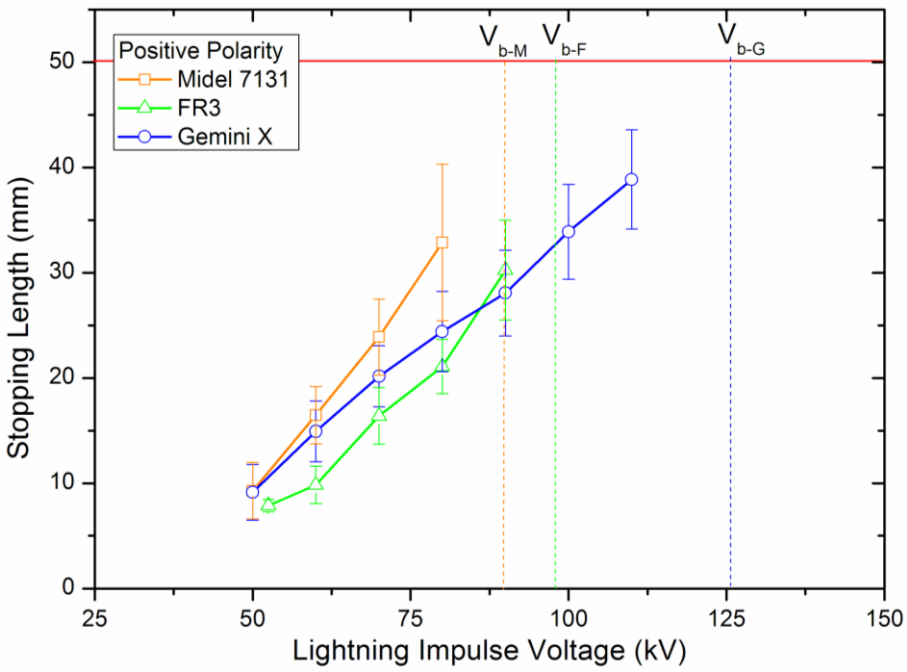

Figure 5-12 Stopping length versus applied impulse voltage under positive polarity; d=50 mm; error bars stand for one standard deviation, the same as following figures.

Under negative polarity, a significant difference of stopping length characteristic exists between ester liquids and mineral oil. Mineral oil Gemini X increases very slowly from inception voltage to about 140 kV, at which stage the streamer looks like a round cloud with little distinguished branches. Above 140 kV, the streamer propagation in Gemini X then starts to increase rapidly although with relatively larger deviations, which is also documented in [33] under step voltage. Negative streamer of both ester liquids increases rapidly with applied voltage, following the same characteristic under positive polarity but having a lower increasing rate of about 0.27 mm/kV.

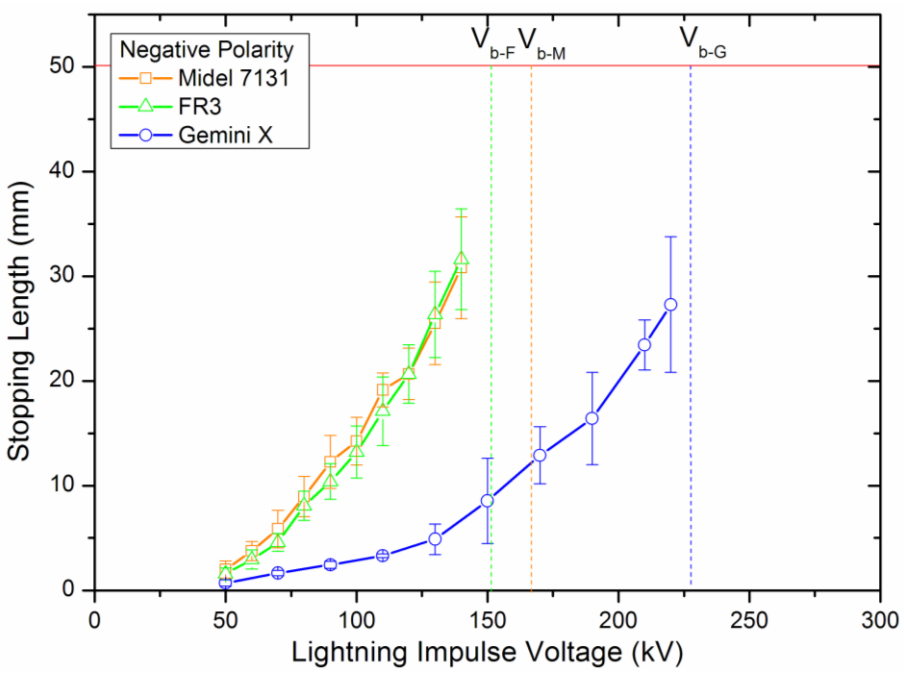

Figure 5-13 Stopping length versus applied impulse voltage under negative polarity; d=50 mm.

5.3.2 Average Propagation Velocity

Before breakdown, average propagation velocity, v_a, is calculated by the ratio of stopping length l_s to propagating time t_p, since streamers propagate typically at a constant velocity, as seen in Figure 3-9 of chapter 3. Once breakdown occurs, v_a is determined by using gap distance d divided by time to breakdown t_b.

Figure 5-14 and Figure 5-15 present results on streamer propagation velocity of ester liquids and mineral oil at a 50 mm gap under both positive and negative polarities. Acceleration voltage [35], at which streamer velocity starts to increase dramatically (fast streamer appears), is determined by the velocity plot, as summarized in Table 5-1 and stated in Figure 5-14 and Figure 5-15 ($V_{a\text{-}M}$, $V_{a\text{-}F}$ and $V_{a\text{-}G}$ stand for acceleration voltage of Midel 7131, FR3 and Gemini X respectively).

Under positive polarity, there is a big difference of streamer velocity between ester liquids and mineral oil. $V_{a\text{-}G}$ is about 2.6 times of $V_{a\text{-}M}$ and $V_{a\text{-}F}$ under positive polarity. Below acceleration voltage, velocity of Gemini X increases slightly from about 1.3 km/s to 3.2 km/s. Ester liquids behave similar at this stage: FR3 increases from about 0.7 km/s to 2.2 km/s; Midel 7131 about 1.2 km/s to 2.8 km/s. Once over acceleration voltage, velocity of ester liquids increases much more quickly with applied voltage than mineral oil. The maximum velocity measured for ester liquids is 50 km/s at about

130 kV, since the test stopped when the parameter time to breakdown reached 1μs, at which breakdown occurred immediately after the voltage rose to peak.

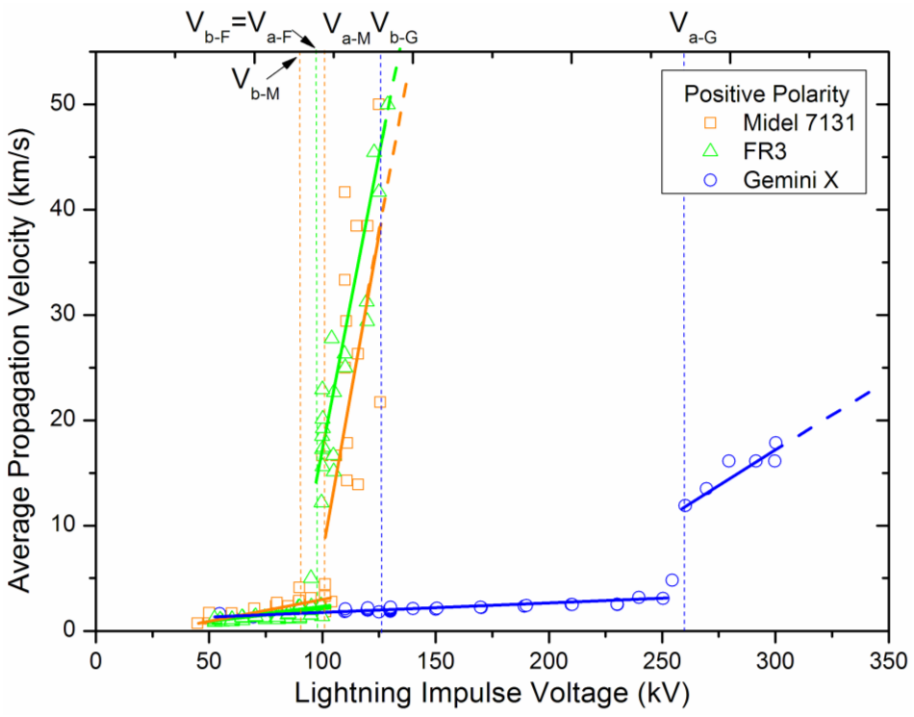

Figure 5-14 Average propagation velocity versus applied impulse voltage under positive polarity; d=50 mm.

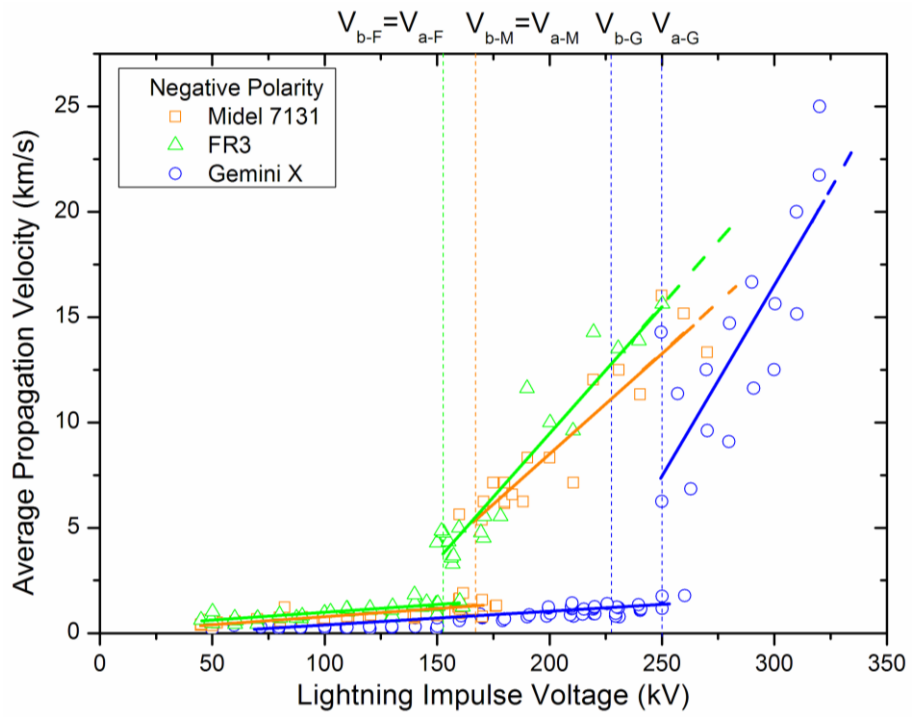

Figure 5-15 Average propagation velocity versus applied impulse voltage under negative polarity; d=50 mm.

The difference of negative streamer velocity between ester liquids and mineral oil becomes smaller. $V_{a\text{-}G}$ is about 1.6 times of $V_{a\text{-}M}$ and $V_{a\text{-}F}$ under negative polarity. The velocity below acceleration voltage is also lower than that under positive polarity. Gemini X increases from about 0.3 km/s to 1.2 km/s, FR3 about 0.6 km/s to 1.3 km/s and Midel 7131 about 0.5 km/s to 1.2 km/s. At the same voltage, streamers in ester liquids still propagate faster than in Gemini X. Over the acceleration voltage, all of them increase rapidly with applied voltage, but still not so quickly as positive streamer in ester liquids.

Furthermore, acceleration voltage of mineral oil is obviously higher than 50% breakdown voltage, especially for positive polarity. In contrast, V_a and V_b of ester liquids are almost the same except for a slight difference in Midel 7131 under positive polarity. Reference [13] shows the similar phenomenon, i.e. V_a equals to V_b, in natural ester occurring at a larger gap of 200 mm under step impulse voltage. However in the present study, it can occur at a much smaller gap of 50 mm under lightning impulse voltage.

5.3.3 Possible Reason for Velocity and Shape Characteristics of Negative Streamers in Ester Liquids

In the review paper [45], the authors stated that *molecular structure has a significant effect on the streamer propagation. The main parameter affecting streamer propagation is the electronic affinity of the liquid molecules*. For example, presence of a single atom of chlorine in chlorocyclohexane increases the negative streamer velocity compared to cyclohexane [27].

In mineral oil, electron scavenger property of the aromatic compounds increases the velocity of negative streamer [42]. Systematic study on the effect of electron-scavenger additives on negative streamer in cyclohexane was documented in [62], where it was confirmed that increase of scavenger concentration could accelerate the negative streamer propagation and make the structure more defined and branched. In addition, it was found that electron attachment cross-section is better than electron affinity to describe the electron accepting capacity of a molecule [62].

Highly electronegative oxygen atoms exist in ester molecular structure, which might be the reason for less favourable performance of negative streamer in ester liquids: at the same voltage before breakdown negative streamer of ester liquids propagates obviously further (Figure 5-13) with higher velocity (Figure 5-15) and more branches (Figure 5-2) than in mineral oil.

5.4 Breakdown at Various Gaps

5.4.1 Breakdown Tests at Gaps from 15 mm to 100 mm

Lightning breakdown tests of ester liquids and mineral oil at gaps from 15 mm to 100 mm were carried out by using the same procedure stated in section 5.3. 50% breakdown voltages under both positive and negative polarities increase with the gap distance as shown in Figure 5-16 and Figure 5-17.

Under positive polarity, breakdown voltages at a 25 mm gap are almost identical for ester liquids and mineral oil. However with gap distances increased, both ester liquids show lower breakdown voltages than mineral oil.

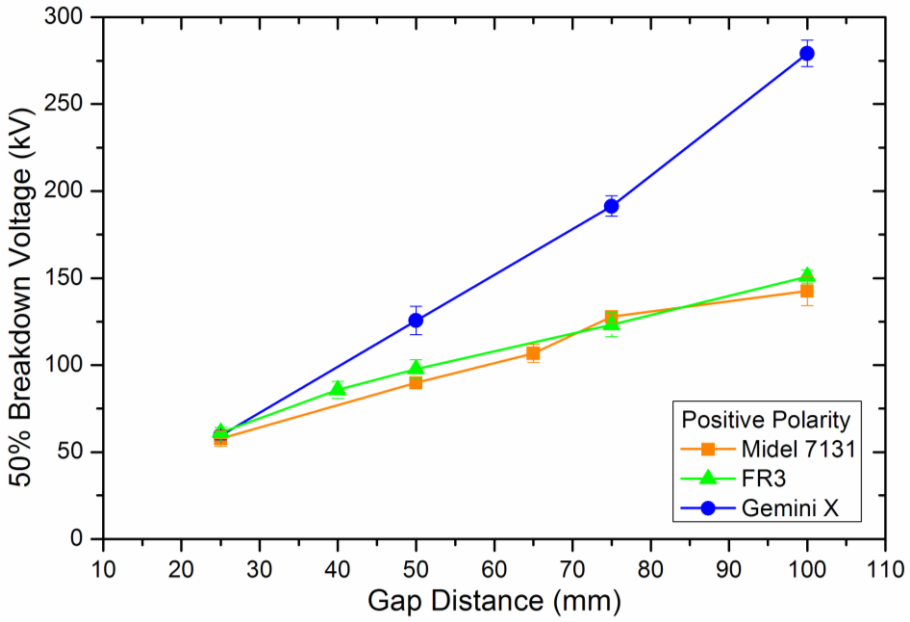

Figure 5-16 50% breakdown voltage versus gap distance under positive polarity.

Under negative polarity, breakdown voltages of ester liquids are lower than that of Gemini X for all gaps observed, and the differences become bigger with gap distances

increased. Breakdown voltage under negative polarity is much higher than that under positive polarity for the same gap distance.

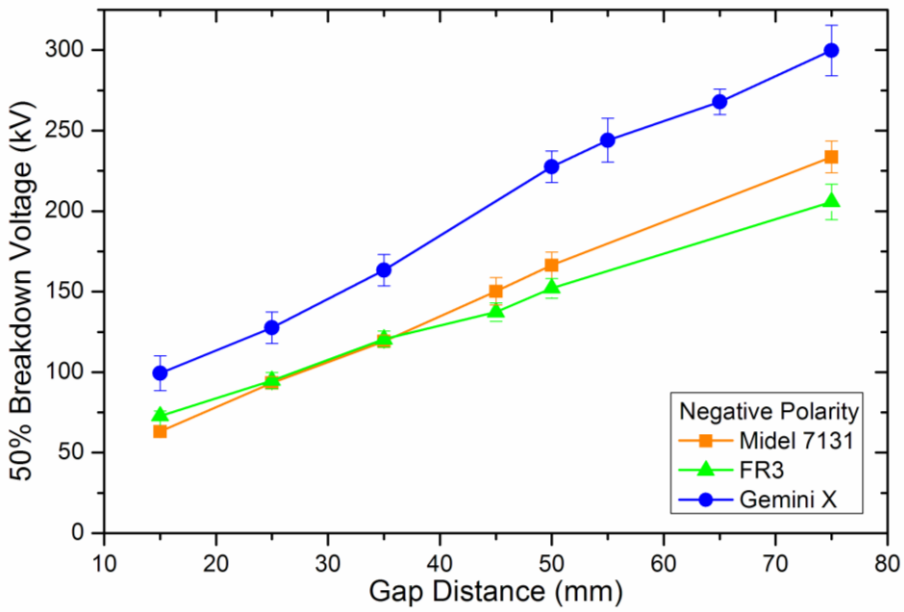

Figure 5-17 50% breakdown voltage versus gap distance under negative polarity.

Besides breakdown voltage, another useful parameter, time to breakdown t_b was also recorded and shown in Figure 5-18 and Figure 5-19 in the form of deduced average velocity, i.e. gap distance d divided by t_b.

Under positive polarity, it can be found in Figure 5-18 that average velocity of streamers which lead to breakdown in all three liquids is as low as 2 km/s at the gap distance of 25 mm. With gap distances increased, the average velocity of streamers leading to breakdown will increase. For FR3, a jump increase of the average velocity occurs at the 50 mm gap distance, since at this distance about half of the breakdowns are induced by fast streamers. It can be seen that for gap smaller than 50 mm, acceleration voltage $V_{a\text{-}F}$ is higher than breakdown voltage $V_{b\text{-}F}$; equal to and larger than this gap distance, $V_{a\text{-}F}$ becomes the same as $V_{b\text{-}F}$. Therefore, this gap distance is named as the transition gap distance. Similarly the transition gap for Midel 7131 is 75 mm. However for Gemini X, fast streamer induced breakdown has not appeared in the investigated gap distance range even at 100 mm, which shows mineral oil has better resistance to fast streamer events in large gaps as compared to ester liquids under positive polarity.

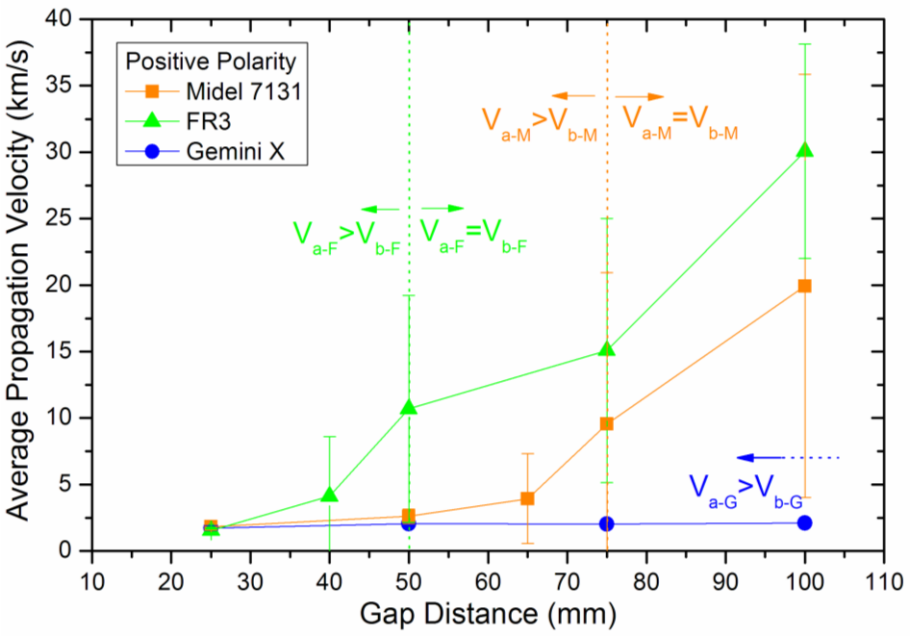

Figure 5-18 Propagation velocity versus gap distance under positive polarity.

Under negative polarity similar phenomenon exists as shown in Figure 5-19. The transition gap distance is at 50 mm for both ester liquids. For Gemini X, the transition gap distance is increased to 55 mm. It seems that the difference between ester liquids and mineral oil in terms of transition gap distance under negative polarity is minor.

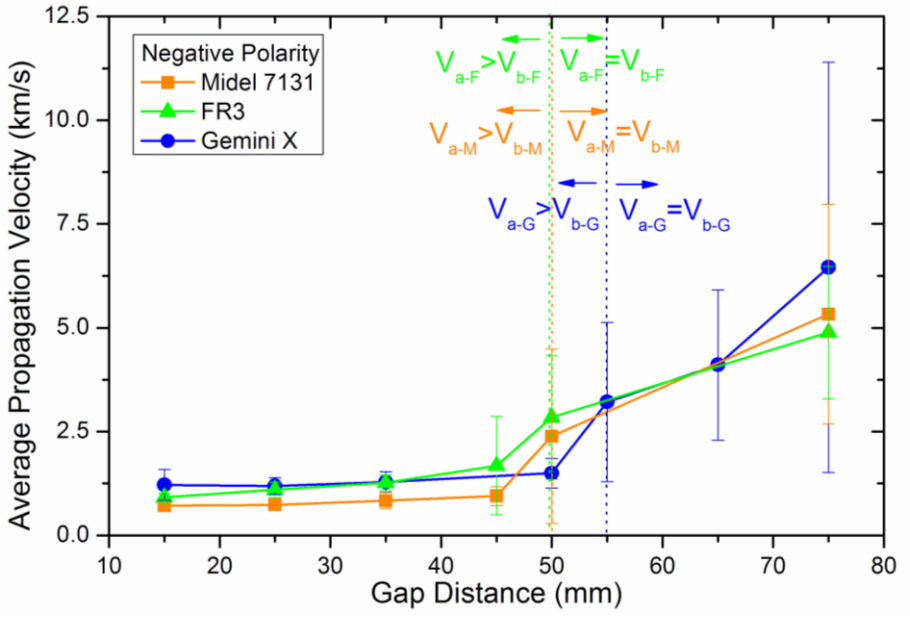

Figure 5-19 Propagation velocity versus gap distance under negative polarity.

In summary, at small gaps breakdown is caused by slow streamers of which the average propagation velocity is low. With gap distances increased, fast streamer appears at breakdown voltage level and starts to take over the control of breakdown. There is indeed a range of transition gap distance where both slow and fast streamer induced

breakdowns can occur. Once over this transition range for very large gaps, breakdown will be purely controlled by fast streamers. Early appearance of this transition gap distance in ester liquids, especially under positive lightning impulse, implies their relatively poor ability to withstand high-voltage at very large gaps.

5.4.2 Prediction of Breakdown at Very Large Gaps

Breakdown voltage of ester liquids at very large gaps is important for their application in large power transformers. In this part, the relationship between the results under lightning impulse and the previously published data under step voltage will be built up so that the breakdown voltages of ester liquids at very large gaps are extrapolated.

At first, it was found that breakdown voltages of mineral oil in the present work match fairly well with previously published data of mineral oil, even those under very large gaps till about 1000 mm by using rod-plane electrodes [14, 36]. Since breakdown under large gaps is mainly controlled by streamer propagation, rather than streamer initiation influenced by tip radius of point electrode [30], a good power law relationship between breakdown voltage $V_{b\text{-}Mineral}$ (kV) and gap distance d (mm) was obtained as seen in Figure 5-20. Based on all these data, empirical formulas for lightning breakdown voltages under both positive and negative polarities were deduced as follows. In addition, the 95% confidence bands of the curve fitting are shown in Figure 5-20.

$$V_{b-\text{Mineral Oil}-\text{Negative}} = 19.077 \times d^{0.636} \tag{5-1}$$

$$V_{b-\text{MineralOil}-\text{Positive}} = 11.620 \times d^{0.684} \tag{5-2}$$

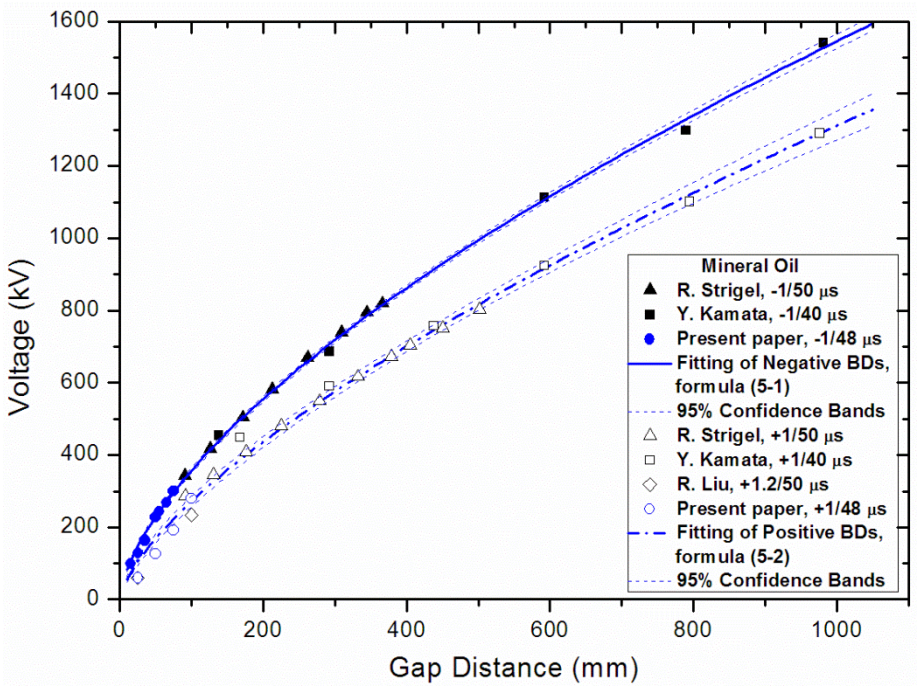

Figure 5-20 General curve of breakdown voltage with gap distance for mineral oil based on the present results and previously published data [14, 36].

The breakdown voltage results of mineral oil under lightning impulse were then compared with breakdown voltage and acceleration voltage under step voltage (0.4/1400 μs) [33], taking the ones under negative polarity for demonstrative purposes as shown in Figure 5-21. At very small gaps, lightning breakdown voltage is identical as breakdown voltage obtained under step voltage. With gap distances increased, lightning breakdown voltage becomes higher than the breakdown voltage under step voltage, probably due to the short tail of lightning waveform, but still lower than the acceleration voltage under step voltage. If the gap increases to 55 mm, lightning breakdown voltage is almost the same as the acceleration voltage obtained under step voltage. In last section 55 mm is concluded as transition gap distance for mineral oil under negative polarity, at which stage the lightning breakdown voltage equals to lightning acceleration voltage due to the fact that both fast streamer and slow streamer can lead to breakdown. It is noted here that lightning acceleration voltage also equals to acceleration voltage under step voltage. Above this transition gap distance, lightning breakdown voltage (same as lightning acceleration voltage) is overlapped with the acceleration voltage obtained under step voltage.

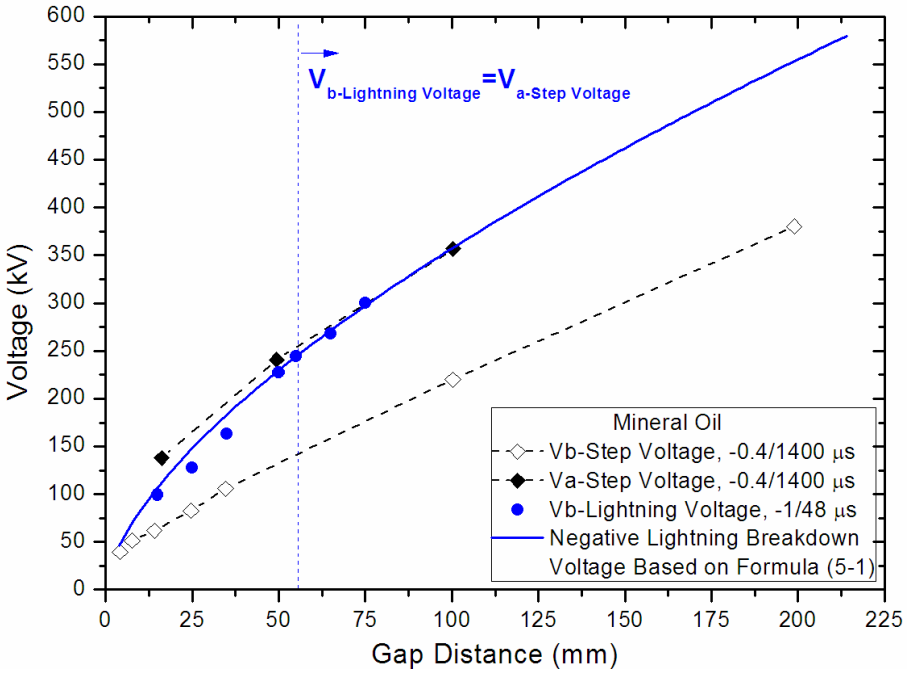

Figure 5-21 Comparison of results under lightning voltage and step voltage [33]; mineral oil, negative polarity.

It needs to be emphasized here that the same relationship is also applicable to natural ester as shown in Figure 5-22, also taking negative polarity for demonstration. The transition gap distance of natural ester under negative polarity is 50 mm, at which lightning breakdown voltage is almost the same as acceleration voltage obtained under step voltage. Over this gap distance, the acceleration voltage obtained under step voltage can be regarded as lightning breakdown voltage.

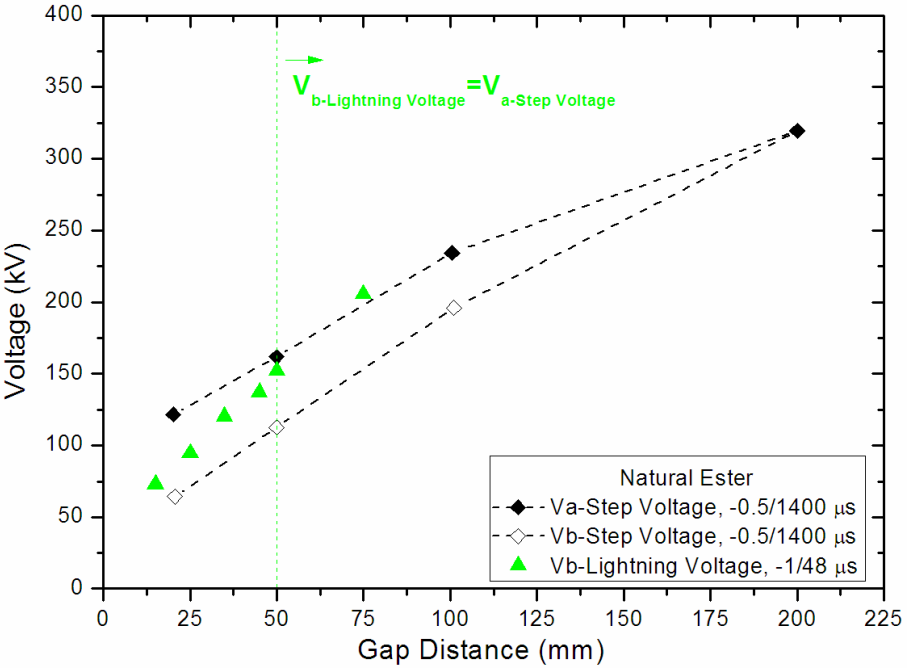

Figure 5-22 Comparison of results under lightning voltage and step voltage [13]; natural ester, negative polarity.

Based on such a relationship, we can combine the lightning breakdown voltages of natural ester in the present experiments together with the acceleration voltages of natural ester obtained under step voltage from 50 mm to 200 mm [13], and use the power law relationship to fit the data. The same methodology can be used for data under both negative and positive polarity. So the breakdown voltages of natural esters $V_{b\text{-}Natural\ Ester}$ (kV) at very large gap distances d (mm) are predicted, as shown in Figure 5-23, and the empirical formulas are given as follows.

$$V_{b-\text{Natural Ester}-\text{Negative}} = 17.658 \times d^{0.552} \tag{5-3}$$

$$V_{b-\text{NaturalEster}-\text{Positive}} = 11.630 \times d^{0.549} \tag{5-4}$$

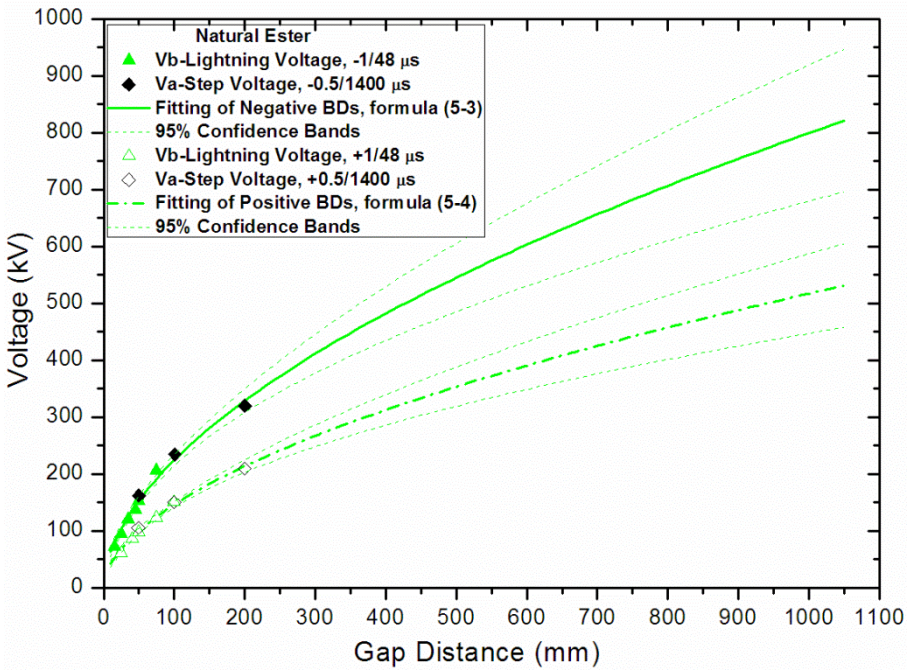

Figure 5-23 Predicted curve of breakdown voltage with gap distance for natural ester based on the present results and previously published data [13].

It needs to be emphasized here that although fundamental understanding indicates that fast streamer led breakdown is highly likely to dominate the large oil gap breakdown and hence the extrapolation curves given in this study, some further experimental verifications, at one or more points of larger gap distance, would be ideal to reduce the uncertainty of prediction as indicated by the 95% confidence bands in Figure 5-23.

There is a lack of sufficient effective data for synthetic ester in the literatures (like the breakdown voltage at a 200 mm gap distance), consequently the prediction of lightning breakdown voltage for synthetic ester at very large gaps is not carried out since it would

have large uncertainty. However, synthetic ester behaves similar to natural ester not only for streamer propagation but also for breakdown property, based on the investigated range in this study.

5.4.3 Application of Ester Liquids in Large Power Transformers

Standard lightning impulse test is one of the factory tests to verify the insulation systems of power transformers. Lightning breakdown strength as BIL is vitally important for the insulation design of power transformer.

At relatively small gaps shown in Figure 5-16 and Figure 5-17, lightning breakdown voltages of ester liquids are generally not less than 65% of that of mineral oil under both positive and negative polarities. However it is surprising that moving to large gaps, lightning breakdown voltage of natural ester becomes much lower than that of mineral oil, based on the results in Figure 5-20 and Figure 5-23 by using empirical formulas. The ratios of breakdown voltage of natural ester to that of mineral oil under both negative and positive polarities are shown in Figure 5-24. At the gap distance of 1000 mm, positive lightning breakdown voltage of natural ester is only about 40% of that of mineral oil, whereas negative lightning breakdown voltage of natural ester is about 50% of that of mineral oil.

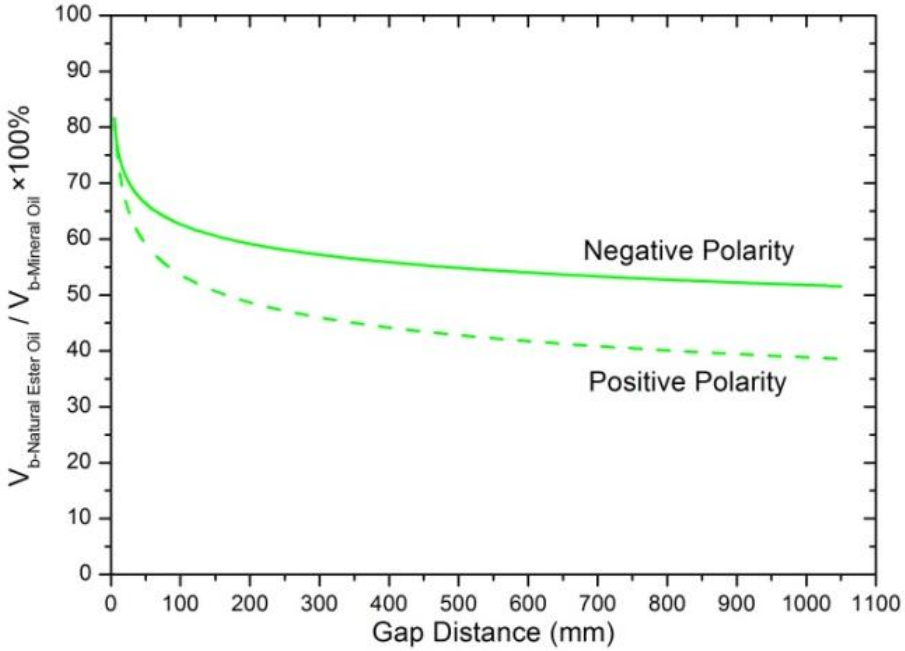

Figure 5-24 Ratio of lightning breakdown voltage in natural ester to that in mineral oil at very large gaps based on experimental data and prediction.

Reviewing the results in this study, it can be summarized that streamer inception voltage in ester liquids is comparable with that of mineral oil; Once incepted, streamer propagation is easier in ester liquids than in mineral oil (Figure 5-12 and Figure 5-13); thus breakdown voltage in ester liquids is lower than in mineral oil (Figure 5-16 and Figure 5-17). Moreover, difference between ester liquids and mineral oil is magnified under higher voltages (Figure 5-14 and Figure 5-15) and at larger gap distances (Figure 5-24).

5.5 Summary

Streamer characteristics, including shape, mode, length and velocity of natural ester and synthetic ester liquids under lightning impulse voltage in a non-uniform field were studied in this chapter. Although streamer inception voltages of ester liquids are comparable to that of mineral oil, at the same voltage level after inception streamer in ester liquids propagates faster and further, with more branches for those negative ones, than in mineral oil. Negative polarity shows the obvious difference between ester liquids and mineral oil in terms of stopping length, whereas positive polarity gives out the significant difference between ester liquids and mineral oil of acceleration voltage which indicates the ability to withstand fast streamer events.

Generally three modes of streamer including slow mode (2^{nd} mode), fast mode (3^{rd} mode) and combination of fast and slow modes (3^{rd}+2^{nd} mode), exist in ester liquids, which conforms to previous knowledge obtained with mineral oil. Moreover streamer shape analysis shows that fast and slow streamers follow the same relationship to applied voltage: the higher voltage, the more branches a streamer has.

Breakdown voltage and associated time to breakdown of ester liquids tested at various gaps from 15 mm to 100 mm under lightning voltage, were combined with previously published data under step voltage to build up the empirical formulas so that breakdown voltages of natural ester at very large gaps up to 1000 mm can be predicted. Lightning breakdown voltages of natural ester at very large gaps could be as low as 40% of that of mineral oil, due to ester liquids' relatively low tolerance to fast streamers.

CHAPTER 6. INFLUENCE OF PRESSBOARD ON STREAMER AND BREAKDOWN OF ESTER LIQUIDS IN NON-UNIFORM FIELD

6.1 Introduction

As pressboards are generally used in transformers as barriers between windings or winding and earth to enhance the dielectric strength of oil gaps, it is necessary to investigate the streamer and breakdown performances of ester liquids by taking into account the presence of pressboard. When a streamer propagates along an oil/pressboard interface, it is called 'creepage discharge', and creepage discharge is attributed to one of the failure modes for large power transformers [64].

A number of previous studies were carried out on the surface of solid materials immersed in mineral oils under impulse voltage [6, 65, 66, 72, 94, 101-104]. As introduced in chapter 2, with pressboard inserted in a perpendicular direction to the electric field, the 50% breakdown voltage was greatly increased compared to that of open oil gap [65]. Such an effect is mainly due to the elongation of streamer propagating path. When the pressboard was in the parallel direction to the electric field, the 50% breakdown voltage was found to be comparable with that of open oil gap, at gap distances up to 150 mm under positive impulse [65, 66] and 100 mm under negative impulse [14]. However, at large overvoltage, the presence of pressboard in parallel direction significantly promoted the streamer velocity leading to the obvious reduction of acceleration voltage under positive impulse [65, 105].

This chapter reports the influences of parallel pressboard surface on the streamer characteristic and breakdown in ester liquids under both positive and negative impulse voltages. Current and light signals as well as high-speed camera captured images are used to characterize the streamer propagation along pressboard surface in ester liquids. Breakdown voltages and acceleration voltages are also determined for various gap distances. For comparison purpose, tests are also carried out in a mineral oil and the mineral oil results are used as the benchmark.

6.2 Streamer Characteristics

6.2.1 Current, Light and Streamer Shape

Current and light signals together with streamer shape feature are usually used to describe the characteristics of streamer propagation, which vary upon the testing conditions [33, 35]. Generally four modes of streamers are classified in transformer liquids mainly according to propagation velocity [30]. In this section, characteristics of streamer propagation before breakdown along pressboard surface in ester liquids under both positive and negative impulse voltages are described.

6.2.1.1 Positive streamer

Figure 6-1 shows an example of positive streamer propagation at a voltage level just above inception, which was obtained on FR3/pressboard interface at the gap distance of 50 mm. Charging process at the wavefront of impulse voltage induces some noises in both current and light signals, and these noises are consequently ignored in the following analysis. A train of discrete intense pulses with increasing amplitude was observed for both current and light signals, which represents the typical recording of positive streamers on ester/pressboard interface at low voltage levels. Light and current pulses usually correspond to each other in time of occurrence. Integral light images of the streamer at the same voltage level obtained in perpendicular and parallel directions are shown in Figure 6-1 (b) and (c) respectively. Small tree-like streamer was observed, of which the intensity is low, since the maximum amplitude of light signals is less than 0.4 arb. unit. The length of streamer in Figure 6-1 (c) is 10.23 mm, and with propagating time of 8.60 μs in Figure 6-1 (a), an average velocity of 1.19 km/s (2^{nd} mode streamer) can be calculated.

With the increase of applied voltage, the current and light pulses become more intense, i.e. larger magnitude, longer sustaining time and higher repetition rate. Especially for streamers on Midel 7131/pressboard interface, a continuous DC component was normally observed for both current and light signals as shown in Figure 6-2 (a), which was obtained at a voltage level close to breakdown for the 50 mm gap. The continuous component might be due to the continuous backward travel of large amount of electrons generated by the intense discharge activities at the streamer heads. Figure 6-2 (b) and (c)

show the integral light images of the streamers at the same voltage level from both perpendicular and parallel directions. It is noted that there is always a bright luminous phase at the root of streamer, which should be the initial short-lived 3rd mode propagation phenomenon, the same as described in open liquid gaps [13, 106]. The length of streamer in Figure 6-2 (c) is 29.03 mm with propagating time of 17.23 μs in Figure 6-2 (a), which shows an average velocity of 1.68 km/s representing the 2nd mode positive streamer. It is clearly seen that streamer propagates along the pressboard surface but with some branches going into the surrounding liquid.

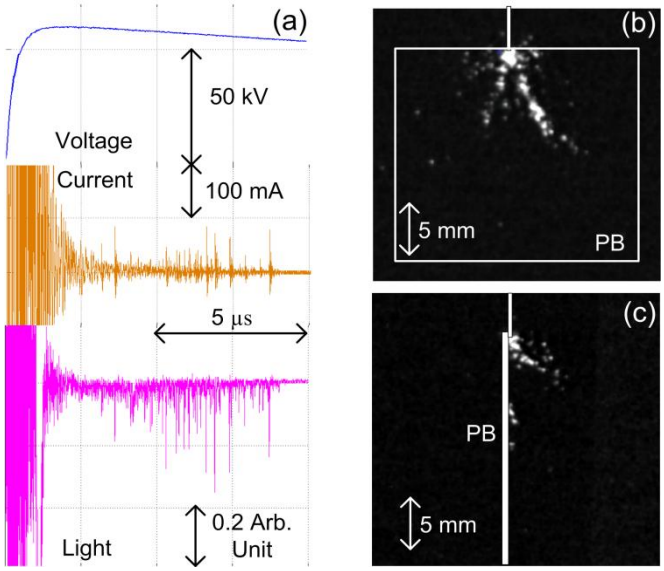

Figure 6-1 Positive streamer propagation on FR3/pressboard interface at low voltage level; d=50 mm, V= 60 kV, (a) voltage, current and light waveforms, (b) integral light image in perpendicular direction, (c) integral light image in parallel direction, corresponding to the signals in (a); PB stands for pressboard, same as the following figures.

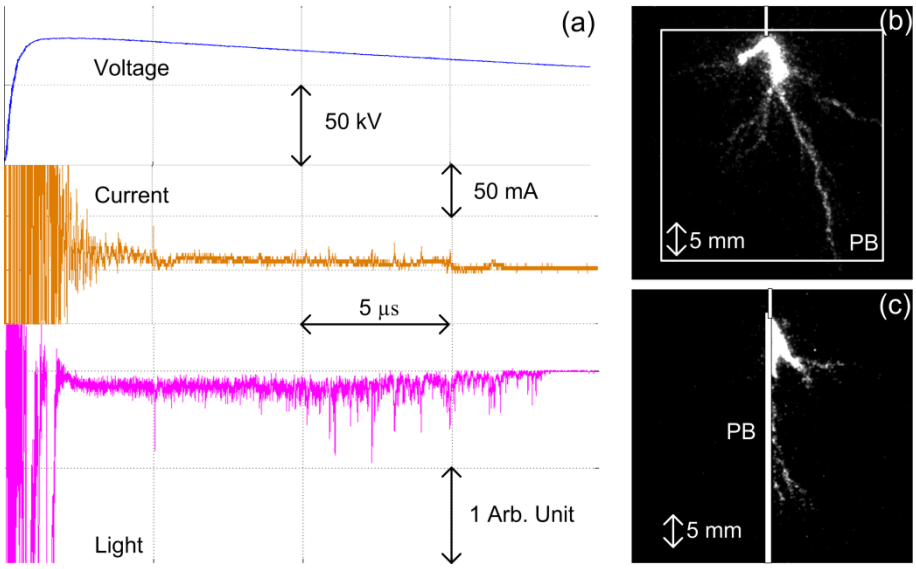

Figure 6-2 Positive streamer propagation on Midel 7131/pressboard interface at high-voltage level; d=50 mm, V=80 kV, (a) voltage, current and light waveforms, (b) integral light image in perpendicular direction, (c) integral light image in parallel direction, corresponding to the signals in (a).

Figure 6-3 shows the typical shadowgraph images of positive streamers along pressboard surface in the three liquids. The channels of positive streamers are so weak (thin) that the observation is made difficult using our present setup. However it can still be seen that positive streamer propagates along the pressboard surface with some other lateral branches injecting into the surrounding liquid, and similar tree-like structures with less branches exist for all the liquids.

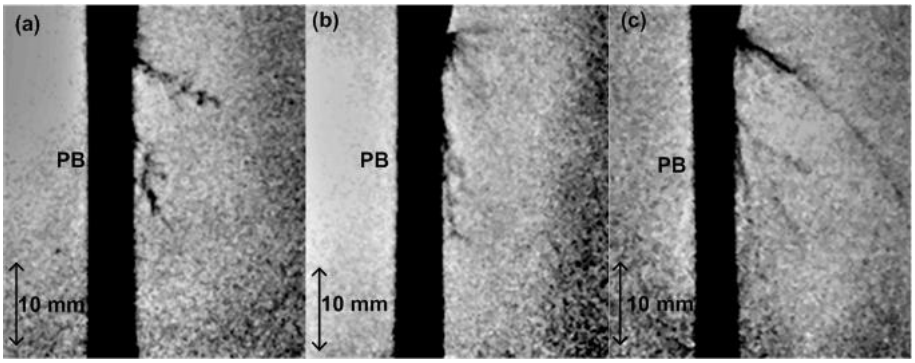

Figure 6-3 Shadowgraph images of positive streamers on liquid/pressboard interface; d=50 mm, (a) Midel 7131, V=70 kV, length 24.83 mm, exposure time 2 μs, (b) FR3, V=80 kV, length 23.98 mm, exposure time 3 μs, (c) Gemini X, V=90 kV, length 28.57 mm, exposure time 3 μs.

6.2.1.2 Negative streamer

Figure 6-4 shows a typical recording of negative streamer propagation at a voltage level just above inception, which was obtained on Midel 7131/pressboard interface at the 50 mm gap distance. A train of clearly recognized discrete pulses with increasing amplitude was observed for both current and light signals, which is similar to what was observed in open gaps [13]. Compared with positive polarity, light and current pulses of negative streamers are less frequent but with larger amplitude. Integral light images of the streamer at the same voltage level obtained in perpendicular and parallel directions are shown in Figure 6-4 (b) and (c) respectively. Small tree-like streamers were observed (Figure 6-4 (b)) and they might even propagate away from the pressboard surface (Figure 6-4 (c)). The length of streamer in Figure 6-4 (b) is 5.42 mm and the corresponding propagating time in Figure 6-4 (a) is 8.72 μs, so the average velocity is deduced as 0.62 km/s, which is slower than that of positive streamer, but still belongs to 2^{nd} mode negative streamer.

With the increase of applied voltage, the repetition rate of current and light pulses does not increase but the amplitude grows greatly as shown in Figure 6-5 (a), which was obtained on FR3/pressboard interface at the 50 mm gap distance. In addition, a series of

large pulses with similar amplitude were always observed at the beginning of both current and light signals, followed by the normal train of pulses of increasing amplitude. This is believed to be the same as the 3^{rd}+2^{nd} mode propagation observed in open gaps [35]. Integral light images of the streamers also support the above description since a luminous zone was always observed at the root of streamer, as shown in Figure 6-5 (b) and (c). The length of streamer in Figure 6-5 (b) is 21.38 mm and the corresponding propagating time in Figure 6-5 (a) is 16.52 μs, thus the average velocity is 1.29 km/s, representing the typical 2^{nd} mode negative streamer.

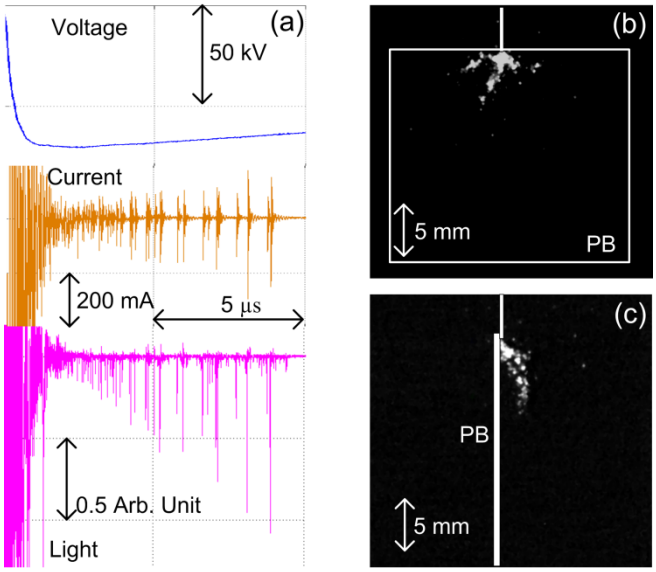

Figure 6-4 Negative streamer propagation on Midel 7131/pressboard interface at low voltage level; d=50 mm, V=-70 kV, (a) voltage, current and light waveforms, (b) integral light image in perpendicular direction, corresponding to the signals in (a), (c) integral light image in parallel direction.

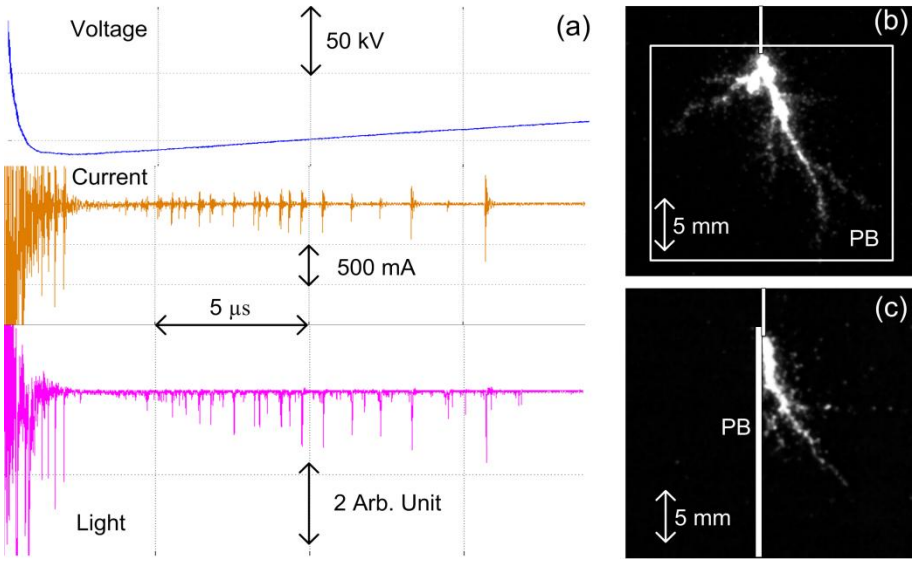

Figure 6-5 Negative streamer propagation on FR3/pressboard interface at high-voltage level; d=50 mm, V=-110 kV, (a) voltage, current and light waveforms, (b) integral light image in perpendicular direction, corresponding to the signals in (a), (c) integral light image in parallel direction.

Figure 6-6 shows the typical shadowgraph images of negative streamers along pressboard surface in the three liquids. Negative streamers have much thicker channels and more side offshoots than positive streamers. The structures of negative streamers on ester/pressboard interface are similar to those observed in open ester gaps [106], only half of which is removed by the presence of pressboard. It was observed that most of the negative streamers in ester liquids propagate along the pressboard surface. As negative streamers in mineral oil normally have less main branches (only one or two) [33, 106], with the pressboard being present, the streamer can propagate either on the pressboard surface or in the adjacent liquid, as shown in Figure 6-6 (c). It is noteworthy that the streamer propagating in the mineral oil seems always to come back and touch the pressboard surface at a later stage.

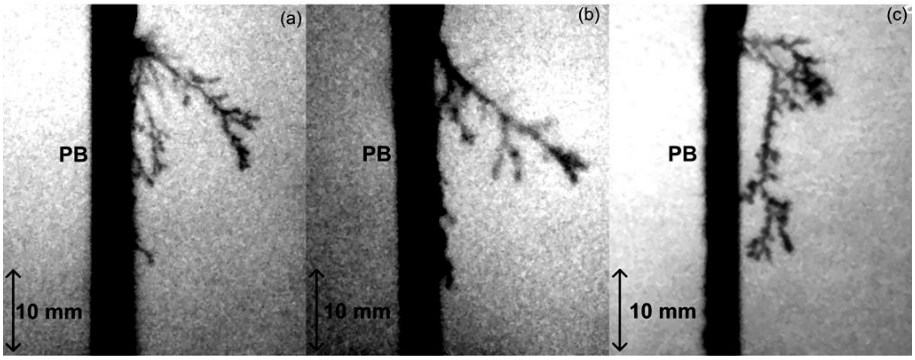

Figure 6-6 Shadowgraph images of negative streamers on liquid/pressboard interface; d=50 mm, (a) Midel 7131, V=-140 kV, length 28.56 mm, exposure time 3 μs, (b) FR3, V=-130 kV, length 31.06 mm, exposure time 3 μs, (c) Gemini X, V= -210 kV, length 28.87 mm, exposure time 3 μs.

6.2.2 Stopping Length

Stopping length means the straight-line distance from the farthest tip point of a stopped streamer to the point electrode. Tests were carried out at voltages from inception to the level close to breakdown with steps of 10 kV or 20 kV. At each voltage level, the average value and standard deviation are given based on about 10 measurements.

6.2.2.1 Comparison between with and without pressboard

Figure 6-7 shows the stopping length of streamers on Midel 7131/pressboard interface under both positive and negative polarities at the 50 mm gap (Dashed line shows the results in open gaps, which are given in section 5.3.1). Streamer length under both polarities increases gradually when the applied voltage is increased. Strong polarity effect exists: at the same voltage level, positive streamer propagates much further than

negative streamers, leading to the lower breakdown voltage under positive polarity. It should be stressed that no promotion effect was observed under both polarities when the pressboard was introduced. Similar trends were observed on FR3/pressboard interface as shown in Figure 6-8. The only difference is that there is a minor increase of stopping length at high-voltage levels with the presence of pressboard.

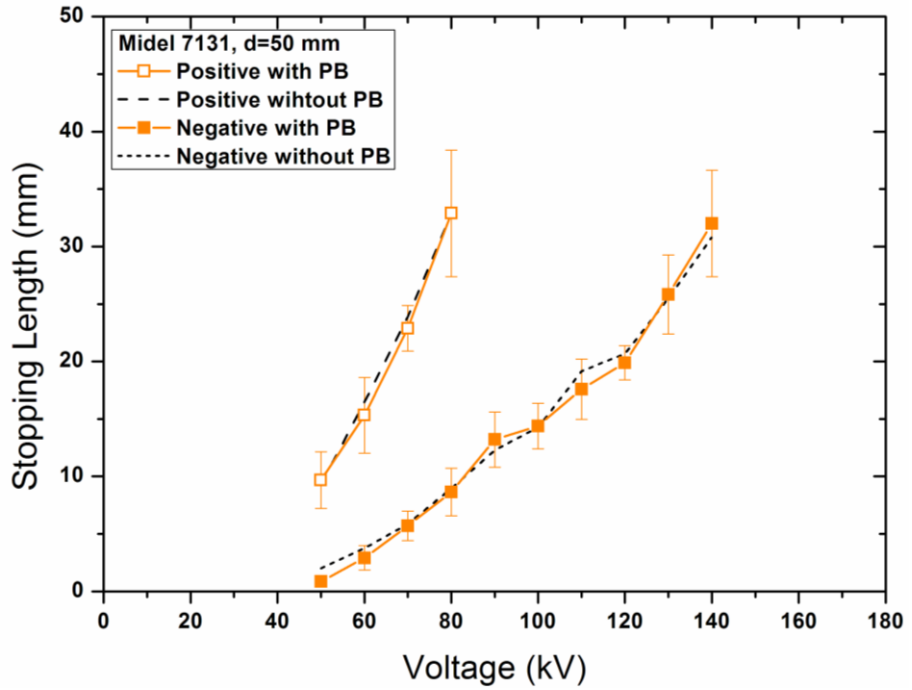

Figure 6-7 Stopping length of streamers on Midel 7131/pressboard interface under both positive and negative polarities and compared with those in open liquid gaps; d=50 mm; error bars stand for one standard deviation, same as the following figures.

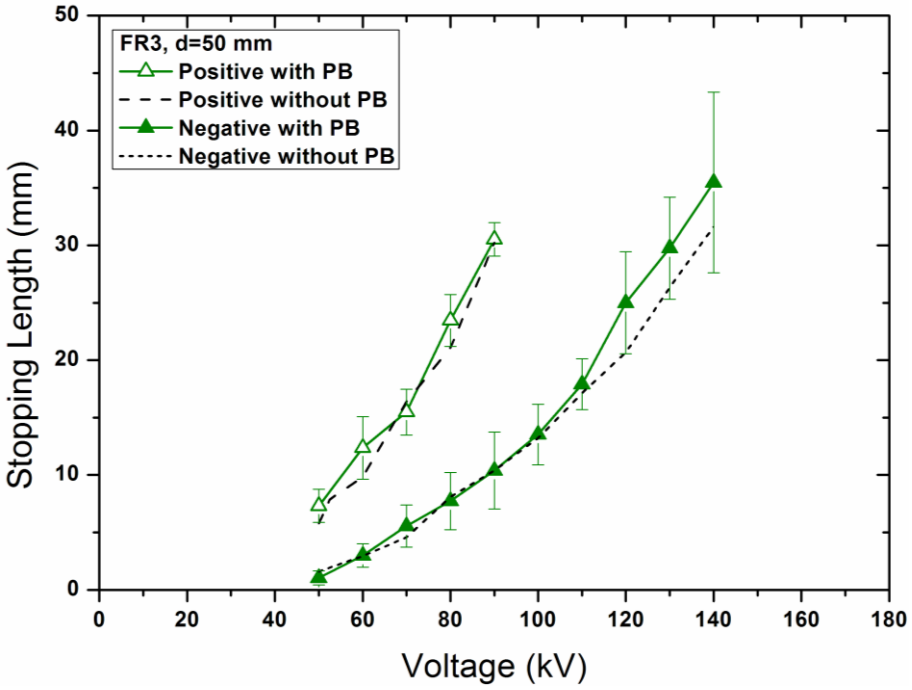

Figure 6-8 Stopping length of streamers on FR3/pressboard interface under both positive and negative polarities, and compared with those in open liquid gaps; d=50 mm.

Stopping length of streamers in mineral oil Gemini X with and without pressboard is shown in Figure 6-9. Under positive polarity, streamer length increases with the applied voltage following the same trend for both on pressboard interface and in open liquid gap. Under negative polarity, it seems that there is a notable increase of streamer length with the presence of pressboard surface at the voltage levels higher than 130 kV. For the tests on Gemini X/pressboard interface, two observations were made on each pressboard sample. Therefore, the small increase of stopping length is mainly due to the accumulative effect, which is to be discussed in section 6.3.2.

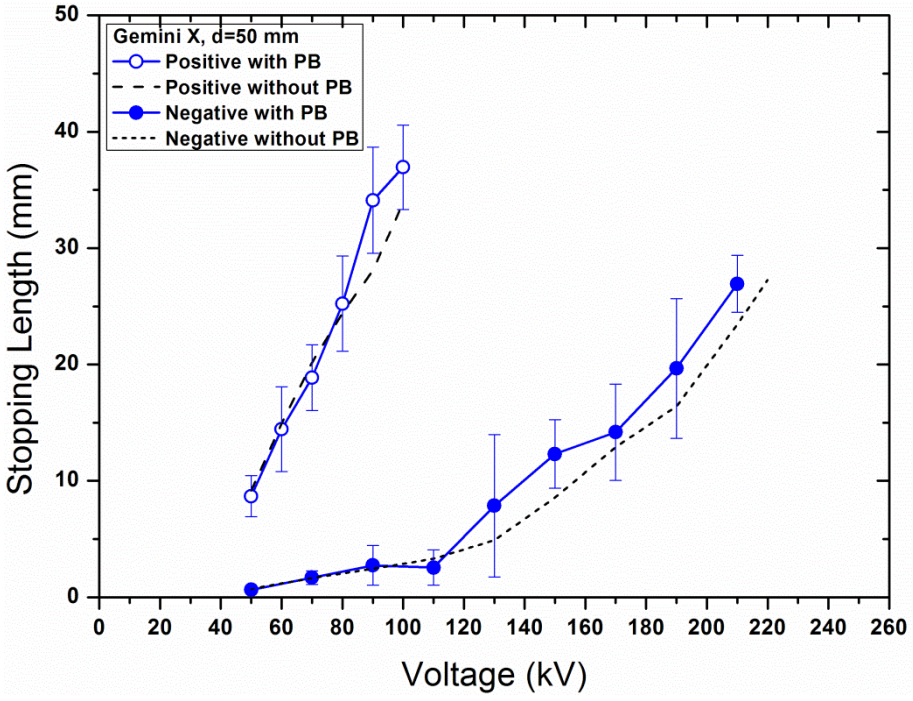

Figure 6-9 Stopping length of streamers on Gemini X/pressboard interface under both positive and negative polarities, and compared with those in open liquid gaps; d=50 mm.

6.2.2.2 Comparison between ester liquids and mineral oil

Figure 6-10 shows the comparison of stopping lengths of positive streamers on pressboard surface in ester liquids and mineral oil at the gap distance of 50 mm. 50% breakdown voltages, $V_{b\text{-}M}$, $V_{b\text{-}F}$ and $V_{b\text{-}G}$, are stated on the figure, which stand for breakdown voltage on Midel 7131/pressboard interface, FR3/pressboard interface and Gemini X/pressboard interface respectively. Below breakdown voltage, the increasing trend of stopping length with voltage seems in a linear relationship. In addition, the difference of trend between ester/pressboard and mineral oil/pressboard is relatively small, which is the same as what was observed in open gaps.

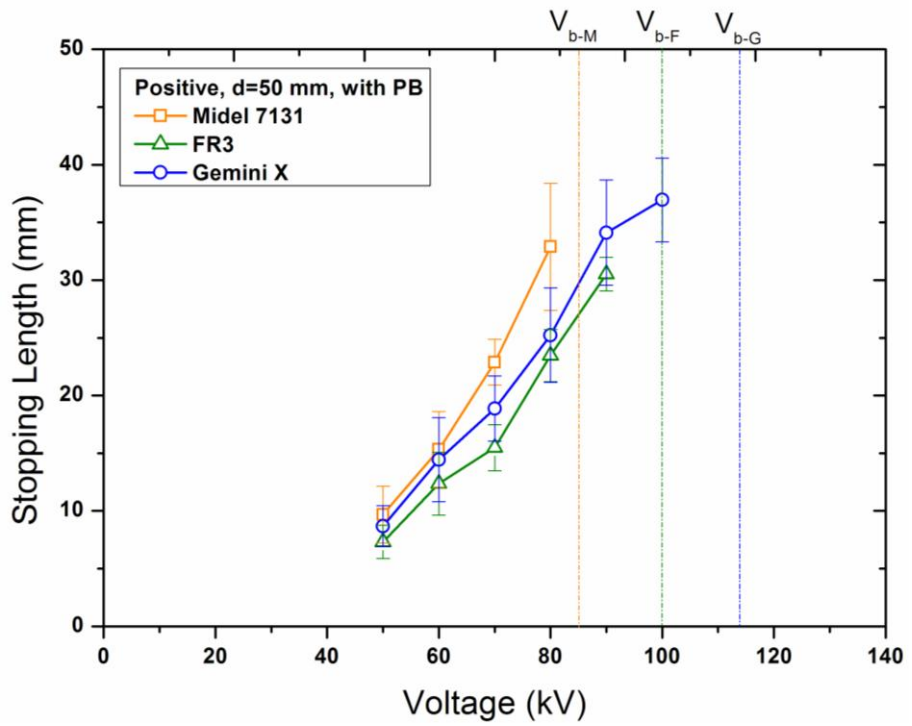

Figure 6-10 Stopping lengths of positive streamers on pressboard surface in the three liquids; d=50 mm.

Figure 6-11 shows the comparison of stopping lengths of negative streamers on pressboard surface in ester liquids and mineral oil at the gap distance of 50 mm. A significant difference between ester liquids and mineral oil was observed. Below 130 kV, negative streamer on Gemini X/pressboard interface grows slowly with voltage. Afterwards its growth increases quickly with voltage, showing the similar trend to streamer on ester/pressboard interface. At the same voltage level, streamer on ester/pressboard interface propagates much further than that on mineral oil/pressboard interface. The overall performance with the presence of pressboard interface is the same as what was observed in open gaps.

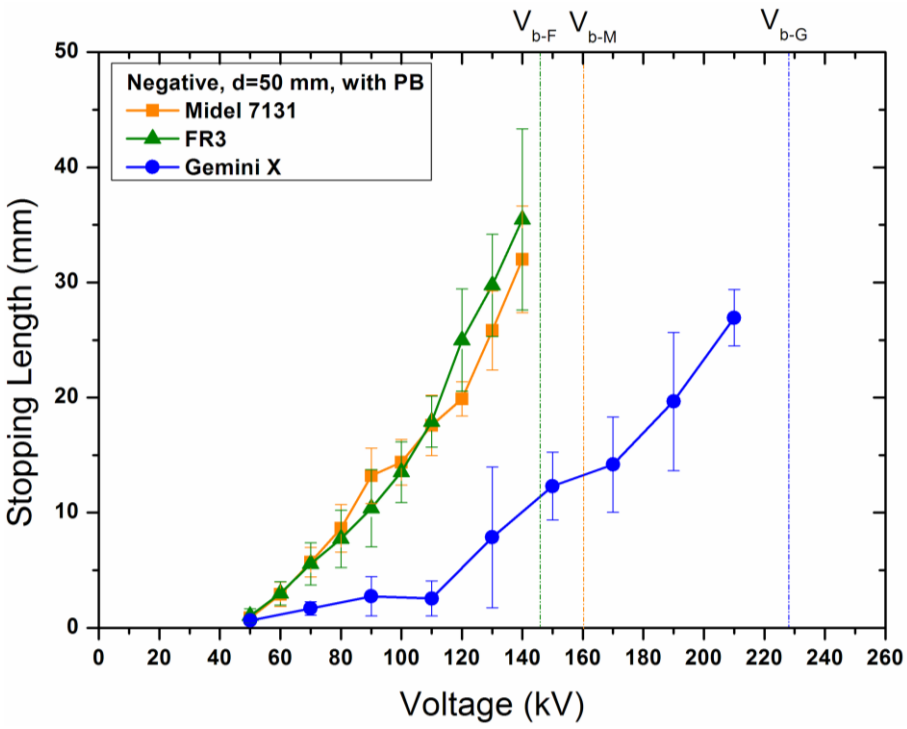

Figure 6-11 Stopping lengths of negative streamers on pressboard surface in the three liquids; d=50 mm.

6.3 Breakdown Voltage

6.3.1 Tests at Various Gap Distances

Breakdown voltage was measured using rising-voltage procedure, i.e. 1 shot per step and at least 3 steps applied before breakdown; the same as stated in section 5.3. Pressboard sample was changed after each breakdown. Five tests were carried out at each gap distance from 25 mm to 75 mm under both positive and negative polarities, of which the average value was taken as the 50% breakdown voltage. Generally an interval of 10 minutes was given between two consecutive tests including the time for changing pressboard samples.

Under positive polarity as shown in Figure 6-12, breakdown voltage increases gradually with gap distance. At 25 mm, breakdown voltages are similar on ester/pressboard interface to that on mineral oil/pressboard interface. With larger gap distances, breakdown voltage on mineral oil/pressboard interface becomes higher than that on ester/pressboard interface. The difference was further enlarged at gap distances of 100 mm and 200 mm as reported in [14]. Introduction of pressboard almost does not reduce the 50% breakdown voltage in both ester liquids and mineral oil.

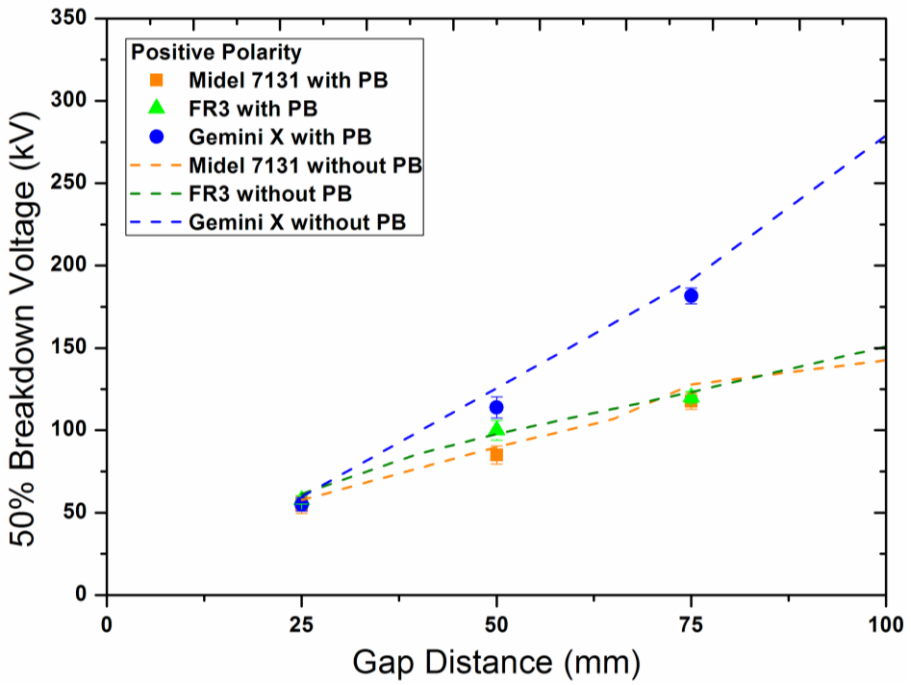

Figure 6-12 50% Breakdown voltages on pressboard surface in the three liquids at various gap distances under positive polarity.

At breakdown voltage levels under positive polarity, no obvious mark or damage was observed due to breakdown on both ester/pressboard and mineral oil/pressboard interfaces for all the gap distances up to 75 mm.

Under negative polarity as shown in Figure 6-13, breakdown voltage increases with gap distance as well. The breakdown voltages on mineral oil/pressboard interface are always higher than those on ester/pressboard interface for all the gap distances investigated in this study. Introduction of pressboard has no influence on the breakdown voltage in ester liquids, but seems to weaken the breakdown voltage in mineral oil at large gap distances, e.g. 20 kV reduction for the 75 mm gap distance.

However such a reduction in mineral oil was found to be caused by the accumulative effect of pre-stresses during the step voltage increase before breakdown, which is to be discussed in next section. Therefore, the procedure was improved to that pressboard was changed after each shot rather than after each breakdown, based on which the breakdown voltages obtained were exactly the same as those in open mineral oil gaps. Similar procedure was also recommended in [14], of which the breakdown voltages were not weaken by the presence of pressboard in both ester liquids and mineral oil at the gap distance of 100 mm.

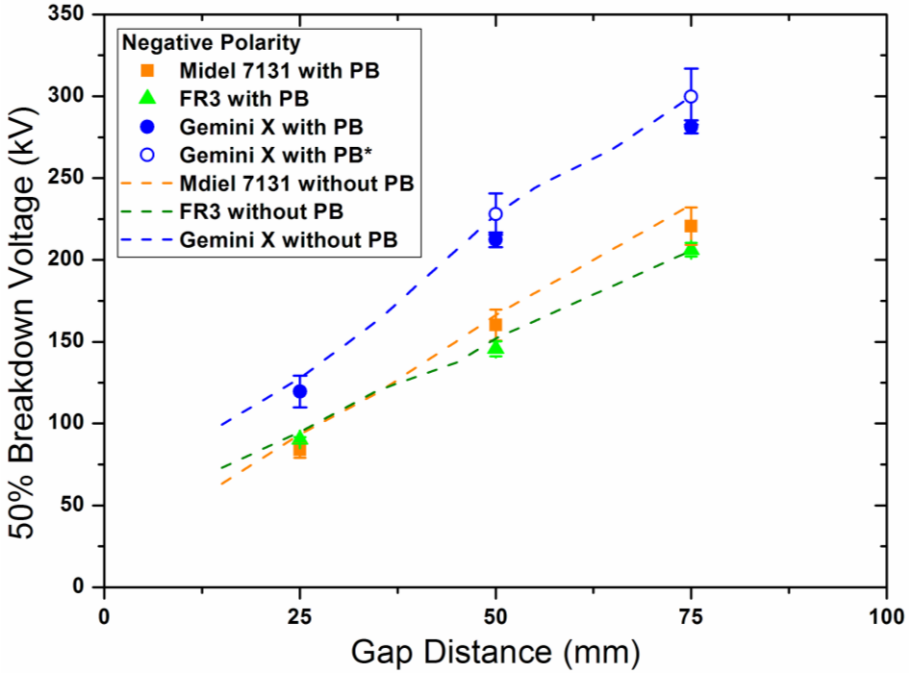

Figure 6-13 50% Breakdown voltages on pressboard surface in the three liquids at various gap distances under negative polarity.* Tests were carried out by changing pressboard after each shot rather than each breakdown.

At breakdown voltage levels under negative polarity, permanent black scar was usually observed on ester/pressboard interface at the gap distance of 75 mm, as shown in Figure 6-14 (a). For Gemini X/pressboard interface, it was observed at both gap distances of 50 mm and 75 mm, as shown in Figure 6-14 (b) and (c). A long full-path black scar was normally left by the breakdown arc at the 75 mm gap distance. In addition tree-like white mark was sometimes observed on Midel 7131/pressboard interface at the 75 mm gap distance, as shown in Figure 6-14 (d), which is not permanent damage and disappears in a short period when exposed to air environment. Therefore white marks are more likely some enclosed gaseous channels, which are formed by 'burning' the oil out of the pressboard surface during the flashover. It was noted that the main path of flashover arc tends to produce black scars when the other sub-branches tend to create white marks.

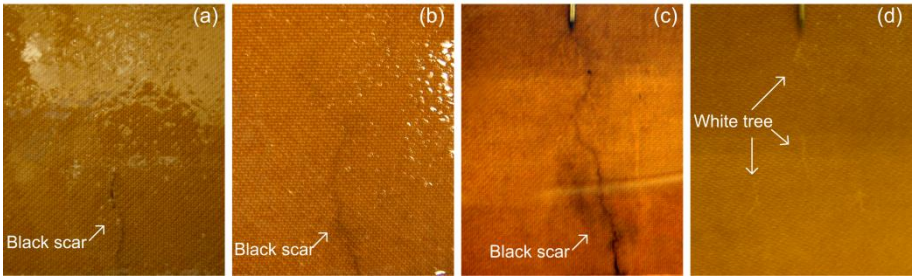

Figure 6-14 Surface mark on pressboard at breakdown voltage levels under negative polarity; (a) black scar on Midel 7131/pressboard interface, d=75 mm, V=-210 kV, (b) short black scar on Gemini X/pressboard interface, d=50 mm, V=-230 kV, (c) long black scar on Gemini X/pressboard interface, d=75 mm, V=-290 kV, (d) white tree on Midel 7131/pressboard interface, d=75 mm, V=-240 kV.

6.3.2 Accumulative Effect in Breakdown Voltage Tests

In lightning tests, multiple shots are inevitably applied on the testing samples before a breakdown occurs, therefore a time interval between two consecutive shots is normally required in standards to avoid the possible accumulative effect: minimum 30 seconds in ASTM D 3300 and minimum 60 seconds in IEC 60897 are specified. To verify the accumulative effect in ester liquids and mineral oil with pressboard involved, the following procedure was defined: a series of 25 shots with 60 seconds interval at the same voltage level below the breakdown voltage, were applied on the same position of a pressboard sample. Streamer images were regularly taken, and the stopping length was used as the criterion for justification of the existence of accumulative effect.

Figure 6-15 shows the results of multiple-shot test on ester/pressboard interface under both positive and negative polarities. Applied voltage was chosen at which the streamer usually propagates to half of the gap distance and breakdown would never occur. It was found that streamers were kept stable during the series of 25 shots on ester/pressboard interface under both positive and negative polarities. In other words, no accumulative effect exists on ester/pressboard interface, or if there is any cause for accumulative effect, 60 seconds interval is long enough to eliminate it.

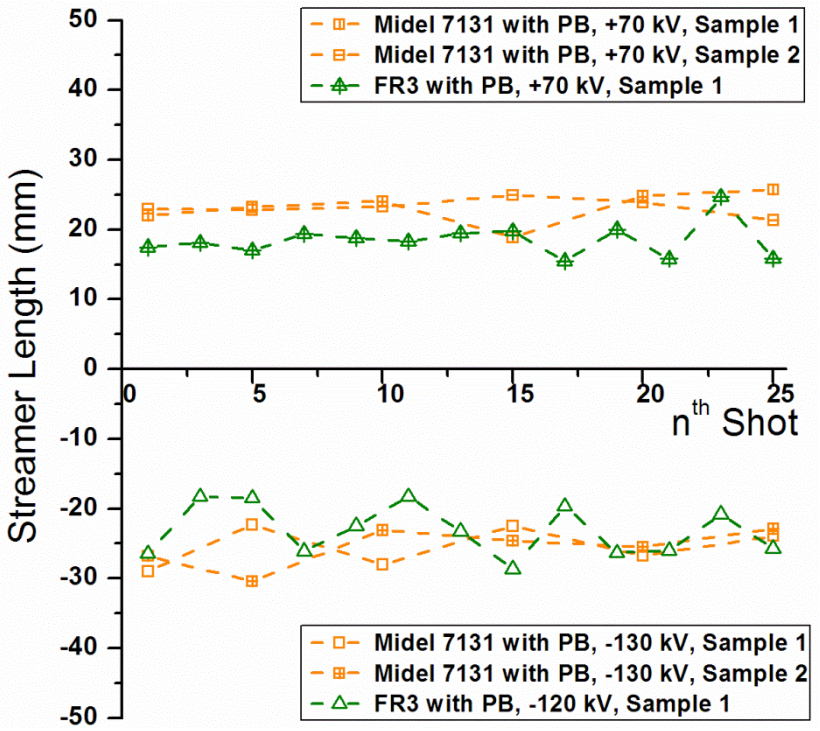

Figure 6-15 Multiple-shot tests on ester/pressboard interface under both positive and negative polarities; d=50 mm.

Figure 6-16 depicts the results of multiple-shot tests on mineral oil/pressboard interface under both positive and negative polarities. Under positive polarity, the streamer length decreases slightly with increasing impulse shots, which is, however, in a reasonable scattering range. Under negative polarity, the streamer length increases gradually with each subsequent shot. At -190 kV, breakdown even occurred after the 9th or 12th shot for two different samples respectively. Therefore strong accumulative effect on negative streamer propagation was clearly found on mineral oil/pressboard interface.

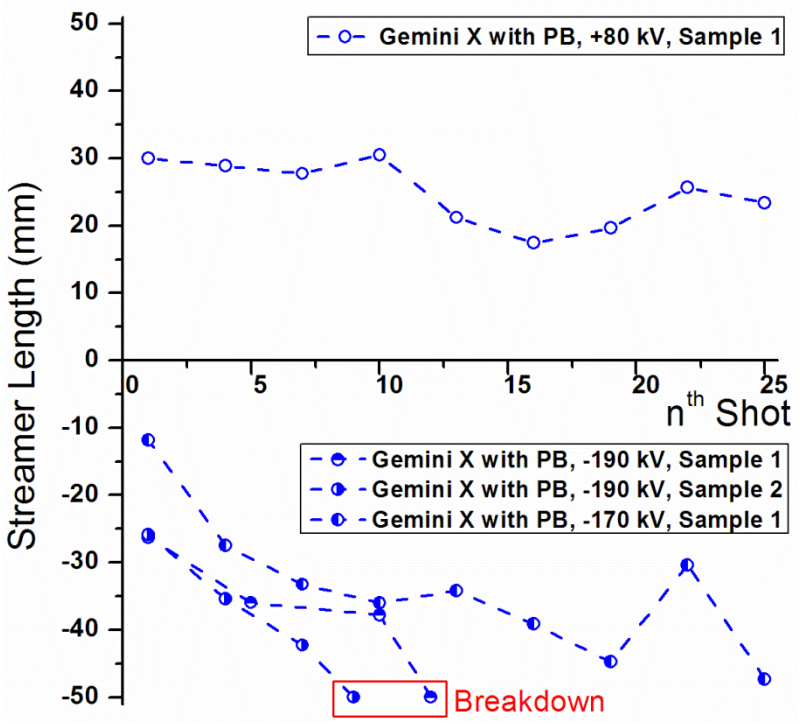

Figure 6-16 Multiple-shot tests on mineral oil/pressboard interface under both positive and negative polarities; d=50 mm.

Further tests indicate that the accumulative effect does not exist in open mineral oil gaps as shown in Figure 6-17, so it is confirmed that mineral oil impregnated pressboard is the key in promoting streamer propagations under the accumulative stress condition. Such an accumulative effect may lead to the underestimation of breakdown voltage, as shown in the last section.

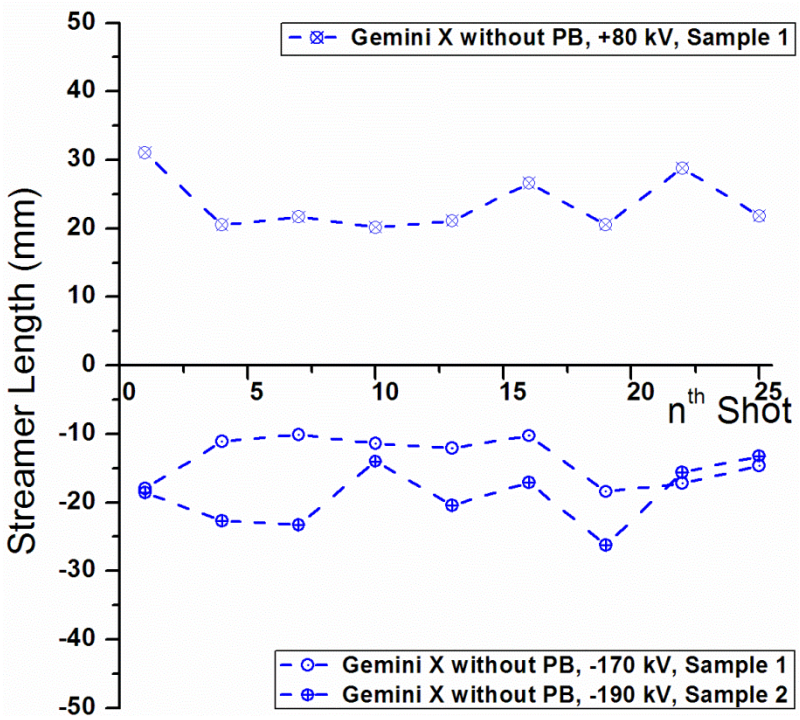

Figure 6-17 Multiple-shot tests in open mineral oil gap under both positive and negative polarities; d=50 mm.

It was noted that accumulative effect was only observed on mineral oil/pressboard interface under negative polarity. Effects of charge storage and bubble residence on the pressboard surface are considered to explain the observed accumulative effect [107]. In terms of the difference between liquids, charge storage might be dominant: the time constant of space charge dissipation on mineral oil/pressboard interface is much longer than that on ester/pressboard interface [108, 109], so the residual space charges on mineral oil/pressboard interface could distort the local electric field on the pressboard surface and thus accelerate the subsequent streamer propagation. As for the difference between polarities, bubble residence might be dominant: the gaseous channels of negative streamers are thicker than positive ones, and this could mean more micro bubbles are generated after the collapse of negative streamer and reside on the pressboard surface, thus promote the subsequent streamer propagation. To fully understand the underlying mechanisms, further studies on this phenomenon are needed.

6.4 Acceleration Voltage

When applied voltage is increased further, streamer propagation can switch from slow modes (1st and 2nd) to fast modes (3rd and 4th), of which the transition voltage is called acceleration voltage [35]. Tests were carried out at gap distances of 25 mm and 50 mm under both positive and negative polarities.

6.4.1 Under Positive Polarity

Figure 6-18 and Figure 6-19 show the average propagation velocities of positive streamers on pressboard surface in the three liquids at gap distances of 25 mm and 50 mm respectively.

Below acceleration voltage, the streamer velocity increases slowly with increased voltage level, generally in the range of 1.0 km/s to 3.0 km/s, for both cases of with and without pressboard interface and for all three liquids. Once the transition into fast mode is made, the streamer velocity increases quickly with increased voltage level, finally reaching 25 km/s for the 25 mm gap distance and 50 km/s for the 50 mm gap distance in the present study. The acceleration voltage on Gemini X/pressboard interface is much higher than that on ester/pressboard interface. It should be emphasized here that introduction of pressboard does not influence the streamer velocity in ester liquids, but significantly promotes the streamer velocity in mineral oil at overstressed voltages leading to a large reduction of acceleration voltage: about 60 kV for both 25 mm and 50 mm gap distances. Similar phenomenon was also observed at the 100 mm gap distance in [14], of which the acceleration voltage of streamers on mineral oil/pressboard interface was reduced by about 60 kV as well.

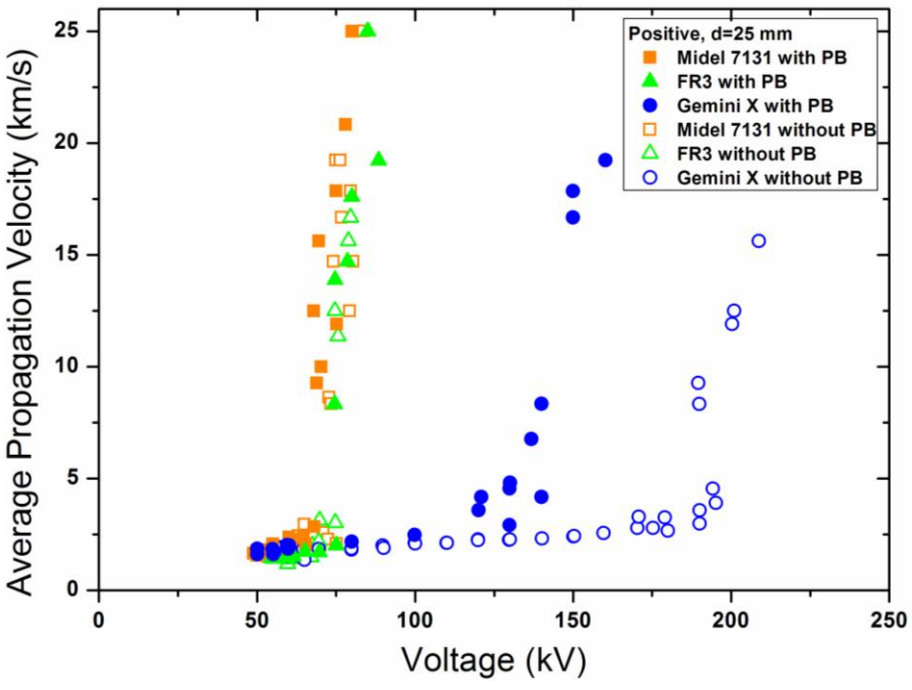

Figure 6-18 Average propagation velocity of positive streamers on pressboard surface in the three liquids; d=25 mm.

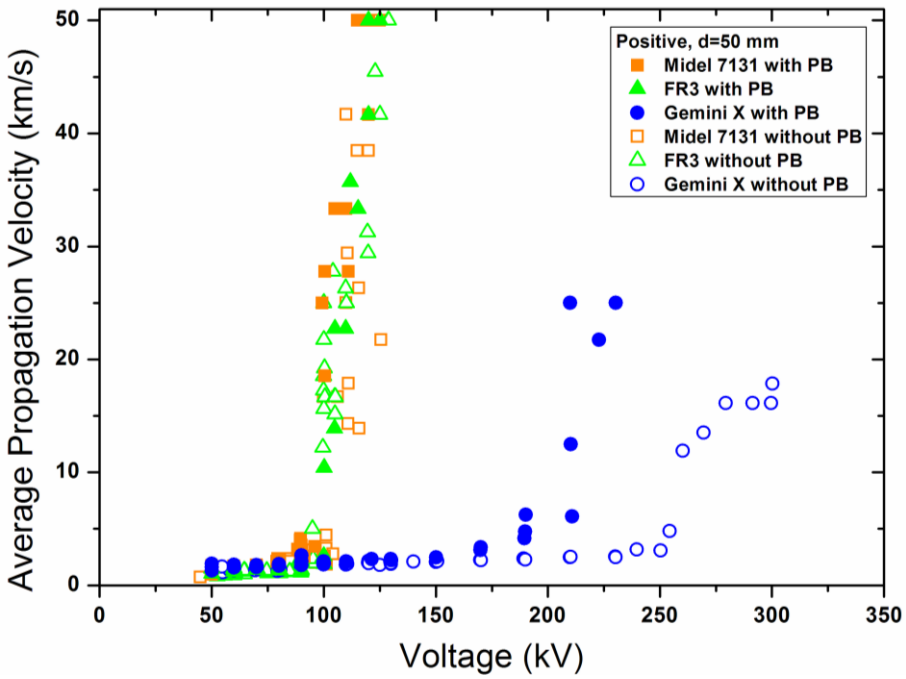

Figure 6-19 Average propagation velocity of positive streamers on pressboard surface in the three liquids; d=50 mm.

At overstressed voltages, still no significant damaging mark was left by flashover on ester/pressboard interface under positive polarity. As shown in Figure 6-20 (a), only minor scar was observed at the bottom of pressboard. Similar phenomenon of weak marks on ester/pressboard interface was also reported in [14] at the gap distance of 200 mm. However, significant black scar was seen on Gemini X/pressboard interface at an extreme overstressed voltage level of 230 kV, which is 120 kV higher than 50% breakdown voltage, as shown in Figure 6-20 (b).

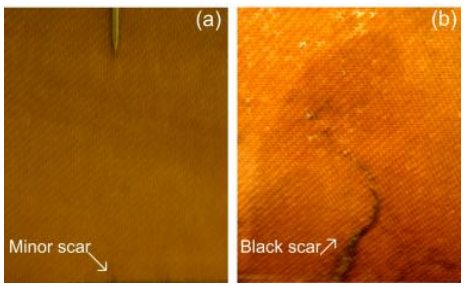

Figure 6-20 Surface mark on pressboard at overstressed voltage levels under positive polarity; (a) minor scar on Midel 7131/pressboard interface, d=50 mm, V=110 kV, (b) long black scar on Gemini X/pressboard interface, d=50 mm, V=230 kV.

6.4.2 Under Negative Polarity

Figure 6-21 and Figure 6-22 depict the average propagation velocities of negative streamers on pressboard surface in the three liquids at gap distances of 25 mm and 50 mm respectively.

Similar to those under positive polarity, below acceleration voltage, the streamer velocity increases slowly with increased voltage level, in a lower range of about 0.5 km/s to 1.5 km/s. Over acceleration voltage, streamer velocity starts to increase gradually with the increase of voltage level, but not as quickly as under positive polarity. In addition, the difference of acceleration voltage between ester/pressboard and mineral oil/pressboard becomes smaller under negative polarity.

At the gap distance of 25 mm, it was found that introduction of pressboard has no influence on the streamer velocities in both ester liquids and mineral oil, as shown in Figure 6-21. With gap distance increasing to 50 mm, acceleration of velocity by pressboard was observed at very high-voltage levels (higher than acceleration voltage) in ester liquids, as shown in Figure 6-22. Such an effect is more obvious at the large gap distance of 100 mm, of which the velocity acceleration by pressboard occurred earlier at lower voltage levels for both ester liquids and mineral oil, as reported in [14]. Overall, if taking acceleration voltage as the only criterion, pressboard has no influence for negative polarity in the investigated range.

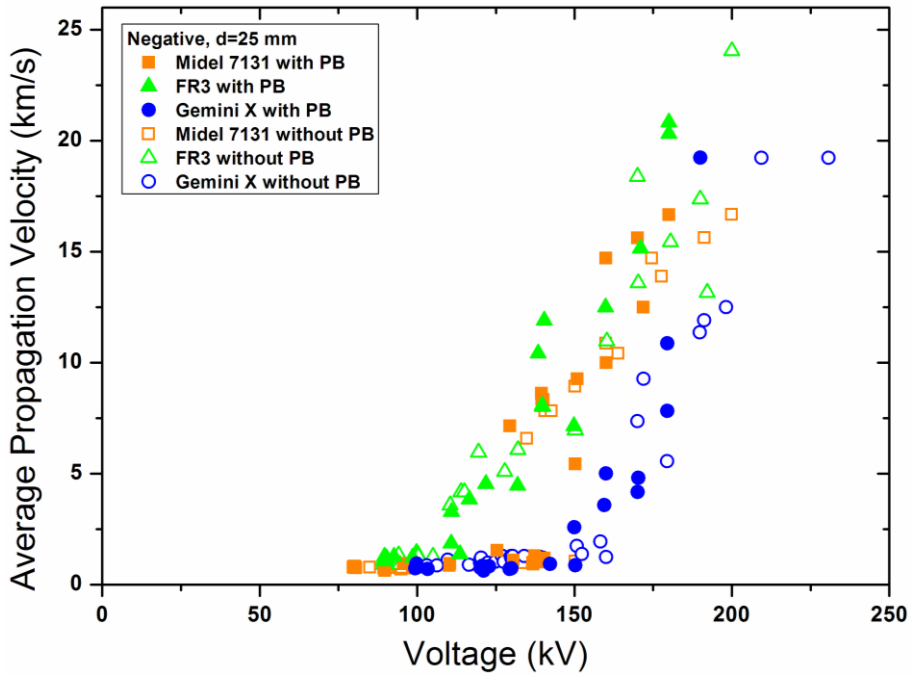

Figure 6-21 Average propagation velocity of negative streamers on pressboard surface in the three liquids; d=25 mm.

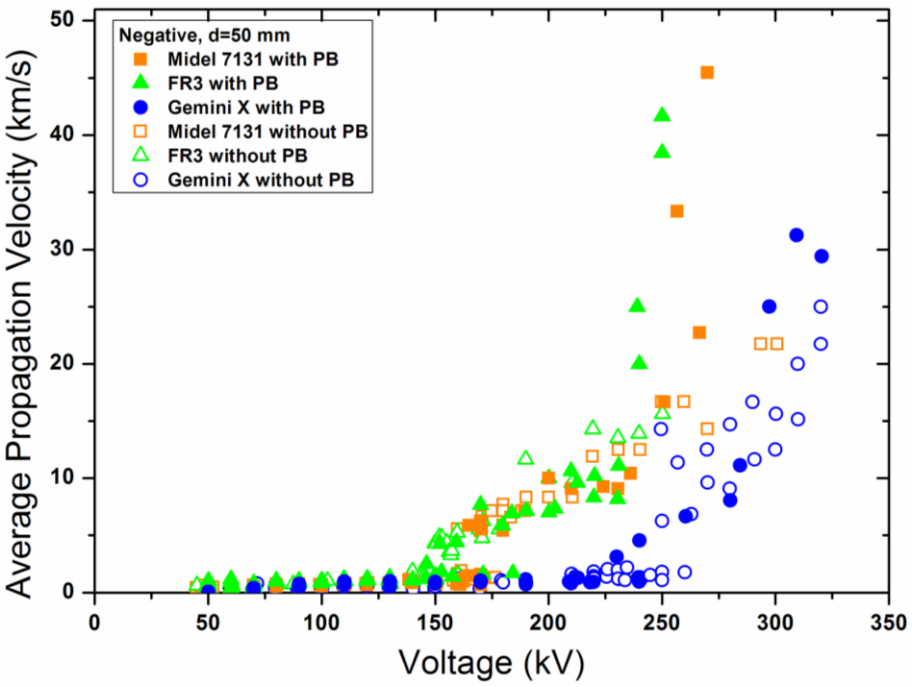

Figure 6-22 Average propagation velocity of negative streamers on pressboard surface in the three liquids; d=50 mm.

At negative overstressed voltages, long black scar which connects point and plane electrodes was observed on ester/pressboard interface, as shown in Figure 6-23 (a). It is interesting to see the existence of both black scar and white mark on the ester/pressboard interface, as shown in Figure 6-23 (b). For Gemini X/pressboard interface, long thick black scar was usually observed at overstressed voltages as shown in Figure 6-23 (c). With further increased voltage, bulk protrusion caused by excessive energy could be occasionally observed, which seems to indicate the under-surface damage of pressboard, as shown in Figure 6-23 (d).

Figure 6-23 Surface mark on pressboard at overstressed voltages under negative polarity; (a) long black scar on FR3/pressboard interface, d=50 mm, V=-250 kV, (b) black scar with white mark on Midel 7131/pressboard interface, d=50 mm, V=-255 kV, (c) long thick black scar on Gemini X/pressboard interface, d=50 mm, V=-310 kV, (d) black scar with bulk protrusion on Gemini X/pressboard interface, d=50 mm, V=-320 kV.

6.5 Summary

Streamer characteristics and breakdown in synthetic and natural ester transformer liquids with pressboard interface were investigated under both positive and negative lightning impulse voltages. Experiments were carried out in a non-uniform point-plane field at three stages of pre-breakdown, breakdown and overstressed conditions.

At pre-breakdown stage, streamers on ester/pressboard interface resemble the characteristics of streamers in open gaps and introduction of pressboard interface has no influence on the streamer stopping length. Streamers on ester/pressboard interface generally propagate further than on mineral oil/pressboard interface at the same voltage level, especially under negative polarity.

Presence of pressboard does not weaken the 50% breakdown voltage under both positive and negative polarities at the investigated gap distances up to 75 mm. Breakdown voltages on ester/pressboard interface are lower than those on mineral oil/pressboard interface, and this difference is magnified at larger gap distances. Surface damages on the pressboard were only observed after breakdown under negative polarity, which are more obvious in mineral oil than in ester liquids. Care should be taken for breakdown tests on mineral oil/pressboard interface under negative polarity, since an accumulative promoting effect from streamer on subsequent streamer propagation was observed, which, however, did not occur on ester/pressboard interface.

At overstressed conditions, introduction of pressboard interface significantly reduces the positive acceleration voltage in mineral oil, however this does not occur in ester liquids. Surface mark after positive breakdown can be seen on mineral oil/pressboard interface but hardly for ester/pressboard interface. Under negative polarity, presence of pressboard tends to accelerate the streamer velocity at larger gap distances and under higher voltages in both ester liquids and mineral oil. Obvious surface marks including long thick black scar and white tree were observed on pressboard after negative breakdown. Overall, acceleration voltages on ester/pressboard interface are still lower than those on mineral oil/pressboard interface, which indicates the lower tolerance to faster streamers on ester/pressboard interface.

CHAPTER 7. SECONDARY REVERSE STREAMER OF ESTER LIQUIDS IN NON-UNIFORM FIELD

7.1 Introduction

In the field of surface discharge, phenomenon of back discharge, having opposite polarity to the applied voltage, has been observed on solid surfaces under both positive and negative impulse voltages. The solid surface was sandwiched in between the needle and plate electrodes and exposed in the air environment [110, 111]. During the falling (or ending) period of impulse voltage, the needle electrode exhibited opposite polarity with respect to the previously charged surface. If the reverse electric field induced by the surface charge was strong enough, back discharge could be observed. Similar phenomenon was also reported on a solid surface immersed in mineral oil under lightning impulse voltage [71]. A 'secondary' back discharge occurred approximately 100 μs after the main discharge evidenced by the current waveform. It is well known that back discharges on solid surface take advantage of the charge memory effect of solid dielectrics, which helps trapping the residual space charges on the surface thus further leading to the reverse electric field. Therefore it is not expected to observe such phenomenon in open liquid gaps i.e. without the presence of solid surface.

This chapter, however, depicts a newly observed streamer-in-liquid phenomenon which occurs subsequently and well after the extinction of the primary streamer (PS) propagation within a single shot of impulse voltage and has the reverse polarity to the PS as well as to the applied impulse voltage. This phenomenon is similar to the back discharge phenomenon on solid surface. However 'streamer' is commonly used to describe a discharge phenomenon in liquids, and its occurrence is secondary and polarity is reverse to the PS, which prompt us to name this newly observed phenomenon as 'secondary reverse streamer (SRS)'. The tests are carried out in a point-plane gap. Characteristics of SRS including length, velocity and time of occurrence under both positive and negative polarities at the gap distances from 25 mm to 100 mm are described. In addition, the formation mechanisms of SRS are discussed and the effect of tail-chopped impulse on the SRS is investigated. The majority of the tests are carried out in synthetic ester Midel 7131; however the influence of liquid nature on SRS is also presented.

7.2 Phenomenon of Secondary Reverse Streamer (SRS)

SRS was accidentally discovered during the pre-breakdown study on ester liquids, since the normal observation focused maximally on the complete propagation of a PS so that no effort was 'wasted' on the process after 100 μs or even 200 μs.

To introduce this phenomenon, an example of SRS observed in Midel 7131 at a 50 mm gap under negative 120 kV lightning impulse is shown in Figure 7-1. A global scenario of PS and SRS is shown in Figure 7-1 (a). A cluster of intense current and light pulses was recorded after the onset of applied impulse voltage spreading from the beginning to the end of the PS. This is the complete PS process which is normally the focus of pre-breakdown study. However, we observed a SRS with large magnitude short duration current and light signals, which occurred 184.2 μs after the extinction of the PS. It is noteworthy that the impulse voltage decayed to approximately 5 kV when the SRS appeared.

The zoomed-in current and light signals of the PS are shown in Figure 7-1 (b), of which each is composed of a train of irregularly spaced discrete pulses. Charging process induces some noises in both current and light signals at the rising period of the impulse voltage, and these noises are consequently ignored in the following analysis. Throughout the streamer propagation, the current and light pulses increase in amplitude gradually with time. Most of the light pulses can be correlated to the current pulses in terms of occurrence time, which depict the full re-illumination from the needle tip to the head of streamer [13, 35, 66]. Those light pulses which cannot be correlated to the current pulses, indicate the partial re-illumination that might only exist close to the streamer head [35].

A couple of pulses are further zoomed and shown in Figure 7-1 (c), to indicate the polarity of the PS. As light signals measured by PMT are always unidirectional (negative pulses), the polarity of a streamer is determined by the current signal. Negative current pulses are observed as expected for the negative PS, which conforms to the customary understanding. So it is surprising to see that the SRS is with positive polarity, as shown in Figure 7-1 (d). In addition, maximum light intensity of the SRS is 6.56 arb. unit, which is about 1.6 times of that of the PS, 4.03 arb. unit. In terms of

propagation time as indicated by the current/light signals, it is 26.79 μs for the PS and 0.72 μs for the SRS.

Figure 7-1 (e) shows the integral light images. Frame 1 corresponds to the PS while frame 7 corresponds to the SRS. There is no other streamer image observed at the interval between PS and SRS. PS appears in a tree-like shape with many branches propagating in both paraxial and lateral directions, and the final stopping length is 17.71 mm. The average velocity of the PS is calculated as 0.66 km/s using the stopping length divided by the propagation time, and it is regarded as a 2nd mode streamer. SRS image shows a different feature from that of the PS, with a bright single trunk which is 6.76 mm long. It is assumed that the SRS resembles the PS having a propagation process initiating from the needle tip. Therefore the average velocity of the SRS-A is deduced using the same method as 9.36 km/s, which is over 10 times higher than that of the PS, so it is classified as a 3rd mode streamer.

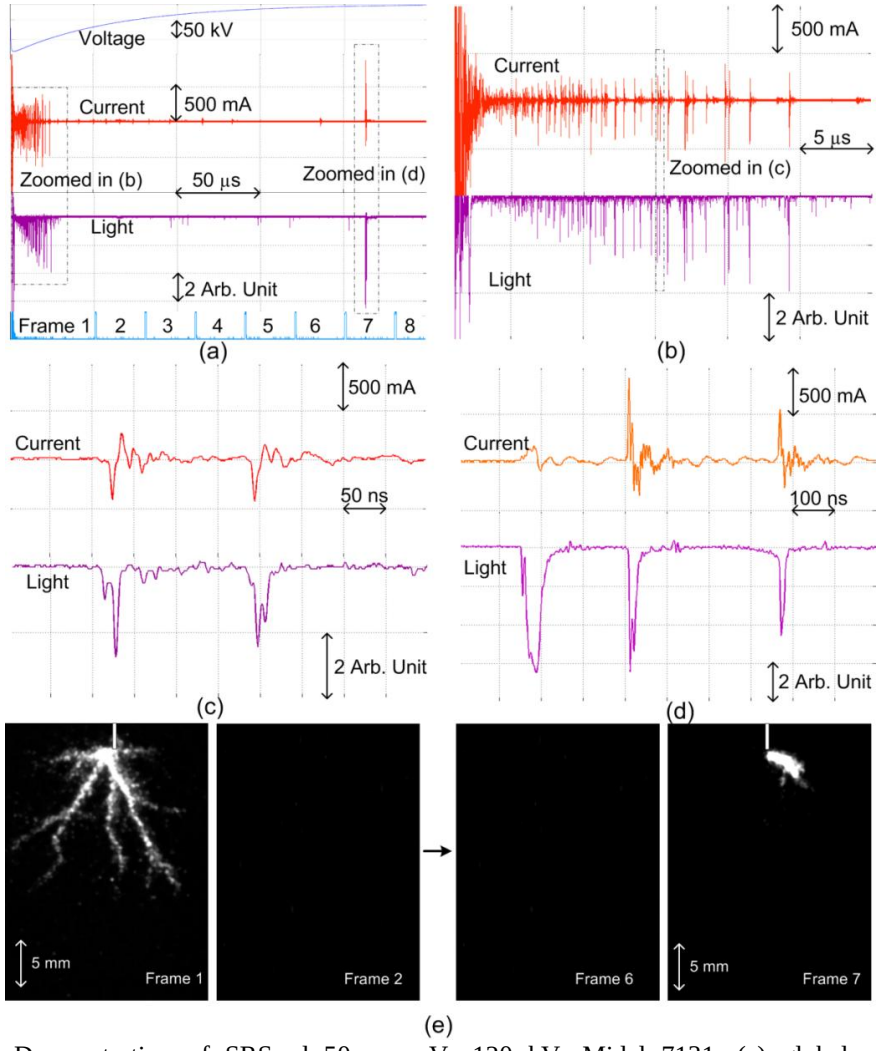

Figure 7-1 Demonstration of SRS; d=50 mm, V=-120 kV, Midel 7131, (a) global scenario, (b) propagation of PS, (c) polarity of PS, (d) polarity of SRS, (e) streamer images; 50 μs exposure time for frame 1 and 30 μs exposure time for frame 2 to 8.

7.3 Polarity Effect on SRS

It was confirmed that SRS can be observed under both positive and negative impulse voltages. In addition two types of SRS were repeatedly observed under negative lightning impulse voltage. In the following figures, light signal from PMT is used to describe the global scenario of PS and SRS, and current signal is supplemented to show the polarity of the streamer discharge.

7.3.1 Under Positive Polarity

Figure 7-2 shows an example of SRS observed at a 75 mm gap under the positive 80 kV lightning impulse. PS initiates after the onset of applied impulse and propagates till 12.89 μs, of which the light signal consists of a train of discrete pulses imposed on a low continuous DC component. A light pulse is zoomed-in and its corresponding current pulse indicates the positive polarity of PS. Frame 1 shows a branch-less positive streamer with a stopping length of 25.25 mm and an average velocity of 1.96 km/s, representing 2nd mode streamer. It is striking that, another train of discrete pulses with increasing amplitude are observed at about 175.84 μs when the instant voltage has decayed to about 5 kV. Integral light image frame 9 proves it is indeed a streamer with a stopping length of 3.04 mm and an average velocity of 0.38 km/s, In addition, the zoomed in pulses indicate that SRS is with negative polarity which is reverse to the PS (positive streamer under positive impulse voltage). It should be mentioned that only one type of SRS is observed under positive polarity.

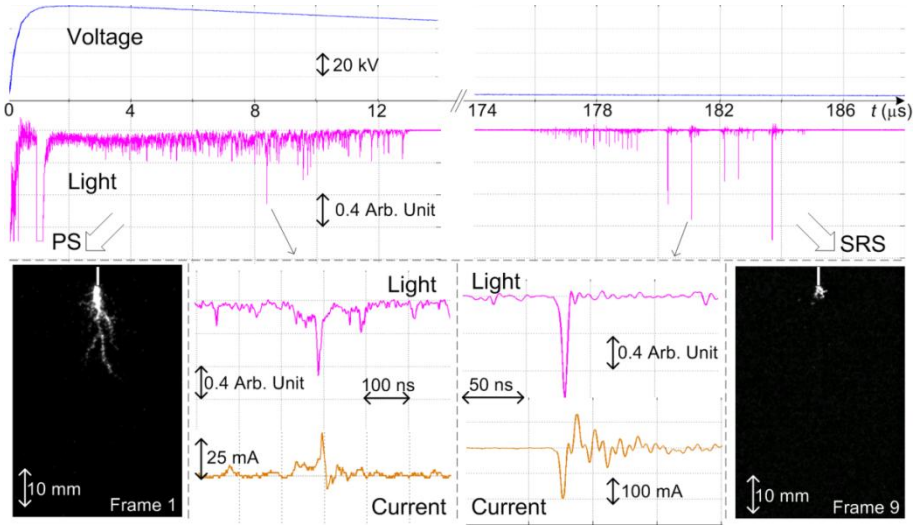

Figure 7-2 Demonstration of a SRS under positive impulse voltage; Midel 7131, V=80 kV, d=75 mm; 30 μs exposure time for frame 1 and 20 μs for the others.

7.3.2 Under Negative Polarity

Under negative impulse voltage, two types of SRS are observed, namely type-A secondary reverse streamer (SRS-A) and type-B secondary reverse streamer (SRS-B).

Figure 7-3 shows an example of SRS-A obtained at a 75 mm gap under the negative 130 kV lightning impulse. PS follows the features of 3^{rd}+2^{nd} mode propagation: it starts from a few large pulses contributing to the initial bright branch-less trunk; then it switches into 2^{nd} mode propagation with a series of increasing pulses resulting in the growth of tree-like branches, as shown in integral light image frame 1. The stopping length and average velocity of the PS are 22.57 mm and 1.15 km/s respectively. Current pulse indicates the PS has negative polarity. When the instant voltage decays to about 2 kV at 292.19 μs, SRS-A is observed which consists of a few large discrete pulses. Integral light image frame 9 shows that SRS-A has a bright thick trunk with a stopping length of 13.57 mm. The average velocity of SRS-A is calculated as 9.19 km/s representing the typical velocity of 3^{rd} mode streamer. SRS-A is with positive polarity which is opposite to the PS with negative polarity.

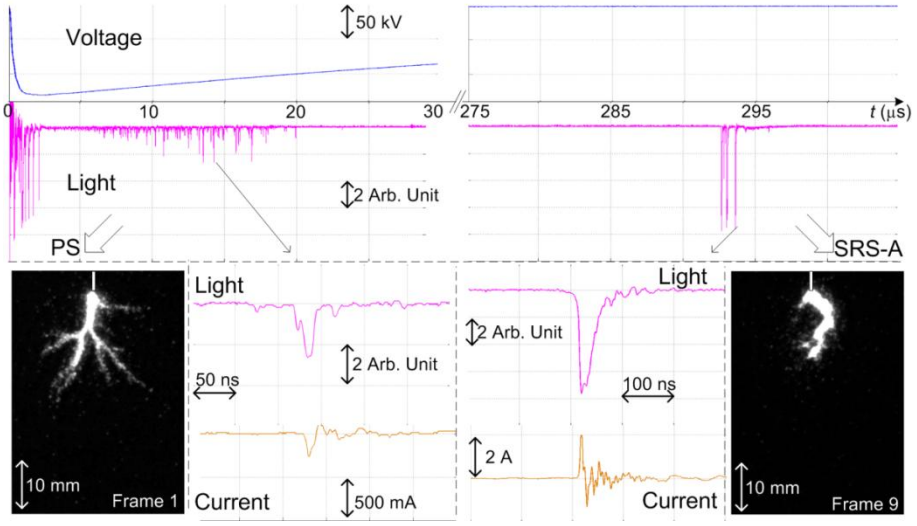

Figure 7-3 Demonstration of a SRS-A under negative impulse voltage; Midel 7131, V=-130 kV, d=75 mm; 75 μs exposure time for frame 1 and 30 μs for the others.

Figure 7-4 shows an example of SRS-B obtained at a 75 mm gap under the negative 170 kV lightning impulse. PS with negative polarity resembles the features of the one described in Figure 7-3, having a stopping length of 28.63 mm and an average velocity of 1.06 km/s. SRS-B occurs at 127.24 μs, at which the instant voltage decays to about

25 kV. Light signal of SRS-B consists of a long-duration DC component imposed by a series of discrete pulses, as shown in Figure 7-4, which is quite different from that of SRS-A. Integral light image frame 3+4 shows that the SRS-B with a stopping length of 16.18 mm is less bright and has more branches than SRS-A. The average velocity of SRS-B is calculated as 1.08 km/s representing the typical velocity of 2nd mode streamer. Similar to SRS-A, it is confirmed that SRS-B has positive polarity which is reverse to the PS with negative polarity.

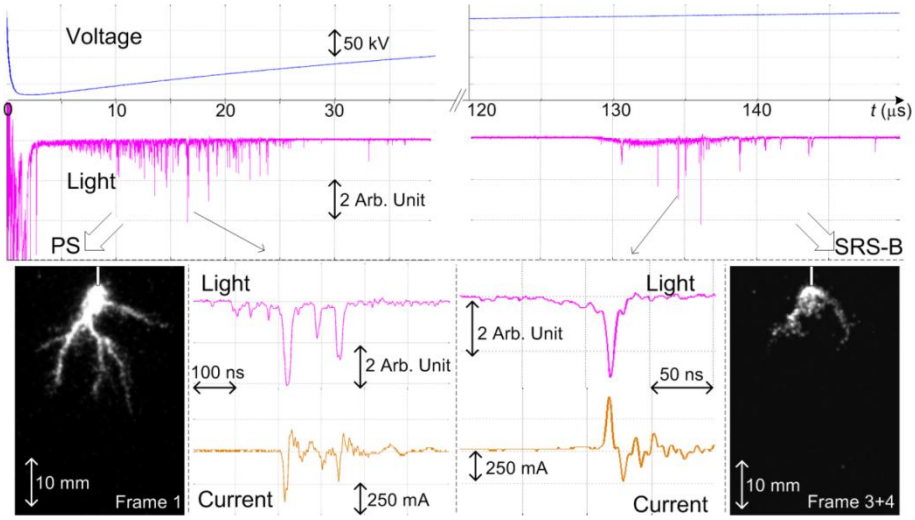

Figure 7-4 Demonstration of a SRS-B under negative impulse voltage; Midel 7131, V=-170 kV, d=75 mm; 75 μs exposure time for frame 1 and 30 μs for the others. Note: the SRS-B occurs half in frame 3 and half in frame 4, so the integral light image frame 3+4 means combination of both frames by photo processing.

7.4 Characteristics of SRS at Various Gap Distances

Characteristics of SRSs including stopping length, propagation velocity and time of occurrence are statistically reported in this section. Tests were carried out at various gap distances: 50 mm, 75 mm and 100 mm for positive impulse voltage; 25 mm, 50 mm and 75 mm for negative impulse voltage. At each gap distance, the tests started from low voltage level till 10 to 20 kV below 50% breakdown voltage. However there were indeed a few breakdowns which occurred at the highest voltage level used. Those breakdowns are neglected in the following analysis.

7.4.1 Stopping Length

Figure 7-5 shows the stopping length of both PSs and SRSs at various gap distances under positive impulse voltage. On average stopping length of PSs grows gradually with

the increase of voltage level at all the gap distances, which conforms to the previous observations [35, 106]. SRSs are much shorter than PSs, with almost no growing trend along with the increasing voltage level. In most of the cases, SRSs have quite weak channels compared to PSs. The longest SRS observed is 10.5 mm under positive 140 kV at the gap distance of 100 mm.

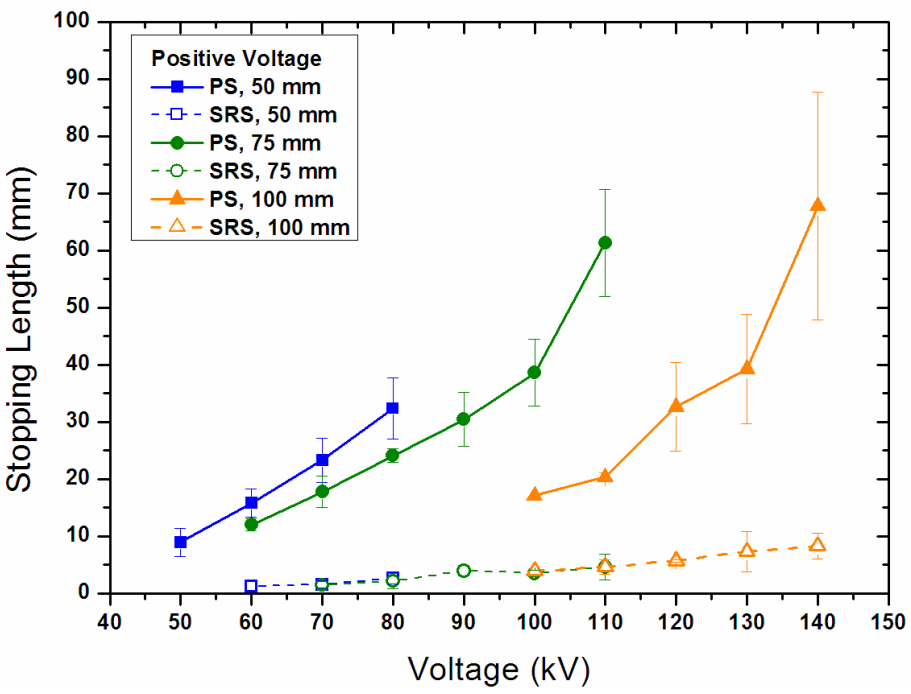

Figure 7-5 Stopping length of PSs and SRSs under positive impulse voltage in Midel 7131.

Figure 7-6 shows the results of stopping length of PSs and SRSs at various gap distances under negative impulse voltage. The two types of SRS under negative impulse voltage are difficult to be differentiated in terms of stopping length, so the stopping length of SRSs at a fixed voltage level is the average of both SRS-As and SRS-Bs. Generally SRSs are shorter than PSs, but both of which increase gradually with the applied voltage level. Both trends somewhat indicate that the inception and strength of SRSs are associated with the strength of the corresponding PSs. The maximum length of SRSs is 26.99 mm observed under negative 190 kV at the gap distance of 75 mm, which has reached about half of that of the corresponding PS.

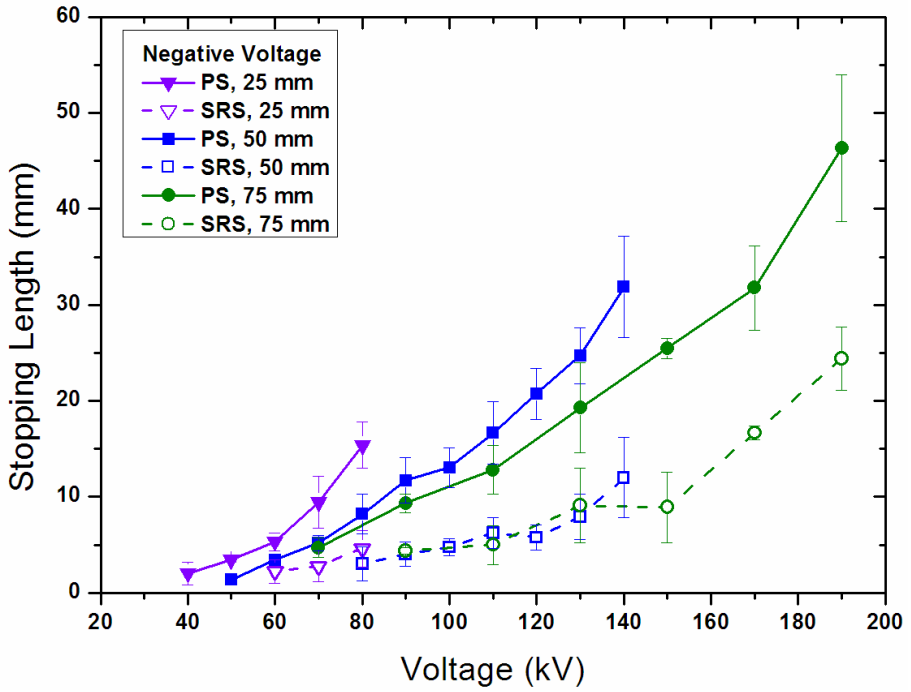

Figure 7-6 Stopping length of PSs and SRSs under negative impulse voltage in Midel 7131.

7.4.2 Average Propagation Velocity

The propagation time was determined by the light and current signals, and the average propagation velocity is deduced by using stopping length divided by the propagation time. It should be borne in mind that SRS has the reverse polarity to the PS under both positive and negative impulse voltages. Figure 7-7 shows the average propagation velocity of both PSs and SRSs at various gap distances under positive impulse voltage. Average propagation velocity of PSs increases slightly with the increased voltage level from about 1.5 km/s to 2.5 km/s, which is the typical range of positive 2nd mode streamer [30, 35]. Average propagation velocity of SRSs keeps stable for different voltage levels and gap distances with a mean value of 0.57 km/s, which is lower than that of PSs but still located into the typical velocity range of negative 2nd mode streamer i.e. from 0.5 km/s to 1.5 km/s [33, 106].

Figure 7-8 shows the results of average propagation velocity of PSs and SRSs at various gap distances under negative impulse voltage. Average propagation velocity of PSs keeps stable in the range from 0.5 km/s to 1.6 km/s, representing the negative 2nd mode streamer. As for SRSs, two groups of data are clearly defined: SRS-A has higher average velocity with mean of 9.87 km/s, representing the positive 3rd mode streamer; SRS-B has lower average velocity with mean of 1.21 km/s, which is close to the typical

velocity of positive 2nd mode streamer. Average propagation velocities of both SRS-A and SRS-B are independent of the applied voltage level.

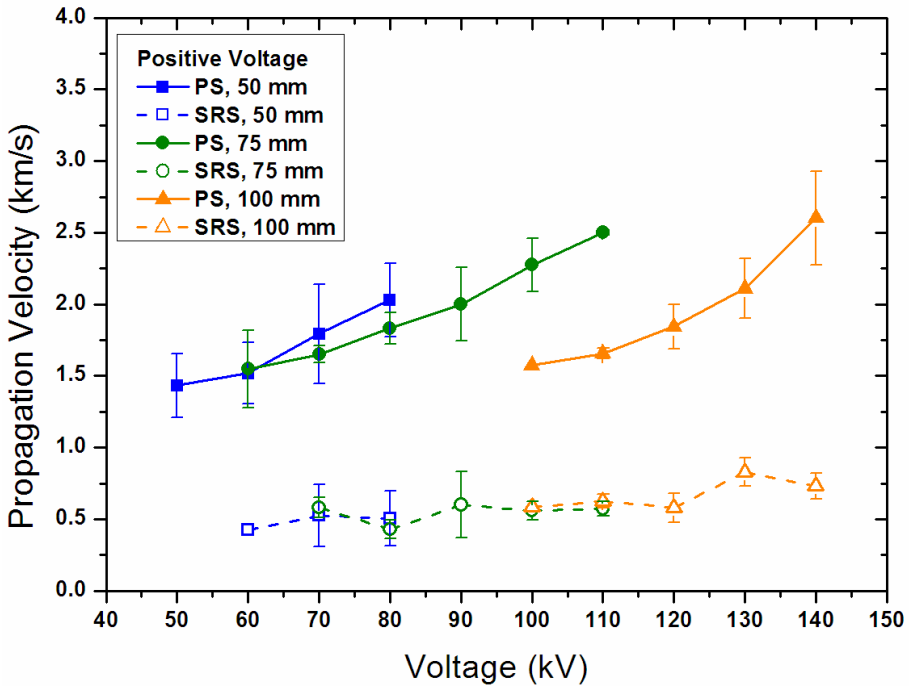

Figure 7-7 Propagation velocity of PSs and SRSs under positive impulse voltage in Midel 7131.

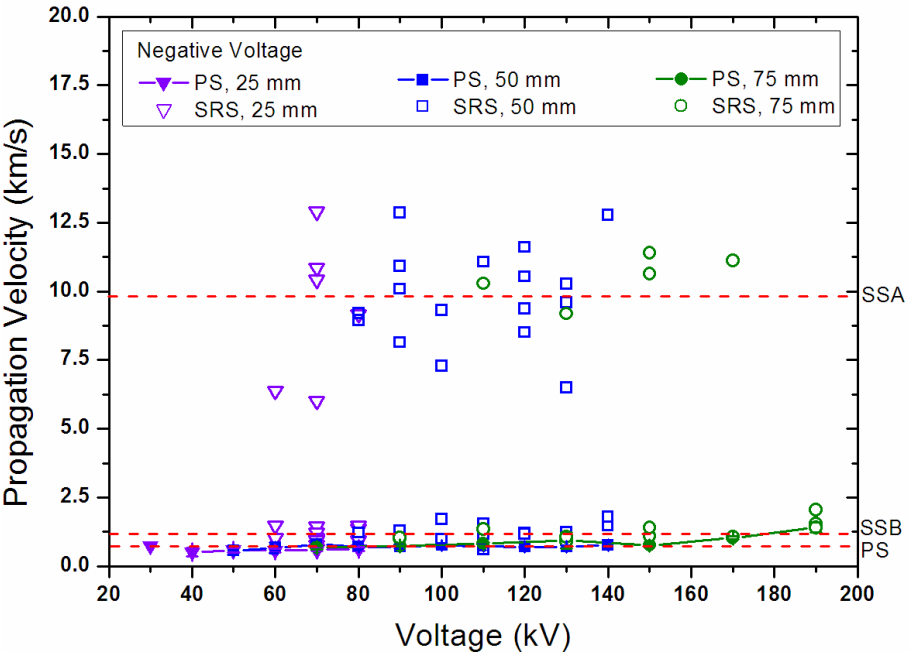

Figure 7-8 Propagation velocity of PSs and SRSs under negative impulse voltage in Midel 7131.

7.4.3 Time of Occurrence

Since SRS appears well after the termination of PS in time sequence, it is worth showing the time of occurrence as a unique parameter for SRS. Figure 7-9 shows the

time of occurrence of SRSs at various gap distances under positive impulse voltage. For a given gap distance, time of occurrence is independent of the applied voltage level. The average value of time of occurrence seems to decrease with the increased gap distance, i.e. 182.34 μs for 50 mm gap distance, 165.87 μs for 75 mm gap distance and 146.36 μs for 100 mm gap distance. However it should be noted that the results are in a so large scattering range that it is difficult to make conclusion in terms of gap distance effect. When the SRS occurs, the instant voltages have decayed to very low values, which are on average 6%, 8% and 11% for 50 mm, 75 mm and 100 mm gap distances respectively.

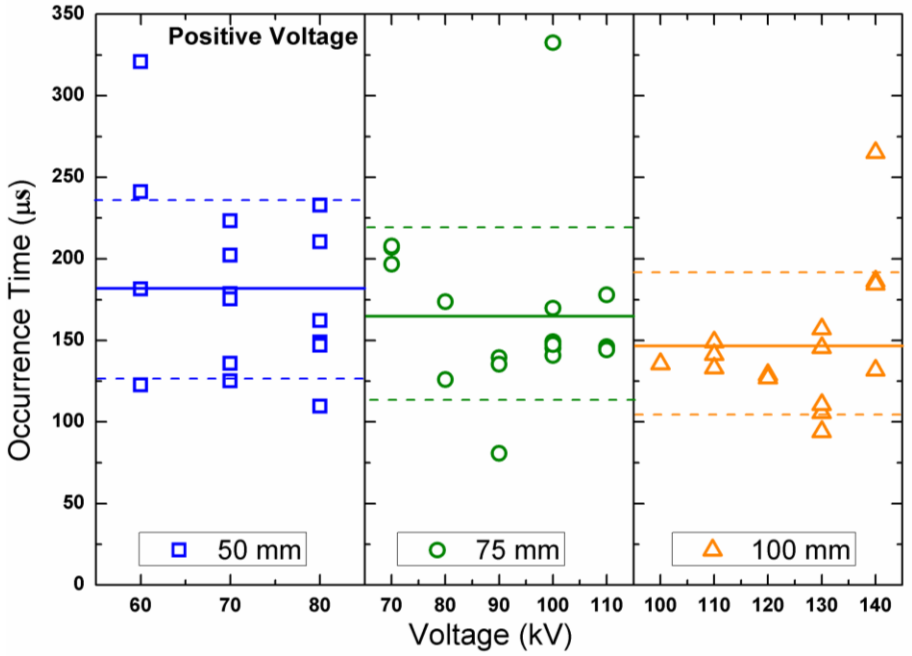

Figure 7-9 Time of occurrence of SRSs under positive impulse voltage in Midel 7131.

Figure 7-10 shows the results of time of occurrence of SRSs at various gap distances under negative impulse voltage. It is noted that SRS-A and SRS-B cannot be separated in the plot of time of occurrence. Similarly to the results under positive impulse, time of occurrence is voltage-independent at a given gap distance and has large scattering at a fixed voltage level. However opposite to the trend under positive impulse, the average value of time of occurrence increases with the increased gap distance, i.e. 117.65 μs for 25 mm gap distance, 142.57 μs for 50 mm gap distance and 191.03 μs for 75 mm gap distance. When the SRS occurs, the instant voltages have decayed to very low values, which are on average 17%, 12% and 6% for 25 mm, 50 mm and 75 mm gap distances respectively.

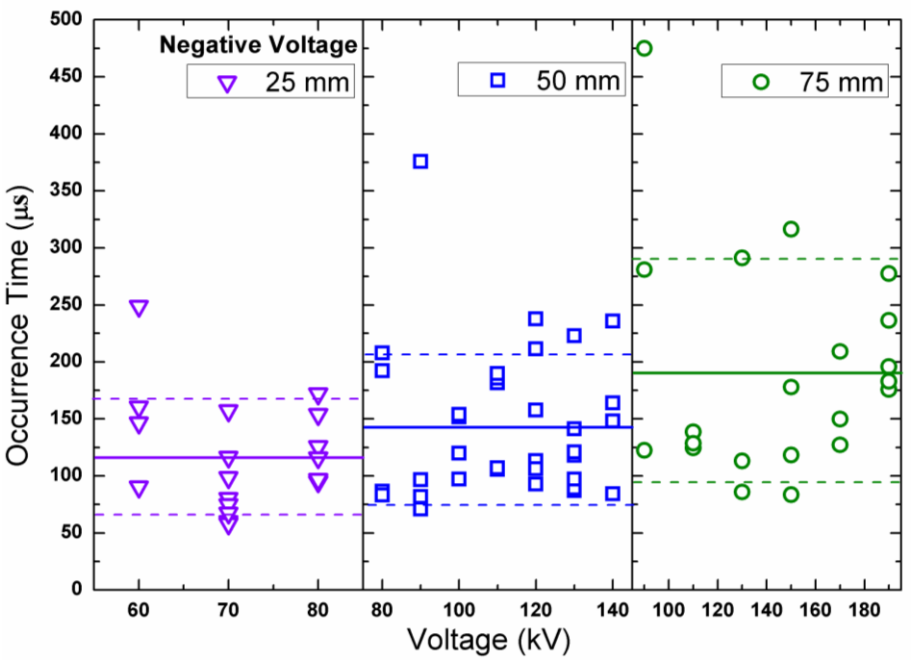

Figure 7-10 Time of occurrence of SRSs under negative impulse voltage in Midel 7131.

7.5 Mechanism and Verification of SRS

7.5.1 Formation Mechanism of SRS

The possible mechanisms leading to the SRS under both negative and positive impulse voltages are shown in Figure 7-11. It is generally acknowledged that both gaseous and electronic processes contribute to the propagation of PS, saying at least for 2nd mode PS, and thus charge injection, local ionization and thermal vaporization could contribute to the streamer initiation and propagation. The consequence of these mechanisms is that a gaseous channel filled with charged particles is left in the liquid when the PS stops.

Under negative impulse voltage as shown in Figure 7-11 (a), the positive charges in the streamer channel move slowly from the streamer head to the needle electrode while the electrons attach to the liquid molecule at the gas/liquid interface during their movement towards ground electrode. It should be stressed that the molecule of liquid Midel 7131 contains electronegative oxygen atoms, which help to trap the free electrons to form negative ions. Therefore many negative ions are accumulated at the gas/liquid interface and its adjacent areas during the PS's propagation.

After the termination of negative PS, the external electric field E_{ex} will still be continuously expelling those negative ions at the streamer head to the ground electrode

and those positive ions mainly in the streamer channels to the needle electrode, even E_{ex} decreases with the decay of applied impulse voltage; On the other hand after a short period of expansion, the gaseous channel gradually dissipates itself into the surrounding liquid, overall the channel shrinks in dimensions. In Figure 7-11 (b), with further decay of the external field, the negative charges are not necessarily moving towards the ground electrode, which could travel back towards the needle electrode due to the process of charge diffusion. In addition, shrinkage of the streamer channel helps to bring the negative charges, those around the gas/liquid phase, back towards the needle electrode. Lastly, most of the positive charges get attached to the needle electrode. Compared to the surrounding negative charges, needle electrode exhibits positive and therefore space charge induced electric field E_{sc} with reverse polarity is built up. Moreover there is still gaseous phase remained in this area, which could offer an easier environment for the initiation of SRS. So SRS occurs eventually near the needle electrode with reverse polarity, which is supported by Figure 7-1, Figure 7-3, Figure 7-4 and Figure 7-6.

In general, observation of SRS is repeatable under every shot of impulse voltage above the inception level. At the same applied voltage, the appearance of either SRS-A or SRS-B is, however, random, since formation of SRS is determined by the internal dynamic processes e.g. space charge generation, distribution and channel dissipation. When a strong reverse electric field is built up, SRS-A should be observed since the initiation of a 3rd mode streamer requires high electric field. Otherwise SRS-B would be observed at a relatively weak reverse electric field. Measurement of space charge distribution may offer more evidence on the dynamic process and help to explain the type difference of SRS, so it is worthy of further investigation.

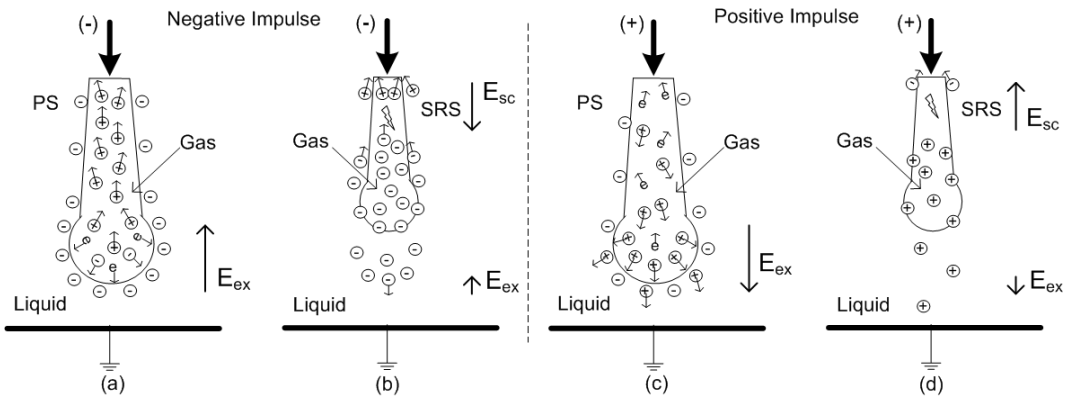

Figure 7-11 Schematic illustration of formation of SRSs under both negative and positive impulse voltages; (a) PS termination under negative impulse, (b) SRS formation under negative impulse, (c) PS termination under positive impulse, (d) SRS formation under positive impulse.

Under positive impulse voltage as shown in Figure 7-11 (c), the electrons in the streamer channels move quickly to the needle anode while the positive charges move slowly and accumulated around the streamer head. The positive charges could also attract some negative ions from the surrounding liquid which enhances the local electrical field and further promotes the streamer propagation. Both the electrons in the channels and the negative ions at the interface could result in more local recombination with positive ions during the streamer propagation.

Therefore after the termination of positive PS, probably less residual charges are expected. In addition, the positive streamer is normally thinner than negative streamer, so less residual gases are expected as well after the termination of positive PS. Other processes like charge separation and diffusion, channel dispersion and shrinkage are similar to those under negative impulse voltage. As shown in Figure 7-11 (d), SRS with reverse polarity finally occurs near the needle electrode but is much weaker than that under negative impulse voltage. This is supported by Figure 7-2 and Figure 7-5.

It is noted that time of occurrence of SRSs decreases with increased gap distance under positive impulse voltage (Figure 7-9) but reversely increases with gap distance under negative impulse voltage (Figure 7-10). Assuming there is indeed such a trend in terms of gap distance effect, the possible mechanisms are speculated as follows.

Under positive impulse voltage, residual space charge could be the dominant factor. At a larger gap distance, PS is larger on average thus more charges are generated. Besides, generally a lower average external field (i.e. applied voltage divided by gap distance) is expected at a larger gap distance, so more residual space charges could accumulate and the induced reverse electric field might exceed the external field at an earlier time for larger gap distances. In addition, initiation of a negative SRS is easier. Overall SRS could occur earlier at larger gap distances under positive impulse voltage as shown in Figure 7-9. Since it is negative SRS observed under positive impulse voltage, the propagation of negative streamer is more difficult (lower velocity) thus stopping lengths of SRS observed under positive impulse voltage are very low at all the gap distances as shown in Figure 7-5.

Under negative impulse voltage, channel dispersion could be the dominant factor since abundant residual charges exist after negative PS propagation. At a larger gap distance,

longer and wider PS channels are generally observed which result in longer dispersion time until they finally shrink to concentrate around the needle electrode. In addition, initiation of a positive streamer is generally more difficult, so the space charge induced reverse electric field should become strong enough in order to trigger the positive SRS. Therefore, SRS could occur later at larger gap distances under negative impulse voltage as shown in Figure 7-10. However once the positive SRS is initiated, the propagation is easier (faster velocity) thus stopping lengths of SRS observed under negative impulse voltage are much longer at all gap distances shown in Figure 7-6.

Once initiated, the SRS propagates preferably following some of the residual channels of the PS. However there are exceptions that new channels are developed especially in the case for SRS-A.

7.5.2 Effect of Tail-chopped Impulse on SRS

A remarkable feature for the occurrence of SRS is that the instantaneous voltage has to decay to a certain low level, which seems to be a necessary condition to form the SRS. Therefore in this section, the effect of tail-chopped impulse on the SRS was investigated at a 50 mm gap under negative polarity. With the previous experience on the propagation time of PSs, the tail of applied impulse voltage was chopped accordingly to ensure that the voltage was there to support the full propagation of PSs but disappeared much earlier than the normal occurrence time of SRSs.

The detailed chopping time at each applied voltage level is given in Table 7-1. Variance of time interval T_{Chop}-$T_{PS\text{-}Stop}$ inevitably occurred in the range of 10±8 μs and this is mainly due to two reasons: firstly the limitation of the chopping device to control the exactly desired chopping time T_{Chop} of an impulse shot at high-voltage levels; and secondly the natural scattering of the stopping time of a primary streamer $T_{PS\text{-}Stop}$. Nevertheless, this verification test still serves the purpose of validating the mechanism proposed in section 7.5.1 by removing the externally applied E_{ex} and leaving the internally formed E_{sc} as the only responsible parameter for SRS, despite the variance of the time interval T_{Chop}-$T_{PS\text{-}Stop}$.

Table 7-1 Chopping time at the tail of impulse waveform, Midel 7131.

Voltage (kV)	$T_{PS\text{-}Stop}$ (μs)	T_{Chop} (μs)	T_{Chop}–$T_{PS\text{-}Stop}$ (μs)
60	4.63	7.26	2.63
70	11.00	15.12	4.11
80	15.94	25.37	9.44
90	12.56	25.44	12.89
100	20.40	37.71	17.31
110	24.39	37.17	12.78
120	25.14	39.09	13.96
130	31.57	37.46	5.88

Figure 7-12 shows an example to demonstrate the effect of tail-chopped impulse on the SRS, obtained under negative 100 kV impulse voltages. As shown in Figure 7-12 (a) under full-wave impulse voltage, a normal SRS-A with a length of 3.49 mm, was observed at 153.78 μs, well after the termination of PS. The length of the PS is 11.17 mm. In Figure 7-12 (b), the tail of impulse was chopped at 37.71 μs after the full propagation of PS which stopped at 19.75 μs with a length of 13.78 mm. It was found that the occurrence of SRS was advanced in time, occurring just after the impulse was chopped. Therefore the time of occurrence of SRS under tail-chopped impulse was the same as the corresponding chopping time. Afterwards, there was nothing observed neither in light signal nor in streamer images. Unfortunately the light signal of SRS is overlapped with the discharging noise induced by the chopping wave, however it is evidenced in integral light image frame 2 that SRS with a length of 6.58 mm does occur and has very bright thick channels resembling the features of SRS-A under the full-wave impulse.

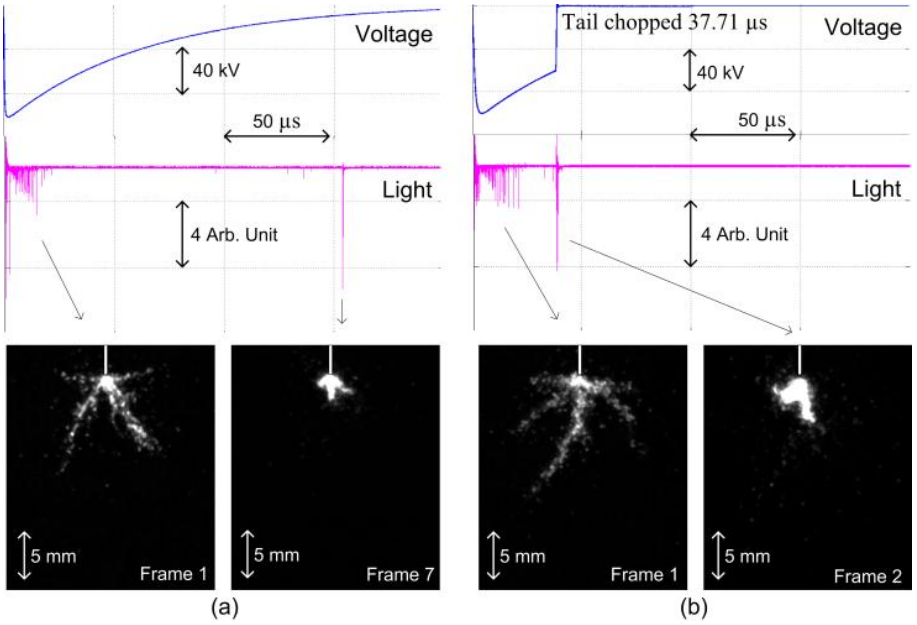

Figure 7-12 Effect of tail-chopped impulse on the SRS under negative impulse; Midel 7131, V=-100 kV, d=50 mm, (a) full waveform, 50 μs exposure time for frame 1 and 20 μs for the others, (b) tail of waveform is chopped at 37.71 μs, 30 μs exposure time for all the frames.

Figure 7-13 shows the stopping length of both PSs and SRSs under full-wave and tail-chopped impulse voltages. Since the impulse was chopped after the full propagation of PSs as indicated in Table 7-1, it is understandable to see the stopping lengths of PSs under tail-chopped impulse voltages are similar to those under full-wave impulse voltages. However SRSs are not only advanced in time, but also promoted in length by the tail-chopped impulses. As seen in Figure 7-13, the stopping lengths of SRSs under tail-chopped impulse voltages are generally larger than those under full-wave impulse voltages.

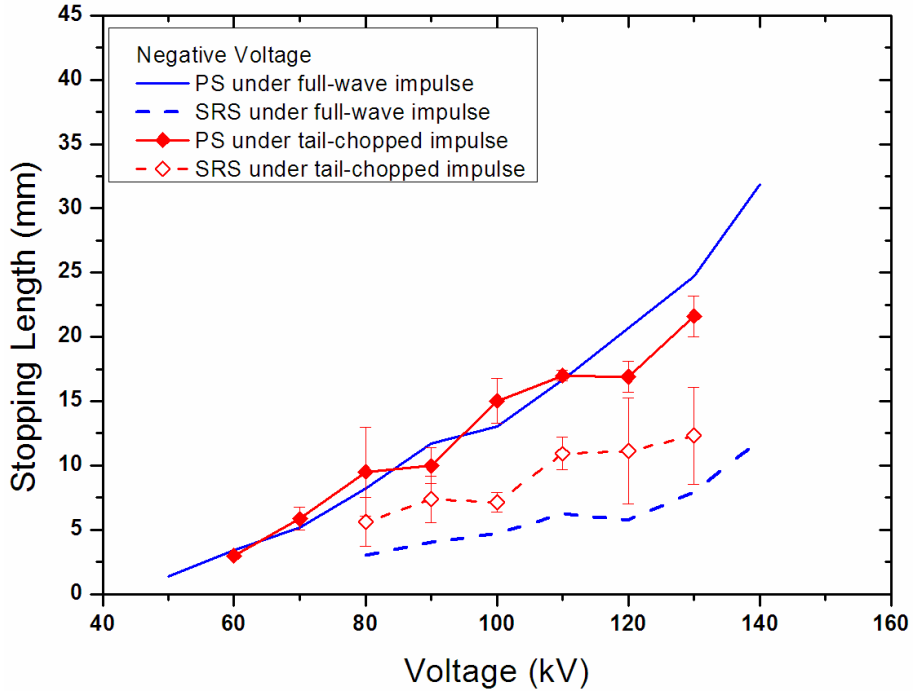

Figure 7-13 Stopping length of PSs and SRSs under full-wave and tail-chopped impulse voltages; d=50 mm, Midel 7131.

The shape features of SRS under tail-chopped impulse voltages are shown in Figure 7-14. Since SRSs under tail-chopped impulse resemble the feature of SRS-As under full-wave impulse, the integral light images of SRSs under tail-chopped impulses are compared with those of SRS-As under full-wave impulses. It is striking that SRSs under tail-chopped impulses have more branches and much thicker channels than SRS-As under full-wave impulses, especially at higher voltage levels. In addition the multi-branch shape of SRS radiating from the needle point as shown in Figure 7-14 (b) supports the assumption that the SRS is most likely to be developed in the direction from the needle point to the surrounding liquid.

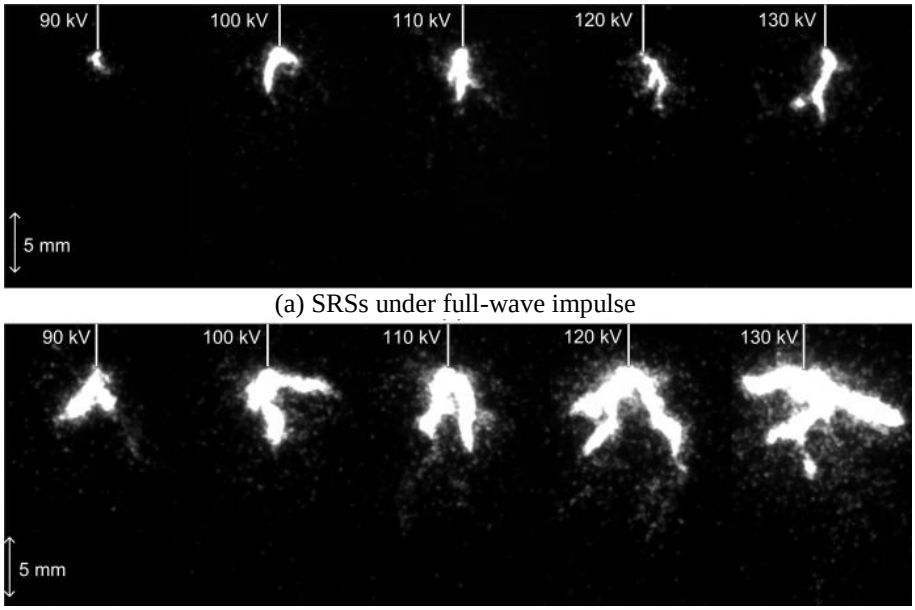

(a) SRSs under full-wave impulse

(b) SRSs under tail-chopped impulse

Figure 7-14 Images of SRSs under negative full-wave and tail-chopped impulse voltages; d=50 mm, Midel 7131.

As illustrated in section 7.5.1, space charge plays an important role in building up the reverse electric field E_{sc} to compete with the external field E_{ex} produced by the full wave impulse voltage. Hence there has to be a certain time of delay for the external field decaying to a low level so that the net field (E_{sc}-E_{ex}) can reach the inception threshold of SRS. The full-wave experiments so far show that this could take approximately 157.64 μs on average; during this period, some of the residual charges are indeed lost into the cathode or anode or through recombination.

Chopping at the tail of impulse after the full propagation of PS firstly makes sure that space charges are generated by the PS and secondly removes the effect of the external field completely and instantaneously, i.e. E_{ex}=0. Therefore the net field (E_{sc}-E_{ex}) under tail-chopped impulse is much higher than the case under the full-wave impulse when E_{ex} is non-zero, and thus the SRSs occur immediately after the tail-chopping and are much stronger than those under full-wave impulse. Consequently tests under tail-chopped impulse further confirm the important role of space charges in the formation of SRS.

7.5.3 Effect of Liquid Nature on SRS

Verification tests of SRS were also carried out in other two liquids i.e. natural ester FR3 and mineral oil Gemini X at the gap distance of 50 mm under both positive and negative polarities. It was confirmed that SRS also exists in the natural ester FR3. The results of

stopping length of SRSs in FR3 under positive and negative polarities are shown in Figure 7-15 and Figure 7-16 respectively.

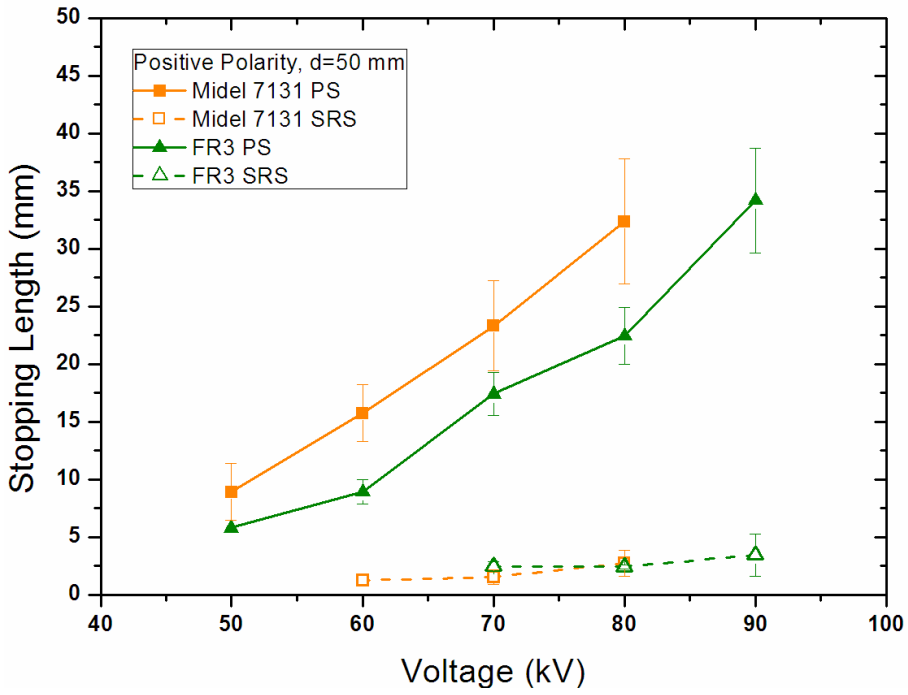

Figure 7-15 Comparison of stopping lengths of SRSs between synthetic ester Midel 7131 and natural ester FR3 under positive impulse voltage; d=50 mm.

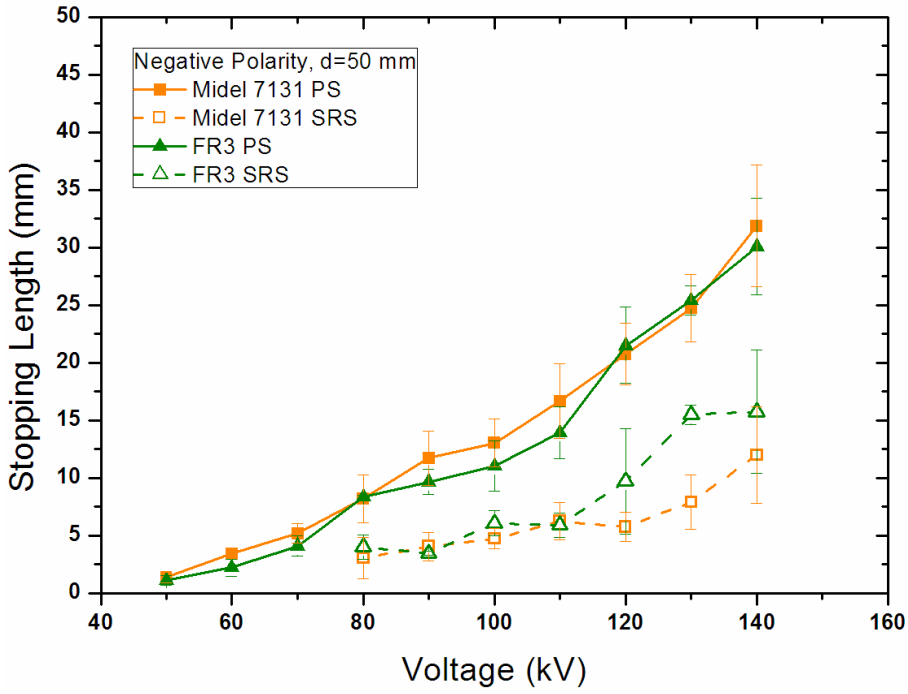

Figure 7-16 Comparison of stopping lengths of SRSs between synthetic ester Midel 7131 and natural ester FR3 under negative impulse voltage; d=50 mm.

Under positive polarity, SRSs with short stopping length were observed in FR3, which conform to those observed in Midel 7131, as shown in Figure 7-15. The average

velocity and time of occurrence for SRSs in FR3 under positive polarity are 0.75 km/s and 190.45 μs respectively.

However under negative polarity, only the slow type SRS (SRS-B) with average velocity of 1.24 km/s was observed in FR3. The time of occurrence for SRSs in FR3 under negative polarity is 107.36 μs on average. It is noted that the lengths of SRSs in FR3 are slightly longer than those in Midel 7131 at high-voltage levels from 120 kV to 140 kV.

Figure 7-17 shows an example of the SRS in FR3 obtained at the negative 120 kV impulse voltage. The negative PS takes the typical combination of 3^{rd}+2^{nd} mode propagation, with a stopping length of 24.39 mm and an average velocity of 1.27 km/s. The positive SRS occurs at about 97.68 μs latter than the extinction of PS, with a stopping length of 14.98 mm and an average velocity of 1.45 km/s. Compared with SRS-B in Midel 7131 (Figure 7-4), the light signal of SRS in FR3 has less continuous DC component but more regularly increasing discrete pulses.

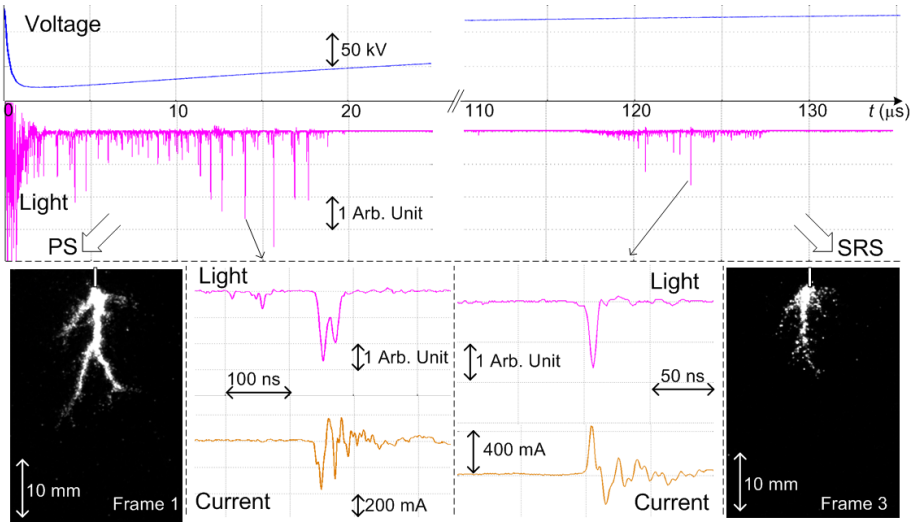

Figure 7-17 Demonstration of a SRS under negative impulse voltage in FR3; V=-120 kV, d=50 mm; 50 μs exposure time for frame 1 and 30 μs for the others.

Further verification tests revealed the remarkable difference between ester liquids and mineral oil. As for mineral oil Gemini X under positive polarity, it was too difficult to identify the SRS since many luminous spots rather than a streamer were observed at different periods after the termination of the PS. Under negative polarity, partial re-illuminations were usually observed just after the main propagation of PS. These partial re-illuminations were randomly distributed in the formed streamer channels and

could last for tens of microseconds. As a large number of space charges were consumed in this process, it was difficult to form the SRS. Most of the images showing the possible SRS were quite weak, except for a few cases at very high-voltage levels.

Figure 7-18 shows an example of SRS in mineral oil obtained at the negative 210 kV impulse voltage, which is relatively clear and can be identified from the other noises. The stopping length and average velocity of the negative PS are 27.34 mm and 0.96 km/s respectively. After the propagation of PS, there are still a lot of discrete light pulses observed, and Frame 2 and 3 show the partial re-illuminations just after the PS propagation. The positive SRS occurs at 311.64 μs, with a length of 21.32 mm and an average velocity of 1.69 km/s.

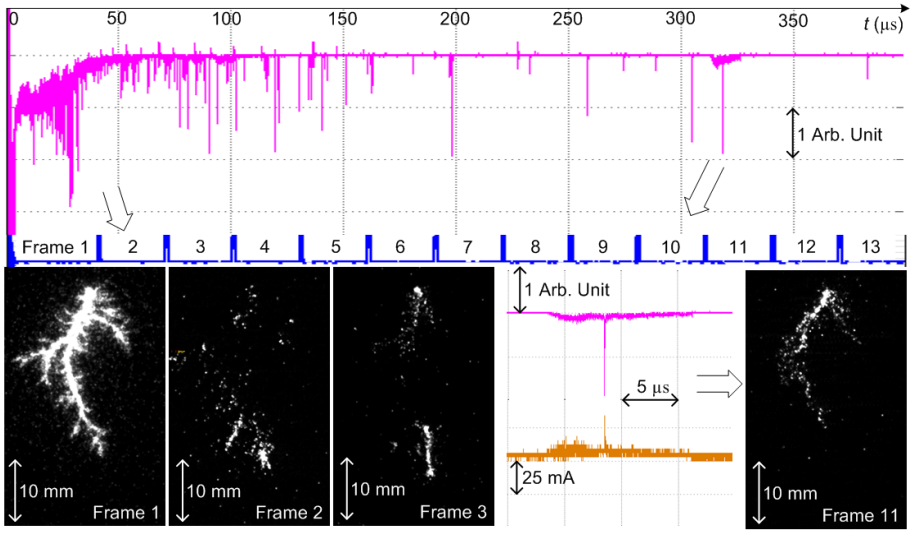

Figure 7-18 Demonstration of a SRS under negative impulse voltage in Gemini X; V=-210 kV, d=50 mm; 40 μs exposure time for frame 1 and 30 μs for the others.

To form a SRS, two dynamic processes of space charge and gaseous channel are involved. It is qualitatively reasonable to see the difference of SRS between ester liquids and mineral oil, since ester liquids having the electronegative molecular components are more polar than mineral oil, which could help the accumulation of space charges in ester liquids. In addition the viscosity of ester liquids is much higher than that of mineral oil, which might slow down the dissipation of gaseous channels in ester liquids. However the detailed dynamic processes especially when it is involved with different liquids are too complex to be speculated without any further sensitive study.

At last it is worth mentioning that two SRSs could rarely be observed within a single impulse shot for ester liquids at high-voltages. Figure 7-19 shows an example of two consecutive SRSs obtained in Midel 7131 under a negative 130 kV impulse shot at a 50 mm gap. The length of PS is 23.31 mm as normal at the voltage level. The former SRS with a length of 6.56 mm occurs earlier at 97.16 μs while the latter SRS with a length of 5.52 mm occurs even at 447.84 μs. As two SRSs seem to share the residual space charges, both of them are relatively weak compared with the formation of a single SRS.

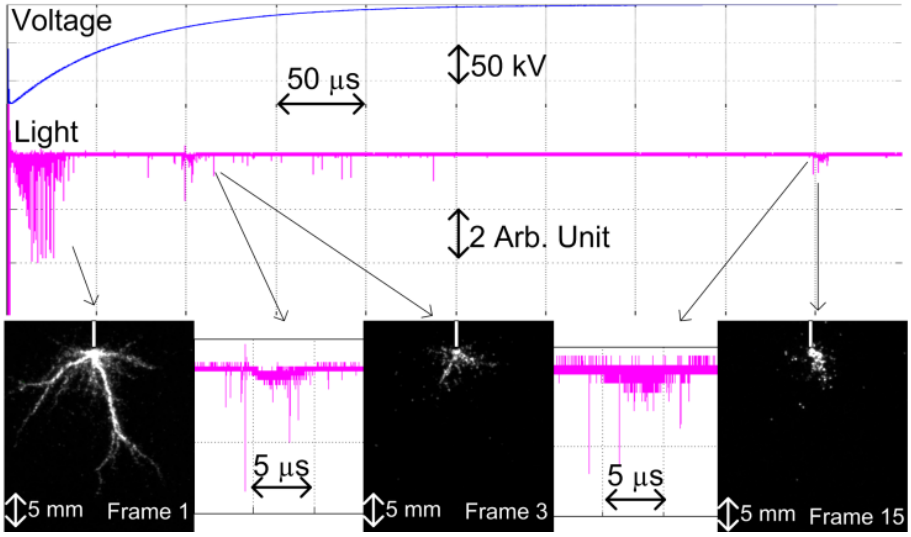

Figure 7-19 Demonstration of two SRSs under a single negative impulse shot in Midel 7131; V=-130 kV, d=50 mm; 50 μs exposure time for frame 1 and 30 μs for the others.

7.6 Summary

SRSs were observed in synthetic ester Midel 7131 under both positive and negative impulse voltages at various gap distances. Under positive impulse voltage, the lengths of SRSs are much shorter than those of PSs, with almost no growing trend along the increasing voltage level. The velocity of SRSs is very stable at an average of 0.57 km/s. SRSs have weaker channels compared with the PSs. Under negative impulse voltage, two types of SRS were observed. SRS-A has bright trunks with high average velocity of 9.87 km/s belonging to the 3rd mode streamer while SRS-B has weak tree-like channels with low average velocity of 1.21 km/s resembling the 2nd mode streamer. Generally SRSs are also shorter than PSs, but both of which increase gradually with the applied voltage.

It was confirmed that SRS also exists in natural ester FR3 under both positive and negative impulse voltages; however only the slow type SRS (SRS-B) was observed under negative impulse.

It was difficult to see a clear SRS in mineral oil except at very high-voltage levels under negative polarity.

A characteristic feature of SRS is the reverse polarity to the PS as well as to the applied impulse voltage i.e. negative SRS observed under positive impulse and positive SRS under negative impulse. Therefore space charge induced reverse electric field is probably the mechanism to produce a SRS. To sum up, the formation of SRS under both negative and positive polarities probably needs the following three conditions: 1) a decayed impulse waveform; 2) sufficient residual space charges; 3) a favourable gaseous environment.

CHAPTER 8. CONCLUSIONS AND FUTURE WORK

8.1 Conclusions

8.1.1 General

This thesis focuses on the pre-breakdown and breakdown performances of synthetic ester and natural ester transformer liquids under impulse voltage by considering the effects of field geometry, voltage polarity, gap distance and solid interface. Through experimental investigations and data analyses, the research objectives are achieved and thus some useful conclusions or findings are made.

Research topics covered in this thesis are:

- ❖ Breakdown strength of ester liquids in a quasi-uniform field
  - Standard lightning and switching tests
  - Influence of testing methods
  - Determination of withstand voltage
- ❖ Pre-breakdown and breakdown phenomena of ester liquids in a non-uniform field
  - Streamer characteristics including shape, mode, length and velocity
  - Breakdown voltages at various gap distances
  - Prediction of lightning breakdown voltage at very large gaps
- ❖ Pre-breakdown and breakdown phenomena on ester/pressboard interface in a non-uniform field
  - Influence of parallel pressboard surface on streamer propagation
  - Influence of parallel pressboard surface on breakdown and acceleration voltages
- ❖ Phenomenon of secondary reverse streamer in ester liquids in a non-uniform field
  - Introduction of secondary reverse streamer
  - Characteristics of secondary reverse streamer
  - Discussion on formation mechanism and its verification tests

8.1.2 Summary of Results and Main Findings

As the majority of the electric fields inside a transformer e.g. between turn to turn, disk to disk and winding to winding, are quasi-uniform fields, impulse breakdown strengths

of ester liquids were examined at a 3.8 mm sphere-sphere gap. It was found that lightning impulse tests tend to show relatively larger difference between ester liquids and mineral oil than switching impulse and AC tests. Various testing methods including rising-voltage method, up-and-down method and multiple-level method, have notable influence on the absolute breakdown voltages, but do not affect the ranking of liquids for the purpose of comparison. No matter which method was used, ester liquids showed lower breakdown voltages than mineral oil, and their reductions compared to mineral oil are generally less than 20%. By using Weibull distribution fitting to the probability curve produced by all the thousand of shots, 1% withstand voltages of ester liquids were deduced, which are close to those of mineral oil. Incorporating the published results in the literatures, it was concluded that **lightning impulse strengths of ester liquids for both breakdown or withstand, are comparable to those of mineral oil at various gap distances in a quasi-uniform field**.

Although a strongly non-uniform field is avoided to the upmost in the transformer design and manufacture, there is always the possibility for existence of manufacturing defects e.g. protrusion on the copper conductor, and contaminations resulting from long term in-service degradation e.g. particle and moisture in the oil, all of which could cause local electric field enhancement (non-uniform field) and thus might initiate a discharge. Therefore streamer characteristics including shape, mode, length and velocity of ester liquids were studied under lightning impulse voltage in a strongly non-uniform point-plane field. Although streamer inception voltages of ester liquids are comparable to that of mineral oil, at the same voltage level after inception, streamers in ester liquids propagate faster and further, with more branches for those negative ones, than in mineral oil. Combining the breakdown tests at various gap distances under lightning impulse voltage and previously published data under step voltage, empirical formulas were made so that breakdown voltages of ester liquids at very large gaps can be predicted. It was found that **lightning breakdown voltages of ester liquids at very large gaps of approximately 1000 mm could be as low as 40% of that of mineral oil, due to ester liquids' relatively low tolerance to fast streamers.**

As pressboards are generally used in transformers as barriers, the discharge could propagate along the pressboard surface driven by the tangential electric field. Therefore the influences of pressboard surface on streamer propagation and breakdown were investigated in the same point-plane gaps. It was found that **introduction of parallel**

pressboard interface has no influence on the streamer propagation and thus does not weaken the 50% breakdown voltage under both positive and negative impulse voltages. So similar to results in open liquid gaps, breakdown voltages on ester/pressboard interface are lower than those on mineral oil/pressboard interface, and this difference is magnified at larger gap distances. At overstressed conditions, **introduction of pressboard interface significantly reduces the positive acceleration voltage in mineral oil, however this does not occur in ester liquids. Under negative polarity, presence of pressboard tends to accelerate the streamer velocity at larger gap distances and under higher voltages in both ester liquids and mineral oil.** However, acceleration voltages on ester/pressboard interface are still lower than those on mineral oil/pressboard interface, which indicates the lower tolerance to faster streamers on ester/pressboard interface.

It should be highlighted that secondary reverse streamer (SRS) is a newly observed phenomenon, which depicts a streamer in liquids that occurs subsequently and well after the extinction of the primary streamer (PS) propagation within a single shot of impulse voltage and has the reverse polarity to the PS (as well as to the applied impulse voltage). It was confirmed that SRS generally exists in ester liquids at various gap distances of point-plane field geometry under both positive and negative lightning impulse voltages. It should be emphasized that it is difficult to see a clear SRS in mineral oil except at very high-voltage levels under negative polarity. A remarkable feature of SRS is the reverse polarity to the PS i.e. negative SRS observed under positive impulse and positive SRS under negative impulse. Therefore space charge induced reverse electric field is most likely to be the mechanism of SRS. The formation of SRS probably needs the following three conditions: 1) a decayed impulse waveform; 2) sufficient residual space charges; 3) a favourable gaseous environment.

8.2 Future Work

In this thesis, some useful conclusions are made on the electrical performances of ester transformer liquids under impulse voltage. Meanwhile there are new questions raised and more work could be done in the future study.

For quasi-uniform field study:

i. The results under different voltage waveforms showed that the shorter duration of the waveform, the larger difference the breakdown voltages of ester liquids have from that of mineral oil. Meanwhile a transformer is also examined under tail-chopped (between 2 to 6 μs [17]) lightning impulse voltages during the factory tests. Therefore it is important to know ester liquids' behaviour under such short duration chopped impulse voltage.

ii. In the comparison study of testing method, various test procedures including rising-voltage method, up-and-down method and multiple-level method were used to obtain the breakdown strength of a liquid. Mathematic analysis on the independence of various test procedures can be an interesting topic for further work.

iii. As there is a large scattered initiation time for streamers in quasi-uniform fields, recording of parameter *time to breakdown* is not adequate to deduce the streamer velocity in quasi-uniform fields. Meanwhile the customary understanding on breakdown in quasi-uniform fields is that the breakdown event is mainly controlled by the initiation of a streamer. So it is interesting to investigate the streamer characteristic of ester liquids in a quasi-uniform field. However test method should be carefully designed since initiation site and time of a streamer is difficult to be predicted in quasi-uniform fields.

For non-uniform field study:

i. The work in this thesis focused mainly on streamer propagation and breakdown under impulse voltage. It is also interesting to study the initiation stage of streamers in ester liquids under impulse voltage by considering the effects of voltage polarity, tip radius and probably the hydrostatic pressure as well.

ii. The nature of streamer is generally believed as gaseous phase. As the dissolved gas analysis (DGA) is commonly used in transformer industry as a powerful fault detection tool, a relationship between streamer characteristic and DGA of ester liquids under impulse voltage if there is one, is highly expected in the

future work, which could not only benefit the diagnostic of ester filled transformers but also help to understand the generic mechanism of streamer in liquids.

iii. Pre-breakdown and breakdown behaviours under impulse voltage in a strongly non-uniform field tend to differentiate the liquids by reflecting the liquid nature. During the in-service ageing of transformer liquids, their compositions could be changed as the result of degradation, and more polar compounds could be generated, so it might be worth studying the streamer characteristics of laboratory aged or in-service aged ester liquids under impulse voltage.

For secondary reverse streamer (SRS) study:

i. The propagation phase of SRS needs to be investigated. Although the current and light signals indicate there is a propagation process of SRS which is similar to the primary streamer (PS), the evidence from fast imaging setup should be obtained to offer a solid answer. This test can be carried out under tail-chopped impulse, as in this case the time of occurrence of SRS is predictable.

ii. As the SRS was found to be enhanced by chopping the impulse just after the complete propagation of PS, it is worth systematically studying the influence of impulses chopped at different tail times on the characteristics of SRS. It would be interesting to know whether there is an optimum chopping time to form a stronger SRS. In addition, measurement of the liquid's relaxation time based on conductivity and permittivity is also helpful to understand the mechanism of SRS.

iii. SRS demonstrates the existence of strong space charge effect in ester liquids, so it is important to investigate ester liquids' performance under other unique waveforms e.g. DC and polarity reversal pulse voltages for the potential application of these liquids in HVDC transformers and power electronic devices.

REFERENCES

[1] Nynas Naphthenics AB, "Transformer oil handbook", Printed in Sweden, 2004.

[2] M. J. Heathcote, "The J & P transformer book", Elsevier Ltd, Printed in Great Britain, 2007.

[3] D. Martin, I. U. Khan, J. Dai and Z. D. Wang, "An overview of the suitability of vegetable oil dielectrics for use in large power transformers", Euro TechCon, Chester, UK, pp. 4-23, 28th-30th November, 2006.

[4] C. Perrier and A. Beroual, "Experimental investigations on insulating liquids for power transformers: mineral, ester, and silicone oils", IEEE Electrical Insulation Magazine, vol. 25, pp. 6-13, 2009.

[5] S. Tenbohlen and M. Koch, "Aging performance and moisture solubility of vegetable oils for power transformers", IEEE Transactions on Power Delivery, vol. 25, pp. 825-830, 2010.

[6] S. Arazoe, D. Saruhashi, Y. Sato, S. Yanabu, G. Ueta and S. Okabe, "Electrical characteristics of natural and synthetic insulating fluids", IEEE Transactions on Dielectrics and Electrical Insulation, vol. 18, pp. 506-512, 2011.

[7] T. V. Oommen, "Vegetable oils for liquid-filled transformers", IEEE Electrical Insulation Magazine, vol. 18, pp. 6-11, 2002.

[8] C. P. McShane, K. J. Rapp, J. L. Corkran, G. A. Gauger and J. Luksich, "Aging of paper insulation in natural ester dielectric fluid", IEEE/PES Conference and Exposition in Transmission and Distribution, vol. 2, pp. 675-679, 2001.

[9] C. P. McShane, K. J. Rapp, J. L. Corkran, G. A. Gauger and J. Luksich, "Aging of Kraft paper in natural ester dielectric fluid", IEEE International Conference on Dielectric Liquids (ICDL), Graz, Austria, pp. 173-177, 7th-12th July, 2002.

[10] X. Wang and Z. D. Wang, "Particle effect on breakdown voltage of mineral and ester based transformer oils", IEEE Conference on Electrical Insulation and Dielectric Phenomena (CEIDP), Quebec, Canada, pp. 598-602, 2008.

[11] D. Martin and Z. D. Wang, "Statistical analysis of the AC breakdown voltages of ester based transformer oils", IEEE Transactions on Dielectrics and Electrical Insulation, vol. 15, pp. 1044-1050, 2008.

[12] R. Girgis, M. Bernesjo and G. K. Frimpong, "Detailed performance of a 50 MVA transformer filled with a natural ester fluid versus mineral oil", Cigre Session, Paris, France, paper A2-107, 22nd-27th August, 2010.

[13] C. T. Duy, O. Lesaint, A. Denat and N. Bonifaci, "Streamer propagation and breakdown in natural ester at high voltage", IEEE Transactions on Dielectrics and Electrical Insulation, vol. 16, pp. 1582-1594, 2009.

[14] R. Liu, C. Tornkvist, V. Chandramouli, O. Girlanda and L. A. A. Pettersson, "Ester fluids as alternative for mineral oil: the difference in streamer velocity and LI breakdown voltage", IEEE Conference on Electrical Insulation and Dielectric Phenomena (CEIDP), Virginia Beach, USA, pp. 543-548, 18th-21st October, 2009.

[15] M&I Materials, "Midel 7131 insulated 238kV power transformer", Retrieved 17th August 2011, from http://www.midel.com/power.htm, 2010.

[16] Cooper Power Systems, "Medium and large power transformer users list Envirotemp FR3 fluid", Retrieved 17th August 2011, from http://www.cooperindustries.com/content/public/en/power_systems/products/dielectric_fluid/envirotemp_fr3_fluid.resources.html, 2011.

[17] IEC 60076-3, "Power transformers part 3: insulation levels, dielectric tests and external clearances in air", International Electrotechnical Commission, 2000.

[18] J. K. Nelson and C. Shaw, "The impulse design of transformer oil-cellulose structures", IEEE Transactions on Dielectrics and Electrical Insulation, vol. 13, pp. 477-483, 2006.

[19] CIGRE Brochure 157, "Effect of particles on transformer dielectric Strength", Working Group 17 of Study Committee 12, 2000.

[20] H. Miyahara, A. Yamagishi, H. Sampei, Y. Shirasaka, Y. Hamadate, and H. Miyao, "Influence of micro particles in fluid on the impulse and AC breakdown strengths of low-viscosity silicone liquid immersed insulating systems", International Conference on Electrical Engineering (ICEE), Okinawa, Japan, paper O-146, 6th-10th July, 2008.

[21] N. V. Dung, F. Mauseth, H. K. Hoidalen, D. Linhjell, S. Ingebrigtsen, L. E. Lundgaard, and M. Unge, "Streamers in large paraffinic oil gap", IEEE International Conference on Dielectric Liquids (ICDL), Trondheim, Norway, paper 113, 26th-30th June, 2011.

[22] N. G. Trinh, C. Vincent, and J. Regis, "Statistical dielectric degradation of large-volume oil-insulation", IEEE Transactions on Power Apparatus and Systems, vol. PAS-101, pp. 3712-3721, 1982.

[23] L. E. Lundgaard, D. Linhjell, J. B. Sund, and G. Jorendal, "Influence of simultaneous ac-stress on impulse breakdown in oil-paper insulation system", International Symposium on High Voltage Engineering (ISH), Yokohama, Japan, pp. 231-234, 23rd-27th August, 1993.

[24] A. H. Sharbaugh, J. C. Devins and S. J. Rzad, "Progress in the field of electric breakdown in dielectric liquids", IEEE Transactions on Electrical Insulation, vol. EI-13, pp. 249-276, 1978.

[25] H. Yamashita, H. Amano and T. Mori, "Optical observation of pre-breakdown and breakdown phenomena in transformer oil", Journal of Physics D: Applied Physics, vol. 10, pp. 1753-1760, 1977.

[26] E. O. Forster, "Critical assessment of the electrical breakdown process in dielectric Fluids", IEEE Transactions on Electrical Insulation, vol. EI-20, pp. 891-896, 1985.

[27] A. Beroual and R. Tobazeon, "Pre-breakdown phenomena in liquid dielectrics", IEEE Transactions on Electrical Insulation, vol. EI-21, pp. 613-627, 1986.

[28] P. K. Watson, W. G. Chadband and M. Sadeghzadeh-Araghi, "The role of electrostatic and hydrodynamic forces in the negative-point breakdown of liquid dielectrics", IEEE Transactions on Electrical Insulation, vol. 26, pp. 543-559, 1991.

[29] D. Linhjell, L. E. Lundgaard and G. Berg, "Streamer propagation under impulse voltage in long point-plane oil gaps", IEEE Transactions on Dielectrics and Electrical Insulation, vol. 1, pp. 447-458, 1994.

[30] O. Lesaint, "'Streamers' in liquids: relation with practical high voltage insulation and testing of liquids", IEEE International Conference on Dielectric Liquids (ICDL), Poitiers, France, pp. 120-125, 30th June-4th July, 2008.

[31] F. O'Sullivan, J. G. Hwang, M. Zahn, O. Hjortstam, L. Pettersson, R. Liu and P. Biller, "A model for the initiation and propagation of positive streamers in transformer oil", IEEE International Symposium on Electrical Insulation (ISEI), Vancouver, Canada, pp. 210-214, 9th-12th June, 2008.

[32] Y. V. Torshin, "Initiation and propagation of the negative leader in transformer oil under impulse voltage", IEEE Transactions on Dielectrics and Electrical Insulation, vol. 16, pp. 1536-1542, 2009.

[33] G. Massala and O. Lesaint, "A comparison of negative and positive streamers in mineral oil at large gaps", Journal of physics D: Applied Physics, vol. 34, pp. 1525-1532, 2001.

[34] R. Badent, K. Kist and A. J. Schwab, "Voltage dependence of pre-breakdown phenomena in insulating oil", IEEE International Symposium on Electrical Insulation (ISEI), Pittsburgh, USA, pp. 414-417, 5th-8th June, 1994.

[35] O. Lesaint and G. Massala, "Positive streamer propagation in large oil gaps: experimental characterization of propagation modes", IEEE Transactions on Dielectrics and Electrical Insulation, vol. 5, pp. 360-370, 1998.

[36] Y. Kamata and Y. Kako, "Flashover characteristics of extremely long gaps in transformer oil under non-uniform field conditions", IEEE Transactions on Electrical Insulation, vol. EI-15, pp. 18-26, 1980.

[37] O. Lesaint and T. V. Top, "Streamer initiation in mineral oil, part I: electrode surface effect under impulse voltage", IEEE Transactions on Dielectrics and Electrical Insulation, vol. 9, pp. 84-91, 2002.

[38] H. Yamashita, K. Yamazawa and Y. S. Wang, "The effect of tip curvature on the pre-breakdown streamer structure in cyclohexane", IEEE Transactions on Dielectrics and Electrical Insulation, vol. 5, pp. 396-401, 1998.

[39] O. Lesaint and P. Gournay, "On the gaseous nature of positive filamentary streamers in hydrocarbon liquids. I: influence of the hydrostatic pressure on the propagation", Journal of Physics D: Applied Physics, vol. 27, pp. 2111-2116, 1994.

[40] A. Beroual, "Electronic and gaseous processes in the pre-breakdown phenomena of dielectric liquids", Journal of Applied Physics, vol. 73, pp. 4528-33, 1993.

[41] E. M. Hizal and S. Dincer, "Breakdown time lags and pre-breakdown phenomena in transformer oil, effects of hydrostatic pressure", Journal of Electrostatics, vol. 12, pp. 333-343, 1982.

[42] J. C. Devins, S. J. Rzad and R. J. Schwabe, "Breakdown and pre-breakdown phenomena in liquids", Journal of Applied Physics, vol. 52, pp. 4531-4545, 1981.

[43] S. Ingebrigtsen, L. E. Lundgaard and P. O. Astrand, "Effects of additives on pre-breakdown phenomena in liquid cyclohexane: I. streamer initiation", Journal of Physics D: Applied Physics, vol. 40, pp. 5161-5169, 2007.

[44] S. Ingebrigtsen, L. E. Lundgaard and P. O. Astrand, "Effects of additives on pre-breakdown phenomena in liquid cyclohexane: II. streamer propagation," Journal of Physics D: Applied Physics, vol. 40, pp. 5624-5634, 2007.

[45] A. Beroual, M. Zahn, A. Badent, K. Kist, A. J. Schwabe, H. Yamashita, K. Yamazawa, M. Danikas, W. D. Chadband and Y. Torshin, "Propagation and structure of streamers in liquid dielectrics", IEEE Electrical Insulation Magazine, vol. 14, pp. 6-17, 1998.

[46] J. F. Kolb, R. P. Joshi, S. Xiao and K. H. Schoenbach, "Streamers in water and other dielectric liquids", Journal of Physics D: Applied Physics, vol. 41, pp. 234007, 2008.

[47] R. Bartnikas, "Engineering dielectrics volume III electrical insulating liquids", ASTM, Printed in USA, 1994.

[48] V. Y. Ushakov, "Impulse breakdown of liquids", Springer Berlin Heidelberg, New York, 2007.

[49] S. Ingebrigtsen, "The influence of chemical composition on streamer initiation and propagation in dielectric liquids", PhD Thesis, Norwegian University of Science and Technology, 2008.

[50] S. Ingebrigtsen, N. Bonifaci, A. Denat and O. Lesaint, "Spectral analysis of the light emitted from streamers in chlorinated alkane and alkene liquids", Journal of Physics D: Applied Physics, vol. 41, pp. 235204, 2008.

[51] A. Beroual, "Spectral analysis of light emitted by streamers and gas chromatography in liquid dielectrics", Japanese Journal of Applied Physics, vol. 32, pp. 5615-5620, 1993.

[52] D. Vukovic, S. Tenbohlen, J. Harthun, C. Perrier and H. Fink, "Breakdown strength of vegetable-based oils under AC and lightning impulse voltages", IEEE International Conference on Dielectric Liquids (ICDL), Trondheim, Norway, paper 116, 26th-30th June, 2011.

[53] Y. V. Torshin, "Prediction of breakdown voltage of transformer oil from predischarge phenomena", IEEE Transactions on Dielectrics and Electrical Insulation, vol. 10, pp. 933-941, 2003.

[54] T. V. Top and O. Lesaint, "Streamer initiation in mineral oil, part II: influence of a metallic protrusion on a flat electrode", IEEE Transactions on Dielectrics and Electrical Insulation, vol. 9, pp. 92-96, 2002.

[55] O. Lesaint, "Pre-breakdown phenomena in liquids and their relation with breakdown properties in high voltage applications", Cigre A2-D1 colloquium, Bruges, Belgium, paper PS1-01, 7th-12th October, 2007.

[56] H. Yamashita and H. Amano, "Pre-breakdown phenomena in hydrocarbon liquids", IEEE Transactions on Electrical Insulation, vol. 23, pp. 739-750, 1988.

[57] R. E. Hebner, "Measurement of electrical breakdown in liquids", The Liquid State and its Electrical Properties, Plenum Press, New York, pp. 519-537, 1988.

[58] O. Lesaint, "Propagation of positive discharges in long liquid gaps", IEEE International Conference on Conduction and Breakdown in Dielectric Liquids (ICDL), Roma, Italy, pp. 161-166, 15th-19th July, 1996.

[59] M. E. B. Pahlavanpour, "Gassing properties of insulating liquid", Fourth Annual Technical Conference Weidman Electrical Technology, 2005.

[60] J. Perret, "Study of the dielectric breakdown of insulating mineral oils under impulse voltages", IEEE Transactions on Electrical Insulation, vol. EI-16, pp. 339-345, 1981.

[61] Y. Nakao, H. Itoh, S. Hoshino, Y. Sakai and H. Tagashira, "Effects of additives on pre-breakdown phenomena in n-hexane", IEEE Transactions on Dielectrics and Electrical Insulation, vol. 1, pp. 383-389, 1994.

[62] S. Ingebrigtsen, H. S. Smalo, P. O. Astrand and L. E. Lundgaard, "Effects of electron-attaching and electron-releasing additives on streamers in liquid cyclohexane", IEEE Transactions on Dielectrics and Electrical Insulation, vol. 16, pp. 1524-1535, 2009.

[63] O. Lesaint and M. Jung, "On the relationship between streamer branching and propagation in liquids: influence of pyrene in cyclohexane", Journal of Physics D: Applied Physics, vol. 33, pp. 1360-1368, 2000.

[64] J. Dai, Z. D. Wang and P. Jarman, "Creepage discharge on insulation barriers in aged power transformers", IEEE Transactions on Dielectrics and Electrical Insulation, vol. 17, pp. 1327-1335, 2010.

[65] O. Lesaint and G. Massala, "Transition to fast streamers in mineral oil in the presence of insulating solids", IEEE International Symposium on Electrical Insulation (ISEI), Montreal, Canada, pp. 737-740, vol. 2, 16th-19th June, 1996.

[66] L. E. Lundgaard, D. Linhjell, G. Berg and S. Sigmond, "Propagation of positive and negative streamers in oil with and without pressboard interfaces", IEEE Transactions on Dielectrics and Electrical Insulation, vol. 5, pp. 388-395, 1998.

[67] L. E. Lundgaard, D. Linhjell, G. Berg and S. Sigmond, "Positive and negative streamers in oil gaps with and without pressboard interfaces", International Conference on Conduction and Breakdown in Dielectric Liquids (ICDL), Roma, Italy, pp. 175-180, 15th-19th July, 1996.

[68] A. Zouaghi and A. Beroual, "Discharge structure and dielectric strength of long oil gaps in the presence of an insulating barrier", IEEE Conference on Electrical Insulation and Dielectric Phenomena (CEIDP), Minneapolis, Minnesota, USA, vol. 2, pp. 660-663, 19th-22nd October, 1997.

[69] A. Zouaghi and A. Beroual, "Barrier effect on the time lag to breakdown of transformer oil gaps under lightning impulse voltage", IEEE Conference on Electrical Insulation and Dielectric Phenomena (CEIDP), Atlanta, USA, vol. 2, pp. 444-447, 25th-28th October, 1998.

[70] A. Beroual and A. Zouaghi, "Barrier effect on the pre-breakdown and breakdown phenomena in long oil gaps", International Conference on Conduction and Breakdown in Dielectric Liquids (ICDL), Roma, Italy, pp. 300-303, 15th-19th July, 1996.

[71] L. Kebbabi and A. Beroual, "Optical and electrical characterization of creeping discharges over solid/liquid interfaces under lightning impulse voltage", IEEE Transactions on Dielectrics and Electrical Insulation, vol. 13, pp. 565-571, 2006.

[72] A. Beroual and L. Kebbabi, "Influence of the voltage waveform and hydrostatic pressure on morphology and final length of discharges propagating over solid-liquid interfaces", IEEE Transactions on Dielectrics and Electrical Insulation, vol. 16, pp. 1574-1581, 2009.

[73] R. Badent, K. Kist and A. J. Schwab, "Pre-breakdown behavior of a composite liquid-solid insulation system under impulse conditions", IEEE Conference on Electrical Insulation and Dielectric Phenomena (CEIDP), Millbrae, USA, vol. 1, pp. 196-199, 20th-23rd October, 1996.

[74] L. E. Lundgaard, D. Linhjell, and G. Berg, "Streamer/leaders from a metallic particle between parallel plane electrodes in transformer oil", IEEE Transactions on Dielectrics and Electrical Insulation, vol. 8, pp. 1054-1063, 2001.

[75] K. J. Rapp, J. Corkran, C. P. McShane and T. A. Prevost, "Lightning impulse testing of natural ester fluid gaps and insulation interfaces", IEEE Transactions on Dielectrics and Electrical Insulation, vol. 16, pp. 1595-1603, 2009.

[76] K. J. Rapp, C. P. McShane, J. Vandermaar, D. Vukovic and S. Tenbohlen, "Long gap breakdown of natural ester fluid", International Conference on High Voltage Engineering and Application (ICHVE), New Orleans, USA, pp. 104-107, 11th-14th October, 2010.

[77] T. A. Prevost, "Dielectric properties of natural esters and their influence on transformer insulation system design and performance-an update", IEEE Power & Energy Society General Meeting (PES), Calgary, Canada, pp. 1-7, 26th-30th July, 2009.

[78] M. Hemmer, Y. Julliard, R. Badent and A. J. Schwab, "Streamer inception and propagation in rape-seed oils and mineral oils", IEEE Conference on Electrical Insulation and Dielectric Phenomena (CEIDP), Kitchener, Canada, pp. 548-551, 14th-17th October, 2001.

[79] A. B. Eriksson, R. Liu and C. Tornkvist, "Differences in streamer initiation and propagation in ester fluids and mineral oil", IEEE International Conference on Dielectric Liquids (ICDL), Trondheim, Norway, paper 40, 26th-30th June, 2011.

[80] H. Q. Moser, "Transformerboard", Special print of Scientia Electrica, USA, 1979.

[81] R. Badent, M. Hemmer, U. Konekamp, Y. Julliard and A. J. Schwab, "Streamer inception field strengths in rape-seed oils", IEEE Conference on Electrical Insulation and Dielectric Phenomena (CEIDP), Victoria, Canada, vol. 1, pp. 272-275, 15th-18th October, 2000.

[82] R. Badent, Y. Julliard, K. Kist and A. J. Schwab, "Behaviour of rape-seed-oils under impulse voltages", IEEE Conference on Electrical Insulation and Dielectric Phenomena (CEIDP), Austin, USA, vol. 2, pp. 638-641, 17th-20th October, 1999.

[83] O. L. Hestad, S. Ingebrigsten and L. E. Lundgaard, "Streamer initiation in cyclohexane, Midel 7131 and Nytro 10X", IEEE International Conference on Dielectric Liquids (ICDL), Coimbra, Portugal, pp. 123-126, 26th June-1st July, 2005.

[84] O. L. Hestac, G. Berg, S. Ingebrigtsen and L. E. Lundgaard, "Streamer injection and growth under impulse voltage: a comparison of cyclohexane, Midel 7131 and Nytro 10X", IEEE Conference on Electrical Insulation and Dielectric Phenomena (CEIDP), Boulder, USA, pp. 542-546, 17th-20th October, 2004.

[85] M. T. Do, A. Nysveen, L. E. Lundgaard and S. Ingebrigtsen, "An experimental study on the effect of DC bias on streamer initiation and propagation in a dielectric liquid under impulse voltage", IEEE Transactions on Dielectrics and Electrical Insulation, vol. 16, pp. 1623-1631, 2009.

[86] N. Aka, A. Beroual and C. Perrier, "Pre-breakdown phenomena in synthetic ester and silicone oils for power transformers", IEEE International Conference on Dielectric Liquids (ICDL), Poitiers, France, pp. 194-197, 30th June-4th July, 2008.

[87] C. T. Duy, O. Lesaint, A. Denat, N. Bonifaci and Y. Bertrand, "Streamer propagation and breakdown in rape-seed oil at high voltage", IEEE International Conference on Dielectric Liquids (ICDL), Poitiers, France, pp. 149-152, 30th June-4th July, 2008.

[88] C. T. Duy, O. Lesaint, N. Bonifaci, A. Denat and Y. Bertrand, "High voltage breakdown and pre-breakdown properties in rape-seed insulating oil", IEEE Conference on Electrical Insulation and Dielectric Phenomena (CEIDP), Vancouver, Canada, pp. 623-626, 14th-17th October, 2007.

[89] D. Viet-Hung, A. Beroual and C. Perrier, "Comparative study of streamer phenomena in mineral, synthetic and natural ester oils under lightning impulse voltage", International Conference on High Voltage Engineering and Application (ICHVE), New Orleans, USA, pp. 560-563, 11th-14th October, 2010.

[90] L. Lewand, "Laboartory evaluation of several synthetic and agricultural-based dielectric Liquids", Doble International Client Conference, USA, 2001.

[91] M. Eklund, "Mineral insulating oils; functional requirements, specifications and production", IEEE International Symposium on Electrical Insulation (ISEI), Toronto, Canada, pp. 68-72, 11th-14th June, 2006.

[92] IEC 60897, "Methods for the determination of the lightning impulse breakdown voltage of insulating liquids", International Electrotechnical Commission, 1987.

[93] ASTM D 3300, "Dielectric breakdown voltage of insulating oils of petroleum origin under impulse conditions", ASTM International, USA, 1994.

[94] R. Liu and A. Jaksts, "Breakdown processes in transformer insulation under LI voltages", IEEE International Conference on Dielectric Liquids (ICDL), Coimbra, Portugal, pp. 75-78, 26th June-1st July, 2005.

[95] F. McCluskey, A. Denat and O. Lesaint, "Breakdown and pre-breakdown phenomena in liquids under positive impulse voltages", IEEE Transactions on Dielectrics and Electrical Insulation, vol. 1, pp. 377-382, 1994.

[96] ASTM D1816, "Dielectric breakdown voltage of insulating oils of petroleum origin using VDE electrodes", ASTM International, USA, 2004.

[97] W. Hauschild and W. Mosch, "Statistical techniques for high-voltage engineering", J. W. Arrowsmith Ltd., Bristol, UK, 1992.

[98] IEC 60060-1, "High-voltage test techniques part 1: general definitions and test requirements", International Electrotechnical Commission, 1989.

[99] V. Lopatin, M. D. Noskov, R. Badent, K. Kist and A. J. Schwab, "Positive discharge development in insulating oil: optical observation and simulation", IEEE Transactions on Dielectrics and Electrical Insulation, vol. 5, pp. 250-255, 1998.

[100] P. Rain and O. Lesaint, "Pre-breakdown phenomena in mineral oil under step and ac voltage in large-gap divergent fields", IEEE Transactions on Dielectrics and Electrical Insulation, vol. 1, pp. 692-701, 1994.

[101] J. C. Devins and S. J. Rzad, "Streamer propagation in liquids and over liquid-solid interfaces", IEEE Transactions on Electrical Insulation, vol. EI-17, pp. 512-516, 1982.

[102] H. Yamamoto, S. Uozaki, R. Hanaoka, S. Takata, Y. Kanamaru and Y. Nakagami, "Creeping discharges in transformer oil under lightning impulse voltages over 100 kV peak value", IEEE International Conference on Dielectric Liquids (ICDL), Poitiers, France, pp. 130-133, 30th June-4th July, 2008.

[103] R. Hanaoka, T. Kohrin, Y. Genba, R. Ishibashi, T. Miyamoto and T. Nishi, "Impulse creeping discharge along the surface of polyethylene wire immersed in transformer oil", Electrical Electronics Insulation Conference and Electrical Manufacturing & Coil Winding Conference, pp. 113-117, 18th-21st September, 1995.

[104] Y. Nakao, M. Naruse, Y. Suzuki, H. Itoh, Y. Sakai and H. Tagashira, "Influence of insulating barrier on the creepage discharge in transformer oil", IEEE Transactions on Dielectrics and Electrical Insulation, vol. 4, pp. 775-779, 1997.

[105] G. Massala and O. Lesaint, "Positive streamer propagation in large oil gaps: electrical properties of streamers", IEEE Transactions on Dielectrics and Electrical Insulation, vol. 5, pp. 371-381, 1998.

[106] Q. Liu and Z. D. Wang, "Streamer characteristic and breakdown in synthetic and natural ester transformer liquids under standard lightning impulse voltage", IEEE Transactions on Dielectrics and Electrical Insulation, vol. 18, pp. 285-294, 2011.

[107] Q. Liu, Z. D. Wang, P. Dyer and D. Walker, "Accumulative effect on streamer propagation of lightning impulses on oil/pressboard interface", IEEE International Conference on Dielectric Liquids (ICDL), Trondheim, Norway, paper 56, 26th-30th June, 2011.

[108] T. Chao, G. Chen, M. Fu and L. Rui-jin, "Space charge behaviour in multi-layer oil-paper insulation under different DC voltages and temperatures", IEEE Transactions on Dielectrics and Electrical Insulation, vol. 17, pp. 775-784, 2010.

[109] K. Nakamura, K. Kato, H. Koide, K. Fujii and H. Okubo, "Kerr electro-optic measurement of electric field distribution in rapeseed ester oil and pressboard composite system", IEEE International Conference on Dielectric Liquids (ICDL), Coimbra, Portugal, pp. 405-408, 26th June-1st July, 2005.

[110] T. Shimazaki, "Flashover characteristics and surface processes under negative impulse voltage in atmospheric air", IEEE Transactions on Electrical Insulation, vol. 27, pp. 488-495, 1992.

[111] Y. Murooka and S. Koyama, "Nanosecond surface discharge study by using Dust figure techniques", Journal of Applied Physics, vol. 44, pp. 1576-1580, 1973.

APPENDIX I LIST OF PUBLICATIONS

Peer-reviewed Journal Papers:

[1] **Q. Liu** and Z.D. Wang, "Streamer characteristic and breakdown in synthetic and natural ester transformer liquids with pressboard interface under lightning impulse voltage", IEEE Transaction on Dielectric and Electrical Insulation, in press, 2011.

[2] **Q. Liu** and Z.D. Wang, "Secondary reverse streamer observed in an ester insulating liquid under negative impulse voltage", Journal of Physics D: Applied Physics, vol. 44, issue 40, pp. 405203, October 2011.

[3] Z.D. Wang, **Q. Liu**, X. Wang, P. Jarman and G. Wilson, "Discussion on possible additions of IEC 60897 and IEC 61294 for insulating liquids tests", IET Journal of Electric Power Applications, vol. 05, issue 06, pp. 486-493, July 2011.

[4] **Q. Liu** and Z.D. Wang, "Streamer characteristic and breakdown in synthetic and natural ester transformer liquids under standard lightning impulse voltage", IEEE Transaction on Dielectric and Electrical Insulation, vol. 18, issue 01, pp. 285-294, February 2011.

International Conference Papers:

[5] P. Jarman, G. Wilson, P. Dyer, F. Perrot, D. Walker, M. Lashbrook, J. Noakhes, **Q. Liu**, X. Wang, X. Yi and Z.D. Wang, "Electrical performance of ester insulating liquids for power transformers", CIGRE SC A2&D1 Joint Colloquium, Kyoto, Japan, paper PS2-O-5, 11th-16th September, 2011.

[6] **Q. Liu**, Z.D. Wang, P. Dyer and D. Walker, "Accumulative effect on streamer propagation of lightning impulse on oil/pressboard interface", IEEE International Conference on Dielectric Liquids (ICDL), Trondheim, Norway, paper 56, 26th-30th June 2011.

[7] Z.D. Wang and **Q. Liu**, "'Breakdown voltage vs. gap distance' curves for ester transformer liquids under standard lightning impulse voltage", CIGRE 2010 Session Proceedings, A2, Paris, France, 22nd-27th August, 2010.

[8] Z.D. Wang, **Q. Liu**, X. Wang and X. Yi, "Pre-breakdown study on ester transformer liquids under lightning impulse and AC voltage", CIGRE 2010 Session Proceedings, D1, Paris, France, 22nd-27th August, 2010.

[9] **Q. Liu**, Z.D. Wang and F. Perrot, "Impulse breakdown voltages of ester-based transformer oils determined by using different test methods", IEEE Conference on Electrical Insulation and Dielectric Phenomena (CEIDP), Virginia Beach, USA, pp. 608-612, 18th-21st October, 2009.

[10] **Q. Liu**, Z.D. Wang, P. Jarman, N. Azis, W. W. Sampson and R. Heywood, "Assessment of ageing conditions through paper tensile strength analysis of scrapped transformers", International Symposium on High Voltage Engineering (ISH), Cape Town, South Africa, pp. 264-269, 24th-28th August, 2009.

[11] **Q. Liu** and Z.D. Wang, "AC and lightning breakdown strength of mineral oil Nytro Gemini X and 10GBN", International Electrical Insulation Conference (INSUCON), Birmingham, UK, pp. 14-19, 26th-28th May, 2009.